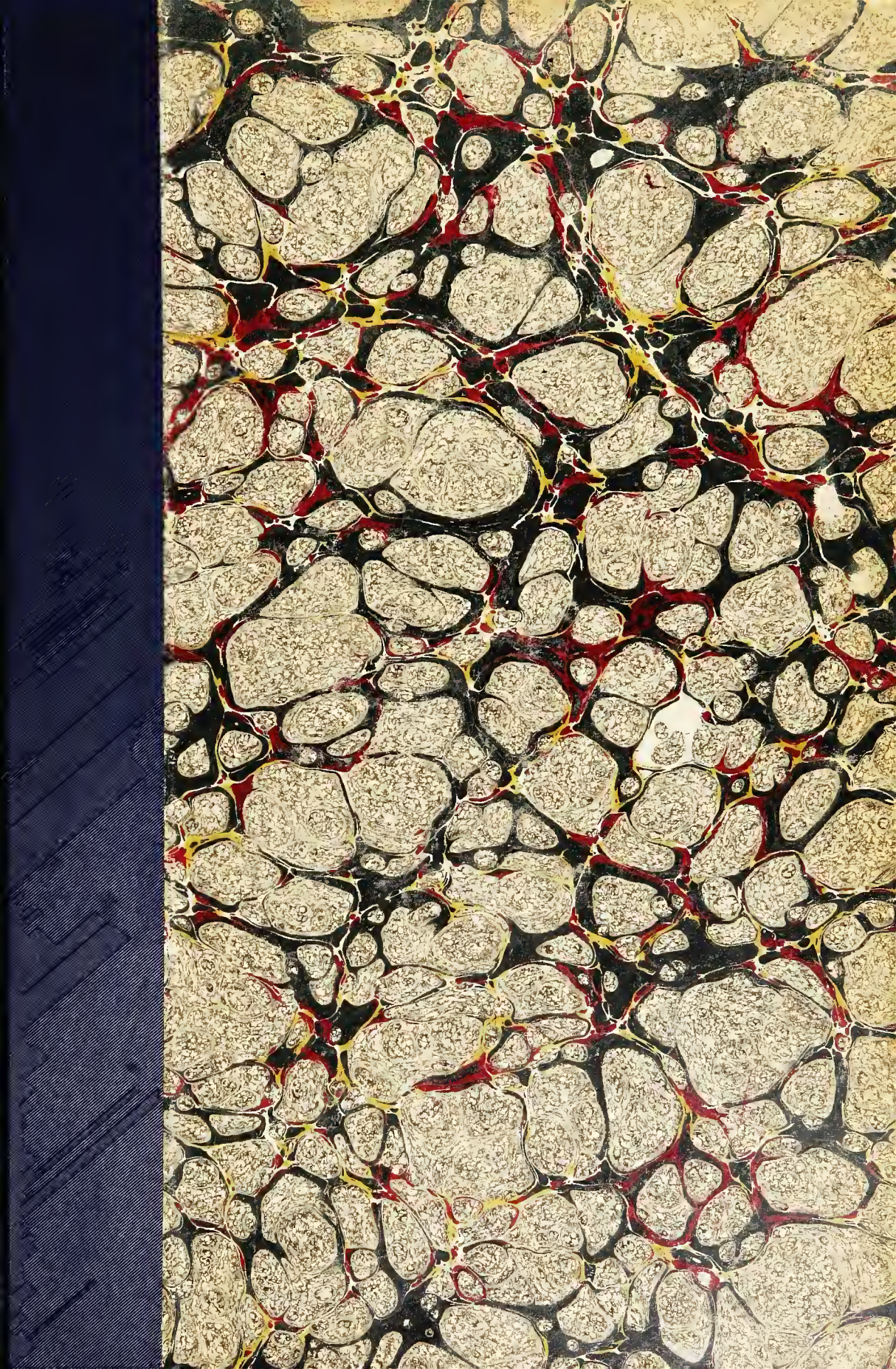

CONDENSATION OF VAPOR AS INDUCED BY NUCLEI AND IONS

By CARL BARUS
Hazard Professor of Physics, Brown University

WASHINGTON, D. C.:
Published by the Carnegie Institution of Washington
May, 1907

CARNEGIE INSTITUTION OF WASHINGTON
PUBLICATION NO. 62

PREFACE.

The chief purpose of the present volume is the development of a fog chamber of simplest practical character, capacious enough to admit of the measurement of the largest available coronas, and efficient up to the highest exhaustions applicable; *i. e.*, those which do not uselessly overstep the optical limits of the experiment, where fog particles become so fine as to be virtually inactive in diffracting or scattering white light. This I think has been accomplished, and the results, as far as they go, seem to indicate an efficiency not inferior to Wilson's piston apparatus. I have not, however, been able to get much beyond the large green-blue-purple corona, no matter whether the nuclei selected were effectively large, like the ions, or effectively small, like the colloidal nuclei. The forms beyond are flimsy and so nearly colorless as to be useless for measurement; but the steam-jet nevertheless reveals a whole order of axial oranges and yellows, lying beyond, which to my knowledge have not been detected in any form of fog chamber whatever.

As used in most experiments, including my own earlier work, the fog chamber with a plug stopcock seems to be of very inferior efficiency in comparison with the piston form. This, however, in a properly designed apparatus, is the case only when the attempt is made to obtain the isothermal drop in pressure observationally at the fog chamber, closed at once after exhaustion. The datum needed can only be found by computation, and the initial pressures in the fog and vacuum chambers and their final pressure when in contact, always at the same temperature, suffice for this purpose. Though I was prepared for some corrections, I did not anticipate so large a difference between the apparent drop and the true drop of pressure, as actually appears. In the experiments which follow, the ratio is in fact as 1,000 to 775, a difference of nearly 25 per cent. Hence it will be necessary to restandardize the coronas with this result in view, an undertaking which I hope to begin in the near future. Indeed a large number of incidental results would have made this desirable in the interest of other investigations. For similar reasons I have (as a rule) continued to refer the nucleations of the present volume to the drop in pressure *observed* at the fog chamber; and such reference is sufficient for the comparisons aimed at, if the same type of apparatus is used throughout, as was the case.

Having improved the fog chamber to the degree shown in Chapters I and II, it was made use of in Chapter III for certain incidental experi-

ments. I have already shown in case of dust-free air and the persistent nuclei produced by intense X-radiation that the distribution of nuclei within the fog chamber is a most remarkable feature of the experiment. The same, however, is true of the ions. Whether produced by X-rays acting from long distances or by radium, the density of ionization is as a rule very different in different parts of the fog chamber, showing the important effects due to the presence of secondary radiation within. Again, the change of nucleation produced when the exciting cause (X-ray bulb or radium tube) is removed at different distances from the fog chamber was to be reinvestigated. Associated with this experiment is the occurrence of minima of nucleation for certain distances, supposing the exhaustion to be sufficiently high to induce condensation of ions and colloidal nuclei in presence of each other. Finally, if the rate of decay of ions can be inferred from independent electrical experiments, a method for the standardization of coronas is presented which bids fair to be the most satisfactory solution of the problem suggested. The method admits of a determination not only of the relation of the nuclei corresponding, in a given case, to two different coronas (*cæt. par.*), but of the absolute nucleation involved. There is also a possibility of detecting in this way how a given mass of precipitated water is distributed among nuclei of different sizes when occurring together—one of the most important of the problems outstanding in connection with this apparatus.

Chapter IV adduces a variety of results for colloidal nuclei in media other than air-water. It is shown, for instance, that there is no evidence to prove the colloidal nuclei in a medium of carbon dioxide and water are larger than in the normal case of air and water, in spite of the presence of the coercible gas in which groups of larger molecular aggregates would be anticipated. On the other hand relatively large colloidal nuclei do seem to occur in a medium of air and alcohol vapor. Thus it is suggested that colloidal nuclei in dust-free wet air are to be associated with the saturated vapor and that the gas is only secondarily involved.

In Chapter V, undertaken by Miss L. B. Joslin under my direction, a systematic comparison is worked out of the relations between the number of ions in the atmosphere and the corresponding dust contents in the lapse of time. No direct connection is apparent, whence it follows that as the nucleation is largely of local origin, other sources must be looked to for the ionization, or that the enormous local output of ions from an industrial community vanishes so rapidly as to be quite negligible. On the other hand, it may be possible to detect evidences of "absorption" in the curves obtained. Incidentally the nucleation of the atmosphere of Providence during nearly four years is exhibited.

Finally, in Chapter VI, I return to the problem begun in Chapter I, to see whether there is any change in the colloidal nucleation of dust-free air, such as might be ascribed to the ionization produced by some penetrating cosmical radiations coming from without; for it was to be the plan of these researches to study the ordinary dust content of the atmosphere with regard to its variation in the lapse of time first, and thereafter to continue in the same way with the nucleation of the dust-free atmosphere. This nucleation is found to *increase* synchronously with the *decrement* of the barometer; but as the amount of adiabatic cooling, *i. e.*, the efficiency of the apparatus (*cæt. par.*), follows the same conditions, it is extremely difficult to disentangle the two effects. Nevertheless the results are of considerable interest and they are therefore reported in their present state of progress.

My thanks are due to Miss L. B. Joslin, who not only gave efficient assistance in the preparation of the manuscript and of the drawings for the press, but contributed much of the work in Chapter III, section 62, and Chapter V.

CARL BARUS.

CONTENTS.

CHAPTER II.—*Later and Final Stages in the Efficiency of the Fog Chamber due to a Gradual Increase in the Bore of the Exhaust Pipes.*

CONNECTING PIPES NOT LARGER THAN 1.5 INCHES IN DIAMETER.

CONNECTING PIPES 2 INCHES IN DIAMETER.

COLLOIDAL NUCLEI IN DUST-FREE AIR. EXHAUSTION PIPES AND STOPCOCKS 4 INCHES IN DIAMETER.

CHAPTER III.—*Miscellaneous Experiments.*

CHAPTER IV.—*Distribution of Colloidal Nuclei and of Ions in Media other than Air-water.*

COLLOIDAL NUCLEI AND IONS IN WET DUST-FREE CARBON DIOXIDE AND IN WET COAL-GAS.

CHAPTER I

EARLY SUCCESSIVE STAGES OF THE EFFICIENCY OF THE FOG CHAMBER AND ALLIED RESULTS.

Before beginning the main subject of this chapter (see section 2), it is advisable to add a few measurements of the distributions of ions produced within the fog chamber by the X-rays or by radium acting from without, since these occurrences must be kept in mind throughout the measurements. Again, the effect of different classes of nuclei (persistent nuclei, ions, and colloidal nuclei) in presence of each other is similarly important and direct light must be thrown upon it preliminarily.

Under all conditions the fog chamber is attached to a large vacuum chamber by a rigid passage-way of the length and diameter specified, the ratio of the volumes of the two chambers being about as 6 to 100, respectively. Moreover, it was customary to read off the drop of pressure (δp) at the fog chamber (isolated immediately after exhaustion from the vacuum chamber) when isothermal conditions had been reestablished. The observed datum suffices for the comparisons of nucleation when the same chambers are used throughout; but it will be shown in Chapter II that it is much in excess of the true drop of pressure and that the latter is to be computed from the initial pressures in fog and vacuum chambers and the final pressure when both are in contact, all under isothermal conditions.

After completing the work of section 2 of this chapter, a few applications were made with the apparatus in its state of partial completion for the purpose of ascertaining whether there is any discernible change of colloidal nucleation and by implication of ionization in the stagnant air within the scope of the method. Several months of observation showed none. The early data have been added to the chapter for convenience in chronology, though they slightly interrupt the continuity of the research. The question of time variation is taken up again by a different method in Chapter VI.

DISTRIBUTION OF NUCLEI WITHIN THE GLASS FOG CHAMBER, WHEN THE AIR IS ENERGIZED BY THE GAMMA-RAYS OR THE X-RAYS.

1. Introductory.—I may recall at the outset that there are three classes of nuclei to be considered in this chapter, the first of which includes the ordinary dust-like or persistent kind. They may be sepa-

rated from the air by the filter and they require the smallest degree of supersaturation of water vapor to precipitate condensation. They are usually but not always (necessarily) foreign bodies in the air; at least they are producible in dust-free air by the X-rays of sufficient intensity and by other radiation. The second class comprises the fleeting nuclei. They are often charged and then called ions. They persist for very short periods of time, usually vanishing within a minute. They can be maintained, therefore, only in the presence of radiation, corpuscular or undulatory, from which their intimate association with electrification or with ultra-violet light is manifest. Such radiation may occur spontaneously within the body of a gas during the state of generation. The sizes of these nuclei are intermediate between the first or dust-like class and the third class. This comprises the colloidal nuclei of dust-free air, which are *virtually* persistent, inasmuch as they are a structural part of the body of the gas and are reproduced as soon as removed. They require the highest degrees of supersaturation for condensation and are without electrification.

All these groups may be made to pass continuously into each other.

I shall use the term "nucleation" to denote the number of nuclei per cubic centimeter observed in any experiment. It will be understood that this means the *efficient* nucleation; for nuclei may be and usually are present, which are not detected by the exhaustion. They are computed in the present chapter from the angular diameter ($\phi = s/30$, nearly) of the coronas, for a given supersaturation. To specify their number one must come to a conclusion as to whether nuclei are removed more rapidly by the exhaustion than they can be replaced by the molecular system, or whether the reverse is the case. If fleeting nuclei and colloidal nuclei are supposed to be instantly reproduced we shall call the number n. None are then virtually removable by the sudden exhaustion. Otherwise the nucleation (corrected for the volume expansion) is called N. In this case the exhaustion is more rapid than the reproduction of nuclei. Both n and N, as well as s, will usually be given in the earlier tables; for the discrimination between n and N is not possible, and s is specially favorable to the small nucleation which are apt to be crowded out of the diagrams for n and N.

Returning to the subject of this section, I may state that the radium used was a weak sample (10 mg., 10,000×) hermetically sealed in a thin aluminum tube. In an earlier paper I showed that whereas the nucleation produced decreased very rapidly with the distance of the energizer from the outside of the cylindrical glass fog chamber, the number of nuclei within was apparently the same throughout the length of the axis. Pressure differences, however, were usually kept below the fog limit of

air. As the aluminum tube was carefully sealed (ground screw plug and wax) the beta- and gamma-rays are here alone in question, and as the bottom of the fog chamber through which the radiation passes may be 1 cm. thick and the walls are everywhere more than 0.2 cm. thick, only the more penetrating beta-rays are active to reenforce the gamma-rays. In fact the earlier work showed that the rays after passing 1 cm. of lead produced an amount of nucleation only 30 per cent less than in the absence of the dense barrier. Thus the whole phenomenon is practically a question of the intensity of the gamma-rays.

In the course of the work, curiously enough a number of contradictory conclusions were reached, and it will therefore be advisable to report the results chronologically, beginning with the data for low pressure differences.

TABLE 1.—Distribution of nucleation within the glass fog chamber (43 cm. long, 14 cm. in diameter); nucleator, radium in thin aluminum tube. $\delta p = 21$ cm. Radium at D cm. from end, axially without. Lines of sight (two goniometers, s_1 and s_2) 15 cm. and 35 cm. from end nearest radium, or 20 cm. apart.

D	s_1	s_2	$N_1 \times 10^{-3}$	$10^{-3} \times N_2$	Mean $\begin{cases} N_1 \\ N_2 \end{cases}$	Per cent.
0 cm.	3.5	3.3	19	16	17,200	...
	3.2	3.0	14	11	16,200	100
	3.4	3.4	17	17	.....	...
	3.4	3.6	17	21	.....	...
	3.5	3.3	19	16	.....	...
20 cm.	2.5	2.5	7	7	7,000	45
	2.4	2.5	6	7	8,000	...
	2.6	2.8	8	9	.....	...
40 cm.	1.8	2.0	3	3	4,000	24
	2.3	2.3	5	5	4,000	...
	2.3	2.3	4	4	.....	...
∞ (air)	.0	.0	0	0	.....	...

2. Data.—The cylindrical glass fog chamber (fig. 1), rigorously free from leakage, was placed, with its axis horizontal, in such a way that a prolongation of the latter intersected the radium tube at a distance, D. Two goniometers with their lines of sight about 20 cm. apart, and 15 and 35 cm. from the end (bottom) of the fog chamber nearest the radium tube, were used nearly at the same time for the measurement of the apertures of the coronas seen along the axis. Both were placed with the pins nearly contiguous to the walls of the cylinder, so that the eye was at a minimum distance of 30 cm. off. All the phenomena may in this case be more clearly observed and the small coronas are less liable to drop out before the measurement has been completed. The source of light

(Welsbach mantle) was 250 cm. beyond the fog chamber. Usually the angular diameter of the coronas is about $s/30$. In table 1, s_1 refers to the goniometer nearer the radium, s_2 to the other, and N_1 and N_2 are the corresponding nucleations, when D is the distance of the radium tube from the end of the cylinder.

After the influx of filtered air, time was always allowed for the dissipation of convection currents. There was some difficulty in reading both goniometers consecutively without loss of time, as the small coronas soon vanish with the subsidence of the fog particles. It was necessary to cleanse the walls carefully before beginning the work to obviate deposits of dew.

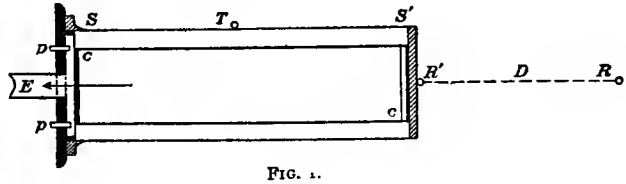

FIG. 1.

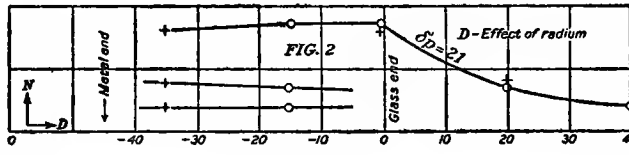

FIG. 2.

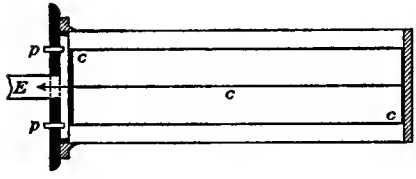

FIG. 3.

FIG. 4.

FIGS. 1, 3, 4.—Types of cylindrical fog chamber. Axial section. E, exhaust pipe; c, cloth partitions.

FIG. 2.—Nucleation (N) due to weak radium at different distances from and on top (side of cylinder) of the fog chamber. Table 1.

The table gives evidence of a small difference between N^1 and N^2, but this is here unquestionably an observational error, particularly as its sign is often reversed. The chart (fig. 2) then shows the mean number of nuclei within, when the radium is at $D=0$, 20, and 40 cm. from the end; and while the nucleation drops off rapidly from 100 to 45 and 24

per cent, respectively, the nucleation within is about constant throughout the 45 cm. of length of cylinder. At least an internal drop to less than one-fourth is out of the question, as the diagram shows. It must be remembered that the nucleation is produced instantly to saturation, that all nucleation will vanish with the removal of the radium to infinity within a few seconds, and that the ions here in question are relatively large nuclei as compared with the colloidal nuclei of dust-free air. The latter, moreover, are quite ineffective at the observed pressure difference, $\delta p = 21$, used. If larger pressure differences appear the results are usually quite different.

3. Explanation.—To account for these remarkable results is difficult. Convection is probably out of the question, though it will be quite eliminated in the following experiments. One may hazard the suggestion that the effective agency outside of the cylinder are the gamma-rays directly, whereas within the cylinder the ionization produced by those rays secondarily is in question. In other words, the gamma-rays do not act here directly, but the nuclei are produced by corpuscles set free by these rays. The medium within the cylinder is thus in a state resembling an electrolytic medium having the same ionic pressure throughout. It is this ionic pressure depending on the density and speed of the corpuscles which is transmitted instantaneously from end to end of the cylinder. To refer to the phenomenon as diffusion would be obscure without a statement as to what diffuses. The ionic nucleus is relatively a fixture and could not diffuse, in the time specified, to the far end of the cylinder, quite apart from decay.

4. Further experiments with radium. High exhaustions.—In the preceding experiments the wet cloth partition was about 10 cm. above the surface of the water below. In the new chamber shown in fig. 3, the distance has been reduced to 5 cm. Under these circumstances a very marked gradation of the number of efficient nuclei was observed for the first time. This is not, however, due to the supposed elimination of convection, but rather to the large pressure difference applied in the experiments. The result follows in table 2. When the radium tube is placed at T (fig. 1) symmetrically on the side, the metal cap virtually becomes the source of nuclei, or better, it seems to become secondarily active more intensely than the remainder of the glass chamber. The coronas obtained with two goniometers at distances 11 and 36 cm. from the brass end and 35 and 10 cm. from the glass end are rapidly larger as the brass end is approached. The ratios of the n-values is greater than 2:5. These conditions are retained indefinitely so long as the radium is

present, showing that the result is not incidental. As both ends of the chamber were about equidistant from the radium, it would appear to be the excess of the secondary radiation from the metal cap which is in question.

TABLE 2.—Distribution of nucleation within the glass fog chamber (as in table 1) and allied results.

	s.	$N \times 10^{-3}$.	$N \times 10^{-3}$.
I. Radium tube on side of glass fog chamber. Two goniometers, I at 11 cm. and II at 36 cm. from brass cap, 46 cm. from glass end. $\delta p = 26.0$ cm.			
No. I	6.6	95	147
No. II	4.7	38	59
[1] No. I	6.6	95	147
[1] No. II	4.4	30	46
II. Radium on glass end, 1 cm. thick; observation I at 10 cm. and II at 35 cm. from end. $\delta p = 26$.			
No. I	60	76	118
No. II	47	38	59

	s.	$N \times 10^{-3}$.	$N \times 10^{-3}$.
III. Radium at ∞. Lapse 10 m.			
26.5	3.2	11	17.4
30.8	[2] 7.4	114	195
IV. Radium on brass plate, 1 cm. thick.			
30.6	4.0	24	42

[1] Three hours later no interference. [2] w r g.

5. The same, continued. X-rays.—After finding that the fleeting nucleation within the fog chamber was unequally distributed under the excitation of radium, similar experiments were tried with the X-rays, using the fog chamber (fig. 4) with four horizontal wet cloth partitions 2 to 3 cm. apart to obviate convection. The results given in the first part of the following table are definitely affirmative. When the X-ray bulb is near the fog chamber, the nucleation nearer the bulb is decidedly in excess. Thus when the line of sight is 30 and 50 cm. from the anti-cathode, the farther nucleation is about 60 per cent of the nearer.

If, however, the bulb is relatively far away ($D = 100$ or 200 cm.), the end of the fog chamber *farthest* from the bulb and *near* the brass cap is more actively ionized. In other words, under these circumstances the secondary radiation from the brass cap predominates. The nucleation at 10 and 30 cm. from the latter shows a decrement of 20 per cent, for

instance, passing continuously from the high to the lower values. This experiment throws light on the function of the walls in producing distributions in case of persistent nuclei. Obviously the effect of secondary radiation decreases rapidly as the distance from the walls increases. The nucleation within the fog chamber is probably largely due to this kind of radiation.

6. The same, continued. Miscellaneous tests.—In the second part of table 3, experiments with radium are resumed for comparison. The gradation of number, decreasing from the brass end to the glass end, for a symmetrical position of the radium tube at T, fig. 1, is very marked, as usual; while the case for radium at R, fig. 1, again shows the largest coronas at the end of the tube, the distribution being more nearly uni-

TABLE 3.—Distribution of ions within glass fog chamber. Metallic (brass) cap at one end, glass end opposite 1 cm. thick. Lines of sight 10 cm. (s_{10}) and 30 cm. (s_{30}) from brass end, 15 cm. and 35 cm. from glass end. X-rays acting from distance D.

Lead case.	D.	s_{10}.	s_{30}.	$N_{10} \times 10^{-3}$.	$N_{30} \times 10^{-3}$.	δp.
	cm.					
I off.....	15	G B P	W P cor	130	156	24.5
	15	w P cor	w r g	180	255	30
	15	w P cor	w o g	180	300	30
	1	w P cor	w o g	180	300	30
	[1]100	6.9	6.3	121	91	30
		w o	w g			
	[1]200	6.5	6.1	102	84	30
II off:						
On middle of side at T.	...	6.8	5.4	114	63	30
		6.6	5.0	106	48	30
On glass end at R...	...	5.6	5.2	69	56	30
On side near cap at S.	...	4.4	3.3	33	14	30
On middle of side at T.	...	6.4	4.5	96	36	30
On side near glass end at S'.....	...	4.8	4.8	45	45	30

[1] Large coronas near brass cap. Secondary radiation preponderating.

form. Thereafter the radium was placed in positions S, T, S', on top, successively, with the results for T graded about as usual. Radium at S still evokes gradation, but the coronas are even much smaller than when the radium is placed on the thick glass end at R. When radium is placed at S' near the glass end gradation is nearly absent, but the coronas are again small. The results are therefore not as simple as was anticipated and do not admit of an explanation merely in terms of the glass penetrated.

When the radium tube is attached to the glass end (about 1 cm. thick), similar gradations are observed, but this time with the large coronas near the radium tube. (See fig. 5.) The ratio of n-values is now about 2 for the given distances. The law of variation is difficult to obtain in any of these cases, but when the brass end is predominatingly active, the reduction of n-values is nearly proportional to distance, if the usual mean values of s be taken together with the special observations.

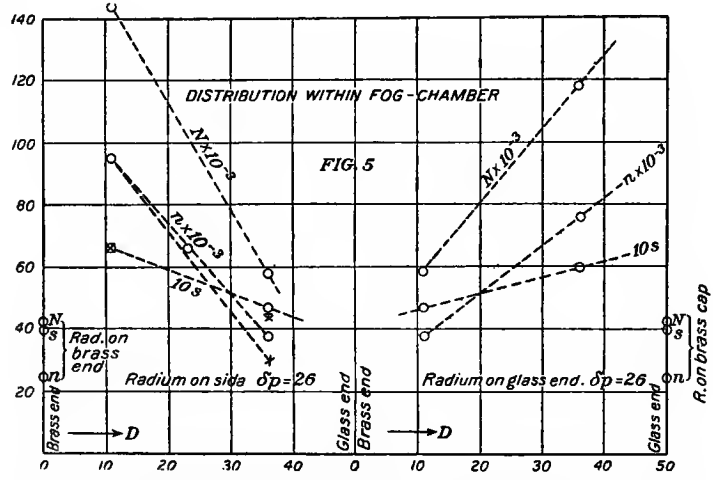

FIG. 5.—Density of ionization (N) within the fog chamber at different distances (D) from the brass end. Table 2.

In view of the action of the glass end when the radium is attached to it, it seems possible that the glass, large thicknesses of which are always penetrated and permeated obliquely by the radiation, may be active in both cases, but special inquiry is needed here. The glass cylinder was found to be thinner (about 0.15 cm.) near its equatorial parts (T), and to increase in thickness towards both ends. If, however, the phenomena were due to thickness of glass the coronas should be largest near the middle and taper down toward both ends of the fog chamber. This is not the case, as the coronas for a symmetrical position of the radium tube decrease regularly from the brass to the glass end of the apparatus.

If the radium tube is placed on the outside of the brass cap, one cm. thick or more, there is the usual moderate reduction of nucleation here, from $n=65$ to $n=24$ thousands (63 per cent); but the change of diameter of coronas within is of the same kind, decreasing from the brass to the glass end, as above.

7. Distance effects of radium.—To throw further light on present and preceding questions at issue, I shall next anticipate some of the work below and describe certain experiments specially adapted for the purpose. By "dust-free air" I mean atmospheric air filtered with extreme slowness (through large wide filters of packed cotton) and thereafter left without interference for two or more hours. Such air shows a high fog limit. In the fog chamber used the condensation began at an observed pressure difference of about $\delta p = 26$ cm.; rain-like condensation at $\delta p = 21$ cm.

In the present experiments all tests are made at $\delta p = 41.5$ cm., at a pressure difference therefore much above the fog limit, and probably approaching the condensing power of the apparatus. The number of nuclei computed from the coronas observed is an estimate merely, as the constants needed for the very large range of variation in question are not available. Nevertheless if the same δp is used throughout, the nucleations obtained are immediately comparable. With these reservations the number of nuclei found in the dust-free air and at the δp in question is about $N = 380 \times 10^3$ to 400×10^3, per cubic centimeter. It is obvious, moreover, that these nuclei are excessively small, much smaller than ions, smaller even than those which would respond to smaller δp's exceeding $\delta p = 26$ cm.

Let the fog chamber (fig. 1) be subjected to the radiations from weak radium (10,000×, 10 mg.) contained in a thin hermetically sealed aluminum tube. As the walls of the fog chamber are 0.1 to 0.3 cm. thick and the end (bottom) toward the tube nearly 1 cm. thick, γ-rays only will penetrate into the inside, apart from the secondary radiation there produced. As shown in fig. 1 (cylindrical fog chamber) the radium tube R is at an axial distance D from the nearer end. In addition to this the radium was also tested at T (top) in the figure, where it is nearest the body of dust-free air under experiment.

The data investigated are shown in table 5 and in the curve (fig. 6), where the abscissas are the distances D and the ordinates the number of efficient nuclei per cubic centimeter.

It follows from the graph that as the radium is brought in an axial direction from ∞ to the end of the fog chamber, the number of efficient nuclei in the dust-free air contained is gradually but enormously reduced to a minimum for $D = 25$ cm. (about), after which the number again increases to the maximum at $D = 0$. Curiously enough, when the radium was further approached to the body of the air by being placed at T, the mean number of nuclei did not increase.*

*This result is to be further interpreted in special experiments below.

If the radium is inclosed in a long, thick lead tube (60 cm. long, walls 0.5 cm. thick), the nucleation is but moderately reduced (see crosses in fig. 6), showing that gamma-rays are in question.

TABLE 4.—Radium effect at high pressure differences. $\delta p = 41.5$ cm.; s (air) $= 7.5$; D, distance from end of fog chamber.

D.	s.	$n \times 10^{-3}$.	D.	s.	$n \times 10^{-3}$.
On top..	3.9	27	50	4.8	51
	3.9	27		4.9	54
25.....	3.3	16	100	6.3	104
	3.4	17		6.8	129
0.....	4.8	51	∞	7.5	160
	4.7	48	End	4.8	51
On top..	4.0	27		4.7	48
	4.1	31	Top	4.6	44
0.....	4.4	37		4.7	48
	4.7	48	End	4.7	48
25.....	3.3	16	Top	4.7	48
[1]0.....	4.1	31	[2]End	4.7	48
On top..	4.0	27	∞	6.1	97
[1]On top..	3.9	27			

[1] Radium tube in lead pipe walls 5 cm. thick. [2] Lead radiation.

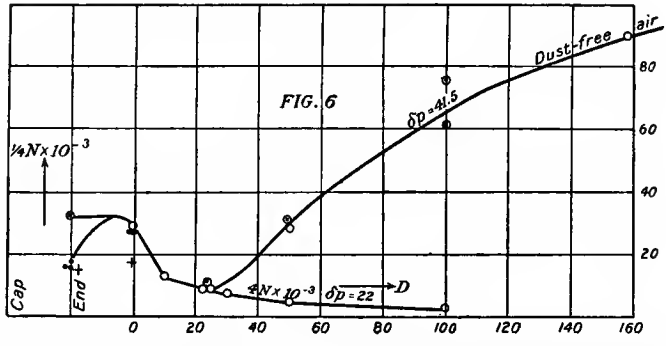

FIG. 6.—Efficient nucleation (N) near the middle of the fog chamber, for different distances (D) of radium from the end and for different exhaustions (δp). Table 4.

8. Cause of the minimum and the maximum.—This is easily explained, since the ions are relatively large bodies and relatively few in number as compared with the nuclei of dust-free air for the same δp. Hence the ions capture the moisture more and more fully as their number, with diminishing distance D, becomes greater. At $D = 25$ cm. probably the whole of the moisture is condensed on ions, and as their number increases as D vanishes the minimum in question results. In fact, it

was shown elsewhere that below the fog limit of air, the nucleation observed and due purely to radium at different distances, D, is, for example ($\delta p = 22$),

D.....	0	10	30	50	100
$N \times 10^{-3}$....	120	50	32	20	12 etc.,

agreeing in character as far as may be expected with the data here in question. These data multiplied by 4 (in other words $4n \times 10^{-3}$) are also given in fig. 6 for comparison. Hence the ions caught at $\delta p = 41.5$ are about four times more numerous than at $\delta p = 22$, and correspondingly smaller. They behave, therefore, as if they were markedly graded, but nevertheless, as a group, throughout much smaller than the nuclei of dust-free air so long as the radiant field is appreciable. While the number of nuclei continually grows smaller, with diminishing D, the efficient nuclei may nevertheless increase again below a certain D, seeing that the colloidal nuclei in dust-free air are enormously in excess, only a few of which are caught even in the absence of radium.

TABLE 5.—Distance effect of radium. D measured from side. $\delta p = 35$ cm.

D.	s.	$n \times 10^{-3}$.	$n \times 10^{-3}$.
cm.	*cm.*		
250	[1]7.6	160	300
200	[2]7.6	150	285
150	[2]7.6	145	270
100	[3]7.3	136	255
50	[4]5.1	56	105
25	4.4	35	66
12	4.2	30	57
0	4.7	45	84
Radium at ∞. Lapses 15[s] and 3[m].			
∞	4.1	27	51
∞	[1]7.6	160	300

[1]GBP. [2]gyog'. [3]wog. [4]wrg.

It would be more difficult to account for the result that the same nucleation is observed wherever the radium touches the outside of the elongated fog chamber. In other words, radium at the end of the chamber in the earlier experiments seemed to produce the same mean nucleation as when at the top, although the distances from the center of mass of the glass are as 3 to 1; but the above experiments have already suggested that this result was probably an incidental case.

9. Further experiments with radium.—Incidental experiments corresponding to those of the preceding section are given in table 6, showing the reduction of the efficient nucleation of dust-free air when the radium tube is gradually approached to the sides of the chamber. They are shown graphically in fig. 7, both in relation to s, n, and N, and need little discussion. The minimum position lies very near the chamber and about 10 cm. from it. The action of radium is hardly perceptible beyond 1 meter, chiefly because the green-blue-purple corona happens to be involved. Sharper results could therefore be obtained at lower pressure differences, where white-red-green coronas are in question. But on the whole it is clear that radiation which appreciably lowers the asymptote corresponding to dust-free non-energized air must be of an intensity exceeding the effect of 10 mg. of weak radium (10,000×), at a distance of 1 meter. There does not, therefore, seem to be much hope of observing cosmical radiations in this way. Finally the second part of table 6 (and other data below) shows how soon the high nucleations of dust-free air (non-energized) is regained after the removal of the radium tube. The rapidity with which ionized nuclei fall apart is obtainable in this way and well worthy of special research. (Cf. Section 62 *et seq.*)

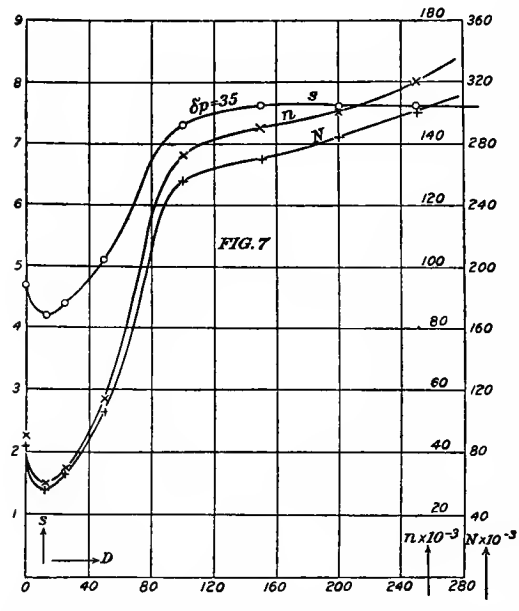

FIG. 7.—Efficient nucleation (N) and coronal aperture (S) for different distances (D) of radium from end of fog chamber and for different exhaustions (δp). Table 5.

10. Distance effect of penetrating X-radiation.—The question at issue was whether the rays which have penetrated lead are characterized by the same marked distance effect which is observed for radium. The fog chamber was inclosed in a close-fitting lead casket with two narrow side-windows for observation. The end of the casket toward the bulb

was provided with a lid to be opened or closed at pleasure. When the distance is $D=50$, about 8 per cent of the radiation passes through; when $D=10$ cm. the amount is about 17 per cent. Unfortunately the observation through the window is not satisfactory and no doubt a certain amount of radiation enters here secondarily. It is therefore difficult to carry out the comparison.

TABLE 6.—Penetration through lead. Lead-cased glass fog chamber. Plates of lead 0.14 cm. thick. $\delta p=24.5$.

Lead case—	D.	s.	$n\times 10^{-3}$.
On; end closed.....	50	2.7	6.7
		3.1	9.5
On; end open.....	50	g B P.	100
On; end closed.....	10	3.8	19.5
On; end closed.....	10	3.5	16.5
On; end closed.....	10	3.5	16.5
Off; plate only.....	15	w o g 7.0	104
Off; no plate.....	15	g B P to	130
		w P cor.	156

Large coronas near brass cap. Secondary radiation.

11. General inferences.—The occurrence of a continuous succession of groups or gradations of nuclei in the curve of figs. 6 and 7, each of which groups constitutes a condition of chemical equilibrium for the given radiating environment, is suggestive. In the first place, it may be recalled that the nuclei of dust-free air are an essential part of this body as much as the molecules themselves. Such nuclei, if withdrawn by precipitation, are at once restored. Again, air left without interference for days shows a maximum of this nucleation for the given conditions of exhaustion when all foreign nucleation must have vanished. Indeed, the water molecules themselves may be treated as a continuous part of the nucleation in question, the frequency of occurrence being a maximum for the molecular dimensions. It is best, however, to reserve discussion for a later paragraph (section 43).

THE NUCLEATION OF FILTERED AIR IN RELATION TO DIFFERENT SUPERSATURATIONS OF WATER VAPOR.

12. Successive series of results.—Before proceeding with an account of the change of the efficient colloidal nucleation of atmospheric air in the lapse of time and other like problems, it is expedient to consider the behavior of filtered air when subjected to different exhaustions. I will

proceed chronologically, taking the earliest experiments first. These may be given with sufficient detail in a chart like figure 8, in which the lower graph (I) shows the data obtained in the earlier memoirs with a wooden fog chamber. The observed pressure differences (supersaturations) are laid off horizontally, the apertures of the coronas ($s = \phi/30$, nearly, where ϕ is the angular radius to the outside of the first ring, when the eye and the source of light are at distances 85 and 250 cm. on opposite sides of the fog chamber) and the nucleations vertically. No particular attention was given to the occurrence of rain, and the measurements cease at the lower end with the measurably visible coronas. It is seen that the curve very soon reaches an asymptote, showing hopelessly poor efficiency. As the work was carefully done, the only explanation would seem to be that the speed of filtration was insufficiently slow and the exhaustion insufficiently rapid (small vacuum chamber). The same remarks apply to the graph (figure 8, II), obtained in a decreasing march of pressure difference, at the beginning of the work with the glass fog chamber (fig. 1); but the asymptote is higher. The fog limit in this case is lower and attributable to nuclei which have entered unobserved, as it is much below the values for more carefully filtered air. The first observation, having been made with the apparatus at rest for 12 or more hours, shows a very high but probably more nearly correct result.

Figure 8 also contains the corresponding nucleations, N, so far as they can be computed, supposing that the nuclei are removed faster than they can be restored. For high pressure differences the data are necessarily estimates. Naturally the differences between the data obtained after long waiting (12 hours or more), and those obtained in succession after intervening intervals of a few minutes, are enormously accentuated.

It follows from these results that if normal data were to be reached it would in the first place be necessary to perfect the method of filtration. This was done by providing the filter with a very fine screw stopcock, by which the rate of flow through the filter could be diminished very gradually to a vanishing value.

The next group of results, obtained on May 21, 23, and 30, and on June 3, were found under conditions of very slow filtration. They are sufficiently reproduced in the graphs (figs. 9, 10, 11), in which the abscissas are the pressure differences and the ordinates the coronal diameters (s) and the nucleations (n and N), respectively, as specified. The graphs for s are perhaps most suitable for discussion, although s exhibits the small nucleations with very great advantage. The data for May 21 are in the main much above those in fig. 8, but they are still far too low and

irregular. The other data are much larger and as far as $\delta p = 30$ lie sufficiently near together to show that limiting conditions are being approached. Beyond this the curves diverge widely. The highest results reached are those of May 30. On June 3 a change takes place during the course of the experiment, as the result of which the incoming and outgoing curves differ. In all cases there is a distinct tendency to approach a limit after δp exceeds 37 cm., due to the limitations of the apparatus.

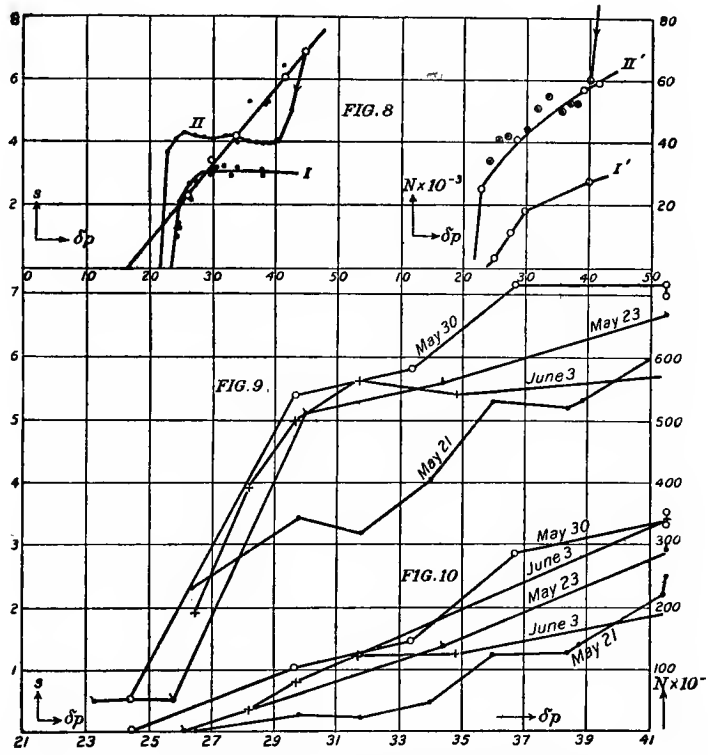

FIGS. 8, 9, and 10.—Early data of efficient nucleations (N, n) and coronal diameter (s), appearing at different exhaustions (δp) in dust-free air. Imperfect fog chamber.

The characteristic feature of all the nucleation curves is the rapid increase between $\delta p = 27$ and 30 cm.; that is, during the early coronal stages. Below this the relatively large nuclei are present at least as far as $\delta p = 21$ to the extent of a few thousand per cubic centimeter. Nevertheless, it is their variation which brings about the sinuous outline of the curves above $\delta p = 33$, seeing that large nuclei are overshadowingly effective.

On the 5th and 6th of August a series of experiments was made to test the effect of long and short lapses of time between the observations, as well as the displacements of lower limits of the curves. The results of August 6 at $\delta p = 35$ show that 15 minutes was an insufficient time between observations, but that intervals exceeding 30 minutes (very

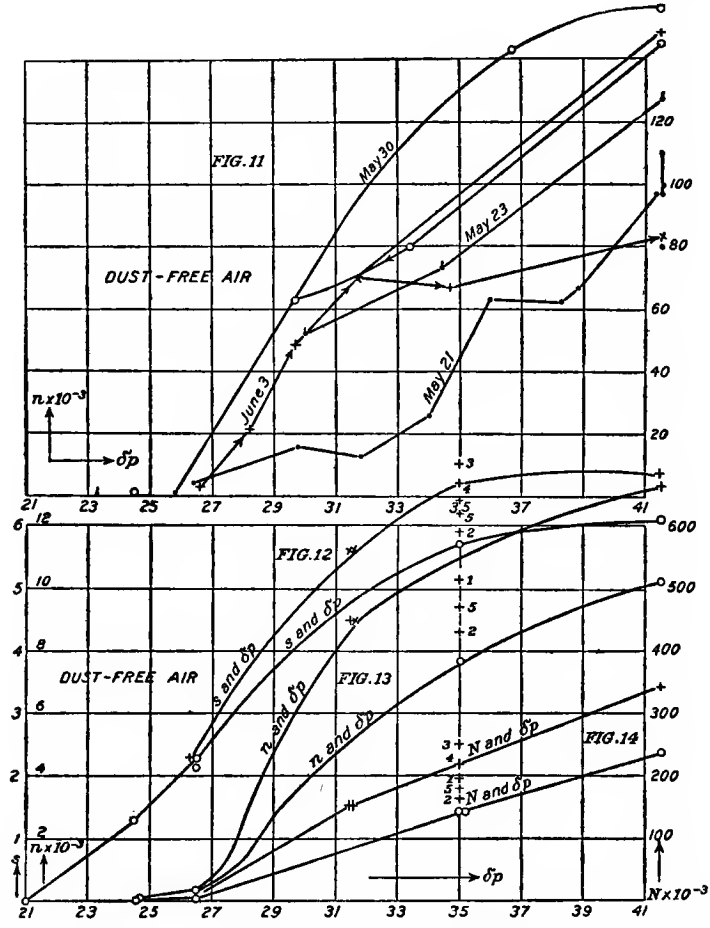

FIGS. 11, 12, 13, and 14.—Early data of efficient nucleations (N, n) and coronal diameter (s), appearing at different exhaustions (δp) in dust-free air. Imperfect fog chamber.

slow filtration presupposed) are liable to show the true efficient nucleation at the time of experiment. Direct experiments made under conditions show that intervals of from one to two hours will in all cases be sufficient for the decay of extraneous nuclei.

TABLE 7.—Nucleation of dust-free, non-energized and energized air, different exhaustions, δp. Lapse about 15 min. Barometer, 75.97 cm. Piping and stopcock of 1-inch gas pipe.

δp.	s.	$n \times 10^{-3}$.	$N \times 10^{-3}$.
I. Dust-free air not energized.			
35.1	6.2	94	180
26.0	2	2.7	3.9
26.3	2.3	3.8	5.8
24.2	1.2	1.4	2.1
22.6	(?)	(?)	(?)
22.6	[1].5	.2	.3
21.0	[2].0	.0	.0
II. Radium on middle of side of fog chamber.			
21.0	3.3	11	15
19.0	(?)	(?)	(?)
19.0	[1].5	.2	.3
20.1	2.1	2.5	3.4
22.4	4.8	37	53
24.1	4.9	41	61
26.0	5.2	52	80
30.0	5.2	55	93
35.0	5.1	56	106
III. Dust-free air.			
35.0	6.2	94	180
33.0	5.8	80	143
31.1	5.5	68	117
29.3	5.2	54	91
27.6	3.1	10	16
28.1	3.8	21	34
26.3	2.1	3	4.7
28.1	3.8	21	34
29.6	4.7	41	70
31.2	5.3	60	103
33.1	5.8	80	143
35.2	[3]5.8	82	155
IV. X-ray bulb. $D = 100$ cm.; fronting bottom.[4]			
42.0	[5]7.0	146	338
41.4	[5]7.0	145	332
35.0	[5]7.0	134	255
30.7	[5]7.2	131	222
26.2	6.5	94	146
24.0	6.2	79	113
IV (continued). X-ray bulb. $D = 100$ cm.; fronting bottom.[4]			
22.7	5.6	59	85
20.9	4.9	37	53
18.8	[6]?.9	.9	?1.1
19.0	?1.0	.9	?1.2
19.0	1.2	1.2	1.6
V. X-ray bulb. $D = 50$ cm.			
19.0	1.2	1.2	1.7
VI. X-ray bulb. $D = 25$ cm.			
19.2	1.7	1.8	2.4
19.2	[7]1.3	1.3	1.8
18.2	.0	.0	.0
18.2	.0	.0	.0
VII. $D = 50$ cm. above[8] fog chamber.			
19.0	1.2	1.2	1.6
19.9	2.9	6.7	9.1
20.9	4.4	26	36
21.3	5.6	54	77
22.7	5.8	63	91
24.4	wrg 7.3	117	175
26.2	wog' 7.8	130	200
27.7	wo'g 7.8	135	217
29.8	gBP 8.3	150	249
[9]33.0	gBP	156	281
34.9	gBP	160	303
38.3	gBP	167	346
42.0	wog' 7.9	?174	?400
VIII. $D = 600$ cm. from end.			
35.0	[10]4.4	35	67
33.7	4.6	41	75
31.0	4.6	40	68
28.0	4.6	37	60
25.8	4.6	36	56
24.2	4.6	35	52
22.7	4.3	26	38
20.9	3.0	7.7	11
19.7	1.3	1.3	1.8

[1] Vanishing at once and faint, only just visible.
[2] Nothing (fog or rain) observed.
[3] Accidental slow reopening: same result.
[4] Exposure 2 minutes. No increment of N results.
[5] All large w r g coronas.
[6] Coronas clear but too small.
[7] Bottom of glass 1 cm. thick, interferes with formation of persistent nuclei even at short distances like 25 cm. $= D$.
[8] Persistent nuclei just begin to be generated. $s < 0.5$ cm. maximum for fleeting nuclei.
[9] Next day.
[10] Smaller than air coronas; s always taken.

13. Effect of X-rays and gamma-rays. Data.—To interpret the above results it will be necessary to vary the nucleations of the dust-free air artificially, by acting on it from the outside of the chamber with the X-rays, or with the gamma-rays of radium.

In these experiments the glass fog chamber (fig. 1), rigorously free from leakage, was used with a framework of wet cloth within. Filtration was throughout excessively slow and all other precautions were taken. The radium in the hermetically sealed aluminum tube was pasted to the top of the fog chamber at T. The X-ray bulb was adjustable, so as to act from different positions at distances D.

Table 8 shows results where δp is the pressure difference, $s/30$ the angular coronal diameter, when the distances of the eye and the lamp are 35 cm. and 300 cm. from the fog chamber. The small distances D (35 cm.) enabled the observer to see even the smallest coronas distinctly. The nucleation n is obtained by supposing that the nuclei are restored faster than they can be removed by exhaustion. In case of N this is not the case, so that the correction for volume expansion is added. For high pressure differences the absolute numbers are not trustworthy, but the data given nevertheless show the relations satisfactorily.

TABLE 8.—Persistent nuclei. Exposure 2^m. D measured from anticathode to top of fog chamber. Thick (1 mm.) aluminum screen (earthed) interposed.

D.	δp.	s.	$N \times 10^{-3}$.	Lp.	D.	δp.	s.	$N \times 10^{-3}$.	Lp.
cm.	*cm.*			*min.*	*cm.*	*cm.*			*min.*
12	18.0	7.8	140	0	30	18.2	3.0	9	1
20	18.6	5.3	56	0		18.2	3.2	12	0
	18.4	5.7	67	1	50	18.4	.0	0	0
30	18.0	2	....	0	40	18.3	2.7	7.2	1
	18.0	[1]4.0	22	1		18.0	1.0	1.2	1
	17.5	3.0	9	2		18.0	1.0	1.2	1
	18.2	2.7	7	0	50	18.0	[2].5	.1	2
	18.2	[1]3.1	10	1		....	.5	.1	1

[1] Spontaneous generation. [2] Just visible before falling.

The data of table 8 are constructed in the charts, figs. 15 to 17, showing the s, n, and N curves in succession, for increasing supersaturations. They will be useful for comparison with the advanced work below.

14. Persistent nuclei.—Table 8 gives the corresponding data for persistent nuclei. Distances are here measured from the sides of the fog chamber where the glass was thinner (about 0.2 cm.) than at the end (1 cm.). No persistent nuclei were obtained when the radiation

passed through the end of the fog chamber as in table 7. To guard against direct inductive action the fog chamber was covered with an earthed plate of aluminum, 0.5 mm. thick, though this precaution is superfluous. The table shows the distance (D) of the anticathode above

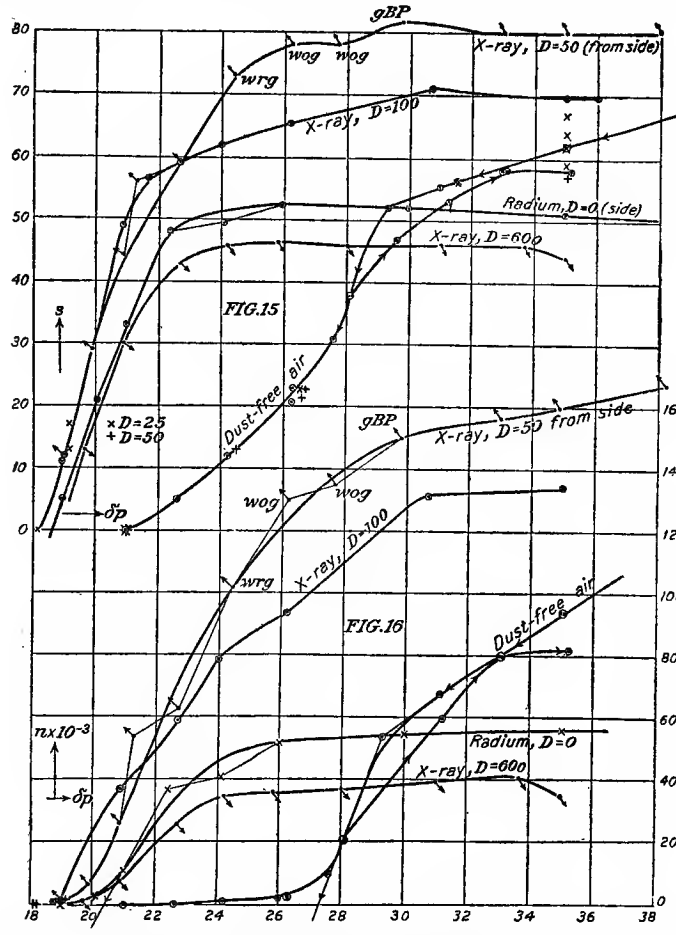

FIGS. 15 and 16.—Early data of efficient nucleations (N, n) and coronal diameter (s), appearing at different exhaustions (δp) in dust-free air. Imperfect fog chamber. (Illustrating table 7.)

the fog chamber, the coronal diameter ($s/30$), the nucleation (N; n would have no meaning here), and the time elapsing (Lp), after the radiations are cut off until the observations are made. The time of exposure was uniformly 2 minutes. Longer exposures would have produced seriously

distorted coronas. These data are constructed in fig. 18, the s values being dotted and the N values drawn in full.

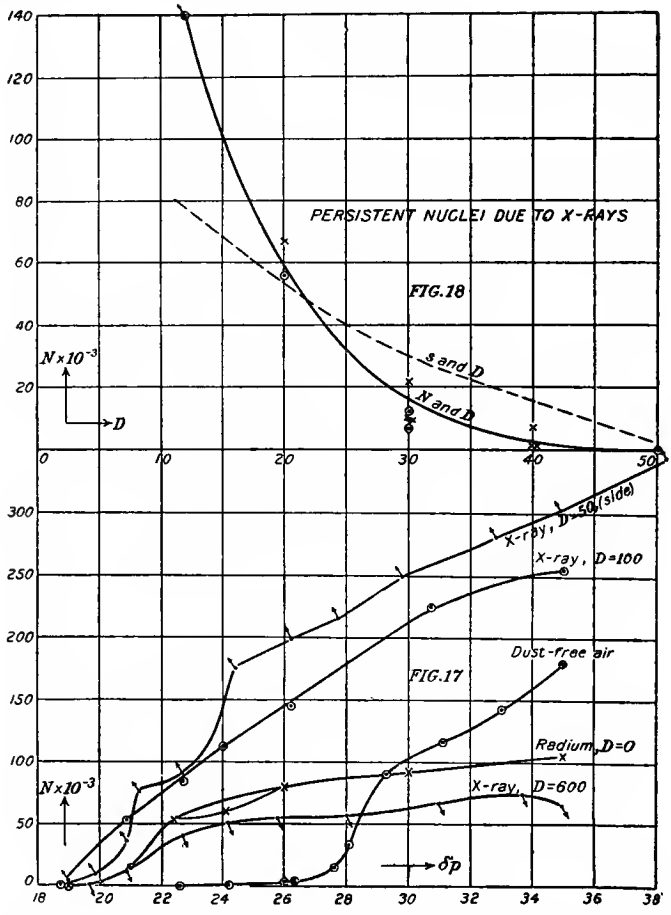

FIG. 17.—Nucleation (N) for different exhaustions (δp) and radiations. Bulb distance.

FIG. 18.—Persistent nucleation (N) produced by X-rays acting from different distances (D) from the glass fog chamber. Table 9.

15. Persistent nuclei generated through tin plate.—In view of the ease with which the cylindrical fog chambers may be made rigorously air-tight, it seemed worth while to endeavor to produce persistent nuclei through a plate of tinned sheet-iron, 0.03 cm. thick and 14 by 20 inches square. In the following trials exposures for 2 minutes to the

X-ray bulb, at a distance of about 12 cm. between the anticathode and the glass wall (0.3 cm. thick) of the fog chamber, are in question. The earthed iron plate was placed between bulb and chamber, resting on the latter. A lapse of time of 1 minute was allowed after the radiation had been cut off. This suffices to show that nuclei of the persistent kind have been entrapped. Naturally the pressure difference used precipitated no appreciable fog in the absence of radiation.

These results show conclusively that persistent nuclei may be produced through earthed tin plate, provided the thickness used is not excessive.

TABLE 9.—Persistent nuclei through earthed tinned iron plate, 0.03 cm. $\delta p = 25$ cm., practically below fog limit. Exposure to X-rays, 2 minutes; lapse, 1 minute; observation during exposure.

X-rays—	s.	$n \times 10^{-3}$.
On.....	2.0	2.5
Off	.0	.0
On.....	2.0	2.5
Off.....	.0	.0
On.....	[1]Weak	....

[1] $\delta p = 24.5$; corona too faint for measurement, but definitely present.

16. Discussion.—The simplest of the graphs are those of figure 18, showing the decrease of persistent nuclei as the bulb is gradually removed (D increasing and measured from the side of the chamber) from the apparatus. This decrease is very rapid and implies that if the anticathode were actually in contact with the glass walls the production of persistent nuclei in 2 minutes would be enormous. The distortion of the coronas resulting under these circumstances, as detailed in the last memoir, is not, therefore, surprising. It should be remembered that the rays have to penetrate more than 2 mm. of glass. On the whole the action is very much like what C. T. R. Wilson describes for ultraviolet light.

As in the earlier case, there is *secondary generation; i.e.*, the number of nuclei is larger if the observations are made at 1 or 2 minutes or more after the radiation has been cut off.

With the given apparatus, persistent nuclei were still produced for a distance of 0.5 meter between the X-ray bulb and fog chamber, though the coronas in that case were but just discernible and vanished too rapidly for measurement. The corresponding intensity of ionization

is then near the point of transition from persistent to fleeting nuclei, a result which will presently be made use of.

The pressure difference ($\delta p = 18$ cm.) used throughout is (for the given apparatus) far below the fog limit for dust-free air ($\delta p = 21$ to 26).

In case of the fleeting nuclei or ions, the generation is instantaneous and it will be necessary to represent the data (s, n, N) for a continuous series of supersaturations for each of the five intensities of ionization applied, beginning with non-energized dust-free air. These are given for both increasing and decreasing values of δp, the latter being at times larger (as would be expected from the removal of larger groups on condensation); but on the whole the data are very satisfactory.

Remembering that the number is roughly as the cube root of s, the region of ions ($\delta p = 21$ to 26) is particularly well represented. They increase slowly but regularly in number until the coronal stages are reached. Beyond these the increase is again slow; but that it is real is shown by the top curve for X-ray nuclei, which fails to ascend.

The lowest pressure at which the suggestion of a corona could be observed in the given apparatus was $\delta p = 21$ cm. The coronal fog limit is best found from the other curves.

The succeeding curves (X-ray, $D = 600$; radium, $D = 0$; X-ray, $D = 100$, 50, 25 from end and 50 cm. from side) correspond to gradually increasing ionization. It may be noticed that the fog limits slowly move to the left into smaller supersaturations, while the initial slope of the curves gradually rises. Persistence sets in when the slope is nearest the vertical. All the curves eventually approach a limit, which for weak radiation is practically reached near the fog limit of air, but for strong radiation much beyond it. In the upper curves the green-blue-purple corona first appears at $\delta p = 30$ cm. It is noteworthy that the asymptote is reached later as the ionization is stronger.

The relation of these results as to numbers of nuclei is best shown by the n-curves, fig. 16, though the scale is now too small for the ions of non-energized air. In this case (n) it is assumed that the nuclei are reproduced faster than they can be removed by expansion. The curves throughout have the same characteristic, being doubly inflected and showing definite stages in which nucleation increases most rapidly. If these branches are prolonged backwards the coronal fog limit may be specified for each, as shown in the figures. This quantity decreases at a retarded rate, while the ionization grows more intense.

The effect of weak ionization (radium, or X-ray at $D = 600$) is to increase the number of ions. It has been supposed above that the result of this is to mask the corresponding increase of any of the colloidal nuclei originally present, should such an increase occur.

The curves, moreover, throw important light on the distance effect D. Thus at $\delta p = 22$, the effect of increasing D from 1 to 6 meters is a fall of n from 50,000 to 20,000—about 60 per cent. At $\delta p = 30$ the fall is from 130,000 to 40,000—about 69 per cent. Owing to the uncertainties of observation these numbers may possibly be the same, in which case the gradation of size of the nuclei would be the same for all intensities of ionization.

The initially slow increase of the upper curves ($D = 50$ cm.) is possibly due to the formation of persistent nuclei, as stated at the beginning of this section, these capturing much of the moisture.

Finally, the evidence given by the N curves, fig. 17 (assuming that the nucleation is not restored faster than it can be removed by the exhaustions), is much the same as that just detailed. The curves are often straighter than heretofore, and continually rise as the result of the increasing volume expansion; but the double inflection remains. In fact, the rise of all the upper curves is eventually at about the same rate as for air. In the latter case the scale is again too small to show the increase in the region of ions.

At $\delta p = 22$ the distance effect for 1 and 6 meters is a decrease of 60 per cent, at $\delta p = 30$ a decrease of 71 per cent, naturally nearly the same as above.

Both the N and n curves show that while within the limits of observation intense radiation increases the nucleation of dust-free air, this is not the case for weak ionization. Here the curves cross at about $\delta p = 29$ cm. Above this the presence of radiation must decrease the efficient nucleation of non-energized dust-free air; below this it will increase it. At high pressure differences like $\delta p = 41$ cm., as used below, the variation of the efficient nucleation must therefore be a sensitive criterion for the variation of the ionization of air. Similarly the direct experiments of sections 7 and 9 find their explanation in the manner already pointed out.

17. More rapid exhaustion. Apparatus and data.—The preceding set of experiments correspond to the particular exhaustion cock used. This was an inch plug gas cock. As almost the whole resistance to flow was encountered here, the advisability of enlarging it seemed evident. In fact, on opening the cock suddenly to an amount corresponding respectively to about 1/4, 1/2, 3/4, 1/1, the nucleations obtained were about $N \times 10^{-3} = 40$, 100, 180, 350 for $\delta p = 41$ cm., showing that not even an approach to the limit is reached in the extreme case. There is a further objection in having the large resistance in the stopcock, as the coronas will vary with the degree of opening.

TABLE 10.—Nucleation of dust-free air, energized or not. New apparatus, 1½-inch stopcock; connections of inch gas pipe. Barometer 76.23 cm. Walls of fog chamber 0.3 cm. thick. Three horizontal wet cloth partitions within chamber.

δp.	s.	$n \times 10^{-3}$.	$N \times 10^{-3}$.
	I.		
44	[1]7.7	180	440
42	[1]7.6	175	400
	7.6	175	400
	7.6	175	400
35	[1]7.6	160	300
	7.6	160	300
30.8	[2]7.5	137	235
26.1	2.6	62	9.7
24.3	.7	.2	.4
	.5	.1	.2
25.3	1.4	1.7	2.6
26.1	2.6	6.2	9.7
27.0	3.6	17	27.5
27.6	5.0	46	75
28.6	5.4	60	99
29.3	6.3	92	153
30.5	7.0	125	212
35.0	[1]7.7	160	300
35.0	[1]7.8	160	300
30.5	[2]7.5	136	230
	II. Radium tube added on side. Barometer 76.05 cm. (Mean values.)		
43.6	4.4	40	95
35.0	5.4	67	126
30.8	5.6	69	120
26.4	5.6	64	97
24.2	5.6	60	87
22.8	5.6	57	87
21.2	5.6	55	74
20.0	4.1	20	28
18.8	0	0	0
19.0	0	0	0
19.0	.5	.1	.1
19.6	2.6	5.2	6.9
20.4	4.9	37	51
21.0	5.2	43	60
	III. X-rays. $D = 50$ cm. from side.		
48.9	[3]7.6	190	560
43.6	[4]8.0	216	530

δp.	s.	$n \times 10^{-3}$.	$N \times 10^{-3}$.
	III (continued). X-rays. $D = 50$ cm. from side.		
35.2	[6]9.0	240	450
30.8	[5]9.3	258	440
26.6	[5]9.2	229	360
22.8	[3]8.0	137	200
21.5	[3]7.3	120	170
20.8	[6]7.2	100	138
19.5	5.1	39	52
18.6	1.1	1	1
18.3	?0	?0	?0
	IV. X-rays. $D = 12$ cm. from side.		
18.9	2.2	2.7	3.7
20.0	5.7	54	74
21.0	[3]7.4	117	165
23.0	[7]7.3	125	180
24.5	[6]9.5	195	290
29.3	[8]10.5	290	490
35.0	[8]10.7	320	610
43.7	[9]10.3	306	750
52.2	[4]9.4	240	760
	V. Dust-free air. Fog chamber with 4-sheeted wet cloth. 2 to 3 cm. apart. Barometer 76.36 cm.		
28.8	5.1	....	....
27.0	3.4	....	....
25.3	?.0	....	....
25.8	2.1	....	....
25.3	?.0	....	....
25.8	2.3	....	....
	2.1	....	....
	2.3	....	....
30.8	[8]7.3	....	....
31.6	[5]7.4	....	....
32.3	([8])	....	....
33.1	[8]7.7	....	....
34.0	[9]7.8	....	....

[1] g′BP corona steadily repeated, but not quite clear. [2] w o g. [3] G B P. [4] w P corona.
[5] w r g. [6] w y g. [7] g y o g′. [8] w o g′. [9] Vague.

Accordingly the inch stopcock was replaced by a 1½-inch plug gas cock, retaining the same inch tubing. The resistance in this case was least at the stopcock, which accounts for the remarkable steadiness of the results obtained in successive exhaustions.

Furthermore, the fog chamber was modified by inserting three wet cloth partitions, horizontal and about 5 cm. apart, as shown in fig. 3. The new form was not merely favorable to better saturation, but all convection currents were more effectually cut off. This was at first (though incorrectly) supposed to be the reason for the appearance of distributions of nuclei within the chamber produced by the action of radium kept outside of it, a result already detailed above, but which here appeared for the first time in a very marked degree. In the later experiments four cloth partitions were inserted, as in fig. 4.

The results are given in the successive parts, table 10, in the usual way, dust-free air being examined with and without the interference of external radiation. It is not probable that any errors are now introduced by the filter.

In view of the intense ionization used, the usual cycle of measurable coronas is exceeded, and the resulting data become more and more fully relative, both on this account and because of the high pressure differences applied. Absolute values are, however, of little interest, and it is precisely from the relations obtained that conclusions are to be drawn. The quantities s, n, N, δp have been frequently defined. D is measured from the side of the apparatus, so that all action takes place through 0.3 cm. of glass. No aluminum screen was interposed.

18. Remarks on the s-curves. Non-energized air.—The present s-curves for non-energized air, fig. 19, are in strong contrast with the preceding. Variability in the lapse of time has been nearly eliminated. The curves have moved bodily somewhat farther to the left into the region of smaller supersaturations, as is shown by comparison with the dotted line in fig. 19 (taken from the preceding fig. 15), evidencing the increase of efficiency referred to. The curves of fig. 19 are in remarkable contrast with the preceding in two respects; they reach a definite asymptote at about $\delta p = 35$, which is retained until the pressure difference is so high that other complications step in. There is certainly an increment after $\delta p = 30$, as proved by the change of coronas. Whether this limit is due to a cessation of further drop of temperature in the apparatus, or whether a distinct group of colloidal air nuclei is in question, remains to be seen. The possibility of the continued succession of groups of this kind is not, *a priori*, improbable.

19. The same, continued.—The other characteristic, which was entirely unforeseen, is the relative absence in what has been called the ionized region (placed in the former curves, fig. 15, between about $\delta p = 21$ and $\delta p = 26$). The contrast is clearly shown in fig. 19. The only explanation which suggests itself to me is this, that what were supposed to be ions were really water nuclei due to the somewhat slower exhaustion of the preceding experiment. In other words, particles caught at the end of the somewhat less rapid expansion evaporated into the larger particles, leaving water nuclei behind. But apart from this, the definite trend with which the curve reaches the abscissa is characteristic, and, so far as coronas go, there seems to be an absence of nuclei below $\delta p = 24$. In other words, the fog limit has been raised, in spite of the general lowering of the necessary supersaturations throughout the curve. The new curve is almost wholly coronal.

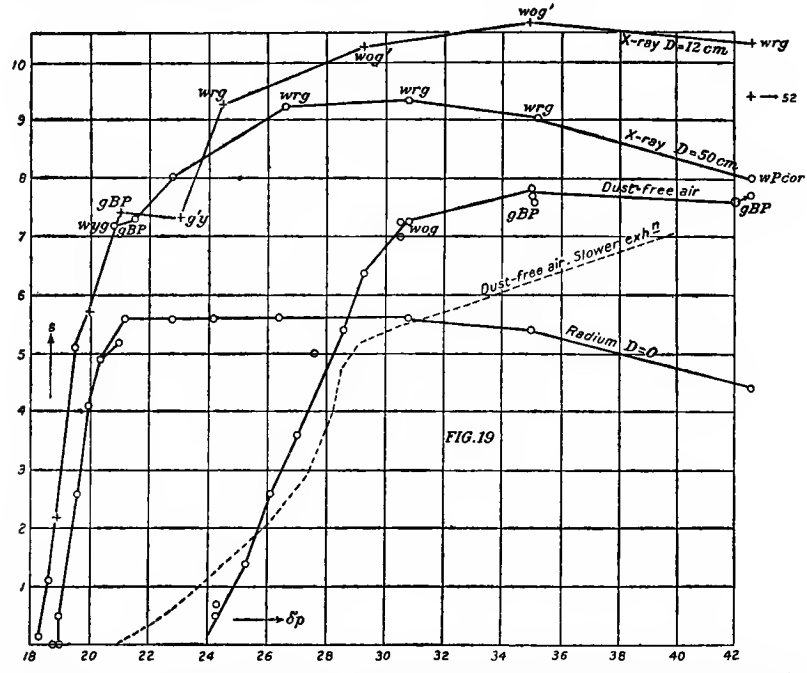

FIG. 19.—Improved fog chamber. Apertures of coronas (s) seen in dust-free air, energized or not, as stated, by radium or X-rays, at different exhaustions (δp). Table 10.

Usually the same results are obtained in a pressure-increasing and in a pressure-decreasing series. There is an equally striking uniformity in the lapse of time.

20. The same, continued. Action of radium.—The action of radium is characterized by a slight rise of the asymptote over the preceding case and of displacement of the curve into smaller supersaturations. This was to be anticipated; nuclei are caught more easily, and a somewhat smaller order of size and increased number is detected in consequence. The other distinctive feature is the smaller range of pressure differences within which practically all condensation occurs. In the preceding experiments this range lay between $\delta p = 18$ and 24, whereas in the present case the marked changes fall between $\delta p = 19$ and 21. There results another apparent rise of the fog limit corresponding to the coronal effects, though it is slight and uncertain. What is noteworthy is the greater steepness of the rising branch of the curve, already indicated. The question may be asked whether for a rigorously instantaneous exhaustion this part of the curve would become even more nearly vertical. One may note that the radium curve eventually passes through a maximum. Furthermore, while in its initial stages it lies very near the former X-ray curve ($D = 50$), the latter shows no tendency to reach a near asymptote.

21. The same. Action of X-rays.—Finally, the results with the X-rays are similar. High asymptotes, a tendency of the curve to lie within a region of lower supersaturations than in table 7, etc., are apparent. Nuclei smaller in size and larger in number have been caught more easily than heretofore. If we regard the present and the earlier curves for $D = 50$, the height of asymptote in the former case is much above the one in the latter case, and moreover passes through the maximum (reached at $\delta p = 26$) as δp increases indefinitely. This corresponds to the result for radium.

It is therefore interesting that if the radiation is further intensified, as in the last case, where $D = 12$ cm., the curve continues to rise apparently throughout higher ranges of pressure. The limits are not reached (δp continually increasing) until nuclei of a size equal in smallness to the order holding for the colloidal nuclei of air have become available for condensation. A final point deserving comment is the break of the X-ray curve near $\delta p = 22$. This is not only marked in both curves of table 10, but similarly apparent in table 7. Unfortunately, the cycle of coronas changes at this point (green-blue-purple corona); but apart from this it seems probable that with intense X-ray radiation, two successive groups of nuclei are in question; the first group prominent below $\delta p = 22$ and the second above $\delta p = 22$.

22. Remarks on the n-curves. Non-energized air.—The n-curves, which assume that the nuclei are replaced sooner than they can be

removed by exhaustion, bring out the points just made with better regard to the actual nucleation, seeing that the *s*-curves are specially favorable to small numbers of nuclei. As a rule the new nucleations obtained are nearly twice as large as the old results. It seems probable that the upper inflection, after passing the nearly straight part, is due

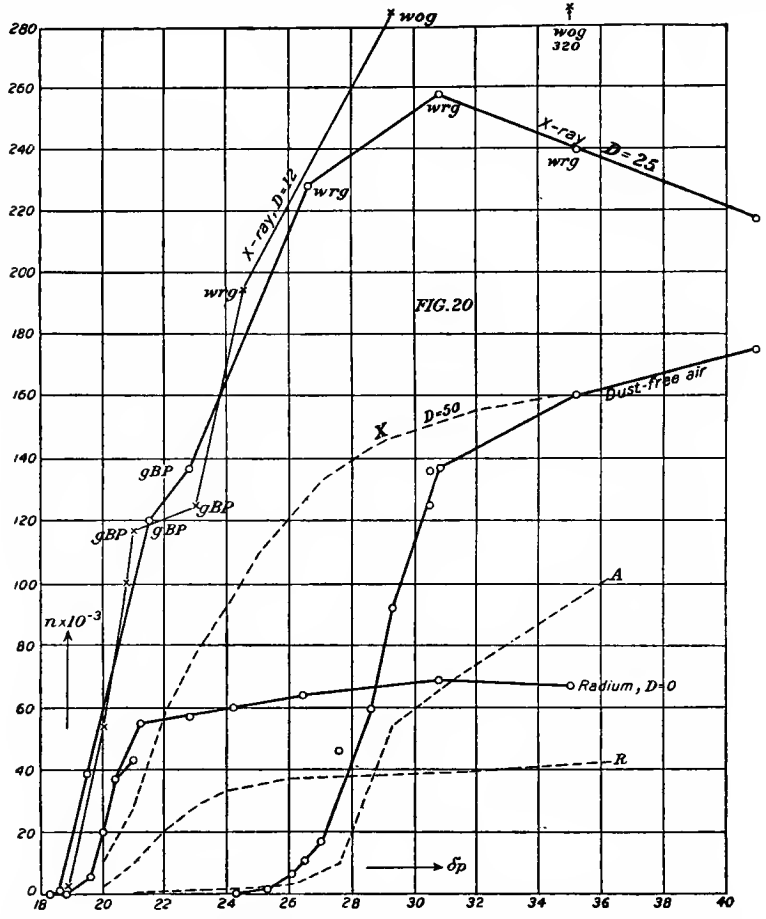

FIG. 20.—Improved fog chamber. Efficient nucleation (n) free air corresponding to fig. 19. Table 10.

to the waning condensing power of the apparatus, and that in the absence of this loss of efficiency the middle region of the doubly inflected curve would continue indefinitely. One may note, too, that both in case of tables 7 and 10 the parts in question are nearly parallel, or that the increment of nucleation corresponding to a given increment of super-

saturation is about the same. This applies even in the following cases, where dust-free air is energized by radium and by intense X-radiation, as far as the middle regions of the curve are concerned.

23. The same. Action of radium.—The small increment of pressure difference (say $\delta p = 19$ to 21) is here in sharp contrast to the gradual increase observed in the old results (say between $\delta p = 19$ and 25). The nucleations which eventually are not quite doubled in the new results, as compared with the older, are therefore at first enormously in excess. In fig. 20 the results of table 10 are given in full, the old results (table 7) in broken lines, and the same method is pursued in the other cases.

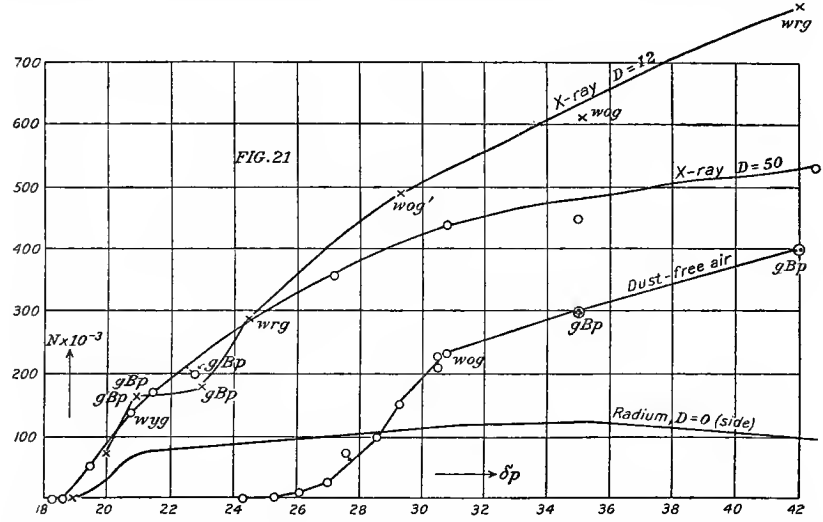

FIG. 21.—Efficient nucleation (N) in dust-free air corresponding to fig. 19. Table 10.

24. The same. Action of X-rays.—Remarks to the same effect may be made with reference to the old and the new data for X-ray ionization when $D = 50$ (broken and full lines in fig. 20). Initially the old curve is even below the present curve for radium, but it eventually intersects the new data for dust-free air at about $\delta p = 35$. The mean nucleations have not been quite doubled. The maxima in cases of $D = 50$ and $D = 12$ lie above the interval of large variation for dust-free air. Finally, the breaks in the curves at $\delta p = 22$ are again quite apparent.

25. Remarks on the N-curves.—With regard to the N-curves, fig. 21, one need merely note that the maxima have in most cases been definitely wiped out, and that the nucleation available for condensation, if it be supposed that removal of nuclei is more rapid than the reproduction, increases continually with the supersaturation up to the highest values.

THE NUCLEATION OF FILTERED AIR IN THE LAPSE OF TIME.

26. Method.—In the above experiments with filtered air, it has been carefully pointed out that all the curves tend to reach asymptotes, the height of which depends on the other (larger) nuclei present. If, then, the ionization of dust-free air is an essentially variable quantity, as shown by the electrometer, the height of the asymptote in question should be correspondingly variable.

Again, it was shown that external radiation (gamma-rays of radium for instance) are powerful nucleators, whether directly or secondarily. Hence external radiation of this type, if variable, might be reasonably sought for in a study of the nucleation of dust-free air.

In relation to the ordinary intensities of radiation, this method of varying asymptotes is exceedingly sensitive. Whether, however, it will apply for cases of much weaker (cosmical) radiation must be left to experiment. Moreover, whether the variable ionization of air can be detected in the manner suggested, or whether it even exists in the fog chamber, is similarly a question requiring experimental solution.

27. Early data.—The method here in question was carried out in a series of experiments begun May 9 and continued until September 2, 1905. In the earlier part of the work it was shown that comparable results could only be expected in cases of excessively slow filtration, the filters for this purpose being 18 inches long, 2 inches or more in diameter, and containing cotton very tightly packed. It was necessary, moreover, to make observations after long intervals (12 to 24 hours) of waiting, the object being to allow all nuclei which might have passed through the filter time to decay. Apparent variations of considerable interest were obtained in this way; but the work below will show them to have been untrustworthy. Neither changes of temperature nor of the barometer produced any effect.

To additionally safeguard the work, two fog chambers were eventually installed side by side, drawn upon by the same exhaustion system identically in every way. It was then found that the internal partitions of wet cloth were essential, but it was nevertheless impossible to make both chambers agree even when the partitions were increased four-fold. Throughout the work, nucleations passing through maxima and minima within the limits of about 400,000 and 160,000 were obtained, apparently under trustworthy conditions. The data remained consistent even when the fog chambers were exchanged. Small variations of the rate of filtration were quite ineffective, showing that a limit has been reached.

28. Apparatus modified.—The tubing of the preceding apparatus, which consisted of inch plug cock and inch gas pipe, was now taken apart and a 1½-inch brass plug cock was substituted. The advantage of this arrangement is easily seen, inasmuch as the whole resistance to flow is practically in the pipes. The passage-way in the stopcock being larger in area, the rate of exhaustion obtained is independent of slight differences in opening.

As a result of this, all the variations noted above practically disappeared, and the nucleations of dust-free air at a given pressure difference were found to be constant in the lapse of time within the limits of accuracy of the method. Data of this character are shown in the following table:

TABLE 11.—Nucleation in the lapse of time. $\delta p = 30.6$ cm. w o g'; $n \times 10^{-3} = 127$; $N \times 10^{-3} = 227$.

Date.	Corona.	s.	Date.	Corona.	s.
Sept. 5[1]	w o g	7.4	Sept. 12	w o g	....
6	w o g	7.4	13	w o g	7
7	w o g	7.4	14	w o g	7.2
8	w o g	7.4	15	w o g	7
9	w o g	7.4	16	w o g[3]	7.1
9[2]	w o g	7.3	18	w o g	7.2
10	w y' g	7.4	20	w o g	....
11	w o g?	....	21	w o g	7.2

[1] Apparatus with three sheets.
[2] Apparatus with four sheets.
[3] Apparatus with one sheet, 10 cm. above surface of water.

Indeed, the succession of different fog chambers with 1, 2, and 3 cloth partitions all gave the same results. The rate of filtration could be varied without effect within wide limits, and the same corona was obtained after a few minutes or after 24 hours of waiting.

29. Inferences.—It has, therefore, not been possible to detect changes of nucleation, either as the result of the concomitant changes of atmospheric ionization or as the possible result of some form of cosmical or at least external radiation. The consistency of the results obtained for radiation under widely different conditions may be especially pointed out. It does not follow, however, that other methods (not depending on the terminal asymptote) may not be more efficient. In how far this is the case will be shown in Chapter VI.

SUMMARY OF THE RESULTS OF THE CHAPTER.

30. Distribution of ions within the fog chamber.—Within the fog chamber, the coronas due to the ions produced either by radium or by the X-rays acting axially from long distances, as a rule vary in aperture from one end of the long vessel to the other. Hence the distribution of nuclei is not uniform in the direction of the axis of the fog chamber. The reason for this is to be ascribed to secondary radiation. As interpreted from the nucleation produced within the fog chamber containing dust-free moist air, dense bodies (brass cap) produce more secondary radiation than rare bodies (glass end) under like conditions of primary radiation.

If the primary radiation is relatively intense, rare bodies like glass may produce more secondary radiation than dense bodies (like the metals) under less intense primary radiation; or at least the decrement of primary radiation with the distance from the source predominates within the fog chamber.

The secondary radiation is rapidly absorbed by the air, as the diminishing coronas testify.

31. Minimum of efficient nucleation.—When ions and colloidal nuclei are in presence of each other (or in general any two groups of nuclei of different average size), the number of efficient nuclei for the case of a drop of pressure not too small passes through a well-defined minimum, if the number of ions continually increases from zero. This occurs, for instance, when a radium tube is moved from a long distance quite up to the fog chamber. The ions abstract more and more of the available moisture, until the colloidal nuclei are practically inactive (minimum), after which the nucleation increases again with the number of ions.

32. Persistent nuclei.—For the moderately intense X-ray bulb (5-inch spark) and a glass fog chamber several millimeters thick, persistent nuclei may be demonstrably produced when the distance from bulb to chamber increases to about 50 cm. They may even be produced through thin tin plate. The decrease with distance of the number generated within a given time is very rapid, and the number producible if the anticathode could touch the fog chamber would be enormous. In like manner the number increases at an accelerated rate with time of exposure as if the nuclei were themselves active.

If we regard the ionized state of a gas as characterized by a kind of kinetic ionization pressure, we may further conceive the ionized gas to

be subject to something resembling saturation, whereby ions pass into persistent nuclei when the ionization pressure reaches a certain limit very much as a vapor condenses.

33. Dependence of efficiency of fog chamber on the size of the exhaust pipes.—If a (long) cylindrical fog chamber, whose contents are not much in excess of 6,000 c. cm., be exhausted into a vacuum chamber whose contents exceed 100,000 c. cm., through a passage-way 50 cm. in length and about 2.5 cm. in bore, many of the experiments showing the properties of ions and of the colloidal nuclei of dust-free air are consistently producible, provided the plug exhaustion stopcock (opened quite and as quickly as possible) has a wider bore than the pipes. With exhaust pipes of this size, however, the apparatus is as yet very far from its limits of efficiency, and the largest or terminal corona obtainable in case of the colloidal nucleation of dust-free air is, even at the highest exhaustion, the intermediate green-blue-purple type. This leaves the whole order of large coronas outstanding, though the order may be entered if the air is intensely ionized. It follows that efficiency actually stops short because of the smallness of the colloidal nuclei.

The curves showing the nucleation entrapped in case of continually increasing exhaustion all have a common feature; there is an initial low branch of small variation attributable to ions; an intermediate branch showing steep ascent, due to colloidal nuclei; a final asymptotic branch, corresponding to the terminal corona and due to the loss of efficiency of the apparatus. The middle branch in question, or line of representative colloidal nuclei, if it appears at all, has almost the same slope and position (relative to the field as a whole) for all fog chambers, whether their efficiency be small or great. The fog chamber ceases to act almost abruptly; in other words, the terminal corona or largest corona producible as the drop of pressure continually increases, appears in any fog chamber as an almost sudden departure from the representative lines. This corona is larger or smaller, the asymptote higher or lower, as the fog chamber is more or less efficient.

34. Invariable character of colloidal nucleation in the lapse of time.—The terminal corona (in a given type of apparatus), if not too small (Chapter VI), is a fixture as to size in the lapse of time (months). It does not vary appreciably with the departure from normal ionization, to which atmospheric air is incident. Probably the number of available colloidal nuclei is too enormous, as compared with the small variations in number of the relatively large ions, to admit of an observable effect.

CHAPTER II.

LATER AND FINAL STAGES IN THE EFFICIENCY OF THE FOG CHAMBER DUE TO A GRADUAL INCREASE IN THE BORE OF THE EXHAUST PIPES.

CONNECTING PIPES NOT LARGER THAN 1.5 INCHES IN DIAMETER.

35. Introductory.—It will be the object of the present chapter to further determine to what an extent a perfectly efficient apparatus (*i. e.*, one in which the cooling and the moisture precipitated per cubic centimeter actually accords with the drop in pressure) may be approached by gradually enlarging the bore of the escape pipes between the vacuum chamber and the fog chamber. One method of doing this will consist in finding whether the distribution curves eventually reach a fixed limit and a limit maintained for larger as well as smaller nuclei; another by comparing the final results with corresponding data deduced for Wilson's piston apparatus.

In treating the large numbers of observations which follow, it will be convenient to refer the nucleations (as above) to the drop of pressure observed under *apparently* isothermal conditions at the fog chamber. This method of comparison is sufficient if the same fog and vacuum chambers are used throughout, as has actually been done in the sequel. The exhaust cock is always to be closed immediately after exhaustion. In the present experiments the volume ratio of the two vessels was about $v/V = 0.064$, where v is the volume of the fog chamber and V that of the vacuum chamber.

It was customary, as just stated, to open the stopcock between the fog chamber and the vacuum chamber as rapidly as possible and then to close it at once; δp therefore denotes the drop of pressure read off on the mercury gage at the fog chamber after sufficient waiting. As above, s is the angular diameter of the coronas on a goniometer radius of 30 cm., when the eye and the source of light are respectively 40 cm. and 250 cm. on opposite sides of the fog chamber. On the basis of these data n is computed from the quantity* of water precipitated per cubic centimeter and the value s, in the way shown elsewhere.† It is always assumed that the nuclei are more rapidly reproduced than removed by the exhaustion, or (without hypothesis) from another point of view,

* Wilson: Phil. Trans. Roy. Soc. London, vol. 189, 1897, p. 298.

† Smithsonian Contributions, vol. XXXIV, No. 1651, 1905, chap. viii.

that the nucleation of the *exhausted* fog chamber is specified. Otherwise it would be necessary to multiply by the ratio of volumes after and before exhaustion.

Diagrams of the apparatus used have already been given in Chapter II (figs. 1 to 4), and further examples will be shown of the details of the more perfected forms below (figs. 26, 34, 64). In those paragraphs, moreover, I will treat the corrections to be applied (which are much larger than were anticipated) in order to pass from the *observed* apparent δp to the true values. These must be computed from the volume ratio of the two chambers and their respective initial and their final isothermal pressures when in communication.

36. Examples of data for 1-inch connecting pipes.—These were about 18 inches or more in length and the stopcock inserted was 1½ inches in bore, as specified in the preceding chapter. The plug was as usual floated in paraffin oil, absolutely preventing the influx of atmospheric air, though some leakage (which is generally harmless) from the fog chamber to the vacuum chamber could not be prevented. The fog chamber in these exhaustions had a rather larger charge of water than usual, a circumstance to which the higher fog limits may possibly be due, since these vary with the volume ratio.

TABLE 12.—Pipes 1 inch, cock 1½ inches. Non-energized dust-free air. October 24.

δp.	s.	$n \times 10^{-3}$.
30.6	7.4	139
28.9	5.8	74
27.2	4.4	26
25.7	1.5	1.9
24.6	...	0

The results are to be shown below (fig. 22, p. 37) in comparison with the later values and may be passed over here.

37. Data for pipes 1.5 inches in diameter.—Fog chamber and vacuum chamber were now connected by brass gas pipes 1½ inches in diameter and 2 feet long, and the plug stopcock interposed was 2 inches in bore. In the case of table 13 the disposition of apparatus was such as to require the length of piping specified with an elbow. The results are given in the usual way and show a distinct gain in efficiency over the earlier set in table 13, proving that greater width of pipe is still an advantage.

TABLE 13.—Nucleation of dust-free air, energized or not, as stated, at different supersaturations. Plug gas cock, 2 inches; piping 1½ inches in bore, 2 feet long.

δp.	s.	$n \times 10^{-3}$.
I. Non-energized air.		
cm.	*cm.*	
30.7	[1]7.2	151
28.2	5.9	77
26.3	3.7	19.7
24.4	2.7	6.8
22.4	2.3	3.3
20.3	.0	.0
22.0	1.7	2.1
24.7	2.7	6.8
27.6	6.1	80
29.9	[2]7.3	135
34.2	[3]8.1	190
Non-energized air. Experiments.		
34.8	8.4	190
34.7	[4]10.0	270
34.8	[6]8.9	220
34.6	[4]10.7	270
34.5	[6]9.0	220
II. Non-energized air.		
42.1	[6]9.3	250
34.5	[7]10.5	318
32.1	[8]9.2	262
30.0	[9]8.0	150
27.9	6.1	80
26.0	3.8	20
24.3	2.7	6.7
22.5	2.0	2.3
21.1	?1.0	1
17.3	!.0	.0
18.6	!.0	.0

δp.	s.	$n \times 10^{-3}$.
II (continued). Non-energized air.		
19.9	?0.8	0.6
20.4	1.2	1.2
21.0	1.6	1.7
Later.		
43.5	[7]11.2	354
47.9	[7]11.2	372
43.8	[7]10.8	338
39.1	[6]10.1	286
34.9	[10]8.9	192
30.8	[11]7.5	144
III. Air energized by radium, on side of glass fog chamber.		
21.7	6.0	67
20.9	5.7	56
20.2	5.2	42
18.6	1.0	.8
16.5	.0	.0
?18.7	1.2	?1.2
18.8	1.9	2.0
21.0	?5.7	56
20.0	5.4	47
26.4	6.8	104
24.9	6.8	100
23.5	6.8	96
22.0	6.7	89
20.0	5.4	47
29.0	6.5	99
33.2	6.0	88
38.9	5.9	91
43.6	5.7	85

δp.	s.	$n \times 10^{-3}$.
IV. Air energized by X-rays[12]. $D = 20$ cm. from side of fog chamber to anticathode.		
34.7	[13]12.3	400
31.0	[13]12.3	380
26.3	[13]12.3	340
22.0	[14]10.6	207
17.6	1.4	1
16.5	.0	0
17.6	2.1	2
19.6	[15]8.1	140
19.0	4.4	24
V. X-rays. $D = 50$ cm.		
32.1	[16]11.4	310
35.0	[16]11.3	320
26.6	[14]10.7	233
22.1	[17]8.6	145
17.4	?r	0
17.7	?0	0
19.0	2.2	2.7
20.0	6.1	64
X-rays. $D = 20$ cm. after long waiting.		
34.6	[18]11.2	....

[1] g' B p, repeated. [2] g y o b g. [3] w p cor. [4] w v o g, after waiting one or more hours. [5] w' P cor after waiting but a few (10 to 15) minutes. [6] w c g. [7] w o g. [8] w r g. [9] g' B P. [10] w P cor. [11] w y cor. [12] Air non-energized, $\delta p = 34.8$; $\epsilon = 9.6$; and by X-rays. [13] w y g' large. [14] w r g. [15] w c g. [16] w o b g. [17] w P cor. [18] g y o b g.

Long waiting before exhaustion (to remove water nuclei) is often essential. In addition to the dust-free gas, air energized by radium (10 mg. of a weak sample, 10,000×, sealed in aluminum and acting from without) and by the X-rays is treated for comparison.

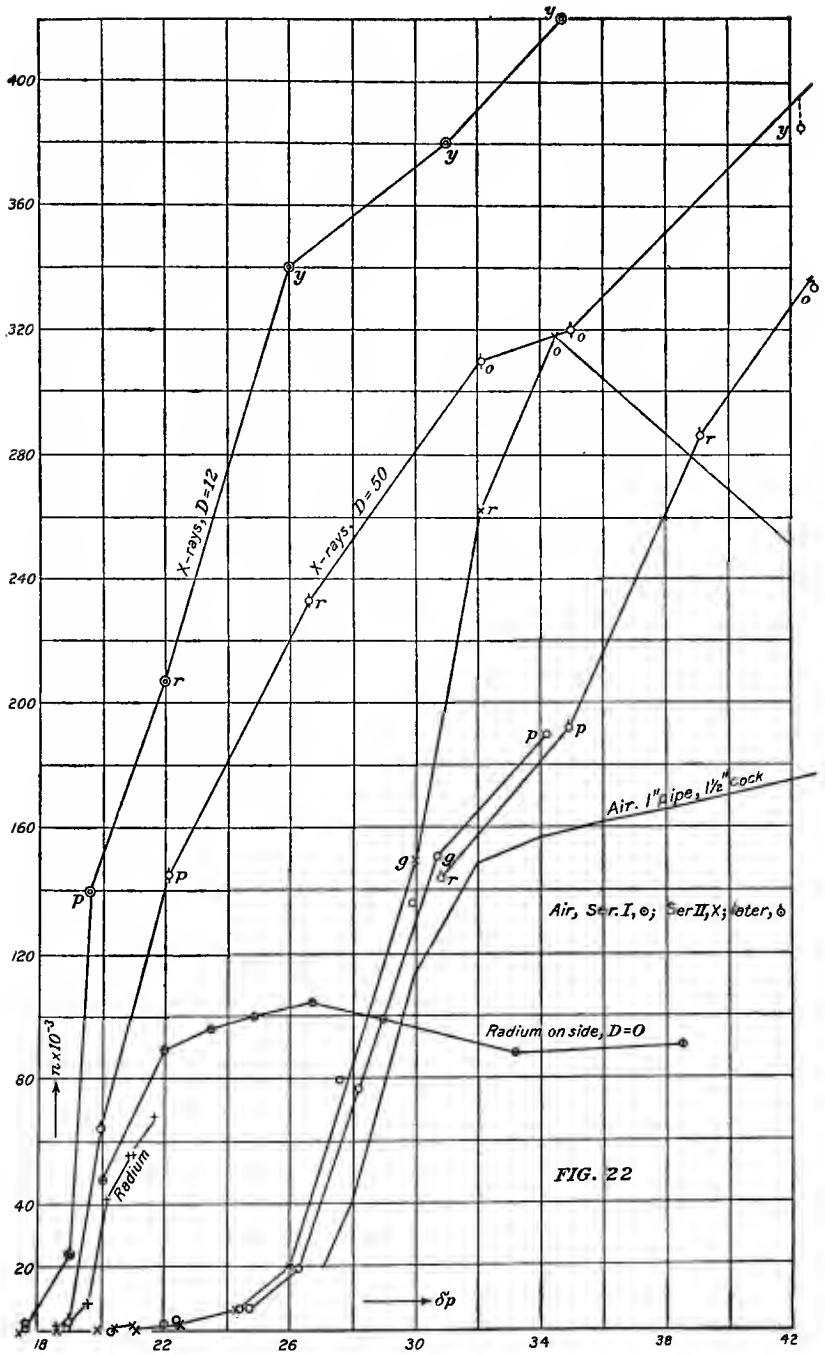

FIG. 22

FIG. 22—Efficient nucleation (n) found in dust-free air energized or not by radium or the X-rays, as stated, from different distances (D), at different exhaustions (δp). [illegible] Table 13

These results, together with the data of table 12, are shown in fig. 22. For the air curve a marked advance beyond the results of table 12 is at once apparent, but it is noteworthy that the slopes of both curves are in the main the same, in spite of the fact that the former rises to but one-half or one-third of the height of the new curve. The efficiency of both fog chambers therefore terminates abruptly in a final or fixed corona or (in the chart) in an asymptote which would be horizontal, if it were not necessary to assume that the quantity of water, m, precipitated per cubic centimeter increases with the drop in pressure. In the different series, irregularities are often apparent which are difficult to explain, though at low values they may be due to cosmical radiation. Thus the second series for non-energized air rises more abruptly than the first and third, results which are possibly associated with the presence of water nuclei and referable to different degrees of leakage from fog chamber to vacuum chamber; but it is also possible that unequally rapid closing of the stop-cock after exhaustion may have left an impression. The results for radium and the X-rays will reappear under better conditions presently, and may then be discussed. One may note that for weak radiation the graphs intersect the graph for non-energized air.

38. Continued. Shorter pipes.—The next step consisted in a remodeling of the apparatus, whereby shorter connecting pipes would suffice. Two 6-inch nipples, 1½ inches in diameter and containing a 2-inch plug stopcock, now joined the fog and vacuum chambers. The results are shown in table 14 and in fig. 23. The fact that the main resistance is still encountered in the gas cock is proved by the need of stops to insure quick and complete opening. Whenever the cock is nearly but not quite opened, however suddenly, low coronas are observed. When this was remedied, fixed coronas thereafter corresponded to each δp. The table contains the usual series of comparative results for air energized by radium and the X-rays.

As compared with the preceding data there is a small shifting of the graph toward lower pressures, while the slopes in the representative parts of the curves are practically the same. The terminal corona, however, and the corresponding asymptote, is markedly raised. Nevertheless, though the large green-blue-purple corona now appears in the case of strongly energized air, it has not yet been reached in the non-energized cases. The limit of efficiency is therefore not yet in sight when a fog chamber of about $v = 6{,}000$ c. cm. empties into a vacuum chamber of about $V = 100{,}000$ c. cm. through 30 cm. of piping about 4 cm. in diameter, with a corresponding plug stopcock suddenly opened between stops to arrest the motion.

TABLE 14.—Nucleation of dust-free air, energized or not, at different supersaturations. Plug gas cock, 2 inches; piping 1½ inches in diameter, 2 × 6 inches long. Long intervals between observations.

δp.	s.	Corona.	$n \times 10^{-3}$.
I. Non-energized air.[1]			
39.8	12.8	g y o b g	460
39.8	13.0	w y b g	420
35.1	13.0	w y g	400
30.8	10.4	w r g	260
28.6	7.4	w r g	108
27.9	5.7	w B P	69
26.0	2.4	cor	4.5
26.4	3.6	cor	17
II. Non-energized air.[1]			
24.3	1.5	cor	1.8
24.4	1.8	cor	2.1
26.2	2.6	cor	6.3
27.3	5.0	cor	46
28.0	6.4	w r g	92
29.3	7.6	g B P	139
29.5	8.0	g B P +	147
30.9	10.0	w r o g	290
30.4	8.4	w c g	230
31.2	9.1	w r g	260
35.0	11.5	w y g′	400
III. Non-energized air.			
31.0	9.8	w r o g	290
31.0	10.3	w r o g	290
31.0	[2]10.4	w r o g	290
35.3	12.0	w y b g	400
35.1	12.0	w y b g	400
39.4	12.0	w y b g	420
44.1	12.5	g y o	490
41.3	12.5	g y o	470
38.6	12.0	w y b g	420
30.7	10.2	w r g	290
IV. X-rays at $D = 20$ cm. from side.			
30.9	13.0	g B P	460
35.4	13.0	g B P	480
33.0	13.0	g B P	470
31.5	13.0	g B P	460
29.2	13.0	g B P	430
IV (continued). X-rays at $D = 20$ cm. from side.			
27.2	12.7	g y o	380
25.6	12.7	g y o	360
24.1	12.2	w y g′	320
22.8	11.9	w o g	250
29.4	12.3	g B P	440
27.1	Vague	g B P	410
20.8	7.7	....	120
23.4	11.7	w o g	250
22.9	11.4	w o g	250
21.4	8.4	g B P	120
20.2	4.6	cor	30
18.7	.0	....	0
18.3	.0	....	0
IV. X-rays. $D = 10$ cm.			
35.1	14.0	[3]g B P	480
40.3	....	g B P	510
37.9	....	g B P	500
33.6	....	g B P	470
31.6	....	g B P	460
30.0	....	g B P	450
28.1	....	g B P	430
26.7	....	g B P	410
25.0	13.5	[4]g B P	400
23.6	12.6	g y o	320
22.3	10.3	w o g	250
21.2	7.1	w o g	100
20.1	4.2	cor	21
18.7	1.3	cor	1.3
V. Air[5] energized by radium, $D = 0$, on side.			
30.8	6.1	cor	87
35.2	6.2	cor	95
40.0	5.9	cor	92
27.6	6.0	cor	79
26.2	6.1	cor	78
24.3	6.3	cor	79
22.9	6.5	cor	85
21.6	6.1	cor	68
21.0	4.7	cor	33
19.7	2.1	cor	2.5
19.2	.0	....	.0

[1] In neither series I or II were stops provided for the exhaust cock. This is the case in series III, et seq.
[2] Filter open 90° without danger. Evaporated corona shows $s = 7.6$.
[3] Coronas at first stone-blue and irregular, soon becoming g B P.
[4] Clear g B P at once.
[5] For air, $s = 9.9$ w o g. $n \times 10^{-3} = 290$. Large coronas fall out, leaving a smaller one behind.

Several interesting features are seen in the radium and X-ray curves in fig. 23, to which special attention may be called. It will be observed that the curves for distances $D = 10$ and 20 cm. of the anticathode from the sides of the fog chamber begin and terminate in nearly coincident curves and coronas, but that they lie at some distance apart in their middle regions. Hence available* nuclei are apparently not more numerous eventually in one case than in the other, but they are larger (virtually) in the middle regions for the stronger radiations; in other words, the asymptote is more quickly approached for the stronger radiation.

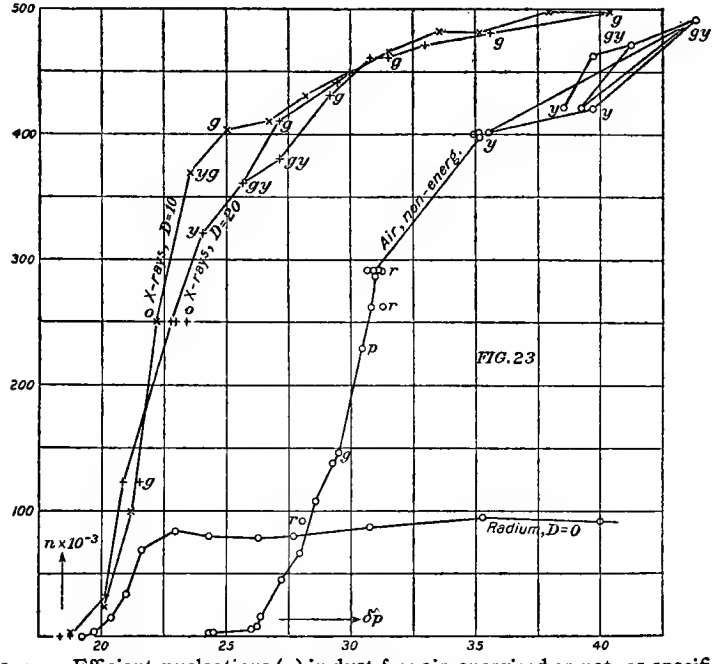

FIG. 23.—Efficient nucleations (n) in dust-free air, energized or not, as specified at different exhaustions (δp). Table 14.

Again, the terminal corona in case of the data for X-rays is reached long after the final coronas for the weak radiation from radium (10 mg. 10,000×); *i. e.*, the number of nuclei (ions) in the case of the weak radiation ceases to increase in a region of lower exhaustion, apparently, than the one observed for the more intense radiation. Hence in case of the latter, finer gradations of nuclei appear to occur, as if the radiation shattered certain of the larger ions. There is, however, another point of

*It will appear below that for nuclei, large or small, the limit is reached with the given *number* of nuclei per cubic centimeter, corresponding to the g B P corona. Nuclei in excess of this, large or small, are inefficient.

view to which some probability may be assigned. In the case of intense radiation relatively large and possibly persistent nuclei are produced in greater numbers, and these may capture much of the moisture and prevent condensation on the smaller ions, until proportionately larger exhaustions have been applied. Examples of these occurrences will be given in the next paragraph.

CONNECTING PIPES TWO INCHES IN DIAMETER.

39. Remarks on the method.—The connection between fog chamber and vacuum chamber was now further enlarged by using two nipples 6 inches long and 2 inches in diameter, on either side of a plug stopcock of $2\frac{1}{2}$ inches bore. The latter was chosen, since much of the resistance was heretofore encountered in this place. Usually observations were taken at long intervals of time apart, to allow for the dissipation of water nuclei due to the evaporation of very small fog particles. Moreover, a considerable period (three days) elapsed before definite results could be recorded. Something of a nuclei-producing character is usually present some time after assembling the parts of the apparatus. The coronas under otherwise like circumstance gradually increase to a maximum. Moreover, in the absence of all leakage inward from without, periodicity of coronal diameter is often in evidence in the successive exhaustions and especially active in case of the very large coronas. The best results appear after long waiting before each observation, whence it follows that evaporation from the heavy paraffin oil used for tightening the stopcocks, leakage of nuclei through the filter or through unknown channels is quite ineffective. Waiting was finally made needless by first exhausting the partially exhausted fog chamber before each definite observation. The effective drop of pressure is then small and only the large nuclei are caught and the fog particles do not evaporate appreciably. The filter, moreover, in all tests gives evidence of entire trustworthiness. It was customary to open and close the plug cock quickly, between stops, a spring opening device having been put in action. In no case was there danger of under-saturation, the wet cloth linings being but 8 or 10 cm. apart, above and below. In the highest exhaustions used, $\delta p = 44$ cm. about, the volume expansion is fully 2.5, so that 60 per cent of the air must thereafter be readmitted freshly through the filter. Naturally in this slow passage it would be not only denucleated but deionized, if there were not fresh sources of penetrating radiation always in action for the reproduction of both types of nuclei. In general the apparatus seems to have behaved faultlessly. Such irregularities as remain must then in large measure have been introduced by the fact that the drop of pressure

was *observed* at the fog chamber when isothermal conditions had been reestablished. It should have been computed from the initial pressures of both chambers and their common isothermal pressure when in communication, in the way shown in the next section. The present results, however, suffice for comparison with the preceding and following work, and it is probable that limiting conditions of efficiency have already been reached. That this is actually the case will also be shown in the next section.

40. Data for pipes 2 inches in diameter, 12 inches long.—The results obtained are fully given in table 15. It appears that coronas, even above the large green-blue-purple type, appeared at the high exhaustions, but this is not quite certain.

Incidentally some data on the effect of X-rays from different distances are included in the tables (part VI *et seq.*). The usual difficulty of an inconstant X-ray bulb appears. Moreover, certain peculiar results on the distribution of the nuclei within the fog chamber in case of symmetrical exposure to weak radium are here again noticed (part V), as in Chapter I, section 4. The results are plotted in fig. 24 and smooth curves obtained therefrom are shown in fig. 25.

TABLE 15.—Air nucleation at different supersaturations. Piping 2 inches in diameter, 12 inches long; plug gas cock, 2½ inches in bore. Wait 30 minutes between observations. Angular diameter of coronas, $2 \sin^{-1} s/60$. Eye 40 cm., lamp 250 cm., on opposite sides of fog chamber. δp observed isothermally at the fog chamber.

δp.	s.	Corona.	$n \times 10^{-3}$.
I. Non-energized dust-free air.			
35.4	14	g B P	480
35.3	14	g B P	480
40.6	14	g B P	510
44.4	14	[1]g B P	540
41.4	14	g B P	520
36.6	14	g B P	490
33.0	14	g B P	470
31.1	....	g y o	410
29.5	10.3	w r′ g	250
27.7	6.4	w r′ g	91
29.3	10.4	w r g	250
28.0	6.7	w r g	104
26.2	2.6	cor	6.3
26.0	3.1	cor	9.9
24.0	1.0	cor	1.2
27.2	7.1	w y′ g	120
I. Non-energized dust-free air—Cont'd.			
28.0	7.7	wPcor	170
28.9	10.6	w r o g	280
30.8	12.5	g y o	410
31.8	12.8	g y o	420
33.0	13.0	g B P	470
II. Air energized by X-rays; $D = 10$ cm.			
33.3	([3])	([3])	470
35.0	....	([3])	480
39.8	13.5	b′ B P	510
31.7	....	b′ B P	460
26.9	....	b′ B P	420
24.5	11.5	b′ B P	390
23.3	11.7	g B P	380
21.0	13	w o bg	230
II. Air energized by X-rays; $D = 10$ cm.—Cont'd.			
20.4	9.0	w c g	170
21.0	11.4	w o bg	230
19.7	6.2	wr bg	190
19.1	4.1	cor	19
18.4	1.3	cor	1
17.4	.0	....	0
Continued, next day; $D = 10$ cm.			
18.5	[4]0	....	0
18.5	0	....	0
18.9	1.6	cor	2
20.3	6.8	w r g	87
20.9	9.3	w c g′	180
21.9	....	g y o	330

[1] Stone-blue colors, above g B P.
[2] Irregular. Shows strong purple band just above water. Coronas diffuse.
[3] Stone-blue.
[4] Left over night seems to diminish rainlike condensation.

TABLE 15.—Continued.

δp.	s.	Corona.	$n \times 10^{-3}$.
III. Air energized by X-rays; $D = 60$ cm.			
17.5	0.0	....	0
19.1	1.7	cor	2
20.3	6.1	w r g	65
21.0	8.7	w c g	180
22.5	11.7	w o g′	250
22.8	12.2	w o g′	270
23.5	[1]13.0	g y o	340
24.8	....	g y o	350
26.6	....	g y o	370
26.6	....	g y o	370
30.9	....	g y o	410
35.8	....	g y o	440
IV. Air energized by X-rays; $D = 600$.			
40.0	8.7	....	250
36.0	7.3	cor	150
31.7	6.1	cor	90
27.2	5.2	cor	52
24.4	5.2	cor	50
23.0	5.2	cor	46
21.0	5.0	cor	39
19.4	.0	....	0
19.4	.0	....	0
18.1	.0	....	0
20.3	3.1	cor	8
21.0	4.8	cor	35
23.0	5.7	cor	60
26.3	5.4	cor	57
31.0	5.8	cor	76
35.3	[2]6.9	cor	130
35.4	6.8	cor	125
39.8	8.1	w r	205
44.3	10.0	w o	322
44.4	[3]10.0	w o	322
V. Air energized by radium (10 mg. 10,000×); $D = 0$, on side.			
44.3	[4]9.7	w o′	305
40.2	7.5	w r′	153
35.9	6.6	w o	115
33.5	6.6	w r	111
30.8	6.5	w r	103
27.0	6.1	w r	79
24.4	5.8	w r	66
23.2	6.2	cor	74
20.9	5.8	cor	60
20.5	4.7	cor	32
19.4	1.3	cor	1.3
18.3	.0	....	.0
VI. Air energized by X-rays.			
[5]22.9	5.5	w r g	55
[6]22.9	7.3	w y g	110
[7]22.9	7.7	w | BP	140
[8]22.9	9.7	w c g	200
VII. Air energized by X-rays; $D = 200$ cm.			
19.0	2.1	cor	2
20.3	6.8	w r g	85
20.9	7.4	w g	105
22.8	7.5	!gBP	125
25.9	7.5	gBP	135
31.1	7.4	w y g	135
30.4	[9]7.4	w o g	130
35.5	7.4	w o g	135
35.1	[9]7.4	w o g	135
40.0	7.4	w o g	145
43.9	7.0	wrog	135
VIII. Air energized by X-rays; $D = 600$ cm.; repeated for contrast.			
43.9	10.7	w o g	300
46.8	10.6	w o g	310
48.8	10.5	w o g	320
IX. Air energized by X-rays; $D = 100$ cm.			
44.4	7.6	w | BP	180
41.9	7.6	w | BP	170
36.2	7.6	g B P	160
31.8	7.6	g B P	150
25.4	[10]8.8	w c g′	200
26.5	9.2	w r g	205
24.0	9.3	w c g	195
21.6	8.2	w | BP	130
20.8	7.4	w y g	105
20.3	5.5	cor	50
19.7	[11]4.1	cor	19
28.0	8.8	w c g′	215
31.6	7.8	g | BP	170
X. Air energized by X-rays; $D = 50$ cm. from end.			
30.8	8.8	w r g	230
35.6	8.7	wPcor	220
40.1	8.2	wPcor	205
XI. The same; $D = 50$ cm. Bulb more efficient.			
31.6	9.8	w c g	245
27.0	10.8	wrog	235
25.2	10.9	wrog	225
22.2	10.0	w c g	200
20.3	6.1	w r g	65
35.1	9.2	w c g	240
40.0	8.3	wPcor	205
44.0	7.8	w | BP	180
48.7	7.7	g | BP	190
32.2	10.4	wrog	260

[1] As intensity of ionization increases there is less shattering.
[2] Next day. Fog chamber absolutely tight. Coronas all blurred.
[3] The final use in response to new conditions.
[4] Coronas blurred and larger at the glass end of fog chamber.
[5] $D = 600$ cm.
[6] $D = 3{,}000$ cm.
[7] $D = 150$ cm.
[8] $D = 75$ cm.
[9] Long waiting (½ hour to 2 hours) without effect.
[10] Passing, as usual, through a maximum.
[11] Fog limit below 20.

41. The same, continued. X-ray bulb inclosed in lead.—In the experiments detailed the X-ray bulb was not inclosed, so that secondary radiation issued from the whole surrounding environment. In the data given in table 17 the bulb is surrounded by a wide lead box, containing a window 7.5 cm. in diameter fronting the fog chamber. The window was in a removable side or lid of the box. This was kept at a long distance ($D = 600$ cm.) in order to furnish weaker ionization than was specified in table 15.

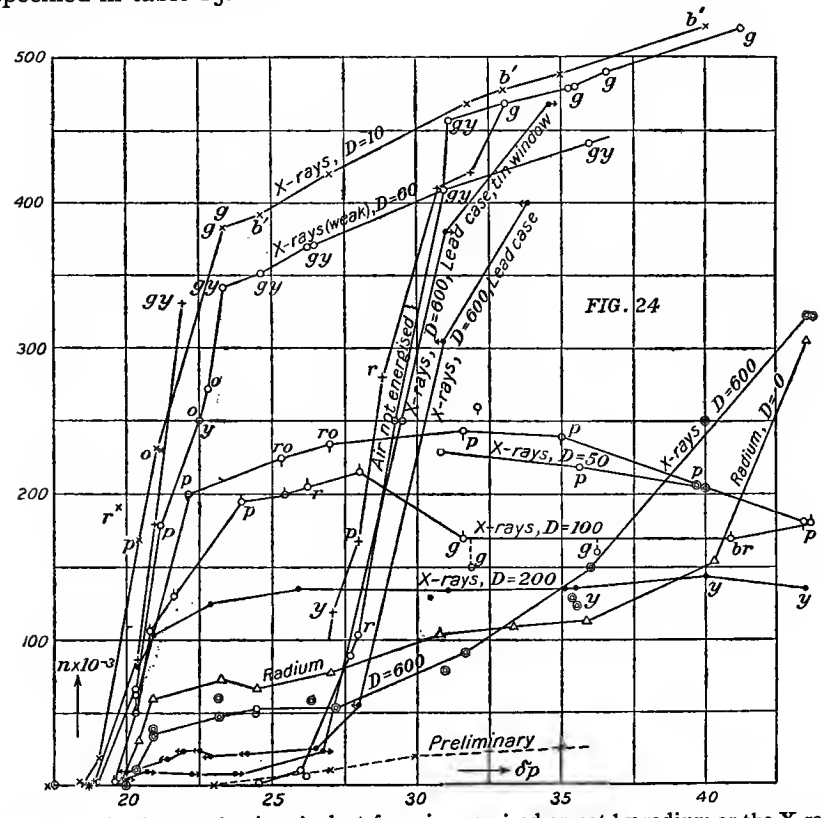

FIG. 24.—Efficient nucleations in dust-free air, energized or not by radium or the X-rays from different distances (D) and different exhaustions (δp). X-ray bulb not within lead case, unless stated.

In the first part of table 16 the exhaustion, $\delta p = 27$ cm., lies below the fog limit of dust-free air. The low degree of ionization is thus shown under different conditions. The second series contains a number of successive exhaustions for an increasing δp, with the radiation passing through a thin tin plate. Parts III and IV of the table are similar

series, with the window open (tin plate removed), the last series being a detail for the initial part of the curve, which is of especial interest. The results are also shown in fig. 24, where their relation to the lowest curve, $D=600$ cm., for the open or non-inclosed X-ray bulb becomes evident. In each of these curves there is a definite horizontal branch within which the ions predominate. Beyond this lies the rise due to the colloidal nuclei, but the curves, and particularly the asymptotes, are depressed in both cases.

TABLE 16.—Nucleations at different exhaustions. 2½-inch cock, 2-inch piping, 12 inches long. X-ray bulb in lead case at $D=600$ cm. from glass fog chamber. Aperture in case 7.5 cm. in diameter.

Lead box.	s.	Cor.	δp.	$n \times 10^{-3}$.
I. Window open.....	3.1	cor	20.5	8.4
Window closed with lead.	.0	cor	20.5	.0
Window open.....	3.4	cor	20.5	11.7
Window closed with tin[1].	2.9	cor	20.5	6.8
Front lead side off[2].....	3.5	cor	20.5	13.0
II. Closed with tin plate...	.0	cor	18.6	.0
	3.0	cor	20.6	7.6
	2.7	cor	22.3	6.4
	2.8	cor	23.7	7.0
	4.1	cor	26.8	24.3
	12.0	w y b g	31.2	380
		g B P	34.7	480
III. Tin plate off.....	....	[3]w y b g	33.8	400
	....	w o g	31.0	305
	5.2	w r	28.0	55
	4.2	cor	26.6	26
	4.1	cor	24.5	23
	4.2	cor	22.5	24
	3.4	cor	20.7	12
	2.6	cor	20.0	5.2
Tin plate on.....	1.7	cor	20.0	1.7
IV. Tin plate off.....	2.5	cor	20.0	4.8
	3.8	cor	21.5	17
	4.2	cor	22.0	24
	4.0	cor	22.7	20
	4.0	cor	24.0	21

[1] Open side over 1 foot square.

[2] Lead sheet 0.12 cm. thick; tin plate 0.03 cm. thick.

[3] After long waiting.

42. Discussion.—It will now be in place to make a more complete survey of the manifestations of nucleation in dust-free air under any conditions. Figs. 24 and 25 are useful for this purpose. With regard to the method I may recall that the difficulties were enhanced by the need of providing rapid exhaustions in case of a fog chamber large enough to measure the coronas and to show the sequence of axial colors.

The earliest results (Chapter I, section 12) scarcely captured the maximum of 30,000 nuclei under the extreme exhaustion corresponding to the limiting asymptote (marked "preliminary" in fig. 24). In proportion as the apparatus was perfected, this asymptote was raised, step by step, until nucleations of at least 500,000 were left in the *exhausted* fog chamber. Probably the asymptote, or more accurately the terminal corona, obtained in any given type of apparatus, indicates that the limit of condensing

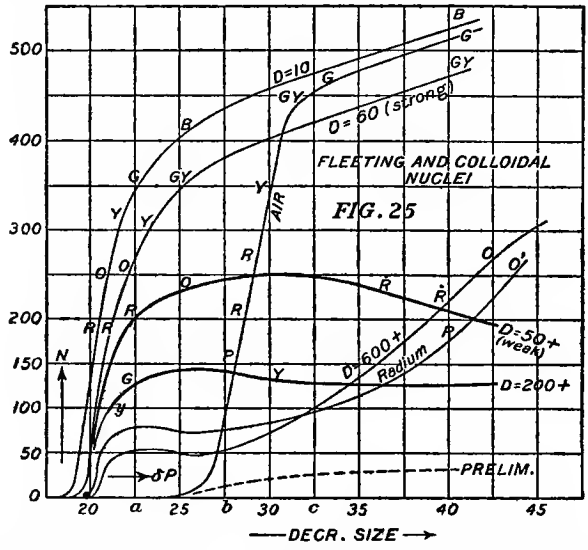

Fig. 25—Smooth curve from fig. 24. Nucleation (N) of dust-free air, in thousands of nuclei per cubic centimeter, energized or not, as stated, by weak radium, or by the X-rays, at different distances (D in cm.). The letters attached to the curves indicate the characteristic colors of the inner field (or its margin) of the largest coronas, the order of colors being R, O, Y, G, B. The abscissas show the *observed* isothermal drop of pressure by which the supersaturation is produced and the nucleations applied relatively to the given apparatus. The line marked "air" shows the behavior of dust-free non-energized air terminating in the large green coronas. In a perfect apparatus supersaturation would increase enormously beyond *a;* the droplets would be at freezing beyond *b*. In the given apparatus efficiency probably ceases beyond *c* when damp air is the medium.

power has been reached. Between the fog limit and the terminal corona the graph rises in a straight upward sweep; and it is remarkable that the rates at which the nucleation decrease with the drop of pressure, or better with the volume expansion, are about the same between fog limit and asymptote, no matter whether they lie within the region of high supersaturation characteristic of the colloidal nuclei or in the region of relatively low supersaturation characteristic of ionized air. Moreover,

they are the same in any apparatus, within the limits of its efficiency. In fact, even the curve which I have endeavored to reduce to the same scale from Wilson's disk colors for non-energized dust-free air (apart from differences in the meaning of δp to be explained in the next section) lies in the same region of pressure difference, and shows a slope quite in keeping with the other curves.* For an imperfect apparatus, on the other hand, the slope terminates abruptly at a lower asymptote and in a region of higher exhaustion. It will be convenient to refer to the nuclei belonging to the slopes specified as representative nuclei.

To obtain the curve for the colloidal nuclei of dust-free air, it is often necessary to wait a week or more, until unknown internal sources of nucleation have spent themselves. Moreover, the isolated observations made with advantage ought to be made hours apart, for it is with the exhaustion that the release of spurious internal nuclei occurs, suggesting that water nuclei due to the evaporation of small fog particles are possibly in question.

The air curve passes through the first two cycles of large coronas, terminating beyond the highest green-blue-purple, actually in the stone-blue or higher coronas, the first of the series producible in the fog chamber by any means whatever. It corresponds with the opaque of the steam jet, beyond which, however, there exists another cycle of yellows, to my knowledge beyond the reach of the fog chamber. It is not probable that the medium is as yet quite optically inactive after the bluish coronas specified, but merely appears so in small thicknesses.

If we turn from the curve of non-energized air to the case of *weak ionization* such as is produced by 10 mg. of impure radium (10,000×) or by the X-rays from a distance of 6 meters, we may note in the first place that the coronal fog limit has enormously decreased as compared with its position in dust-free non-energized air. The nuclei are therefore throughout correspondingly larger in size. The nucleation soon rises with an approach to the characteristic slope referred to, showing that the representative ions lie within a relatively narrow range of sizes, the curve of distribution terminating in a maximum. With increasing exhaustion the nucleation first decreases to a minimum; hence to all appearances the ions are now partially destroyed or else materially reduced in size at low pressure, so as to fail of capture even in the higher exhaustions. Beyond the minimum the final and most interesting stage of variation characteristic of weak ionization may be observed. The nucleation rapidly rises again, eventually to approach the asymptote of dust-free air. In explanation of this phenomenon, we may agree that

*The coincidence between my interpretation of Wilson's disk colors and my own data holds only when the drop of pressure is observed at the fog chamber. See section 48.

further nuclei are destroyed or rendered relatively inefficient by the low pressure until there is a sufficient excess of supersaturation to actually capture the colloidal nuclei of dust-free air more and more fully in the presence of the ions (few in number and small in size) remaining. Possibly the relative number of ions and colloidal nuclei is itself a sufficient reason; but it since seems clear that an apparatus which ceases to produce condensation on colloidal nuclei much below $\delta p = 35$ cm. can not be expected to regain efficiency between $\delta p = 35$ and $\delta p = 45$ cm., unless there is destruction of whatever has been holding down the effective nucleation to low numbers. As the ions decrease either in size or number, there is a reappearance of the normal colloidal nucleation of dust-free air. Its asymptote is less and less depressed.

Under *moderate ionization*, such as is obtained from the X-ray bulb at a distance of 1 to 2 meters, the fog limit is definitely reduced, showing the presence of an order of larger nuclei; the asymptotes are correspondingly higher and they are reached later (*i. e.*, at higher exhaustions), indicating the presence of smaller nuclei than in the preceding cases, as well as larger nuclei, unless the increased presence of the latter retards condensation on the former. The range of sizes within which the representative nucleations lie is definitely extended in both directions, but particularly on the sides of the smaller nuclei. The maximum and the minimum are flattened, though destruction of ions still occurs at low pressure.

The new feature of these curves is their failure to rise from the minimum toward the asymptote of dust-free air. It follows that the ions are now present in too large a number, even relatively to their reduced sizes at high exhaustion (if this obtains), to leave an excess of supersaturation sufficient to catch the colloidal air nuclei; or, from the other point of view, the kinetic ionization pressure is too strong to admit of sufficient rupture of the nuclei even at the lowest pressures applied. (Section 43.)

In the comparison of both series of experiments, the occurrence of the intersection of the curve is noteworthy. In other words, the nucleation, apparently produced at high exhaustion by an X-ray bulb at 6 meters from the fog chamber, may be much larger than the nucleation produced from 200, 100, or even 50 cm., due (as we have supposed) to the reappearing efficiency of the colloidal nuclei in the former case. Similar complications surround the distance effects at other pressures; but under conditions of sufficiently moderate exhaustion, *i. e.*, below the fog limit of filtered air, the distance effects between 50 and 600 cm. remains disproportionately small.

When the ionization is relatively *intense*, as when the anticathode is from 10 to 60 cm. from the thinner side of the glass fog chamber, the

fog limit has decreased somewhat further, showing increased abundance of the larger nuclei; but the slope closely resembles the corresponding case for dust-free air. There is no maximum, but a terminal asymptote, or better, a terminal corona of fixed aperture. This corona, which is here the largest obtainable in the fog chamber, is even at the highest ionizations reached at supersaturations below the coronal fog limits for dust-free air, and long before the apparatus has ceased to function. It is impossible to state whether colloidal nuclei are simultaneously present but inactive or whether their inefficiency is due to actual absence. It thus becomes a problem of great theoretical importance in its bearing on this subject to determine how the precipitated supersaturation is distributed among groups of nuclei of different sizes.

It is finally to be observed that the terminal corona is the same, both for the ionized and the non-ionized state of the gas. The maximum number of nuclei which can be caught per cubic centimeter seems, therefore, to be a constant for the apparatus and the medium inclosed, and to be independent of the size of the nuclei, whether large like the ions or small like the colloidal nuclei. In the above apparatus, with an air-water medium it is difficult to pass beyond the large green-blue-purple corona.

43. Radiant fields.—The occurrence of a succession of groups of colloidal nuclei of (let us say for simplicity) continuously decreasing size and continuously increasing number, is suggestive; for each group is essential in the given natural but otherwise unknown environment. They are at once restored if withdrawn. These conditions may be imitated or varied artificially by approaching the radium tube at different distances from the fog chamber, in which case the efficient nucleation will for weak radiation usually decrease, as the intervening distances are smaller.

Furthermore, in the presence of radium the character of the phenomenon is the same, except that the nuclei are throughout larger. Withdrawn by precipitation they are at once restored. They are an essential part of air in the new (radiant) environment and the nuclei are again graded.

It is natural to compare the particular nuclear status introduced in the latter case by a particular kind of radiation (gamma-rays) with a former case of dust-free air in the absence of recognized radiation. In other words, if we abstract from the details of the mechanism which are unknown for the colloidal nuclei, chemical agglomeration might be considered referable to some radiant field, unknown but otherwise essentially alike in kind, to the much coarser nucleations observed on exposure to the known radiant field. The effect of radium, however distant, is virtually

an increase of size of the efficient air nuclei and a decrease of their number. Hence if we were to fancy that the colloidal nucleation of air responds to its own radiant environment, this would have to be special in kind.

Recently I have made similar tentative inquiries as to whether the ions and persistent nuclei might not be regarded as colloidal nuclei aggregated by kinetic pressure, corpuscular or undulatory; for in view of the occurrence of pronounced secondary action within the fog chamber, the radiation at any point must be considered as sufficiently the same in all directions to be equivalent to a Lesage medium. It is then possible to account for the nucleation in any ionized field, for fleeting and persistent nuclei, for condensational differences of positive and negative ions, for fleeting nuclei otherwise identical but respectively charged and uncharged, for the destructive effect of low pressure and the counteraction in strong ionized fields, for electrical differences in the effect of ultra-violet light and of X-rays, etc., with a single straightforward hypothesis.

While such a view may be worth a statement, it would at the outset encounter very determined opposition; and the distinctive or differentiating evidence to sustain it is uncertain. Briefly, if we admit that with ions sufficiently large and sufficiently numerous, relatively speaking, the colloidal nuclei are virtually non-existent (so far as the fog chamber is concerned), since the former capture all the available moisture, most of the phenomena of nucleation admit of interpretation, and additional hypotheses, however alluring, are not called for. Moreover, so long as the representative colloidal nuclei are definitely smaller than the smaller ions, even in the strongest electrical field—in other words, if what may be called the shattering action of strong fields always fails to reveal ionized nuclei as small as the representative colloidal nuclei—the special interpretation is not warranted.

In conclusion, if we asked what is the most important outcome of researches of the present character, I should refer to the appearances obtained, indicating that a gas, or at least a moist gas, far from being a uniform system, behaves like an assemblage of nuclei which decrease in size and increase in number as the molecular dimension is approached. Every group of nuclei is none the less a structurally essential part of the gas and (be the number of groups few or many) is at once restored if withdrawn, while the molecule itself is distinguished among the many nuclei of its own kind by the maximum frequency of occurrence.

In the above cases (fig. 25) the occurrence of nearly identical slopes for colloidal nuclei and for strong ionization may thus be regarded as the initial branch of a law of distribution of sizes given by the theory of dissociation.

COLLOIDAL NUCLEI IN DUST-FREE AIR. EXHAUSTION PIPES AND STOPCOCKS FOUR INCHES IN DIAMETER.

44. Purpose.—In the above experiments, the efficiency of the fog chamber in regard to the capture of very small nuclei was successively increased by enlarging the efflux pipe in diameter as far as 2 inches. In the present experiments a further step is taken by increasing the diameter to 4 inches. This final step, however, did not show the marked improvement which might have been anticipated, while the difficulty of manipulating a plug weighing 25 pounds is obvious. The limiting coronas here, as above, were the large green-blue-purple type, and in no apparatus of the present kind has it been certainly possible to exceed this in angular aperture. The use of so large a stopcock introduces other difficulties. It is in the first place nearly impossible to make it quite tight. Provision against the influx of *external* air may be made in perfection, by aid of an annular oil bath of the above form; but slow leakage from the fog chamber to the vacuum chamber around the plug could not be avoided. This is an inconvenience, though it need not introduce serious error. With a tightly packed filter the air within the fog chamber is never quite at atmospheric pressure, but a few millimeters below it, so that the exhaustion begins at a lower pressure than 76 cm.

45. Apparatus.—This is shown in fig. 26, where F is the fog chamber, V the vacuum chamber, C the 4-inch stopcock between, P the air pump. The pressure within the vacuum chamber is given by the gage G, which also communicates with the air pump. The latter may be shut off by the glass two-way stopcock c, which serves also for the admission of dust-free atmospheric air when pressure is to be lowered through the filter f. The gage g is in communication with the fog chamber by the rubber pipe ab, which contains a lateral branch (not shown) with a fine screw stopcock through which thoroughly dust-free air may be admitted into the fog chamber from a long well-packed filter (not shown) beyond the cock.

The heavy plug of the stopcock is handled at h and counterpoised by the spring p on a pulley. By properly adjusting the tension (taking care to allow for excess and diminution of air-pressure), the plug may be rotated as easily and quickly as a much smaller valve. There is no evidence that increased speed in the rotation of the stopcock would have increased the efficiency of the fog chamber. The limit reached depends rather on the law of flow, the gradient of which eventually vanishes. The projecting rims, m and n, of the stopcock and lower end of the plug, form annular troughs into which oil or mercury may be

poured (iron stopcock) and the inflow of the external air absolutely avoided. The cock, moreover, is in this way virtually floated in oil; though no such provision is possible to avoid leakage from F to V through C as already stated.

The goniometer for the measurement of the angular diameter of the coronas is shown somewhat indistinctly at D. The small vertical plate which serves as the eye rest is 40 cm. from the axis of the fog chamber, to which it is rigidly attached, but with freedom of rotation about a vertical and horizontal axis and translation along the latter. The arms are 30 cm. long, opened and closed by a tangent screw. The point source of light (not shown, part of a Welsbach mantle) lies 250 cm. behind the fog chamber, in the same horizontal plane.

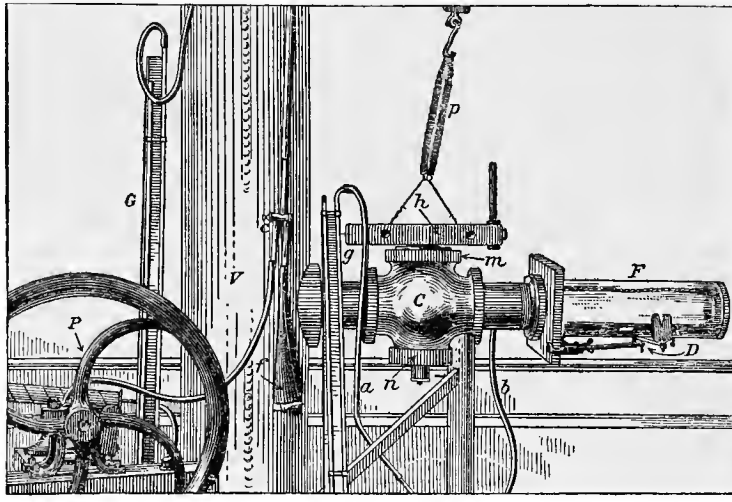

FIG. 26.—Disposition of apparatus in case of fog chamber (F) and vacuum chamber (V) connected by a 4-inch exhaustion pipe, etc.

The X-ray bulb, adjustably placed with the induction coil and interrupter on a table provided with wheels, could be moved as near to the fog chamber, or remote from it, as desirable, with facility.

The fog chamber itself was a cylindrical jar of glass, provided with a metallic face held in place by bolts and tightened by a rubber gasket. Wax-resin cement was used in liberal quantity everywhere, and internal metallic parts were so far as possible covered with a coat of it. In later experiments a cylinder of wet cloth was placed in the tube between C and F, to saturate air, in addition to the rectangular framework within the fog chamber.

46. Exhaustion difficulties.—As the stopcock was not tight internally, the final or isothermal pressure in the fog chamber could not be registered. In any case it is doubtful whether the cock can be closed again quickly enough. It was therefore customary in the following experiments to put the vacuum chamber and the fog chamber in contact for a short time, after isothermal conditions had been reestablished. Long communication between the fog chamber and the vacuum chamber is unadvisable from other points of view, since the character of the nucleation of the latter is not so well guaranteed It is therefore necessary to ascertain the conditions under which exhaustion takes place.

Let v be the volume of the fog chamber, V the volume of the vacuum chamber, k/c the ratio of specific heats of the moist gas, and let p, v, τ, ρ, denote its pressure, volume, absolute temperature, and density, under conditions given by the subscripts. It will be convenient to refer to the vacuum chamber by the same symbols with *accents*. Hence the successive thermal states will be for dry air,

For the fog chamber.....	Initially	$p=76$,	τ	ρ
	Adiabatically (alone).....	p_1	τ_1	ρ_1
	Isothermally(alone).....	p_2	$\tau_2=\tau$	$\rho_2=\rho_1$
	Isothermally (together)...	p_3	$\tau_3=\tau$	ρ_3
For the vacuum chamber..	Initially	p'	$\tau'=\tau$	ρ'
	Adiabatically (alone).....	$p'_1=p_1$	τ'_1	ρ'_1
	Isothermally (alone)	p'_2	$\tau'_2=\tau$	$\rho'_2=\rho'_1$
	Isothermally (together)..	$p'_3=p_3$	$\tau'_3=\tau_3$	$\rho'_3=\rho_3$

The equations describing the transformations are (again for dry air):

$$1 \ldots\ldots\ldots \frac{\tau}{\tau}=\left(\frac{p}{p_1}\right)^{(k-c)/k} \qquad \frac{\tau}{\tau'_1}=\left(\frac{p'}{p_1}\right)^{(k-c)/k}$$

$$2 \ldots\ldots\ldots\ldots \begin{cases} p = R\rho\tau & p' = R\rho'\tau \\ p_1=R\rho_1\tau_1 & p'_1 = R\rho'_1\tau \\ p_2=R\rho_2\tau=R\rho_1\tau & p'_2 = R\rho'_2\tau=R\rho'_1\tau \\ p_3=R\rho_3\tau & \text{or } p_2/p'_2=\rho_2/\rho'_2 \end{cases}$$

$$3 \ldots\ldots\ldots\ldots\ldots \rho v+\rho^1 V=\rho_1 v+\rho'_1 V=\rho_2 v+\rho''_2 V=\rho_3 (v+V)$$

From these one may deduce, relative to the value of p_1,

$$v\,(p^{(k-c)/k}p_1{}^{c/k}-p_3)=V\,(p_3-p'^{(k-c)/k}p_1{}^{c/k})$$

or

$$4 \ldots\ldots\ldots\ldots\ldots p_1{}^{c/k}=\frac{p_3\,(1+v/V)}{p'^{(k-c)/k}+(v/V)\,p^{(k-c)/k}}$$

$$5 \ldots\ldots\ldots\ldots\ldots p'_2+p_2\cdot v/V=p_3\,(1+v/V)$$

where p, p', p_3, are observable with certainty. While equation (5) is variously useful in checking the results, it does not admit of the individual determination of p_2 and p'_2. For this purpose, however, the equations (1) and the second and third of group (2) are available, with the results (for dry air)

$$6 \ldots\ldots\ldots\ldots p_2 = p^{(k-c)/k}\, p_1{}^{c/k} \qquad p'_2 = p'^{(k-c)/k}\, p_1{}^{c/k}$$

since $p_1{}^{c/k}$ is given in equation (4).

Using these equations, the data of table 17 were computed, in connection with incidental results tested for the purpose.

TABLE 17.—Values of adiabatic (p_1) and isothermal (p_2, p'_2) pressure for dry air. Pressures computed from the initial pressures ($p = 76$, p') and the final common isothermal pressure p_3 of the communicating fog and vacuum chambers with other similar data. Volume ratio $v/V = 0.064$; temperature 20°.

Observed.				Computed.*			Observed. $r_1 - t_1 = 273$ $r'_1 - t_2 = 273$		
p.	p'.	p_3.	†p'_1.	p_1.	p_2.	p'_2.	‡p''_1.	t_1.	t'_1.
76	43.0	45.4	48.0	45.7	....	....	....	....	....
	39.5	42.2	45.2	....	....	....	....	....	....
	42.5	45.2	47.9	....	....	....	....	....	....
	43.5	45.5	47.9	45.7	52.9	45.0	45.6	−20.2°	24.3°
	45.5	47.3	49.3	....	....	....	47.4	....	....
	47.5	48.9	50.9	....	....	....	48.9	....	....
	51.5	52.5	54.3	52.4	58.3	52.1	....	− 9.9°	21.5°
	53.5	54.3	56.1	....	....	....	....	....	....
	55.5	—	—	....	....	....	....	....	....
	57.5	58.0	59.8	....	....	....	....	....	....
	59.5	59.7	62.2	59.4	63.8	59.4	—	.2°	20°
	43.5	45.7	48.4	....	....	....	....	....	....
	43.5	45.4	48.0	....	....	....	....	....	....

* Checked $p'_2 + p_2\, v/V = p_3\,(1 + v/V)$.
† Observed as soon as possible at the fog chamber. Nearly same later.
‡ Observed as soon as possible at the vacuum chamber. $p''_1 = p_3$ nearly.

The data of table 17 are computed for dry air throughout and are given in fig. 27*a*, graphically.* The results of the table are very important. In the first place, it will be seen not only that isothermal pressures or nearly isothermal pressures are not observed, but that the effect of the vacuum chamber is preponderating. Thus the pressure at the latter (p''_1) read off as soon as possible and nominally adiabatic is within 1 mm. of p_3. Similarly the computed adiabatic pressure (p_1) is within a few

*The curve (p_2) is of no interest here and should be disregarded.

millimeters of p''_1 and p_3. It follows, therefore, that even an approach to isothermal pressure can not be discerned at the fog chamber at all, to say nothing of adiabatic pressure; or that before the exhaust cock can be closed again, the vacuum chamber has practically regained its isothermal pressure by cooling and that the fog chamber is further exhausted by a corresponding amount. The pressure $p'_1 = p''_2$ observed under isothermal conditions* at the fog chamber exceeds p_1 (computed) by about 1.9 cm. on the average, which might be regarded as the average vapor pressure of water at the temperature at which the observation was made. Leaving this for further consideration, the final result of importance is the following: p_2, the computed isothermal pressure in the closed fog chamber, is from 2 to 5 cm. above the observed (nominally) isothermal pressure $p'_1 = p_2$ (observed), and correspondingly more than this above the common isothermal value (p_3) usually taken. For the region in which colloidal nuclei lie the correction will be in excess of the difference between the pressure regions containing Wilson's data for colloidal nuclei, as reduced elsewhere,† and the region in which my own data as summarized below would lie. In other words, the data in my large coronal apparatus lie in regions of exhaustion at least as moderate as those observed in Wilson's small apparatus; or the two types of apparatus compare in efficiency if the drop of pressure taken is not the apparent experimental value but that deduced for the computed isothermal pressure (p_2) of the fog chamber, as above explained.

47. The same, continued. Case of air in the fog chamber saturated with water vapor.—It will next be necessary to compute the above data with allowance for the vapor pressure of water in the fog chamber, supposing the vacuum chamber to be dry, which may seem to be in a measure true, since it is heated by the same transfer of air which cools the fog chamber. Hence in the summary, if π is the vapor pressure of water, the equations relating to the fog chamber have to be modified to

$$1 \ldots \ldots \ldots \ldots \ldots \ldots \frac{\tau}{\tau_1} = \left(\frac{p-\pi}{p_1-\pi_1}\right)^{(k-c)/k}$$

$$2 \ldots \begin{cases} p - \pi = R\rho\tau \\ p_1 - \pi_1 = R\rho_1\tau_1 \\ p_2 - \pi = R\rho_2\tau = R\rho_1\tau \\ p_3 - \pi = R\rho_3\tau \qquad p_3 = p'_3 = R\rho'_3\tau_3 \qquad \rho v + \rho^1 V = \text{etc.} = \rho_3 v + \rho'_3 V \end{cases}$$

*This pressure varies but slightly.

†Presidential address, Physical Review, XXII, 1906, p. 107.

From these the value of p_1 appears as

$$7 \ldots\ldots\ldots p_1^{c/k} = \frac{p_3 + (p_3 - \pi) \cdot v/V}{p'^{(k-c)/k} + (p-\pi)^{(k-c)/k}(1-\pi_1/p_1)^{c/k} \cdot v/V}$$

where π_1/p_1 occurring with the factor v/V may be neglected. Furthermore

$$8 \ldots\ldots\ldots (p_2 - \pi) = (p-\pi)^{(k-c)/k}(p_1-\pi_1)^{c/k};\ p'_2 = p^{1(k-c)/k}\, p_1{}^{c/k}$$

where π_1 (respectively $\pi = 0.10$, 0.24, 0.51 in comparison with $p_1 = 45.6$, 52.2, 59.3) may again be neglected.

The results of this computation are given in table 18 and fig. 27*b*.

Table 18 also contains the value of δp observed as $p - p_3$ and computed as $p - p_2$, the latter being the correct value. This table of corrections will not apply below the limits of computation, since π_1 now becomes appreciable in comparison with p_1; but above $p - p_3 = 15$ cm., a table may be constructed from which $\delta p = p - p_2$ may be taken at once. In this way the following data will be corrected Since the main data for colloidal nuclei lie between $p - p_3 = 25$ cm. and 32 cm., the correction will lie between -4 cm. and -6 cm.

TABLE 18, corresponding to table 17 for saturated moist air in the fog chamber. Temperature 20°; vapor pressure 1.7 cm.; $p = 76$; $v/V = 0.064$.

δp.		Observed.				Computed.				
$p-p_3$.	$p-p_2$.	p_1.	p_3.	$*p_1'$.	$\dagger p_1''$.	p_1.	p_2.	p_2'.	τ_1.	τ_1.
30.5	25.2	43.5	45.5	47.9	45.6	45.6	50.8	44.9	−18.7	+24.0
23.5	19.9	51.5	52.5	54.3	....	52.2	56.1	52.0	− 8.5	21.2
16.3	14.4	59.5	59.7	62.2	....	59.3	61.6	59.3	+ 1.5	+20

* Observed as soon as possible at the fog chamber; nearly same later.
† Observed as soon as possible at the vacuum chamber; $p_1'' = p_3$ nearly.

TABLE 19.—The results are for $\pi = 1.7$ at 20°.

p.	p'.	p_3.	p_2.		
			$v/V = 1$.	$v/V = 0.064$.	$v/V = 0$.
76−π	43.5	45.5	48.1	50.8	53.1
	51.5	52.5	54.4	56.1	58.4
	59.5	59.7	60.7	61.6	63.7

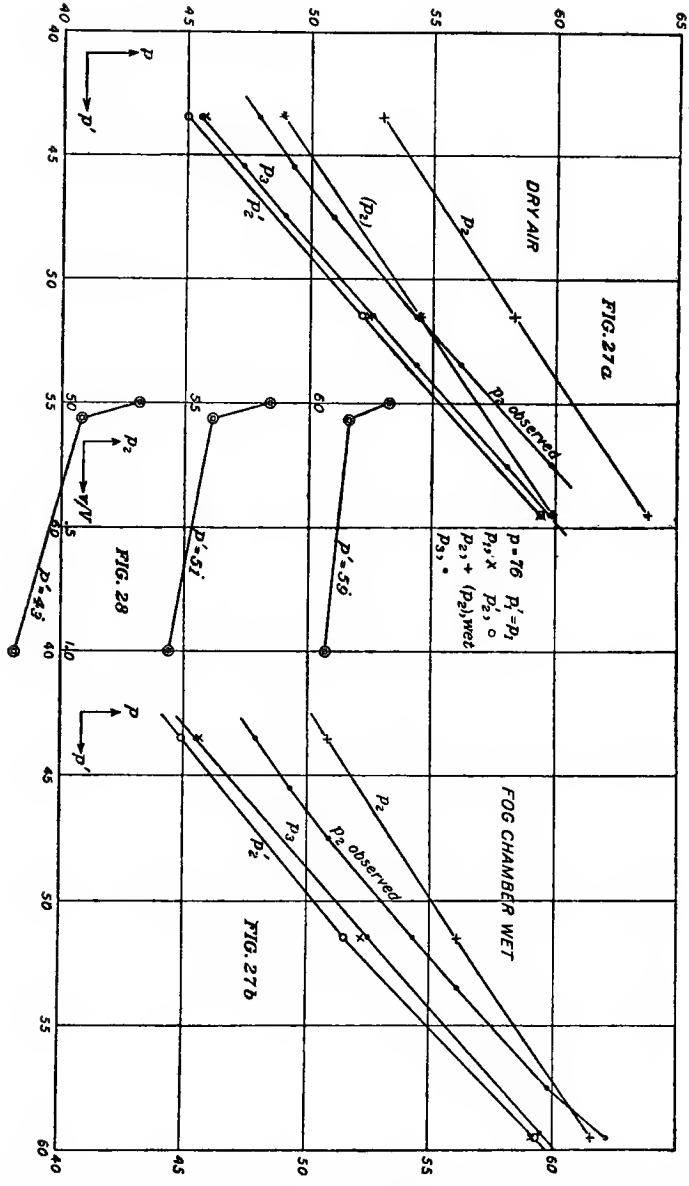

FIG. 27*a*.—Computed pressures in the fog chamber and in the exhaustion chamber for atmospheric pressure, p in the former and p' in the latter. Dry air. Table 17.

FIG. 27*b*.—Wet air in the fog chamber. Table 18.

FIG. 28.—Isothermal pressure in the isolated fog chamber for different volume ratios (v/V) of the fog chamber and vacuum chamber. Table 19.

It may be of further interest to compute the values of $p-p_3$ for $v/V=1$ (a small exhaustion chamber) and for $v/V=0$ (one of immense size) for the same values of p, p', p_3, observed isothermally and initially at the fog chambers and vacuum chambers and finally when both are in communication. The results for 20° are given in table 19, page 56.

These data are charted in figs. 28 and 30, to a first approximation, in terms of v/V and p_3. If expressed in terms of p', they lie nearly on straight lines, as do the above values of p_2 for $v/V=0.064$. The large

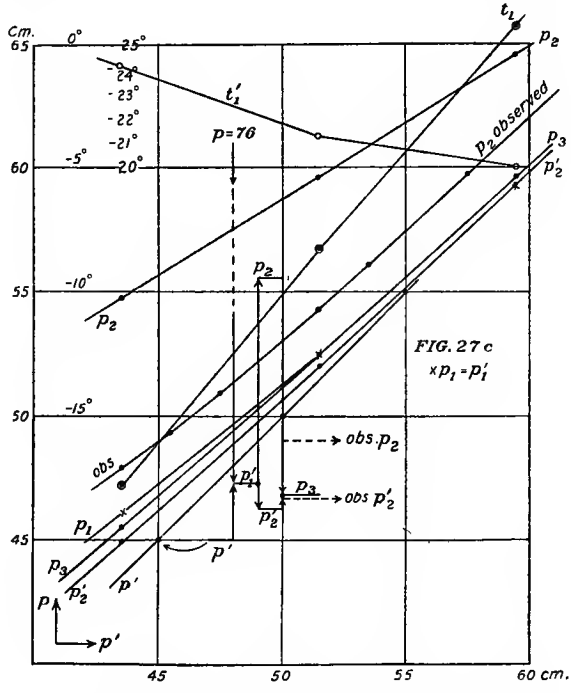

FIG. 27c.—Wet air in both chambers. Table 20.

variation between $v/V=0$ and 0.064 as compared with the small one for $v/V=0.064$ and 1.0 is noteworthy. Hence, in using small vacuum chambers, the observed and computed p_3 and p_2 lie more closely together, but other disadvantages supervene. The rate of variation

$$\frac{\delta p_2}{\delta(v/V)}=p_3(p/p')^{(k-c)/k}\frac{1-(p/p')^{(k-c)/k}}{\left\{1-(p/p')^{(k-c)/k}.v/V\right\}^2}$$

is always negative and proportional to p_3 and $(p/p')^{(k-c)/k}$.

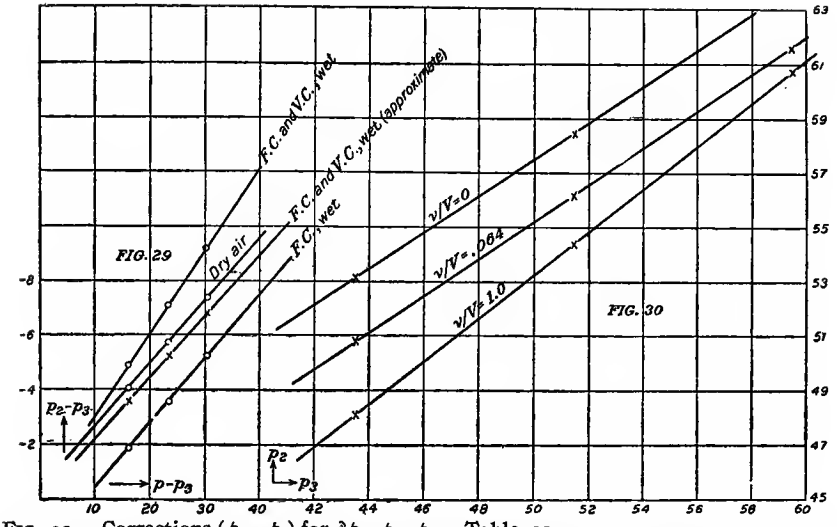

FIG. 29.—Corrections $(p_2 - p_3)$ for $\delta p = p - p_3$. Table 20.

FIG. 30.—Isothermal pressure p_2 in the isolated fog chamber for different isothermal pressures p_3 of the communicating fog chambers and for different volume ratios (v/V). Table 19.

48. Case of saturated air in both chambers.—Here all the pressures of both chambers must be reduced by the corresponding pressure of saturated vapor, except p'_1 where the vapor is slightly superheated. Omitting this the equations become

$$9. \quad \ldots\ldots (p_1 - \pi_1)^{c/k} = \frac{(p_3 - \pi)\ (1 + v/V)}{(p' - \pi)^{(k-c)/k} + (p - \pi)^{(k-c)/k} . v/V}$$

$$10. \quad \ldots\ldots\ldots\ldots\ldots (p_2 - \pi) = (p - \pi)^{(k-c)/k} (p_1 - \pi_1)^{c/k}$$

or the equations again take the original form, though a special computation is needed, since a different initial pressure (p) enters. These results are given in table 20 and in fig. 29.

TABLE 20.—Corresponding to table 18 when both fog chamber and vacuum chamber are saturated. $v/V = 0.064$; temperature 20°; $p = 76$ cm.; $\pi = 1.7$

δp.	Observed.				Computed.				
$p - p_3$.	$p - p_2$.	p'.	p_3.	$*p'_1$.	$p_1\pi_1$.	$\dagger p_2$.	p'_2.	τ_1.	τ_2.
30.5	23.7	43.5	45.5	47.9	43.5	52.4	45.1	−22.5	..
23.5	18.2	51.5	52.5	54.3	50.3	57.8	52.2	−11.5	..
16.3	12.7	59.5	59.7	62.2	57.3	63.3	59.5	− 1.4	..

* Observed as soon as possible at the fog chamber.

$\dagger (p'_2 - \pi) + \frac{v}{V}(p_2 - \pi) = \left(1 + \frac{v}{V}\right)(p_3 - \pi)$

$p-p_3$.	$p-p_2$.	Ratio.		$p-p_3$.	Correction.	Ratio.	
o	o			o	o		
16.3	12.7	$\frac{18.2}{23.5} = 0.7745$	Mean 0.776	16.3	3.6	$\frac{-5.3}{23.5} = 0.226$	Mean 0.225
23.5	18.2			23.5	5.3		
30.5	23.7	$\frac{11.0}{14.2} = 0.7782$		30.5	6.8	$\frac{-3.2}{14.2} = 0.225$	

In view of the low temperature (τ_1) the vapor pressure (π_1) may be neglected for the fog chamber; but this would not be the case of the vacuum chamber, where π'_1 is quite appreciable. As the result of this, the march of pressures in the vacuum chamber is peculiar, but need not be considered here, where p, p', p_3, and p_2 are chiefly in question. The difference between $\delta p_0 = p - p_3$ as observed and $\delta p_c = p - p_2$ as computed now actually vanishes with the former (see fig. 29). In other words, very nearly

$$\frac{p - p_2}{p - p_3} = 0.775, \text{ or } \frac{p_2 - p_3}{p - p_3} = 0.225$$

and therefore $\delta p_0 - \delta p_c = 0.225\ \delta p_0$, nearly. Hence this is a correction to be taken by preference. A table giving $0.225\ \delta p_0$ for the usual ranges of observation was therefore drawn up and used throughout the following work, or the factor 0.775 may be used at once. These corrections are quite sufficient to indicate that the efficiency of the fog chamber as used above is not surpassed by any apparatus.

The preceding correction, in comparison with the cases of sections 46 and 47, seemed to me to be most nearly in keeping with the actual state of the case. The more nearly rigorous solution, when the air in both chambers is continually saturated, leads to transcendental equations for the adiabatic pressures ($p_1 = p'_1$), which can only be obtained approximately. If the vapor pressures (π_1 and π'_1) correspond to p_1 and p'_1, the results would be

$$(p_1 - \pi'_1)^{c/k} = \frac{(p_3 - \pi)\ (1 + v/V)}{(p' - \pi)^{(k-c)/k} + v/V \cdot \left(1 - (\pi_1 - \pi'_1)/(p_1 - \pi'_1)\right)^{c/k} (p - \pi)^{(k-c)/k}}$$

$$(p_1 - \pi_1)^{c/k} = \frac{(p_3 - \pi)\ (1 + v/V)}{\left(1 - (\pi'_1 - \pi_1)/(p_1 - \pi_1)\right)^{c/k} (p' - \pi)^{(k-c)/k} + v/V \cdot (p - \pi)^{(k-c)/k}}$$

where approximate values must be entered for π'_1, π_1, p_1, in the denominator on the right side of the equation.

Similarly

$$p_2 - \pi = (p_1 - \pi_1)^{c/k}(p - \pi)^{(k-c)/k},$$

$$p'_2 - \pi = (p'_1 - \pi'_1)^{c/k}(p' - \pi)^{(k-c)/k},$$

$$\tau/\tau_1 = \Big((p - \pi)/(p_1 - \pi_1)\Big)^{(k-c)/k}, \quad \tau/\tau_1' = \Big((p' - \pi)/(p_1' - \pi_1')\Big)^{(k-c)/k}$$

Making use of the values of table 18, the data of table 21*b* were computed on a single approximation.

TABLE 21*b*.—Corresponding to table 18, when both fog chamber and vacuum chamber are saturated. $v/V = 0.064$; temperature 20°; $\pi = 1.7$; $p = 76$ cm.

*π.	*π'_1.	obs. p'.	obs. p_3.	p_1.	p_2.	p'_2.	t_1.	t'_1.
0.0	2.3	43.5	45.5	46.1	54.7	44.9	− 17.8°	+ 24.1°
.2	1.9	51.5	52.5	52.5	59.6	52.0	− 8.3	21.3
.5	1.7	59.5	59.7	59.3	64.6	59.4	+ .8	19.8

*Assumed from data for t_1, t'_1, in table 18.

$p - p_3$.	$p - p_2$.	$(p - p_2)/(p - p_3)$.	$\bar{\pi}$.	$\bar{\pi}'_1$.	$\bar{t}_1$.	$\bar{\rho}_1/\rho_1$.	$\bar{p}_2$.
0.0	0.0	$\frac{16.4}{23.5} = 0.70$	0.7	2.2	+ 5.2	0.910	49.9
16.3	11.4		.9	1.9	+ 9.4	.929	55.5
23.5	16.4	$\frac{9.9}{14.2} = .69$	1.1	1.7	+12.7	.952	61.5
30.5	21.3						

The corrections (see table 21*b*, and upper graphs in fig. 30) again lie on a curve which passes through zero, but with a larger slope. In fact, they are so much larger than the preceding cases and throw the whole phenomenon into so low a region of pressures that it has seemed best to abide by the data at the beginning of this paragraph, at least for the present. Details are given in table 21*b*.

A few incidental results deserve brief attention. The first of these is the nearly constant difference of about $\delta p_2 = 2$ cm. between the observed value of p_2 (nominal) and p_3. Since for dry air or not

$$(p'_2 - \pi) + v/V.\ (p_2 - \pi) = (p_3 - \pi)(1 + v/V)$$

is constant for a given exhaustion,

$$\delta p'_2 = -v/V.\ \delta p_2.$$

Hence if $\delta p_2 = 2$ cm.

$$\delta p'_2 = 0.064 \times 2 = 0.13 \text{ cm.}$$

The case is illustrated graphically for $p' = 45$ cm. in the notched curves of fig. 27*c* in a way easily understood. It seems probable that whereas the smaller fog chamber has more than returned to isothermal conditions (p_2), the large vacuum chamber is about a millimeter short of it when the cock is again closed. The constancy of this difference is in all probability referable to the systematic method of investigation, though the effect of precipitated moisture has not yet been considered.

Anomalous relations in the data for the fog chamber (as in the case of $p' = 59.5$ cm.) are direct errors of observation. On the other hand, however, since within the ranges of observation and very nearly

$$\begin{gathered} p = a \\ p_2 = a_2 + b_2 p' \\ p_3 = a_3 + b_3 p' \\ (p - p_2)/(p - p_3) = (A_3 + B_3 p')/(A_2 + B_2 p') = A + Bp' \text{ (nearly)}, \end{gathered}$$

where a, b, A, B, etc., are constant. Frequently B is negligible, so that

$$(p - p_2)/(p - p_3) = A = \text{const.},$$

in which case the graph for $(p_2 - p_3)/(p - p_3) = 1 - A$ also passes through the origin as in the two cases (fig. 30). There is no need of this and it is at best an approximation which facilitates computing.

Some remarks may here find place on the moisture precipitated in the fog chamber per cubic centimeter, and on the absolute temperature $\bar{\tau}_1$ to which this precipitation heats the chamber above the adiabatic temperature τ_1. I have shown above that the combination of fog chamber with a large vacuum chamber and a sufficiently wide passageway, though affording superior practical advantages, and little if any inferiority in efficiency to the piston apparatus within the range of measurable coronas, nevertheless does not give the volume expansion of the air within the fog chamber either under adiabatic or under isothermal conditions. It makes no difference how rapidly the stopcock is manually closed. The conditions of the vacuum chamber are always impressed upon the fog chamber. The adiabatic and isothermal data may, however, be computed if the volume ratio of the fog and vacuum chambers and the pressures before exhaustion (when the chambers are isothermally separated) and after exhaustion (when the chambers are isothermally in communication) are known; and these computations are simple because the reductions are practically linear.

When the vacuum chamber is large, moreover, its pressures vary but slightly, and therefore the pressure observed at the vacuum chamber after exhaustion, when the two chambers are in communication, is very nearly the adiabatic pressure of the fog chamber. This result makes it

easier to compute the water precipitated per cubic centimeter (without stopping to compute the other pressures) with a degree of accuracy more than sufficient when the other measurements depend on the size of coronas.

To prove this, let d, L, and π refer to the density, latent heat of evaporization, and pressure of water (or other) vapor; let ρ, k, c, t, denote the density, specific heat at constant pressure, specific heat at constant volume and temperature of the air, the water vapor contained being disregarded apart from the occurrence of condensation. Let the variables, if primed, refer to the vacuum chamber, otherwise to the fog chamber. When used without subscripts, let them refer to isothermal conditions or to room temperature. Let the subscript $_1$ refer to the adiabatic conditions on exhaustion; the subscript $_2$ to isothermal conditions, if the chambers could be isolated immediately after exhaustion and allowed to heat and cool from the adiabatic state independently. This case is in fact realized in the piston apparatus. Let the subscript $_3$, finally, refer to the isothermal conditions which prevail if the chambers are put in communication at a room temperature after exhaustion. Then the usual equations for heat evolved in the condensation of vapor lead easily to

$$\bar{d}=[d_1]-\rho_2 C(\bar{t}-t_1)/L \qquad (1)$$

where $\bar{d}$ is the density of saturated vapor at $\bar{t}$, where $\bar{t}$ is the temperature to which the wet air is heated from its adiabatic temperature t_1, in consequence of the condensation of water vapor, where $[d_1]$ is the density of water vapor if cooled as a gas, *i. e.*, without condensation, from t to t_1. Moreover

$$[d_1]-\bar{d}=m \qquad (2)$$

the mass of water precipitated per cubic centimeter by condensation or the quantities sought.

If Boyle's law is assumed to hold both for the gaseous water vapor $[d_1]$, and for the wet air, it is convenient to reduce equation (1) to room temperature (isothermal state) and it becomes

$$\bar{d}=d\frac{p_2-\pi}{p-\pi}\quad\rho\frac{c}{L}\frac{p_2-\pi}{p-\pi}(\bar{t}-t_1) \qquad (3)$$

If the vapor density of saturated water vapor is known at a temperature as low as $\bar{t}$,

$$\bar{d}=f(\bar{t}) \qquad (4)$$

so that $\bar{t}$, the only unknown quantity in equation (3), since the equation of adiabatic expansion determines t_1, is found from the intersection of the curves (3) and (4). This is the method of Wilson and of Thomson.

In the piston apparatus p_2 as well as p may be read off by the gages; but, as stated above, this is not true when the fog chamber communicates directly with the vacuum chamber. In this case, however, p_1 is nearly given by p_3. Consequently it is expedient to reduce equation (1) to the adiabatic conditions, whence (if τ refers to absolute temperature),

$$d = d\left(\frac{p_1-\pi_1}{p-\pi}\right)^{c/k} - \frac{\rho c}{L}\left(\frac{p_1-\pi_1}{p-\pi}\right)^{c/k}(\bar{t}-t_1) \qquad (5)$$

$$\tau_1 = \tau\left(\frac{p_1-\pi_1}{p-\pi}\right)^{(k-c)/k} \qquad (6)$$

$$m = \frac{\rho c}{L}\left(\frac{p_1-\pi_1}{p-\pi}\right)^{c/k}(\bar{t}-t_1) \qquad (7)$$

Here π_1, the vapor pressure at t_1, is usually negligible (about 0.5) as compared with p_1, and p_1 may, in practice, where great accuracy is not demanded, be replaced by p_3, which, like p, is read off while π holds at t, which is also read off.

In illustration I will give a numerical example taken from table 21*b* where

$p = 76$ cm.	$p_3 = 45.5$ cm.	$t_1 = -17.8°$ C.
$\pi = 1.7$ cm.	$p_1 = 46.1$ cm.	$\bar{t} = 5.25°$ C.
$\rho = 0.00118$	$p_2 = 54.7$ cm.	$t'_1 = 24.1°$ C.
$p' = 43.5$ cm.		

If equation (3) is taken

$$m = 5.36 \times 10^{-6} \text{ grams per cubic centimeter}$$

If equation (5) is taken

$$m = 5.35 \times 10^{-6}$$

If equation (5) is taken and p_1 replaced by p_3

$$m = 5.30 \times 10^{-6}$$

the error being 1 per cent of the true value, which is quite near enough in practice and admits of easy correction.

Finally one may compute $\bar{p}_2$, the pressure which would be observed at the fog chamber instead of p_2 if allowance is made for the water precipitated in the fog chamber, whereby additional air escapes into the vacuum chamber, since the former is heated from τ_1 to $\bar{\tau}_1$. The chambers are supposed to be separated (cock closed) immediately after condensation and no further loss of air is to take place from fog chamber to vacuum chamber while the absolute temperature of the fog chamber passes from $\bar{\tau}_1$ to atmospheric τ. Without giving the full discussion for which there is no room, I will merely add that

$$p_2 - \pi = \frac{\bar{\rho}_1}{\rho_1}(p_2 - \pi)$$

where $\overline{\rho_1}$ is the density of the air at $\overline{\tau_1}$. The ratio is equal to

$$\frac{\overline{\rho_1}}{\rho_1} = \frac{(\overline{\pi'_1} - \overline{\pi_1}) - (\pi'_1 - \pi_1) + (p_1 - \pi_1)\,(1 - v/V \cdot \tau'_1/\tau_1)}{(p_1 - \pi_1)\,(\overline{\tau_1}/\tau_1 + v/V \cdot \tau'_1/\tau_1)}$$

if the vapor pressures π are designated like the temperatures and pressures with which they are associated. Usually

$$\frac{\overline{\rho_1}}{\rho_1} = \frac{1 + v/V \cdot \tau'_1/\tau_1}{\tau_1/\tau_1 + v/V \cdot \tau'_1/\tau_1}$$

suffices, the term involving the vapor pressures (π) being a correction of about 1 per cent. The computation, to which I shall return elsewhere, shows that $\overline{p_2}$, computed, is always above $\overline{p_2}$, observed, so that the fog chamber begins to heat itself above the temperature $\overline{\tau_1}$ before the cock can be closed again and contains less than its normal allotment of air. Thus, in the example given, $\overline{\rho_1}/\rho_1 = 0.91$; $\overline{p_2} = 47.9$, observed; and $\overline{p_2} = 49.9$, computed. Hence p and p_3 alone have any definite meaning for the fog chamber.

49. Observations with 4-inch exhaust pipes.—The observations of this paragraph, apart from the exhaustion difficulties already discussed, were made peculiarly difficult by the unavoidable leak from fog chamber to vacuum chamber through the large exhaust cock. It was therefore essential to wait many hours for each observation, since the coronas corresponding to the second, third, etc., of successive exhaustions were smaller than the first. This can not be due to any other cause than the presence of water nuclei from the fog of the first exhaustion. A given corona, moreover, was apt to decrease in aperture as much as one-half during the period of subsidence, showing growth of certain particles at the expense of others, the latter being afterwards detected in the water nuclei specified. This must also be attributed to the continued slow exhaustion due to the leak in question.

In table 21 and fig. 31 the earlier data with 4-inch pipes are given, chiefly with the object of direct comparison with foregoing results with 2-inch pipes. The meaning of the data is clear from the earlier tables, and the δp here mentioned is the isothermal value observed at the fog chamber as heretofore.

On March 16 to 18 the data are irregular in the way common to observations in a newly adjusted apparatus. The effective nucleation is too small from the presence of interior sources of relatively bulky nuclei. A fairly complete series was undertaken on March 19. The outgoing and incoming branches do not quite coincide, and the data, as a whole, still lie below the corresponding results with 2-inch exhaustion pipes. This is indicated in fig. 31. Of later observations (March 22),

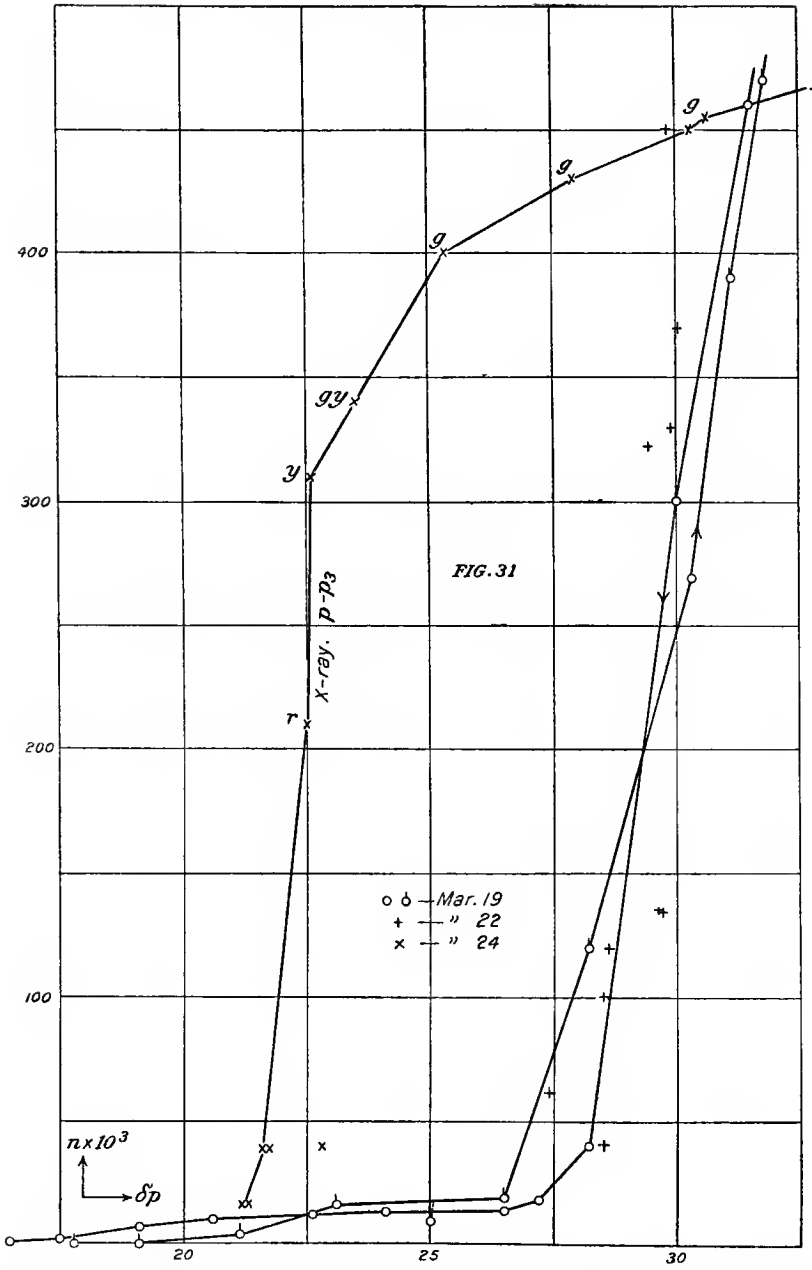

FIG. 31.—Nucleations (n) observed in dust-free air and dust-free X-air at different exhaustions (δp); 4-inch pipes. Table 21.

TABLE 21.—Colloidal nuclei in air. New apparatus. Glass fog chamber. Piping 12 inches long, 4 inches in diameter; 4-inch plug stopcock.

	Observed δp.	s.	Cor.	$n \times 10^{-3}$.
I.				
Mar. 16	25.4	3.8	.....	20
Later...	25.4	2.0	.....	3
	25.4	[1]3.8	.....	20
	29.0	3.5	.....	[2]16
	29.0	4.2	.....	27
II.				
Mar. 17	20.4	.0	.....	0
	25.1	3.3	.....	12
	25.1	4.2	.....	25
	29.1	5.1	.....	51
	29.1	3.7	.....	20
	29.1	4.2	.....	28
	33.5	[3]7.3	w y′	140
	33.5	11	w y	315
	33.5	11	w y	315
	38.0	[3]7.2	w B P	165
	38.0	11	w y′	330
	42	10	w o	350
	42	11	w y	350
Later...	33.5	12.0	g y o	425
	33.5	4.2	cor	30
	33.5	[2]9.5	w o	315
III.				
Mar. 18	33.5	11.5	g y o	425
	....	8.8	w p cor	190
	....	9.8	w o	315
	....	[2]4.6	cor	41
	....	[2]11.8	y′ o b g	390
IV.				
Mar. 19	33.5	[2]13	Stone-blue	
	33.5	7.0	w y	
	33.5	12.0	g y o	
	46.4	[4]13	g B P	540
	42.2	13	b′ B	510
Incoming series.	38.0	13	g B P	500
	33.4	....	g y o to g B	[4]425
	31.5	....	g B P	460
	30.0	11	w o g	300
	28.2	4.7	cor	40
	27.2	3.6	cor	18
	26.5	3.4	cor	14
	24.1	3.4	cor	13
	22.6	3.4	cor	12
	20.6	3.3	cor	10
	19.1	2.9	cor	7
	17.5	1.9	cor	2

	Observed δp.	s.	Cor.	$n \times 10^{-3}$.
Incoming series.	16.5	....	Rain	1
	15.1	....	Rain	1
Later...	16.5	....	Just seen	1
Outgoing series after several hours' rest.	17.8	0	No corona	0
	19.1	0	No corona	0
	21.1	2.2	cor	3
	23.1	3.6	cor	16
	25.0	3.1	cor	9
	26.5	3.7	cor	19
	28.2	7.1	w y g	120
	30.3	9.7	w o g′	270
	32.1	11	w y b g	390
	32.8	12	g B P	470
Promiscuous results.				
V.				
Mar. 20	[5]29.8	....	g B P	450
Later...	30.0	....	y o b g	370
	30.3	....	g B P	450
	28.0	....	g y o	390
	27.3	11	w r′ g	250
	26.2	....	w p cor	165
VII.				
Mar. 22	28.6	[5]6.9	g B P	120
	26.3	4.5	cor	33
	27.4	5.5	cor	62
	29.9	10	y o b g	330
	33.9	11	g B P	475
Later...	33.8	11	g B P	475
	32.7	....	g y o	420
X.				
X-rays; $D = 20$ cm.	33.6	11	g B P	470
	30.6	11	g B P	455
	27.9	11	g B P	430
	25.3	11	g B P	400
	21.7	5	cor	39
	21.6	5.0	cor	39
	22.5	10.5	w r g′	210
	23.5	....	g y o	340
	22.8	5.0	cor	40
	22.6	10	w y g	310
	21.5	3.6	cor	16
	21.6	3.7	cor	17

[1] $s = 3.8$ persistently except on first exhaustion.
[2] Many periods follow.
[3] Blurred; other coronas very clear, often multi-annular.
[4] Periods usually omitted.
[5] Fog chamber greasy.
[6] Followed in next exhaustion by small corona.
[7] Apparatus cleaned again.

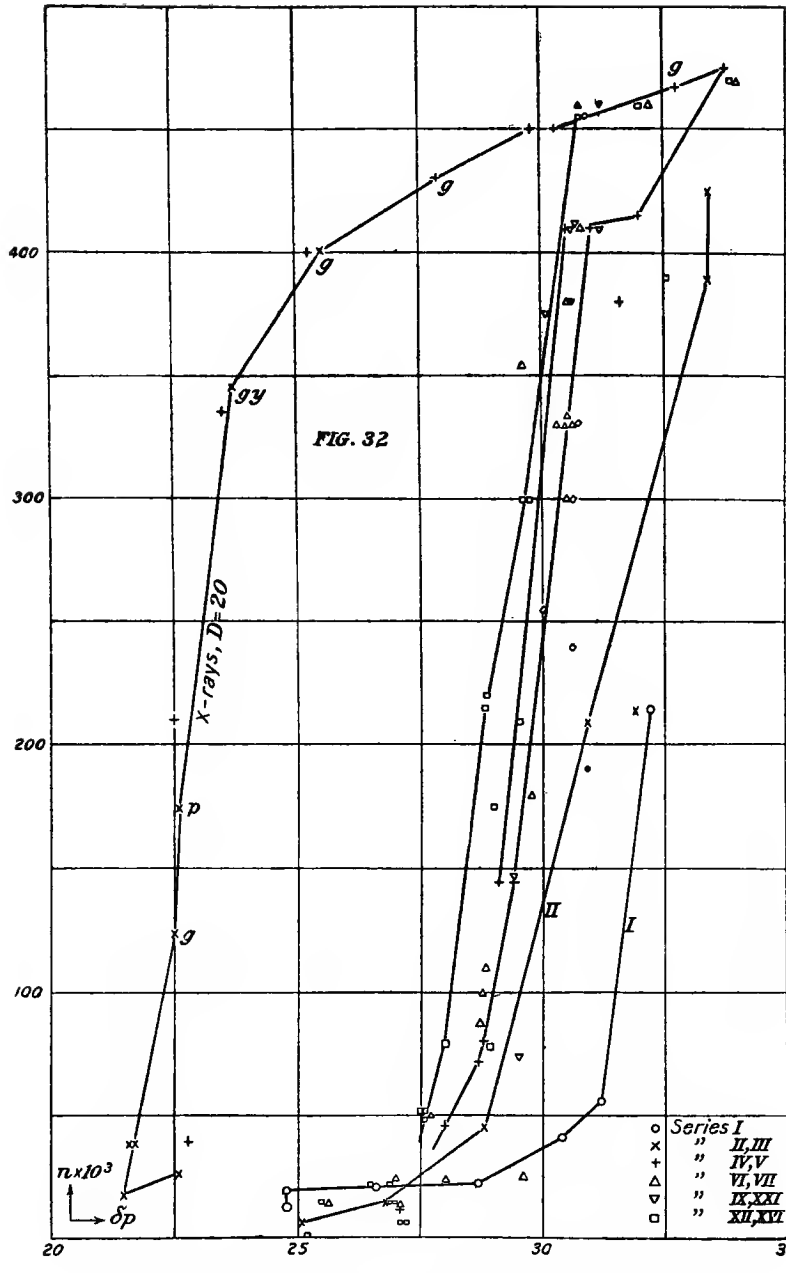

FIG. 32.—Nucleations (n) observed in dust-free air and dust-free X-air at different exhaustions (δp); 4-inch pipes. Table 23.

TABLE 22.—Systematic work. Third cleaning of apparatus. Isothermal $\delta p = p - p_n$; $p = 76$ cm.

	δp.	s.	Cor.	$n \times 10^{-3}$.		δp.	s.	Cor.	$n \times 10^{-3}$.
I.					VII.				
Mar. 26	24.8	3.4	cor	13	Mar. 30	30.5	11.5	yo bg	330
	24.8	3.8	....	20		30.5	10.7	w o g	300
	24.8	3.9	....	20		28.8	6.5	w r g	100
	26.6	3.9	cor	21		29.6	10.5	w r g	25
	28.7	4.0	....	23		33.0	13	g B P	470
	30.4	4.7	....	42	Later...	32.2	12	g B P	460
	31.2	5.2	w b r	56	VIII.				
	32.2	8.6	w p	215	Mar. 31	30.8	11.5	g B P	460
II.						30.8	12.5	g y o	410
Later...	33.4	13	g y o	425		29.6	11.5	y′ y bg	355
	33.4	9.5	w p cor	240		27.7	5.2	w r	50
	33.4	11.5	w y b g	390	IX.				
	33.4	9.5	w b r	250	Apr. 1	31.2	12	g B P	460
	30.4	8.7	w p cor	210		31.2	13	gyo	410
	28.8	5.0	cor	46	Later...	30.6	12	gy o	410
	26.8	3.5	cor	15		30.1	11	w y bg	375
	25.1	2.7	cor	7	X.				
	22.0	2.1	Faint cor	2	Apr. 2	30.7	12	gy o bg	410
						30.6	12	y′ g bg	380
III.						30.6	7.8	w b r b	180
X-rays	21.5	3.8	cor	18	XI.				
from	23.7	11	Vague g y o	345	Apr. 3	29.4	7.7	w P B	147
$D = 20$						29.5	5.8	cor	74
cm.	22.6	4.4	cor Vague	27	XII.				
					Apr. 4	29.7	11	yo bg	300
	22.5	6.7	g B P	124		29.6	11	w o g	300
	22.6	8.7	w p cor	175		28.8	8.8	w P B	220
	25.5	....	g Fog	400		29.0	[3]8.3	w P ?	175
IV.						28.0	6.0	cor	80
Mar 27,	[1]30.5	....	g y o	410	XIII.				
2d day.	31.6	10	yo bg	380	Apr. 6	33.9	[3]13	g B P	470
	29.1	10	w o g	145		26.5	3.9	cor	22
V.						26.9	3.9	cor	22
Later...	31.0	12	g y o	410		27.6	5.2	cor	52
	30.4	4.8	cor	45		28.8	8.9	w P	215
	29.4	7.4	wp	145		27.6	7.3	w y	120
	28.7	5.8	cor	72	XIV.				
	28.0	5.0	cor	46	Apr. 7	27.5	7.4	w r g	120
	27.1	3.3	....	12		27.5	....	cor	....
	28.0	4.2	....	27		27.5	5.2	cor	52
	28.8	6.0	w y	80		27.6	5.1	cor	49
					XV.				
	30.0	7.2	w B P	150	Apr. 8	27.2	[2]2.7	cor	7
	30.6	8.1	wP cor	180		27.0	3.5	cor	15
	31.4	7.0	w y	130		26.9	[4]3.5	cor	15
	32.0	11	gy	415		25.5	3.0	cor	15
	33.8	....	g B P	475	Series Apr. 8				
VI.					(55)	25.2	1.3	cor	1.5
Mar. 28,	34.0	13	g B P	470	(56)	27.1	2.6	cor	6.4
3d day.	32.0	13	g y o bg	415	(57)	28.9	5.9	wrg	78
	30.5	12	w y b g	380	(57′)	....	8.4	wP cor	210
	29.8	8.0	w b r b	180	(59)	32.5	12.5	w y g	390
	28.8	6.5	w r g	110	XVI.				
	28.0	4.1	cor	24	Apr. 10				
	27.0	4.1	cor	24	(58)	32.0	13	g B P	460
Later...	30.5	10.6	y o g′	330		30.8	13	gy o	455
	28.7	6.3	cor	88	XVII.				
	27.1	3.4	cor	14	Apr. 13	30.0	10.5	w r g	255
	25.6	3.4	cor	14		30.6	9.5	w r g	240
VII.					Apr. 14	30.7	12.5	y g bg	380
Mar. 29,	30.3	....	yo bg	330		30.6	11.5	w o g	300
4th day.	30.6	11	yobg	330	Apr. 15	30.9	13.	g y to g	455
	30.6	9.4	w c g	230					

[1] Alternate observations.
[2] Apparatus (fog chamber) blurred.
[3] After thorough cleaning.
[4] Warming with burner clears the glass.

while there is evidence of slight improvement, irregularities are at times increased. The final data in the table relate to the effects of X-rays from short distances ($D = 20$ cm. to anticathode), and the peculiar feature here is the steepness of the line as compared with earlier results. The reason is in part due to the admission here of $\delta p = p - p_3$ instead of the *observed* δp as heretofore, the effect being to displace upper observations relatively more to the left. It is already quite clear, however, that neither for X-air nor for ordinary air have the earlier data been much improved. The highest corona attained in both cases is again the green-blue-purple type.

TABLE 23.—Atmospheric air. Two observations daily. Water nuclei removed by low exhaustion. $\delta p = p - p_3$. Aug. diameter $s/30$ nearly. Fog chamber 40 cm. from eye, 250 cm. from light.

Date.	Observed.				Computed.	
	δp.	s.	Cor.	$n \times 10^{-3}$.	$p - p_2$.	$n \times 10^{-3}$.
May 17	30.6	....	g B P	450	23.7	385
	30.8	12	g B P	450	23.9	385
May 19	29.0	11	w y o g	320	22.5	270
May 20	28.8	11	w r o g	290	22.3	245
May 19	27.2	4.2	cor	27	21.1	22
May 21	27.4	3.6	cor	18	21.3	15
May 22	27.1	2.9	cor	8	21.0	7
Mar. 24;	33.6	....	g B P	....	26.0	410
X-rays	30.6	....	g B P	....	23.7	385
from D	27.9	....	g B P	....	21.6	360
$= 20$.	25.3	....	g B P	....	19.6	335
	21.7	5	cor	....	16.8	32
	21.6	5.0	cor	....	16.7	32
	22.5	10.5	w r g′	....	17.4	175
	23.5	....	g y o	....	18.2	290
	22.8	5.0	cor	....	17.7	34
	22.6	10.0	w y g	....	17.5	260
	21.5	3.6	cor	....	16.6	13
	21.6	3.7	cor	....	16.7	14
Mar. 26	21.5	3.8	cor	....	16.6	15
	23.7	11	gyo	....	18.3	290
	22.5	6.7	g B P	....	17.4	105
	22.6	8.7	wp cor	....	17.5	145
	25.5	....	g fog	....	19.8	335

50. Observations, continued.—In the experiments of table 22 much difficulty was experienced with the apparatus, as the use of oil with the large stopcock was often liable to show itself in the blurred walls of the fog chamber whenever this was wetted with water. It is usually sufficient to heat these walls gently, in order to evaporate the suspicion of

an oil film which has here collected, after which the walls remain clear for some time on wetting. Prior to the systematic investigation of table 23, however, the apparatus was thoroughly overhauled and cleaned. The δp referred to is henceforth to be $p - p_3$, *i. e.*, the difference between atmospheric pressure and the pressure (p_3) observed when fog chamber and vacuum chamber are in communication at the given temperature.

Some time having elapsed since the last observation, the first experiments (parts I, II, etc.) of the tables show low nucleation, due to the presence of large nuclei originating internally, as already specified. Series III, with X-rays, agrees very fully with the preceding cases (table 22) and there is nearly the same steepness of curve ($\delta p = p - p_3$) already instanced. Conformably with this, series IV, V, etc., also show increased steepness of curve, the nucleation, moreover, being higher because the interior sources of relatively large nuclei have been gradually removed. But there is throughout much irregularity, and periods are frequent. Remembering that above the δp referred to is the drop of pressure observed in the fog chamber, while at present $\delta p = p - p_3$, a slight advance of the highest nucleations over the preceding cases is discernible.

51. Observations, continued.—In table 24 observations are recorded, made once or twice a day, far enough apart to allow water nuclei to vanish by time loss. After each measured corona a low exhaustion was (as usual) made to remove the greater number of such nuclei at once in the large particles of the small corona produced. The pressure difference (δp) is again $p - p_3$, as explained in section 48, so that the correction there adduced may be applied. The fog chamber was rigorously tight as regards the influx of external air, but air flowed slowly from fog chamber into the vacuum chamber, through the leaky stopcock. Between the exhaustions the air was kept at low pressure for about ten hours, and new air was admitted, just before exhaustion, through the filter into the fog chamber, until the barometer pressure had been reached. As the whole apparatus had been left standing a long time, dust-free air only was present in the fog chamber and vacuum chamber. The walls of the former were rubbed clean before beginning the work.

The table also contains the above data for air energized by the X-rays with anticathode distant 20 cm., observations being made while the radiation acted and immediately after the exposure began, to avoid the presence of persistent nuclei. The computed values for the drop in pressure ($p - p_2$, where p_2 is the computed isothermal pressure in the isolated fog chamber alone), and the corresponding values of n, are also given. The nucleation refers as usual to the exhausted fog chamber. The results are constructed graphically in fig. 33.

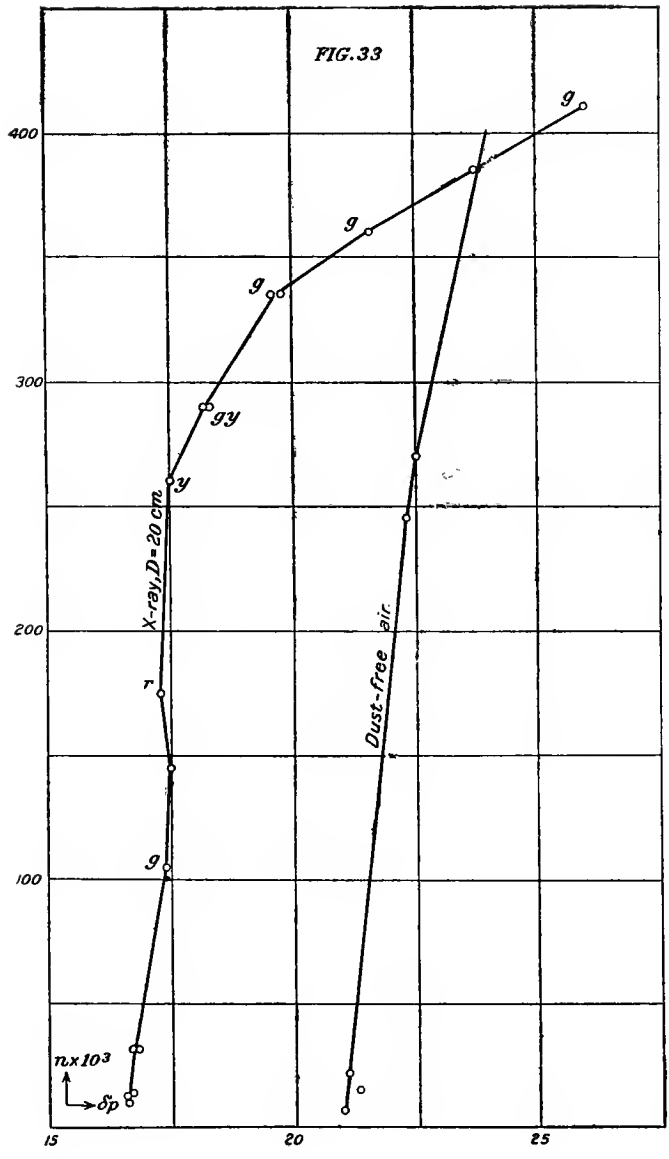

FIG. 33.—Nucleations (n) observed in dust-free air and dust-free X-air at different exhaustions (δp); 4-inch pipes. Table 23.

52. Discussion.—The new curves (fig. 33) lie nearer together for the energized and non-energized states of the gas. This obviously results from the correction applied to the observed values of δp. Neither do the graphs ascend as highly as they did before, for the same reason, remembering that the nucleation (n) always refers to the exhausted fog chamber. Again, the new curves must be steeper than the old; but both of them, *i. e.*, the curves for the non-energized and for the energized gas, have about the same slope, so far as can be made out for the case of such steep curves as those under consideration. Nevertheless, it is probable that there is some other reason implied in this, which is yet to be made out. For the ionized state the observations frequently suggest a kind of saturation beyond which the ions pass into persistent nuclei very much as a vapor condenses. In other words, a maximum ionization pressure, determined by a definite number of ions per cubic centimeter, which can be approached as the radiation is more and more intense, but not exceeded, is a useful conception in connection with many of the experiments given.

53. Summary.—The general summary of this chapter has already been given in sections 42, 43, and 52, particularly in the former, with regard to fig. 25, and need not, therefore, be repeated here. The highest order of available coronas has been invaded and surpassed.

It appears that the limits of efficiency of the practical fog chamber with rapidly opened plug cock have been reached when the long cylindrical vessel of about 6,000 c. cm. is exhausted into a vacuum chamber of about 100,000 c. cm. through a pipe not less than 5 cm. in bore nor more than 50 cm. long, with a stopcock of wider diameter (7 to 8 cm.) interposed. To test this again, such a fog chamber was adjusted as shown in fig. 34 (V vacuum chamber; F fog chamber; G, g, gages at the former and the latter, the whole mounted on casters to admit of shaking the water in F; goniometer attached to fog chamber). The results are given, both for fog chambers Nos. I and II, in tables 24 and 25, with corrections for the barometer as explained in Chapter VI, sections 100 and 101, and they are charted on a small scale with other data (table 23) in fig. 35.

The graph for chamber number II would coincide with data inferred from Wilson's colors for small coronas; but for large coronas it actually lies in a region of lower exhaustion—to which however, too much importance must not be attached, because of the difficulty of identification. The point is that the apparatus of 2-inch pipes is quite the equal, if not the superior, of the apparatus with 4-inch pipes, in the region of both the lower and higher coronas. Curiously enough, the apparatus I

(4-inch cock) gives an excess of ions, whereby the graphs for I and II in the region of lower coronas are consistently distinct. I will pass this over here, as it needs additional investigation.

That the limit of efficiency has been reached for plug-cock apparatus is specifically proved by the fact that the same large green-blue-purple

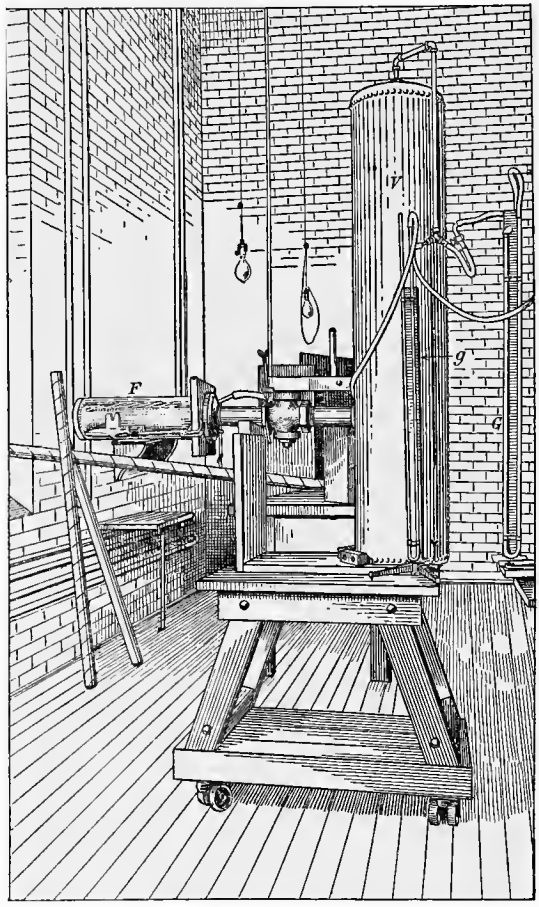

FIG. 34.—Disposition of apparatus in case of fog chamber (F) and vacuum chamber (V), connected by 2-inch pipes and 2½-inch stopcock.

corona terminates the observations, no matter whether the nuclei are relatively large, as in case of the ions and intense X-radiation, or relatively small, as in case of the colloidal nuclei. This is differently proved in the work with alcohol, in Chapter IV.

It is somewhat hard to understand why the efficiency should terminate abruptly, with a certain *number* of nuclei per cubic centimeter, no matter

whether large or small nuclei are in question. One should expect these conditions to depend on the size of nuclei; but (as the data show) even though larger numbers of nuclei are certainly present, they are devoid of efficiency beyond the limit.

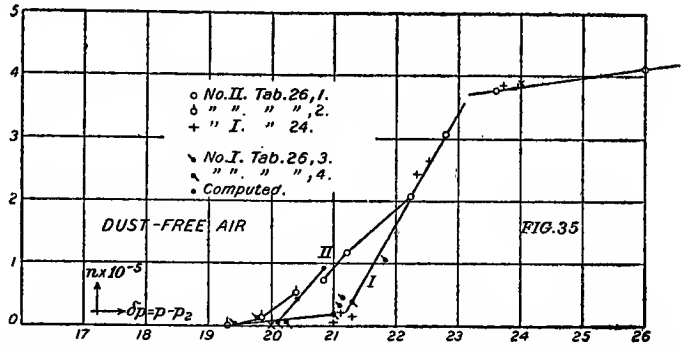

FIG. 35.—Nucleation (n, in hundred thousands of nuclei per c. cm.) observed in dust-free air and in energized air at different exhaustions. $\delta p = p - p_2$. 2-inch and 4-inch pipes and perfected apparatus I and II. Tables 23, 24, and 25. Ions in No. I consistently in excess.

TABLE 24.—Fog chamber and vacuum chamber as in fig. 34, joined by 2-inch pipes, $2\frac{1}{2}$-inch plug stopcock. $\delta p = p - p_3$. Final series for comparison.

	δp.	s.	Corona.	$p - p_2$.	$n \times 10^{-3}$.	s corrected.*	$n \times 10^{-3}$ corrected.
I. Barometer 76.2	25.9	3.2	cor	20.1	9.5	3.4	11.6
	26.9	6.4	w p′ g	20.8	76	6.6	83
	27.4	6.8	g B P	21.2	120	....	....
	28.7	10.2	wr g′	22.2	210	....	....
	29.4	12	yr	22.8	310	....	....
	30.5	13?	g B P	23.6	380	....	....
	33.5	13?	g B P	26.0	410	....	....
II. Barometer 75.5	24.9	1.7	cor	19.3	1.8	1.3	1.4
	25.6	3.6	cor	19.8	15	3.2	9.9
	26.4	5.6	cor	20.5	53	5.2	42

TABLE 25.—The same; 4-inch stopcock, apparatus I.

	δp.	s.	Corona.	$p - p_2$.	$n \times 10^{-3}$.	s corrected.*	$n \times 10^{-3}$ corrected.
III. Barometer $p = 75.8$, July 14.	25.5	? 3.7	cor	19.7	15	3.6	....
	27.2	4.9	....	21.1	37	4.8	....
	25.0	2.4	....	19.4	4	2.3	....
	28.1	7.2	y′ b P	21.8	110	....	....
	27.3	5.3	....	21.1	45	5.2	....
IV. $p = 75.9$, June 3.	27.1	4.2	cor	21.0	22	....	....
	25.9	2.8	....	20.1	6	....	....
	26.1	2.7	....	20.2	6	....	....
	27.4	5.0	....	21.3	40	....	....

*Correction for barometer made as explained in Chapter VI.

In no form of the fog chamber have the initial yellows and browns of the steam jet been approached. Coronas reach but to the equivalent of the opaque zone. Below the large green-blue-purple corona, the computed value of the water precipitated per cubic centimeter may now be considered trustworthy. In Chapter I this was true below the middle green-blue-purple corona. The drop of pressure $(p - p_2)$ actually efficient in producing low temperatures in the fog chamber must be computed from the initial pressure of the isolated fog and vacuum chambers before exhaustion, and their final pressure when in communication after exhaustion, all data taken at the same temperature.

As the intensity of radiation increases, coarser nuclei become much more frequent, but beyond this the coronal method is not adapted to test the lower limit in question. At the upper limit, however, most of the observations show that the finer nuclei become more abundant when the medium is more powerfully energized; or that new gradations of nuclei of continually increasing smallness and continually increasing number are produced by radiation increasing in strength indefinitely. These are important questions, however, upon which I hope in the near future to make some final tests.

CHAPTER III.

MISCELLANEOUS EXPERIMENTS.

54. Objects.—Having perfected the coronal fog chamber to the degree specified in the earlier sections of Chapter II, it seemed expedient to make use of it for a variety of purposes partly corroborating and interpreting my earlier work, partly introducing new results. In particular, the growth of persistent nuclei in a highly ionized medium in the lapse of seconds, the occurrence of solutional nuclei, and like questions may be studied by the *depression* of the terminal asymptote produced by the introduction of relatively small numbers of larger nuclei into the medium. Again, the effects of radiation from different distances on the medium of the fog chamber, the absorption of such radiations, the distributions within the fog chamber, etc., may be elucidated by this treatment. Finally, some consideration of the rates of generation and decay of ions is in place and a method will be shown for the standardization of coronas. Some final remarks will be made on the steam jet and on the relation of its color phenomena to those of the fog chamber.

Throughout this chapter δp refers to the drop of pressure observed at the isolated fog chamber under isothermal conditions, the exhaust cock being closed as soon as possible after the expansion. The necessary reductions (should they be needed) may be made as shown in the preceding section.

55. Growth of persistent nuclei.—In table 26 (illustrated by fig. 36) the time during which the fog chamber was exposed to the X-rays, with the anticathode at a distance of $D=10$ cm. from the fog chamber, is given in the first column. The coronas and the number (n) of nuclei per cubic centimeter follow.

The two series of experiments made show that there is a gradual increase of the number of persistent nuclei, evidenced by the gradual reduction of the number of efficient nuclei. In less than two minutes, however, the phenomenon becomes more stationary, indicating that the full number of persistent nuclei is being approached, or that there are now about as many made as are unmade per second. It is difficult to follow the phenomenon beyond this, for the coronas now become campanulate or otherwise distorted, appearing in association with heavy fogs. The true asymptote is probably far off. These data furnished good illustrations bearing on the remarks of section 42, Chapter II.

TABLE 26.—Persistent nuclei produced after different lapses of time. Method, depression of asymptote. $\delta p = 26.4$ cm.; $D = 10$ cm. above side of cylindrical glass fog chamber; cock $1\frac{1}{2}$ inches; exhaustion during exposure.

Exposure.	s.	Corona.	$n \times 10^{-3}$.
sec.			
0	13	g B P	410
30	12	w y g′	340
60	11	w o g′	270
90	7.5	(1)	140
120	7.6	(1)	140
30	13	w y g′	340
60	11	[1]w r g	230
90	9	(1)	200
0	14	g B P	410

[1] Tempestuous fog and rain, leaving smaller corona. Second exhaustion made for safety, showing small corona.

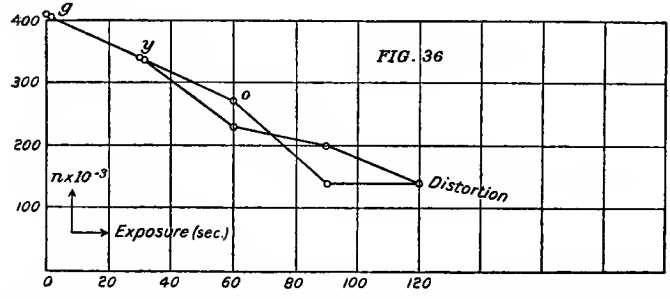

FIG. 36.—Depression of efficient nucleation (n) of dust-free air ionized by strong X-rays at a given exhaustion, by accumulation of persistent nuclei in the lapse of time. Table 26.

56. Water nuclei produced by evaporation.—A beautiful method of demonstrating the production of water nuclei in connection with the condensation of fog consists in leaving the cock for influx of air from the filter slightly open. In such a case the fog begins to evaporate as soon as produced, and there will be less loss from subsidence of fog particles, in proportion as the evaporation is more rapid; in other words, as the stopcock is more widely opened. Table 27 shows results of this kind and they are reproduced in fig. 37, where the abscissas are distributive. In every case the efficient nucleation (n) of dust-free air, after complete subsidence of the preceding fog, is much in excess of n', the nucleation observed when the fog is dispelled by evaporation. The table also proves that the degree to which the filter cock (fine screw valve) is open does not influence the result.

TABLE 27.—Enlargement of nuclei of dust-free air. Glass fog chamber, single wet cloth partition. $\delta p = 30.9$ cm.; s found after complete subsidence of preceding corona; s' after partial subsidence with evaporation.

Date.	s.	s'.	Cock open.	$n \times 10^{-3}$.	$n' \times 10^{-3}$.	s.	$n \times 10^{-3}$.	Remarks.
			°					
Oct. 17	[1]7.0	...	45	135	..	[2]7.4	140	Full subsidence but with quick opening of cock (90°) thereafter.
	[3]7.0	...	45	135	..	7.4	140	
	...	5.8	45	...	76	7.5	140	
	7.0	...	45	135	..	...	...	Same, but with slow influx.
	...	6.0	45	...	84	7.4	140	
Oct. 19	7.1	...	45	135	..			
	[4]7.3	...	45	150	..			
	7.3	...	45	150	..			
	...	[5]5.7	45	...	72			
	[4]7.4	...	45	150	..			
		[5]6.2	45	...	88			
	[4]7.5	...	90	150	..			
	...	[5]3.0	90	...	10			
	[2]7.2	...	90	140	..			

[1] After many days' waiting.
[2] w o g.
[3] After few minutes' waiting.
[4] g B P.
[5] Blurred with much rain.

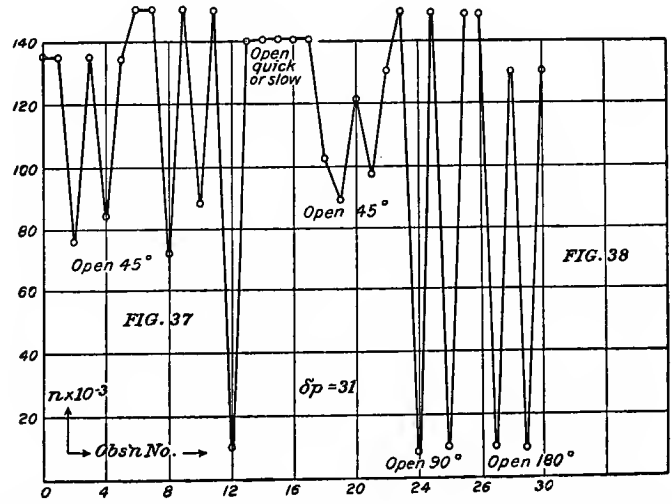

FIGS. 37 and 38.—Periodic variation of efficient nucleation (n) in case of an open filter cock. Tables 27 and 28.

In table 28 and fig. 38 the occurrence of periodic variation in the angular diameter of successive coronas and the corresponding efficient nucleation is shown by the same method of a permanently opened filter cock. The conditions of all of the exhaustions are quite identical; but the small fog particles of large coronas evaporate faster and in greater numbers than the larger particles of smaller coronas. Hence the water nuclei are present in like periodic distribution. The effect is more striking when the stopcock is opened wider. The difference between 180° and 90° in the adjustment of the cock is not marked, because the filter itself introduces resistance to flow.

TABLE 28.—Corresponding to table 27. Periodicity due to permanent open filter cock.

	s.	s'.	Cock open.	n.	n'.
			°		
Oct. 20 ..	..	[1]6.5	45	..	102
	..	[2]6.2	45	..	89
	..	[1]6.9	45	..	121
	..	[2]6.4	45	..	96
	..	[1]7.1	45	..	130
	..	[1]7.5	90	..	150
	..	[3]2.8	90	..	7.8
	..	[4]7.2	90	..	150
	..	[3]3.0	90	..	10.0
	..	[4]7.2	90	..	150
	..	[4]7.4	180	..	150
	..	[3]3.0	180	..	10
	..	[1]7.0	180	..	130
	..	[3]2.9	180	..	9
	..	[1]7.0	180	..	130

[1] w o g.
[2] w r g. Note the periodicity of the series.
[3] Blurred with rain.
[4] g B p.

TABLE 29.—Corresponding to table 27. Effect of δp; cock open during exhaustion.

	δp.	s'.	Cock open.	n'.
			°	
Oct. 22	26	3.6	45	17.1
	26	2.6	45	6.3
	26	2.7	45	7.1
	28	5.9	45	77
	28	4.4	45	31
	28	5.2	45	53
	30	7.0	45	125
	30	6.1	45	85
	30	6.9	45	120
	30	6.0	45	85
	30	6.6	45	105
	..	7.3	Closed	135

In table 29 the effect of different drops of pressure (δp) is investigated for low exhaustions and smaller coronas and there is scarcely any periodicity. As the exhaustion is higher, periodicity in the size of successive coronas is correspondingly marked. The data give an estimate as to the degree in which periods are to be guarded against.

In table 30 experiments similar to the preceding are made with ionized air. It will be seen that the periodicity is in every case just as marked as before. In the absence of evaporation (closed filter cock) the successive coronas are equal. Precipitation at a low drop (δp) of pressure is followed by a relatively large corona at a higher drop of pressure, as the water nuclei have been removed in the former.

TABLE 30.—Periodicity of ionized air. X-rays; $D = 50$ cm. Filter cock permanently just open. Exhaust cock $2\frac{1}{2}''$; $\delta p = 23$ cm. below fog limit of dust-free air.

Exp. No.	s.	Cor.	$n \times 10^{-3}$.
1	10.5	w r g	210
2	6.3	cor	75
3	9.6	w c g	200
4	5.0	cor	41
5	10.4	w r g	210
6	5.6	cor	58
7	9.2	w c g	190
Filter cock closed during exhaustion and subsidence.			
8	[1]9.3	w c g	190
Dust-free air not energized; $\delta p = 31$; repetitions without waiting Dec. 13; internal evolution of nuclei has ceased.			
....	11.5	w y g	335
....	11.5	w y g	335
Dust-free air not energized; $\delta p = 36$ cm.			
....	13.5	g | P	480
....	13.5	g | P	480
Evap. nuclei precipitated at $\delta p = 23.2$ cm. and then tested at $\delta p = 31$.			
1	3.0	cor	8
2	0.0	——	0
3	——	[2]g y o	410

[1] No difference between 7 and 8. [2] Corona enlarged by the preceding precipitation.

Some interesting questions present themselves in connection with this work. Are the nuclei holding positive ions different from those

holding negative ions? Do they retain their charges, or some equivalent of the charges? As there is less mobility and slower recombination in cases of ions entrapped by water nuclei, one would infer greater opportunity for the gravitational separation of the equivalents of the positive and negative charges; for it seems improbable that the water nuclei resulting can be of the same size.

Finally, in table 31 data have been gathered showing the gradual self-purification of the fog chamber, after cleansing and sealing. Nuclei arising from some internal source cease to appear in the mere lapse of time and without further interference. The coronas s_1 and s_2 are observed in successive exhaustions at the time (days and hours) given. Initially the first corona is smaller in marked degree, owing to the spurious nucleation within. After more than three days, however, both coronas s_1 and s_2 are identical.

TABLE 31.—Purification of the fog chamber in the lapse of time. $\delta p = 31$. Exhaust cock $2\frac{1}{2}$ inches; piping 12 inches long, 2 inches in diameter.

Date.	Hour.	s_1.	Cor.	s_2.	Cor.	$n_1 \times 10^{-3}$.	$n_2 \times 10^{-3}$
Nov. 30	10 a. m.	4.6	.....	11.5	.....	40	305
	5 p. m.	7.5	g B P	12.0	w y g′	150	380
Dec. 1	10 a. m.	8.0	w P cor	11.7	w y g′	180	380
	6 p. m.	[1]9.7	w c g′	....	g y o	275	410
Dec. 2	.....	9.2	w r g	11.4	w o g	230	305
13	.....	11.5	w y g	11.5	w y g	305	335
	.....	[2]14	g′	14	g | P	460	460

[1] Vacuum maintained some hours. [2] $\delta p = 36$. Internal source of nucleation absent.

The source of this transient internal nucleation is difficult to detect. There were no leaks. Oil evaporation if harmful would be continuous. The same differences of fresh and stagnant air in relation to s_1 and s_2 are always reproduced. There is no evidence that anything in the vacuum chamber is capable of diffusing into the fog chamber. Some agency therefore, which is productive of relatively large nuclei, and the nature of which is not clear, survives many consecutive precipitations.

57. Distance effects. X-rays.—In the following experiments I endeavored to overhaul the curious results obtained when the X-rays strike the fog chamber from different distances, without, however, reaching very satisfactory conclusions. The object of the following work is to bring to bear the newly improved means on the problem. In table 33 data are given as obtained with the glass fog chamber, the drop of

pressure (δp) being below the coronal fog limit of dust-free air. Hence there are no complications from colloidal nuclei. In parts I and II of the table the X-ray bulb was not inclosed in the windowed lead vessel specified, whereas in part III this is the case; while in part IV a tin plate has been placed over the window.

TABLE 32.—Distance effects due to X-rays. Fog chamber of glass with 2.5-inch gas cock and 2-inch piping 12 inches long. X-ray, 7 cells. $\delta p = 23.8$ cm.

	D.	s.	Corona.	$n \times 10^{-3}$.
I. Bulb not inclosed; meters.....	0.5	10.0	w c g	220
	6.0	6.3	cor	80
	...	6.2	.....	75
	2.0	7.3	w′ B P	115
	...	7.4	w′ B P	120
	.5	11.0	g y o	260
$\delta p = 20.3$ cm.				
II. Same; bulb not inclosed.....	0.5	...	w B P	90
	...	7.2	w B P	100
	2.0	5.2	.....	42
	...	5.2	.....	42
	6.0	3.5	.....	13
	...	3.5	.....	13
	4.0	3.6	.....	15
	...	4.5	.....	28
	1.0	6.4	w r g	75
	...	6.3	w r g	70
	.5	7.2	w y g	100
		7.3	w y g	105
$\delta p = 22.7$; X-ray bulb in lead case[1] with window 7.5 cm. in diameter.				
III. Window open.....	600	4.1	cor	22
	400	4.4	cor	27
	200	6.5	w r g	85
	100	7.5	g B P +	135
	...	7.5	g B P +	135
Lid off.....	...	7.5	g B P +	135
Same. Tin plate[1] over window.				
IV. Tin window	600	2.7	cor	6.5
	200	4.9	cor	40
	100	6.9	w r g	99

[1] Lead sheet 0.12 cm. thick; tin plate 0.03 cm. thick.

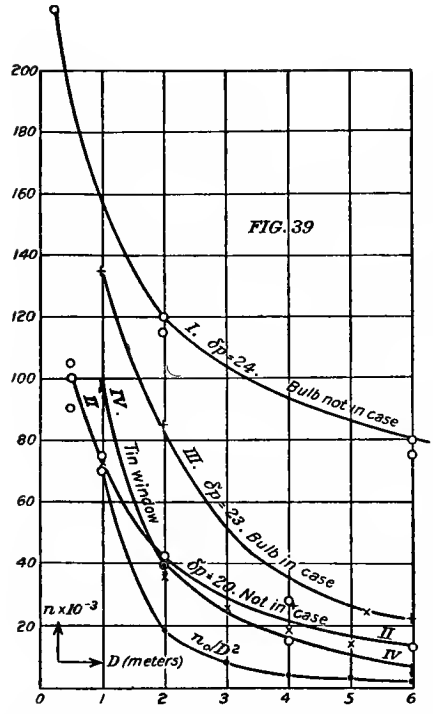

FIG. 39.—Nucleation (ions) produced by a radiating X-ray bulb (cased in lead or not as stated), at different distances (D) from the glass fog chamber. Table 32.

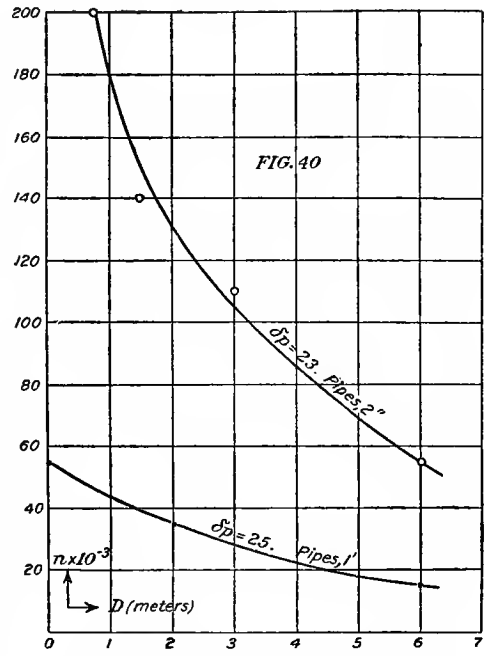

FIG. 40.—The same, illustrating table 15, Chapter II.

The curves I and II, fig. 39, for the free bulbs show different nucleations, compatibly with the different values of δp applied, but are otherwise alike in character. They in no way suggest the law of inverse squares. The curves III and IV for the inclosed bulb are again similar in character, but beyond this very little can be stated. If in case of series II and III, for instance, the law

$$n\,(A+D)^2 = \text{const.}$$

is assumed, the constant A would have to be from 1.2 to 2.7 meters in the first case, and 1.5 to 2.1 meters in the second, which is entirely out of the question for a fog chamber less than 0.5 meter long. If the law

$$n\,(A+D) = \text{const.}$$

is used, in the first case (II) $A = 0.3$ to 0.1 meter; in case III, $A = -0.2$ to -0.6 meter. This decrease would then be too fast in the first case and too slow in the second, or the decrement in case of the open bulb is

slower and in case of the inclosed bulb (lead box with window) faster than the first power of distance.

In fig. 40 I have inserted data incidentally obtained in Chapter II, table 15 (upper curve), together with data of the same kind in the earlier reports (lower curve). The former are the steepest curves obtained and the latter the least so. Here, as elsewhere, it is difficult to conjecture a reason for this apparently erratic difference of behavior, unless it be referred to the facility with which secondary radiation is evoked, and to the degree in which the fog chamber is pervious to it or generates it. Since $dn/dt = a - bn^2 = 0$, where a is the number of ions produced per second, a must vary as the square of the number of ions, n, observed.

58. The same, continued. Small wood fog chamber.—The data of the last paragraph with the glass fog chamber suggest a comparison with the wood fog chamber. The latter is much the more pervious and in the earlier work showed a much smaller distance effect. Table 33 contains eight series of results. In series I, fig. 41, the march is not unlike the case for the glass chamber; but in series II the insignificant difference between a bulb distance of 50 and 100 cm. from the fog chamber (curves III and IV) are similar to I, and often betray the incidental weakening of the X-ray bulb. In the series VI to VIII, change of the drop of pressure (δp) was introduced, but the inherent difficulty of coping with the bulb variations is seen in the details in fig. 43.

It is probable that the ordinates of the curves V to VIII (figs. 42 and 43) are proportional to each other; but a discussion is beyond my present purpose. The slow order of change with distance should, however, be noticed.

59. The same, continued. Large wood fog chamber.—It is with this apparatus that the coronas of almost the same aperture were obtained in the earlier work, while the X-ray bulb was moved from 1 to 6 meters from the fog chamber. Table 34 and fig. 44, however, show that this result must have been due to other conditions, for there are changes of nucleation here registered amounting in case of the distance specified (1 to 6 meters) to $n'/n = 145/104$ at $\delta p = 22$; $77/41$ at $\delta p = 19$. For greater pressure differences, $\delta p = 25$ and 29, the occurrence of terminal coronas would interfere with the comparisons. At higher exhaustions still, the efficiency of air nuclei would be gradually restored, so that the observed nucleation may be greater with the bulb at 6 meters than at 1 meter from the fog chamber (see Chapter II, figs. 24 and 25). At the very low exhaustion $\delta p = 17$ the coronas are too small to be serviceable for comparison.

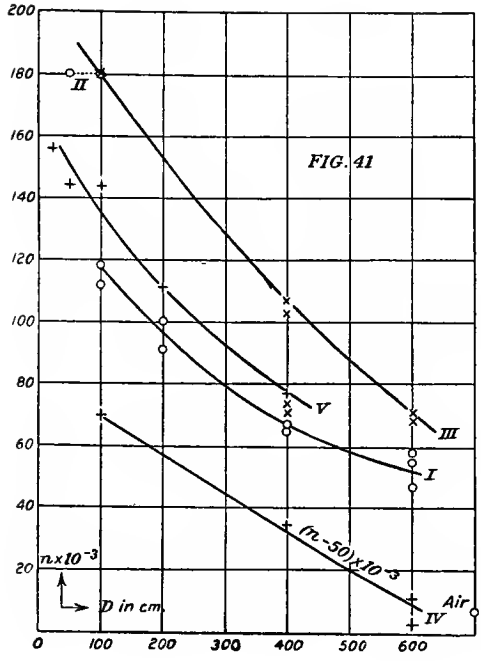

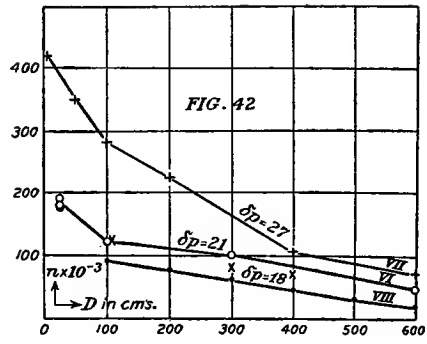

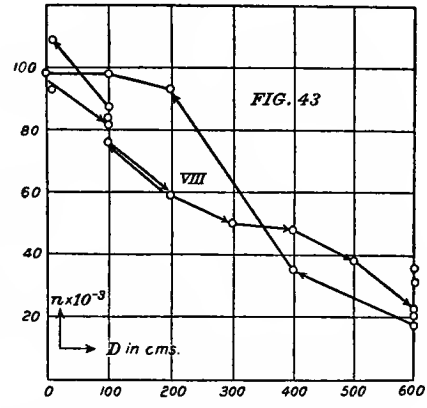

FIGS. 41, 42, and 43.—Nucleatious (ions) produced by a radiating X-ray bulb at different distances (D) from the small wood fog chamber. Table 34.

With regard to the work of table 34 it should be stated that it is always customary to make a second exhaustion to remove the water nuclei left by the first. Again but two distances (1 and 6 meters) were selected to guard against losses of efficiency of the X-ray bulb, so far as possible. The exhaustion was made during the exposure, which was always brief. At the distance $D=6$ meters from the bulb, there is a terminal corona at $\delta p=22$ cm.; at $D=1$ meter it appears a little later at $\delta p=25$. (See Chapter II, figs. 24 and 25.) In fig. 45 the corresponding points are joined by straight lines, for convenience.

60. The same, continued. Discussion.—Experiments of the present kind are hampered by two annoying difficulties, the first being the variability of the X-ray bulb, the other the tendency of the wooden fog chambers to develop slight leaks which often pass unobserved. True, the chamber is tested by a second exhaustion after each of the coronas measured; but the unfiltered atmosphere entering anywhere is liable to

produce a disproportionate amount of distortion, because of the relatively large size of the nuclei contained. Hence it is of little value to attempt to systematize the above results in the absence of a well-digested

TABLE 33.—Revision of distance effect. X-rays. Small wooden fog chamber 15 × 11 × 45 cm. $\delta p = 21.7$ cm.

	D.	*s.*	Corona.	$n \times 10^{-3}$
I.	*cm.*			
X-rays off	....	[1]2.9	.....	7
X-rays on	[2]100	9.0	w r g	180
	600	5.3	.....	47
	600	5.6	.....	55
	600	5.7	.....	58
	400	6.1	w y′	67
	400	5.9	w r	65
	200	7.0	g′ B	100
	200	6.8	g′ B P	91
	100	7.4	.....	112
	100	7.6	w r	118
	100	7.4	.....	112
II.				
X-rays off	....	2.8	.....	7
X-rays on	100	[2]9.2	w r g	180
	50	9.2	w r g	180
	50	9.2	w r g	180
	100	8.7	w r g	180
	100	9.2	w r g	180
III.				
X-rays on	100	9.2	w r	180
	400	7.1	w y	103
	400	7.2	w y	106
	600	[3]5.6	cor	55
	600	6.2	.....	71
	600	6.1	.....	68
Bulb	400	6.3	g′ B P	74
weaker	400	6.2		71
IV.				
X-rays on	200	7.6	g B P	120
	400	6.6	g′ B P	85
	600	[3]4.4	.....	26
	600	5.5	w r g	53
	600	5.8		61
V.				
X-rays on	400	6.4	w b r	77
	200	7.4	w r	112
	100	7.9	w p	144
	50	7.9	w p	144
	25	8.5	wp′ g	156
VI.				
X-rays off	....	[4].0		0
X-rays on	25	9.6	w r g	190
	25	9.0	w p	175

	D.	*s.*	Corona.	$n \times 10^{-3}$
VI.	*cm.*			
X-rays on	25	9.0	wp	175
	100	8.0	w B P	120
	100	7.8	w B P	120
	300	7.3	w r o g	100
	300	7.3	w r o g	100
	600	5.4	w r g	50
	600	5.2	.....	45
High $\delta p = 27.5$.				
VII.				
X-rays off	....	[5]4.6	.....	6.5
X-rays on	600	5.8	.....	70
	400	6.7	w y′	105
	200	9.5	w r g	225
	100	11.0	w y o g′	280
	50	11.5	w y g	350
	10	....	g y o ?	420
VIII.	10	5.9	w y′	59
	....	7.6	w r	93
	100	7.2	w r	87
	10	7.4	g′ B P	109
	100	7.5	w y g′	84
	600	[6]4.1	cor	18
	....	[6]4.7	cor	31
	....	[6]5.0	cor	35
	400	[6]5.0	cor	35
	200	7.0	w r g	93
	100	7.6	w y g	98
	20	7.6	w y g	98
	100	7.3	w r g	82
	200	5.9	w r g	59
	300	5.6	cor	50
	400	[6]5.5	.....	48
	500	[6]5.1	.....	38
	600	[6]4.2	.....	21
	600	[6]4.3	.....	23
	100	[6]6.4	w r g	76

[1] $\delta p = 25.3$, $s = 5.7$. [2] Fresh bulb. [3] Battery current weak.
[4] Second exhaustion without rays made (after the first) to remove water nuclei.
[5] $\delta p = 28.1$, $s = 48$, $n = 57{,}000$; $\delta p = 29.7$, $s = 5.2$, $n = 55{,}000$; $\delta p = 31.9$, $s = 5.6$, $n = 71{,}000$.
[6] Coronas large on the near end and small on the far end of fog chamber. Subsidence oblique.

TABLE 34.—Revision of distance effects. Large wood fog chamber. 20×12×55 cm. Exhaustion during exposure.

	D.	s.	Corona.	$n \times 10^{-3}$.
$\delta p = 19.0$ cm.				
X-rays off	...	1.2	just seen	1.2
X-rays on	600	5.3	.....	43
IX.	600	4.5	.....	26
	100	6.6	.....	77
	600	5.2	.....	41
	600	5.1	.....	39
	600	4.0	.....	18
$\delta p = 21.8$ cm.				
X.	600	5.6	.....	56
	100	8.7	w p	145
	100	8.8	w p	145
	600	6.6	w r′	103
	600	6.5	w y	103
$\delta p = 25.1$ cm.				
XI.	600	6.5	w o g	112
	100	9.5	w r o g′	236
	600	7.0	w y	119
$\delta p = 17.1$.				
XII.	600	1.0	.....	1.0
	100	2.8	.....	5.3
$\delta p = 24.8$.*				
XIII.	100	9.5	w r o g′	236
	$\delta p =$	27.6		
	100	10.0	w r o g	254
	$\delta p =$	29.4		
	100	10	w r o g	265
	600	6.2	w r g	110
	100	10	w r o g	265

*Terminal corona; same for 7 and 9 cells.

theory of the phenomena; but the equations $n = n_0/(A+D)^2$ and $n = n_0/(A+D)$, where A is constant and D the distance between bulb and fog chamber, may be adduced to accentuate the order of values observed. This has been done in case of table 32, showing that for the non-incased bulb even the inverse first power of D varies more rapidly than the observed phenomenon. To a much greater extent is this true for the wood fog chambers. The phenomenon itself is clearly a case of superposition of primary and secondary radiation. The latter, moreover, is furnished not only by the environment of the X-ray bulb, as shown in fig. 39 by surrounding the bulb with a windowed lead case, but also by the immediate environment of the fog chamber. The small distance variation encountered would then seem to be explained by supposing that relatively much secondary radiation is released by relatively weak primary radiation, as compared with a case of strong primary radiation. Under all circumstances the total effect is an integral to be extended over the whole surface and possibly the interior of the room. Finally, one should recall that the rate at which ions are produced by the radiation must vary as the square of the number observed.

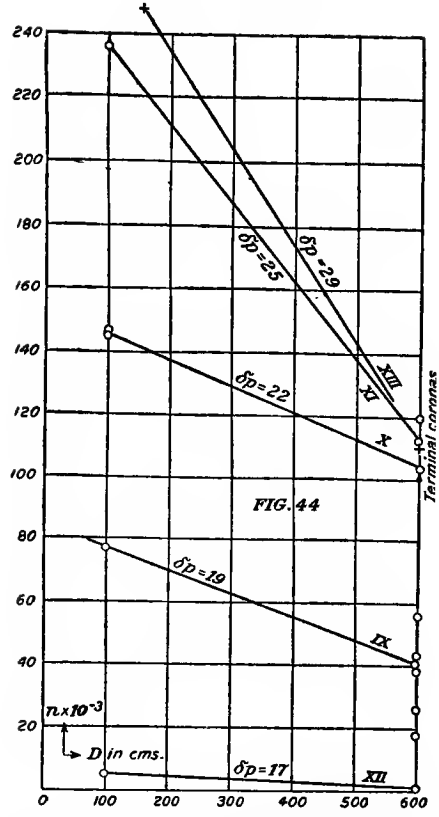

FIG. 44.—Nucleations (ions) produced by a radiating X-ray bulb at different distances (D) from the large wood fog chamber. Table 34.

61. Distance effect and absorption. Radium.—A few experiments were made incidentally with impure radium (10 mg. 10,000×, sealed in aluminum), using the method of depression of the terminal asymptote. In table 36, for instance, results are recorded on the absorption of the γ-rays in lead. Fig. 45 shows the results in relation to the nucleation of dust-free air, the efficient nucleation of which is more and more reduced as the intensity of the radiation increases with the diminishing thickness of the absorbing lead envelope.

After nearly 1.6 cm. of lead have been penetrated, the distance of the curve from the asymptotic air line is still marked. Results of this kind should furnish valuable data for testing any theory on the distribution of precipitated moisture on graded nuclei under any definite conditions.

Table 36 gives an incidental series of distance effects worked out by the same methods. As exhibited in fig. 46, the first series reaches the

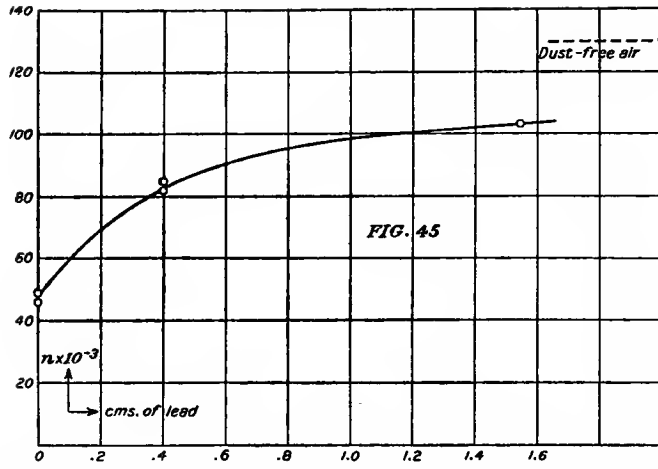

FIG. 45.—Depression of efficient nucleation (n) of dust-free air, ionized by gamma-rays of radium penetrating through different thicknesses of lead. Table 35.

high asymptote for dust-free air practically at a distance of $D = 150$ cm. In the second series the asymptote is lower, due to details in the adjustment in the apparatus, and reached later, *i. e.*, at a distance of $D = 180$ cm. between the radium and the fog chamber. This curve has been worked out completely for $D = 0$ cm., and shows the very interesting feature of a well-developed minimum. In other words, as the radium is removed from the fog chamber, the ions which at first predominate and capture all of the moisture decrease more and more in number, until the conditions are ripe for the simultaneous condensation of moisture on the colloidal nuclei of dust-free air. In proportion as the radium is further removed, the latter predominates, fully so when the asymptote is reached.

TABLE 35.—Absorption of lead. γ-rays of radium 10,000 ×. $D = 100$ cm.; $\delta p = 31$ cm.

Thickness t.	s.	$n \times 10^{-3}$.
∞	7.2	131
1.54	6.0	85
	6.5	103
	6.5	103
0.40	6.0	85
	5.9	82
.0	4.9	49
	4.8	46
∞	7.0	128

The corresponding results when the radium tube is inclosed in a thick lead pipe (walls 5 mm., length 60 cm.) shows a much sharper minimum, occurring at lower exhaustions. Such irregularities as are apparent here may be referred to the unequal distribution of radiation within the fog chamber discussed in Chapter I, sections 4 *et seq.* All of these curves have a similar bearing on the question of the distribution of the precipitate of graded nuclei.

TABLE 36.—Distance effect and absorption of radium rays. D measured from side. $\delta p = 31$. November 2. Lead pipe 0.5 cm. thick, 60 cm. long

	D.	s.	$n \times 10^{-3}$.		D.	s.	$n \times 10^{-3}$.
	cm.			III.	cm.		
II.....	180	6.2	90	In lead pipe..	145	5.6	70
	150	5.9	82		100	4.7	42
	100	4.7	42		50	4.3	32
	50	3.7	21		25	4.1	27
	25	3.7	21		10	4.0	24
	10	4.7	42	On top.....	1	4.9	49
Above fog chamber...	2.2	4.8	46	At ∞	...	7.2	135
On glass.....	0	5.6	70				
	350	6.7	111				
	300	6.8	116				
	250	6.2	90				

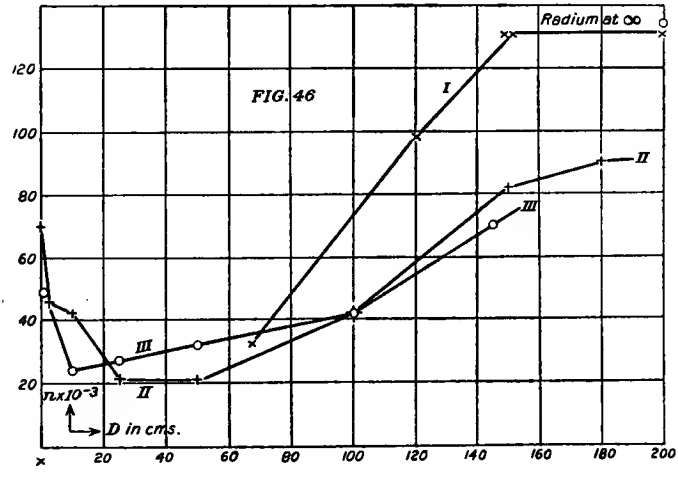

FIG. 46.—Minima of efficient nucleations observed at high exhaustions with radium at different distances (D) from the fog chamber. Table 36.

62. Falling to pieces of ions in the lapse of time.—Miss L. B. Joslin contributes the following interesting observations obtained by the method of depression of the terminal asymptote.

The data summarized in table 37 and fig. 47 were obtained by acting, in the manner stated, on the dust-free moist air contained within a glass fog chamber, with a sample of weak radium (10,000×, 10 mg.), sealed in an aluminum tube. This was placed on the outside of the chamber in contact with its walls (0.2 to 0.3 cm. thick), and was then removed

suddenly at given intervals before exhaustion. Only very penetrating primary rays (β and γ) are therefore in question. The curves show the number of efficient nuclei in thousands per cubic centimeter, observed after the lapses of time shown by the abscissas, and it is supposed that the nuclei are reproduced faster than they can be removed by the exhaustion. In the upper curve the pressure differences applied ($\delta p = 31$) are much above the fog limit of dust-free air, which is below $\delta p_0 = 24$ for the given apparatus. In the lower curve the pressure differences are nearly at the fog limit of dust-free air, while the other curve ($\delta p = 28$) applies for intermediate conditions. The effect of the radiation is therefore, virtually at least, a coagulation (to use a figurative expression) of

TABLE 37.—Falling to pieces of ions produced by radium. Everything ready; cocks closed before removing radium.

Date.	t.*	s.	Cor.	$n \times 10^{-3}$.
	$\delta p = 31$ cm.			
	sec.			
Oct. 19	∞	7.4	w′ o bg	140
	0	5.8	cor	76
	15	4.0	cor	24
	30	5.0	cor	51
	60	5.9	c o y g	82
	90	6.7	w o g	111
	120	7.2	w o g	134
	180	7.5	w o g	145
	$\delta p = 24.5$ cm.			
Oct. 24	0	6.3	....	79
	5	5.1	w r g	45
	10	4.7	w r g	36
	15	3.7	....	18
	20	3.6	....	16
	25	3.2	....	11
	30	2.3	....	3.5
	5	4.8	w o g	45
	10	4.2	w r g	29
	12.5	3.9	w r g	23

Date.	t.*	s.	Cor.	$n \times 10^{-3}$.
	$\delta p = 28$ cm.			
	sec.			
Oct. 25	0	5.8	w r g	72
	15	3.8	w o g	21
	30	3.5	....	16
	45	3.3	....	13
	60	3.4	....	14
	120	4.7	....	40
	180	4.6	....	37
	∞	4.6	....	37
	∞	4.8	....	43
	Oct. 27 Repeated. Decay of ions at $\delta p = 24$.			
Radium on.....	60	2		2.5
Radium at ∞ ...	...	1.3		1.6
Radium on.....	30	3.3		12.1
	†30	3.2		11.4
	15	4.2		25
	10	4.7		36
	0	6.2		77
	Fog limit of air. Radium off.			
$\delta p = 23.6$		1.3		1.5
$\delta p = 22.6$		.0		.0

* Seconds elapsed after removal of radium.

† First coronas dense but fall out rapidly, leaving fainter and *smaller* coronas behind.

the colloidal nuclei of dust-free air into the aggregates much larger in size representing the ions. Hence in the presence of radium under the given conditions the number of *efficient* nuclei decreases either because the ions from their size capture all the available moisture more and more fully, or because the colloidal nuclei have actually been aggregated into fewer but larger systems, which will in turn fall apart in the absence of radium.

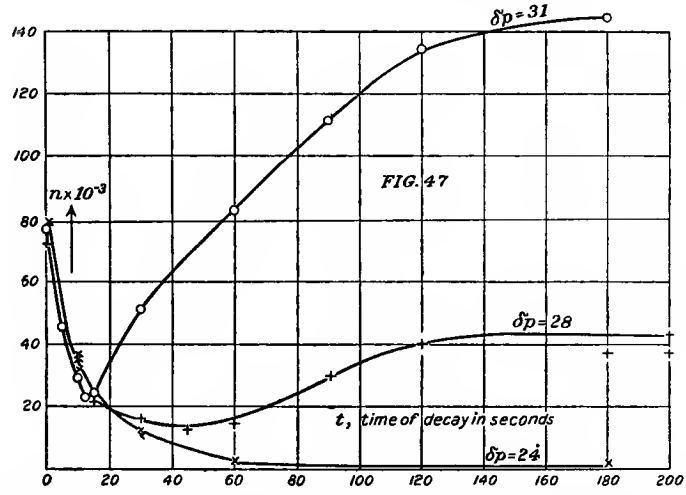

FIG. 47.—Efficient nucleation observed within the fog chamber at different times after exposure to radium applied outside at different exhaustions (δp). Table 37.

It follows from what has been stated that above the fog limit of dust-free air the number of efficient nuclei must increase with the removal of radium at a rate which corresponds to the falling to pieces of the ions. The peculiar feature of the results here in question is the manner in which the efficient nucleation decays from the coarser ionized to the finer non-ionized colloidal stages, when the pressure difference is decidedly above the fog limit of air, so that the latter may be recognized. The curves invariably pass through a minimum when the time after the removal of the radium, *i.e.*, the interval of decay, increases indefinitely.

This minimum, moreover, is very sharp, almost cusp-like, as if one law were passing abruptly into another. Thus below the minimum ($t=13$ sec., about) the curve for $\delta p=31$ nearly coincides with the curve for $\delta p=24$, which is practically independent of the colloidal nuclei of air. The decay may be computed to be of the order of that of ions. After a lapse of 13 seconds the effect of colloidal nuclei is marked for $\delta p=31$; and even after a lapse of 60 seconds, when the ions (lower curve) have

vanished to a few hundred, the upper curve is only half way on its march toward the asymptote. This shows the remarkable sensitiveness of the method as a test for the presence of ions or of any nuclei larger than the colloidal sizes. Moreover, measurement of the large coronas is relatively easy. Finally, the curve $\delta p = 31$, if prolonged backwards, would seem to start nearly from the origin; in such a case one would have to picture to oneself a single particle breaking to pieces, in the absence of radiation, into fragments of continually decreasing size, until the débris ultimately numbers 150,000 colloidal nuclei.

The intermediate curve ($\delta p = 28$) also coalesces* approximately with the other curves for lapses of time less than $t = 13$ seconds. It has its own minimum, however, and from the lower pressure difference, necessarily its own asymptote at $n = 40{,}000$, since only the coarser order of air nuclei fall within the given limits of condensation in the apparatus used. For the same reason the minimum is lower and later, seeing that the ions are present throughout in relatively greater numbers as compared with the efficient colloidal nuclei, than was the case at $\delta p = 31$.

The curves as a whole have so close a resemblance to the data investigated in section 61 for the effect of radium at different *distances* from the fog chamber that the same cause must underlie both series of observations. In the former case (distance effects) any given intensity of ionization between the maximum and the vanishing values may be maintained indefinitely by properly placing the radium tube; in the latter case (decay) all stages are passed through in 2 or 3 minutes. Beginning with dust-free non-energized air, the number of efficient nuclei decreases as the number of ions increases (for either or possibly both of the reasons already given) until the condensation takes place wholly on ions. For greater intensities of ionization the number of ions must increase further, and hence the efficient nucleation rises again while the curve passes through a minimum.

The curves enable us to make certain interesting comparisons, inasmuch as the same nucleation results from radium decaying for a stated length of time, as results from the action of radium at a certain distance from the line of sight. From the importance of secondary radiation in connection with these observations, such comparisons are probably not simple. The essential feature is the passage of the nucleation through the same stages of variation, whether of size or of number, in both cases no matter how the given successive intensities of ionization may be produced, or whether they come from within or without.

---

* Considered relatively to the wide divergence after $t = 13$ sec. is passed. The coalescence need not be perfect. Small coronas fall out too rapidly for close measurement.

63. Decay curve.—Assuming that the rate of decay in the lapse of time (t) is as the square of the number, or that $1/n - 1/n' = b\,(t-t')$ where b is constant, a few incidental attempts were made to compute b.

Table 38 and fig. 48 contain an example of such results, obtained by exhausting the fog chamber at a stated time after the removal of radium. The drop in pressure is below the coronal fog limit of air and all precipitation takes place on ions.

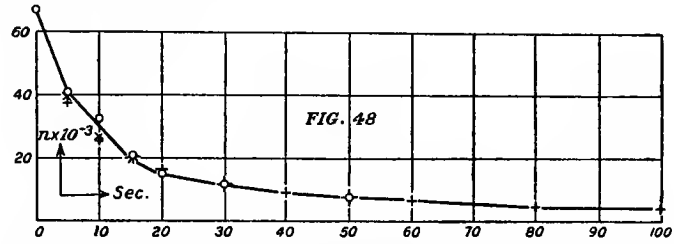

FIG. 48.—Decay of ionized nuclei (n per cubic centimeter) produced by radium in dust-free air, in the lapse of seconds. Table 38.

For the first five seconds $b = 0.0019$, for the first fifteen seconds $b = 0.0022$, etc., the values obtained ranging from 0.002 to 0.003. This is larger than the electrical datum 0.0014. Decay is more rapid than the equation warrants. Initial coronas are too large, final coronas too small, in spite of the presence of air nuclei, the number of which should be deducted at least in part. Other experiments show similar coefficients. Thus the low curve of Miss Joslin would conform to $b = 0.0023$. Naturally the present method for b is much inferior to the electrical method, even if the two coefficients are identical; but the b here is obtained under possible complications with the larger gradations of the colloidal nuclei of dust-free air, though these are probably inefficient.

TABLE 38.—Decay curve at $\delta p = 23$. Radium on top.

t.	s.	$n \times 10^{-3}$.	$n \times 10^{-3}$. $b = .0024$
sec.			
0	5.9	67	67.5
5	5.0	41	37.3
10	4.6	32	25.8
15	4.0	21	19.7
20	3.5	15	15.9
30	3.3	11.6	11.5
50	2.9	7.4	7.4
120	1.7	1.9	3.3
∞	1.0	1.1	....

If the values of $1/n$ be inserted, the curves should be linear, since $1/n = 1/n_0 + bt$, where t is the time dated since the occurrence of n_0. The line passing through the observations at 5, 30, 50 seconds is best adapted to represent the results, and compatibly therewith $b = 0.0024$ (n in thousands of nuclei per cubic centimeter) may be roughly assumed. These computed values of n are given in table 38 and shown in the chart (fig. 48). They are too low initially and too high finally, even if the air

value is quite ignored; but the constant probably reproduces the true conditions better than the observation, remembering that the initial corona ($t = 0$) is not quite invariable.

A very important consequence may be deduced from these results. The equations specified may be written

$$\frac{1}{bt}\left(\frac{n_0}{n} - 1\right) = n_0.$$

Hence if the ratio of nucleations or of ions is known (for instance by the method of geometric sequences), n_0/n is given, and the absolute value of n may be computed if b is known. Now, if b, for the case of ions, may be taken as identical with the value found in electrical experiments, where $b = 0.0014$, roughly and relative to ionization in thousands, $bn_0 = 0.0014\ n'_0$ where n'_0 is the true nucleation. Thus in table 39, $b = 0.0024$, $n_0 = 67{,}500$; therefore $n'_0 = (0.0024/0.0014)\ n_0$ or 115,000 nuclei per cubic centimeter. Quite generally, if n_0/n and b are determined from purely coronal measurements $b/0.0014$ is the reduction factor for all the relative nucleations to absolute values.

Another very important consequence may be drawn. If the coefficient is known from direct experiments, it will then be possible to standardize the residual curve (depressed asymptote) leading to the terminal corona. Thus if $b = 0.0024$ is roughly assumed, as an example derived from the data at $\delta p = 24$ cm. (table 37 and fig. 47), the value of the ordinates of the curve for $\delta p = 31$ would then be given by table 39 and fig. 49.

Moreover, in any such curve, while the ordinates denote the computed number of ions, the abscissas denote the observed number of efficient colloidal nuclei and ions in the course of time, largely the former. Hence the curve gives an indication of the distribution of the precipitated water on the two groups of nuclei, different in size and present in different proportions, for the given supersaturation. Experiments of this kind are of the highest importance and the present cursory treatment is admitted provisionally, in view of a projected restandardization of the coronas of cloudy condensation, which the variety of results since obtained has made necessary. The curve for $b = 0.0024$ is shown in fig. 48; the two curves* i and $n+i$, i and n, in fig. 50. The initial descent of the graph for i and n is clearly steeper than would correspond to any exponential or hyperbola, and an equation of the form

$$i\ (n+A)^B = C$$

is at least needed to express the data. The computation of the constants

*Where i denotes the number of ions, n the number of nuclei per cubic centimeter.

would not be of any value. The table and chart show clearly enough how rapid a reduction of efficient nuclei is produced by the presence of but a few thousand ions. The results would have been much more striking if a more efficient form of apparatus had been used, since for $\delta p = 31$ cm. it is customary to obtain four or more times as many colloidal nuclei in the absence of ions.

TABLE 39.—Graduation of high pressure curve. $b = 0.002$; $n_0 = 75 \times 10^{-3}$; $1/n_0 = 0.0133 = a$.

t.	$n \times 10^{-3}$ at $\delta p = 31$.	$1/n_0 = A = 0.0133$; $b = 0.0024$.		
		$a + bt$.	$n \times 10^{-3}$.	$\{(n+i)^{-i}\} \times 10^{-3} = n \times 10^{-3}$.
sec.				
10	*29	0.0373	†26.8	2
20	32	.0613	16.3	16
30	51	.0853	11.7	39
40	62	.1093	9.2	53
50	74	.1333	7.5	67
60	85	.1573	6.4	79
80	105	.2053	4.9	100
100	120	.2533	4.0	116
120	135	.3013	3.3	132
140	140	.3493	2.9	137
160	...	.3973	2.5	...
180	145	.4453	2.2	143
5	...	.0253[s]	39.5	
15	...	.0493[s]	20.3	

* $(i+n) \times 10^{-3}$. † $i \times 10^{-3}$.

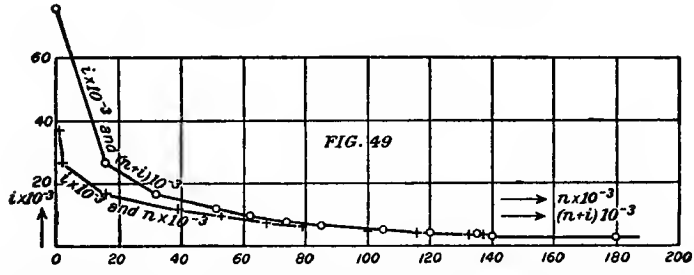

FIG. 49.—Decay of ions (i per cubic centimeter) in dust-free air, evidenced by increase of efficient colloidal nucleation (n per cubic centimeter). Table 39.

64. The same, continued.—In conclusion I may state that a number of experiments were made to test the rate at which the ions are generated. If a is the number of ions produced by the rays per cubic centimeter per second and b the coefficient of decay,

$$dn/dt = a - bn^2$$

This may be written

$$t = -\frac{1}{2\sqrt{b}} \int \frac{d\ (dn/dt)}{(dn/dt)\sqrt{a - dn/dt}} + C$$

from which, after integration,

$$\epsilon^{-2\sqrt{ab}\cdot t + c} = \frac{N - \sqrt{a/b}}{N + \sqrt{a/b}}$$

If

$$\frac{n - n_1}{n \times n_1} = A\epsilon^{-2bn_1 t}$$

where A is a constant and $n_1 = \sqrt{a/b}$,

$$n = n_1 \frac{1 + A\epsilon^{-2bn_1 t}}{1 - A\epsilon^{-2bn_1 t}}$$

If $t = \infty$, $n = n_1$, $a = bn^2$, which is otherwise evident. The coefficient a is here taken as an absolute constant independent of n. In the preceding paragraph it was roughly assumed that $b = 0.002$ if n is reckoned in thousands per cubic centimeter. Hence $a = 0.000002 \times n^2$. Thus if $n = 10^3$, $a = 2$ per cubic centimeter per second; if $n = 10^6$, $a = 2 \times 10^6$, etc. Experiments were tried with the radium tube on a pendulum swinging above the fog chamber; also with the tube on an inclined plane moving rapidly across the chamber. But in both cases the results, which essentially require the opening of the stopcock of the fog chamber, are too involved to have any critical value, and they are therefore discarded here.

65. Condensation phenomena of the inclosed steam jet. Methods and results.—Some time ago (Bulletin No. 12, U. S. Weather Bureau, 1893), I obtained a series of results (shown for example in fig. 52) from observations of the behavior of the steam jet inclosed in a wide tube of thin sheet metal. The jet shown at j in fig. 50 plays into the tube AkA, about 2 inches wide and 2 or more feet long, the steam escaping at B. Sky-light L, from a mirror M, enters the tube axially, through a window a, and is observed through an opposite window, g. Room air enters at C, to cool the steam, and the temperature of the inflowing air is taken, as well as the pressure under which the steam escapes. Fig. 51 shows two such tubes arranged for differential work. These data are used in the construction of fig. 52, where air temperatures in degrees centigrade are horizontal and steam pressures in pounds vertical.

It will be seen that for each temperature of the inflowing air there is a definite steam pressure at which the field of the tube just becomes opaque, and condensation within the jet, therefore, begins to be tumultuous. The edge of the opaque field is sharply marked, and above 15 it is possible to pass through it in a march of continually increasing steam pressures; for the opaque field vanishes with a kind of cusp, dependent for its position, naturally, on the apparatus used.

What the figure imperfectly suggests, however, is the occurrence of similar loci of *axial color*, which run parallel to the edge of the opaque zone, on the clear side of it. The colors follow the spectrum series reversed, v, b, g, y, o, r, growing continually fainter and vanishing into daylight.

The field becomes at once opaque if a strong nucleator like phosphorus is placed near *C*, fig. 50; or any color may be obtained in this way by carefully regulating the additions of nuclei, as shown elsewhere. Mere smokes, like salammoniac, are ineffective; in fact the field made opaque by phosphorus may be cleared by such smoke, added in reasonable quantity.

Ordinary non-filtered air is practically ineffective.—This touches the first point to be made. I have shown elsewhere that the fog chamber and the steam jet mutually supplement each other; the former responding measurably to nuclei reckoned in thousands per cubic centimeter, the latter to nuclei reckoned in millions per cubic centimeter, to speak roughly. In other words, the whole sequence of coronas, of which there are many periods visible in an apparatus of reasonable size, has been passed through when the occurrence of axial color begins, the latter end with particles so fine as to be optically ineffective.

It is for this reason that ordinary non-filtered air, which produces such remarkable effects in the fog chamber, is almost without effect on the steam jet. A faint scarcely discernible pink tinge is all that is seen, and it is therefore possible to omit the filtration of air altogether. The use of dust-free air will not change the conditions, which lie wholly below the scope of the steam jet. This is even the case when the air is artificially dusted by less powerful nucleators like weak X-rays or weak radium, the additions being as a rule relatively insignificant.

As the increase of steam pressure can only increase the supersaturation, it follows that the tumultuous precipitation of the steam jet characterizing the opaque zone *must take place on the nuclei of dust-free air*, for at this stage of the phenomenon the corona-producing dusts are ineffective.

Much attention has been given by Professor Wood in this country, and by others abroad, to the occurrence of optical resonance in con-

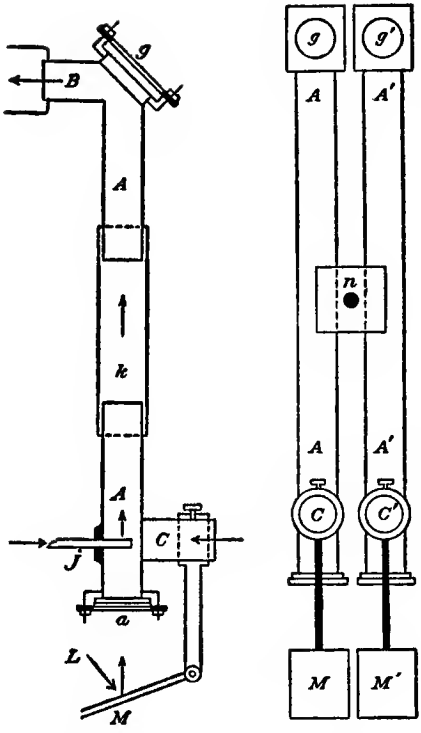

FIG. 50.

FIG. 51.

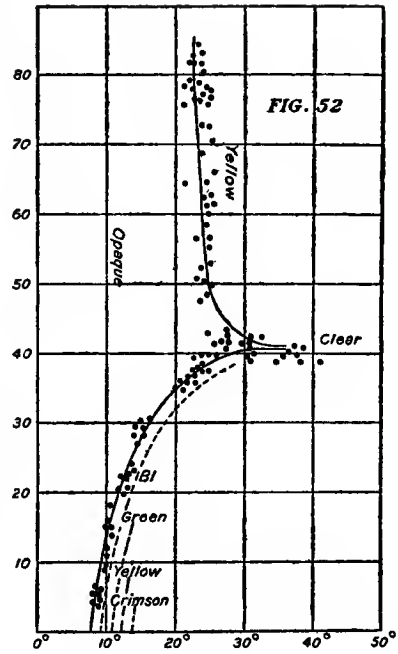

FIG. 52.

FIG. 50.—Section of inclosed steam jet and tube.

FIG. 51.—Binocular inclosed steam jet.

FIG. 52.—Chart showing margin of opaque zone for different steam pressures (pounds per square inch) and temperature of inflowing air.

nection with similar color effects. But the case of the steam jet may be duplicated, in different ways, by the vapors of typical non-ionizing liquids, like gasoline, benzol, carbon bisulphide, etc., with even more saturated axial colors than are observable in steam. Electrical resonance can not, therefore, be effective here, where the fog globules are dielectric. The particles, moreover, are too large to fall within the lines of such an explanation.

Returning to the diagram (fig. 52), it will be seen that at a temperature of about 40° there is no observable condensation; in other words, the steam passes through the tube like a gas, leaving the field quite clear. At 40°, therefore, the supersaturation at which condensation begins to take place on the nuclei of dust-free air is just reached; below it, at the given pressure, the supersaturation is in excess, and steam pressure

must be relieved to reduce the excess before the field clears again, in greater measure as the temperature is lower, until at 9° steam issuing at ordinary pressure (without appreciable pressure above one atmosphere) condenses spontaneously.

The increments of supersaturation below 40° are in fact considerable. Thus, if the saturation at 40° be taken as the standard, these excesses would be roughly as shown in table 40.

TABLE 40.—Estimated supersaturations.

Temperature.....	40°	35°	30°	25°	20°	15°	10°	$10^{-6}g/cm^3$.
Supersaturation.....	0	12	21	28	34	38	42	
Relation.....	1	1.3	1.7	2.2	2.9	3.9	5.5	

These values are to be added to whatever supersaturation preexists at 40°, seeing that the escaping steam is always suddenly cooled down from a temperature much above 100°. In fact, the following data (table 41) may be adduced from the diagram, if t_1 be the temperature of the steam before, t_2 the temperature after, ρ_1 and ρ_2 the densities of the steam.

TABLE 41.—Estimated supersaturations.

t_2.....	40°	35°	30°	25°	20°	15°	10°	
ρ_2.....	50.9	39.3	30.1	22.8	17.2	12.8	9.3	$10^{-6}g/cm^3$
t_1.....	112°	112°	112°	112°	111°	109°	105°	
ρ_1.....	894	894	894	894	865	811	715	$10^{-6}g/cm^3$
$S=\rho_1/\rho_2$..	17.6	22.7	29.8	39.2	50.3	63.3	77	

Nothing more than exhibition of the order of values is intended; but it will readily be seen that in comparison with Wilson's data ($S=4.3$ for rain-like, $S=7.6$ for cloud-like condensation, and $S=9.9$ for the sensitive tint), the supersaturations here are enormous, and that the condensations must take place on something approaching the molecular groups of the system, water—steam—air.

It is therefore scarcely necessary to remark that the data are superior limits, particularly inasmuch as the influx temperature at C, fig. 50, and not the efflux B, were taken. But as the influx of air is swifter as the the steam pressure increases, the difference between these temperatures is not large. The escaping steam is always cool to the hand.

It follows that the color data bear at once on the structure of dust-free air. The occurrence of definite loci for r, y, g, b, v, the fact that any color can be retained indefinitely, if (*cæt. par.*) the pressure-temperature

conditions are fixed, shows that groups of nuclei counted by millions per cubic centimeter must be available for condensation long before the molecular sizes are approached. It is convenient to refer to the molecular aggregates in question by the term "colloidal nuclei." They are necessarily much smaller than ions. The number of such nuclei increases as the supersaturation is greater and the size needed therefore smaller until condensation is actually spontaneous on the molecules themselves.

It is in this stage that one would naturally expect the fog particles of all sizes to produce a medium opaque to transmitted light, as is actually the case provided the fog particles are themselves large in comparison with the wave-length of light. It does not by any means follow, however, that the turbulent phenomenon is complete at the lower edge of the opaque zone. It is much more probable, seeing how gradually the violet drops into the opaque, as the supersaturations increase with increase of steam pressure at a given temperature of the inflowing air, that the number of nuclei continually increases. As this goes on (*i. e.*, in a vertical march through the opaque zone) the time must arrive when the fog particles become small in comparison with the wave-length of light; for although the influx of steam has increased, the air influx increases in the same proportion. Under these circumstances, even though fog particles of widely different sizes are the rule, the Rayleigh effect of scattering is to be looked for.

In fact, the yellows of the first order emerge from the opaque as magnificently saturated orange-browns and thereafter gradually become yellower. Deep crimson at the edge of the opaque does not appear. To prove that the passage from blue to yellow through opaque is due to an *increase* of nucleation, it is merely necessary to add phosphorus nuclei, when axial violet appears in the steam tube at a sufficiently high temperature. Without further change the bluish tone at once passes to yellow. Again, the intense oranges above the opaque may be obtained at once by introducing the fumes of the intensely nucleating sulphur flame into the steam tube. Finally, the probability of the Rayleigh effect is increased by the fact that colors of smaller wave-length than orange and yellow never occur above the opaque zone.

66. Summary.—The present chapter has made use of the method of testing the presence and number of relatively large nuclei by the depression produced in the terminal asymptote obtained when nucleation varies with the drop in pressure, or of the diminution in aperture of the terminal corona corresponding in a given apparatus to dust-free non-energized air. It was thus easily possible to trace the growth in number

of the persistent nuclei produced by relatively intense X-radiation in the lapse of time, showing results similar to Chapter I, sections 14, 15.

In the same way the occurrence of water nuclei in the presence of colloidal nuclei or of ions was clearly exhibited. These are due to the evaporation of small fog particles, until the increase of vapor pressure due to surface curvature is balanced by the decreased vapor pressure due to some independent phenomenon. Hence if the exhaustions proceed with a slightly opened filter cock, such nuclei must be present in greater number as the evaporation is faster, because increasingly more particles evaporate than subside.

The result in the first place is a necessary alteration of aperture of successive coronas, all other conditions remaining the same, since the large ones evaporate more fog particles than those of lower order of size (periodicity of coronal diameter). In connection with this phenomenon it is particularly interesting to observe that not only the colloidal nuclei but the ions are available. Questions arise as to whether the fog particles of positive and of negative ions evaporate to like water nuclei, what becomes of the charges, since it is not clear that they should be dissipated, what phenomena arise from the decreased mobility of the loaded ions, etc.

The means developed in Chapter II were again applied to an effect produced (distance effect), when the radiating source is removed more and more from the fog chamber. The results are necessarily crude; but they show that in case of pervious wood fog chambers the nucleations decrease more slowly than the first power of distance; they decrease faster for the glass fog chamber; faster still when the X-ray bulb is inclosed in a windowed lead case; fastest when the window is closed with a thin tin plate; but in no case do they reach the law of inverse squares. All this points clearly to the importance of secondary radiation in producing nuclei. The radiation arises both near the bulb and near the fog chamber, as well as in the region between. The number of nuclei produced is therefore dependent upon an integral extended over the whole interior surface of the room and throughout the intervening air.

In case of exposure to weak radium (10 mg. 10,000×) the asymptote of dust-free air is not reached until the intervening distance is above 150 cm.; and it is far from appearing after 1.5 cm. of lead have been penetrated.

The occurrence of minima of nucleation, when such weak radium is carried from a long distance quite up to the fog chamber, is again strikingly brought out, provided the drop of pressure is sufficiently above the fog limit of dust-free air. It is also observed when the ions are produced

in the fog chamber by radium and decay in the lapse of time after the radium is suddenly removed. The decay curves all show minima for a drop of pressure above the fog limits of dust-free air; while the curve is normal for pressure differences below the fog limit.

If the coefficient of decay for the ions within the fog chamber is the same as that found by purely electrical investigations, and if the relative numbers of nuclei corresponding in a given apparatus and given conditions of exhaustions are known, then a new method for the standardization of coronas in terms of the number of nuclei involved in their appearance, is suggested; for

$$n_0 = (n_0/n - 1)\, bt$$

if n_0 and n are two successive nucleations observed under like conditions at t seconds apart and if b is the known coefficient of decay. Conversely, if n_0 is given this method lends itself for the determination of nucleation ratios n_0/n, and for the experimental determination of the distribution of a given mass of precipitated water on groups of nuclei different in average size—one of the important of the outstanding problems.

Finally, it was shown that data bearing on the graded character of the colloidal nuclei of dust-free air may be obtained most directly and throughout the widest range from the behavior of the inclosed steam jet. If (*cæt. par.*) the steam pressure is intensified until the originally clear field (air dust being practically inactive), after passing a succession of colors, becomes clear again in consequence of absence of all condensation, it follows that colloidal nuclei in vast numbers and of continually decreasing size must successively become available for condensation until the fog particles are too small to be optically discernible. Each particular color corresponds to a group of colloidal nuclei characterized by their minimum size. It is still to be determined, however, whether these nuclei belong to the system of saturated vapor, or to the air, or to both.

CHAPTER IV.

DISTRIBUTION OF COLLOIDAL NUCLEI AND OF IONS IN MEDIA OTHER THAN AIR-WATER.

COLLOIDAL NUCLEI AND IONS IN WET DUST-FREE CARBON DIOXIDE AND IN WET COAL GAS.

67. Apparatus.—The following experiments were made with the apparatus used in my last experiments* with dust-free air. The conveyance tubes between the exhaustion chamber (5 feet long and 1 foot in diameter) and the condensation chamber (18 inches long and 5 inches in diameter) were about 18 inches long and 2 inches in diameter. The rapid exhaustion thus secured is effective, but has by no means reached a limit; there is still too much resistance in the connecting pipes. The data obtained with such an apparatus are comparable with each other, and nothing further than this is aimed at, since in view of the very high exhaustions needed, the constants for the computations of the absolute nucleations would in any case be lacking. It is a matter of convenience, however, to compute the data at the high exhaustion as if the conditions met with at the low exhaustion were indefinitely applicable, and this is the meaning to be given to n, the number of nuclei per cubic centimeter, in the present paper. Moreover, n refers to the nucleation left in the *exhausted* fog chamber, supposing that the nuclei are restored to the gas faster than they can be withdrawn by exhaustion or that the nucleation encountered is fixed for any definite environment. Otherwise n (to be multiplied by the volume expansion) would be very much larger.

The carbon dioxide used was generated from calc spar and hydrochloric acid. The gas was eventually passed through a solution of sodic hydrocarbonate, a long tube of dry bicarbonate of soda, a solution of silver nitrate, and a calcium chloride drying tube. Then it entered a filter (2 feet long), from which it was conveyed very slowly into the fog chamber. Coal gas taken from a gas pipe was treated in the same way.

68. Data for carbon dioxide.—In table 42, δp shows the drop of pressure on exhaustion, $s/30$ (approximately) the angular diameters of the coronas when the eye is at 30 cm. in front and the source of light 250 cm. behind the fog chamber. The meaning of the other data is obvious, n being the nucleation.

*Phys. Review, XXIII, pp. 31-36, 1906.

TABLE 42.—Condensations in CO_2 generated from $CaCo_3$ with HCl. Gas washed as specified.

δp.	s.	Corona.	$n \times 10^{-3}$.
I. Washed in water, twice.			
31.0	(1)	g y o	410
31.0	10.7	w r g	260
31.0	7.8	w y g	140
31.0	6.4	w r g	100
31.0	5.3	cor	60
31.0	2.7	cor	8
31.0	2.4	cor	5
31.0	2.0	cor	2.9
19.1	2.1	cor	2.4
16.9	2.1	cor	2.2
II. Washed in solution of $NaHCO_3$ and $AgNO_3$.			
31.0	(1)	g y o	410
31.0	10.7	w o g	305
31.0	7.9	g B P	150
31.0	3.3	cor	14.0
31.0	2.4	cor	5.0
31.0	[2]8.4	w r g	230
31.0	[2]11.4	w y b g	380
III. Same, with long tube of $NaHCO_3$.			
31.0	(1)	g y o	410
31.0	11.2	w o g	305
31.0	7.5	w B P	150
31.0	4.3	cor	32
31.0	4.4	cor	33
IV. Same, after 3 hours.			
31.0	[3]4 4	cor	33
17.6	1 ?	cor	1
17.1	0 ?	cor	1
17.7	1–2	cor	1
19.4	1 ?	cor	? 1
21.2	1–2	cor	1.5
24.7	1–2	cor	1.5
28.0	1.2	cor	1.5
31.0	2.0	cor	2.9
31.0	[4]9.6	w r g	240
V. Air bubbling through HCl, CO_2 off.			
31	12.0	w y b g	305
	12.0	w y b g	360
	....	[5]g y o	410
VI. Experiments with CO_2 repeated.			
31	([6])	g y o	410
31	11.0	w o bg	305
31	6.4	w r g	100
31	4.2	cor	29
31	[7]4.0	....	24
31	[8]4.2	....	29
31	2.1	cor	3.3
31	2.0	cor	2.9
35.1	10.0	w o g	320
40.3	...	green	500
31.4	1.8	cor	2.4
32.4	3.2	cor	12.9
33.5	6.7	g′ B P	140
34.7	9.8	w r o g	270
VII. Same.			
35.0	...	y o g	400
36.8	...	g	490
38.0	...	g B P	500
44.0	...	B g B P	550
VIII. Gas ionized. X-ray bulb at $D = 200$ cm.			
41.7	7.3	w y′ g	155
35.9	7.3	w o g	146
28.8	7.3	w o g	130
27.3	7.3	w o g	125
25.8	7.3	w o g	120
24.8	3.8	cor	20
23.3	2.5	cor	5.0
21.7	1.1	Just seen	1.2
24.2	4.2	cor	25
26.0	6.8	w r g	105
25.5	5.6	cor	62

[1] s given for successive coronas beginning with air.
[2] CO_2 off; air inflowing.
[3] Not yet air-free.
[4] Exposure to X-rays.
[5] No trace of HCl gas escapes through the cleaning train.
[6] s given for successive coronas, beginning with air.
[7] After 1 hour.
[8] After 2 hours; other data consecutive.

In parts I to III in the table the exhaustion (δp) is usually kept constant, with the object of observing the behavior of the mixture of gases, beginning with air and terminating with CO_2. In part I about 8 exhaustions lead to the steady behavior of the latter gas. Inasmuch as the original air is still present to the extent of about 1 per cent, an admixture of this amount may be regarded as inappreciable. In the second part of the table, even four exhaustions, reducing the air content to about 11 per cent, nevertheless bring out the behavior of CO_2. The same things happen less certainly in part III. In part II, however, on readmitting air, two exhaustions nearly suffice to restore the air corona. Parts III and IV show that coronas for a given mixture are reproduced after several hours.

The relatively small coronas obtained with CO_2 as compared with air for the same drop in pressure and in the same apparatus gave rise to a suspicion that water nuclei associated with HCl gas might be involved. In part V, therefore, atmospheric air was bubbled through HCl and the gas then passed through the same drying train. After three exhaustions exceptionally high air coronas were obtained, showing that the method of producing the gas is of no consequence, thorough washing presupposed.

Hence, in parts VI and VII of the table, the experiments with non-energized CO_2 were concluded.

In part VIII of the table the gas is ionized by the X-rays with the bulb at a distance of 200 cm. The usual constancy of corona at high exhaustions is observed, while the fog limit is exceptionally high.

69. The behavior of carbon dioxide.—The graphs corresponding to table 42 are given in fig. 53, in connection with the corresponding data for air, both for the non-energized and energized states. It will be seen that in both cases the curves are essentially similar in their contours, but that the CO_2 curves require much higher exhaustion throughout than the air curves. In other words, the same coronas occur in CO_2 as in air, provided that in the former gas all the pressure differences are chosen to about 5 to $5\frac{1}{2}$ cm. higher than in the case of air. Similar relations hold for the fog limits, as was found directly by Wilson* in a different apparatus.

The peculiar feature of these results is the degree of parallelism of the CO_2 and air lines, both for the non-energized and to a somewhat smaller extent for the energized state. Clearly the phenomena in both cases are alike in character, though lying far apart on the chart.

70. Cause of differences.—In view of the more coercible character of CO_2 one would naturally expect larger colloidal nuclei than in the case

*C. T. R. Wilson: Phil. Trans. Royal Soc., vol. 189, p. 288, etc., 1897.

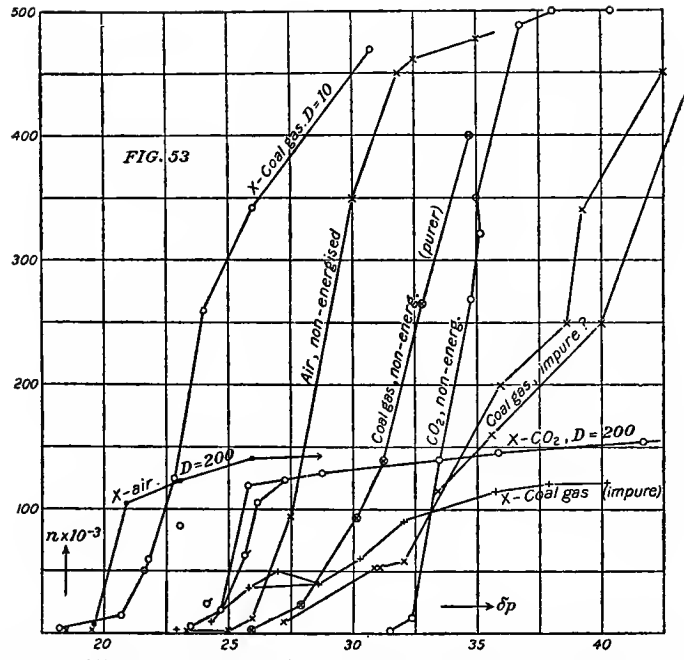

FIG. 53.—Efficient nucleation (n) observed in media water-air, water-CO_2, water-coal gas, energized or non-energized at different exhaustions δp.

of air, and it was with this anticipation that the data were investigated. Taken at their full value, however, they would point to a conclusion exactly the reverse of this. The colloidal nuclei in CO_2 are apparently smaller than in the air, and the same is true (*cæt. par.*) for the ions.

Unfortunately the precise meaning of these results is not clear, for in the first place the amount of adiabatic cooling may be written

$$\log \tau_0/\tau = (\gamma - 1)/\gamma .\ \log p_0/p$$

and thus between two fixed pressures

$$\log \frac{\tau}{\tau_0} = \text{const.} \frac{\gamma - 1}{\gamma}$$

The value of this fraction is for air, 0.29; for CO_2, 0.22; for coal gas, 0.19. In other words, the amount of cooling is less in CO_2 than in air under like conditions, and hence the reduced efficiency of the fog chamber in the former case is qualitatively compatible with the thermal properties of CO_2 gas. Quantitatively, however, this compensation does not seem to be sufficient. For instance, the same corona is obtained in air and CO_2 when the pressure difference is 28 cm. and 33.5 cm., respectively. For

like nuclei this would imply the same degree of supersaturation. Hence, if p_1 and p_2 be the vapor pressures of water before (20° C.) and after exhaustion, and $p=76$ and $p-\delta p$ be the corresponding pressures, the occurrence of like supersaturation implies that

$$\frac{p_1}{p_2}\left(\frac{p-p_2-\delta p}{p-p_1}\right)^{\gamma}=\frac{p_1}{p_2}\left(\frac{p-p_2-\delta p'}{p-p_1}\right)^{\gamma'}$$

where p^1 and γ refer to CO_2 and where γ is the heat ratio for air. Hence

$$\frac{\gamma}{\gamma'}=\frac{\log\,(1-(\delta p'+p_2)/p)-\log\,(1-p_1/p)}{\log\,(1-(\delta p+p_2)/p)-\log\,(1-p_1/p)},$$

where the value for $\frac{\gamma}{\gamma'}=1.10$ as derived for direct experiment.

To compute the value of the same ratio from the coronal experiment it is necessary to know p_2 the vapor pressure on exhaustion and before condensation ensues. This datum is unavailable, but it must be greater than 0 and less than would correspond to the decidedly lower exhaustion $\delta p=17$ (for instance) than the one applied ($\delta p=28$). Hence limits of the value of $\frac{\gamma}{\gamma'}$ may be computed by inserting $p_2=0$ and $p_2=0.2$ respectively. The results are $\frac{\gamma}{\gamma'}=1.28$, both for the superior and inferior limits, as would be otherwise evident.

One may summarize these results as follows: Either the heat ratio of carbonic acid, γ', decreases in comparison with that of air, γ, very rapidly as temperature decreases, so that an average value of $\frac{\gamma}{\gamma'}=1.3$ instead of $\frac{\gamma}{\gamma'}=1.1$ is to be used in the preceding experiments; or the colloidal nuclei in wet CO_2, though distributed in a way closely recalling the case of air, are throughout smaller.

71. Nucleation increases subject to a uniform law of equilibrium.—The most interesting feature of the data for CO_2 is their repetition (under higher exhaustion) of the behavior of air. In other words, the two curves are closely parallel throughout their extent. This seems to imply that both are primarily dependent, not on supersaturation or cooling or on volume expansion, but on a common law of distribution of number with size of aggregates, such as is given by the theory of dissociation. In other words, a given drop of pressure of sufficient rapidity and from a specific initial value in each case generates the same number of colloidal nuclei, though it does not follow that the apparatus in all cases can entrap them. This is even true in different apparatus of different degrees of efficiency, as shown elsewhere.

One might perhaps suppose that cohesion of molecules is more frequent when collisions are less frequent or that effectively more large particles reside in the exhausted gas. There are other cases given below which seem to suggest this peculiar inference.

72. Data for coal gas.—These are given in table 43 in the same way as in table 42, both for the non-energized and for the energized gas when the X-ray bulb is at a distance of 200 cm. from the fog chamber. The measurements were much less satisfactory than the above, the corona being thin and blurred. This may perhaps be due to the fact that mixed gases are under examination.

TABLE 43.—Distributions of nuclei in coal gas, washed in water and $AgNO_3$.

	δp.	s.	Corona.	$n \times 10^{-3}$.
Coal gas	31.0	5.1	cor	55
	31.0	5.1	cor	55
	31.0	5.6	cor	70
	31.0	4.3	cor	30
	33.4	6.7	w y g(?)	115
	35.5	7.8	(Thin)	160
	40.0	8.9	w P(?)	250
	44.1	9.2	w y′	450
	42.1	10.2	w y	450
Same.	39.2	...	y o bg	340
	38.6	9.6	w b r	250
	35.8	7.7	w P	200
	32.0	5.3	cor	60
	27.3	3.1	cor	10
	25.8	3.0	cor	9
	24.5	3.6	cor	16
	23.2	2.2	cor	3
	19.4	1.9	cor	2
	18.4	1.3	cor	1
	15.7	.0	...	0
Coal gas	17.6	.0	...	.0
	19.9	1.7	cor	1.7
X-rays. $D = 200$ cm.				
Coal gas	40.1	6.6	w o g	121
	37.8	6.6	w o g	120
	35.7	6.6	w o g	115
	32.0	6.2	wrg	90
	30.2	5.3	cor	60
	28.6	4.7	cor	40
	27.1	[1]5.2	cor	50
	25.7	4.6	cor	35
	24.3	3.4	cor	13
	22.9	2.3	cor	3.5
	21.7	1.5	cor	1.7
	20.6	[1]2.3	cor	3.1
	19.4	.0	cor	.0

[1] Fluctuation of s not infrequent.

73. Character of the early results for coal gas.—As in case of CO_2, the data for coal gas throughout lie in a region of relatively low pressure; *i. e.*, large drops in pressure are needed to produce the coronas. Fog limits are correspondingly high. This will again be qualitatively in keeping with the low heat ratio γ.

Apart from this, these first results with the hydrocarbon gas differ thoroughly from the character of the results for air and CO_2. In the non-energized gas the nucleations rise to the pressure difference at a rapidly accelerated rate, and this continues to the highest value which δp applied

and long after the air and CO_2 nucleations have become stationary in the given apparatus.

Similarly for the energized gas the increase of nucleation is very gradual and the asymptote is scarcely reached within the interval $\delta p =$ 40 cm. of the experiment. All this is sharply in contrast with the rapidity with which air and CO_2 approach their respective asymptotes, as may be seen by inspection of the chart.

TABLE 44.—Coal gas energized by X-rays at $D = 10$ cm. and in absence of rays. Two-inch pipes. Lead conveyance tubes.

δp.	s.	Corona.	$n \times 10^{-3}$.	δp.	s.	Corona.	$n \times 10^{-3}$.
32.9	(1)	Slate bl.	...	Bulb removed.			
30.8	(1)	g'G	470				
29.0	(1)	Grayish	...				
27.5	(1)	Grayish	...	19.4	.0	....	0.0
26.0	11	w y'	340	22.4	.0	....	.0
21.7	5.7	w r'	58	24.6	?.0	....	.0
20.6	3.5	cor	13	26.0	1.7	....	2.2
18.2	2.1	cor	2.3	27.9	3.8	....	21.5
16.9	.0	....	.0	30.1	6.4	w y	97
24.0	10.5	w y o	260	31.2	7.3	w be	137
22.7	7.8	g'B	125	32.8	9.5	w r o	270
21.5	5.4	w r	50	34.8	10.4	w y	400
				37.3	...	?w y'	410

[1] Coronas too vague for measurement.

74. New data for coal gas.—In case of the above results the large vacuum chamber was not quite filled with coal gas and there may have been diffusion from one vessel to the other. Again, the rubber connecting-tubes of the first experiment (though in advance of the filter) were replaced by lead connecting-tubes, as rubber is pervious to coal gas. Whether from these causes or others, the results came out quite differently after every part of the apparatus had been filled with coal gas. This is also shown in fig. 52 and the results themselves are inserted in table 44.

The new results for coal gas now conform in character with the data for media of air-water and carbon dioxide-water, and for the non-energized state, the coal-gas line lies between the curves for the other two media, as the figure shows. In like manner the curve for coal gas energized by the X-rays now betrays nothing abnormal. In endeavoring to discover reasons for the differences between the data of table 43 and table 44, the presence of rubber tubing in the former case comes nearest to suggesting a solution. Carbon disulphide emits nuclei spontaneously; whether these may pass through the filter has not been tested; but it is

conceivable that the action of coal gas on vulcanized rubber may in a somewhat similar way to carbon disulphide be productive of nuclei.

If these are larger than colloidal nuclei, though they may still be much smaller than ions, they would pass through the filter and give rise to the very phenomenon of depression of asymptote observed in table 43.

75. Conclusion.—Neither from the cases of CO_2 nor of coal gas does it follow that coercible gases have larger colloidal nuclei than non-coercible gases like air. The apparent results are the reverse of this. If the increased difficulties of condensation in the former are due to smaller heat ratios (γ) as compared with air, there is no reason why CO_2, where γ is larger, should show greater condensation difficulties than coal gas where γ is smaller. The distributions of nuclei suggest a common law of dissociation or chemical equilibrium.

COLLOIDAL NUCLEI AND IONS IN DUST-FREE AIR SATURATED WITH ALCOHOL VAPOR.

76. Introductory.—In my report* on the solutional nucleus and elsewhere† I came to the conclusion that the differences in promoting condensation exhibited by positive and negative ions were more probably to be ascribed to the difference in chemical structure or composition involving a difference of size than to the electrical differences as such. Experiments made in Wilson's apparatus by Dr. Donnan‡ with vapors of methyl and ethyl alcohol, carbon tetrachloride, carbon disulphide, benzol, and chlorobenzol show that the supersaturation needed to produce condensation was not necessarily greater in ionizing than in non-ionizing solvents. With similar apparatus Dr. K. Przibram§ recently examined a series of alcohols and other bodies ionized by the X-rays, obtaining among a variety of data a noteworthy result with a direct bearing on the question here at issue. It appears that whereas in the case of water vapor the negative ions are more efficient condensation nuclei than the positive ions, the reverse holds for the alcoholic vapors. In cases of methyl, ethyl, amyl, and heptyl alcohols (including some other bodies like chloroform) the positive ions invariably require less supersaturation to precipitate condensation than the negative ions of the same body.

Interesting differences are therefore manifest in the behavior of vapors, and it seemed desirable to test the nucleation of a medium of

* Structure of the Nucleus. Smithsonian Contrib., No. 1373, p. 161, 1903.

† Ions and Nuclei, Nature, LXIX, p. 103, 1903.

‡ F. G. Donnan: Phil. Mag. (6), III, pp. 305–310, 1902.

§ K. Przibram: Wien Sitzungsber., CXV, pt. IIa, pp. 1–6, 1906.

ethyl alcohol and air in comparison with the media of water-air and water-carbon-dioxide hitherto examined. The former behaves in fact as if the nuclei were throughout larger than in the latter cases.

77. Apparatus and method.—The experiments were conducted with an apparatus in which the connecting pipes between the fog chamber (18 inches long, 5 inches in diameter) and the vacuum chamber (5 feet long, 1 foot in diameter) were 4 inches in diameter, containing a 4-inch counterpoised plug stopcock. The whole connecting system was about 22 inches long, one-half of it belonging to the fog chamber. Experiments made with water vapor, however, did not show any further marked advantage arising from the use of the large passage-way specified, over the former apparatus, in which the corresponding tube was 2 inches in diameter. It is therefore superfluous to adduce for comparison the new data for water vapor. The general method for work was that frequently described in connection with these investigations.

78. Properties of alcohol fog.—While the experiments of my preceding paper with the medium of water vapor and carbon dioxide gas showed unusually high values of the exhaustions needed to produce coronal condensation, the case of alcohol-air shows correspondingly low values of exhaustion as compared with those for water-air. The number of colloidal nuclei entrapped by alcohol vapor are about 3.5 times larger than is the case for water vapor under like conditions. Hence the coronas for alcohol are exceedingly dense by contrast. They are also much less pure in color, and particularly at high exhaustions become fog-like. The phenomenon is coarsened and measurement less satisfactory.

As the alcohol fog particles are larger in size, they subside more rapidly at the same exhaustion than water particles; but the occurrences are in the former case far from simple. While the corona (if not too large) remains nearly the same throughout the slow subsidence of water particles, the corona for alcohol particles decreases one-half or more in size during this period. In other words, the alcohol particles experience very rapid growth during subsidence, from which it follows that many of them must evaporate to compensate in part for the eight-fold or more enlargement in bulk of the survivors. The same fact may account for the blurred coronas; for the true initial corona being very evanescent is probably not seen. Conformably with this view it is impossible to exceed large white-reddish forms in the present apparatus and to reach the high greens observed with water vapor.

79. Number of particles.—In order to determine the number of particles corresponding to a given corona, it is first necessary to compute the amount of alcohol precipitated per cubic centimeter of the exhausted

vessel by the sudden cooling incident upon exhaustion. This may be done by a straightforward approximation* with results shown in the following table, 45, where t_1 is the initial temperature of the saturated air within the fog chamber, t_2 the temperature after sudden exhaustion and before condensation, and t the temperature after the precipitation of the m grams of alcoholic fog per cubic centimeter. The drop in pressure is δp from $p = 76$ cm. at 20° C. The data of the last column will be presently explained.

TABLE 45.—Precipitation of alcohol vapor at different exhaustions (δp), supersaturations (S), and radius (r), of nuclei.

δp.	t_1.	t_2.	t.	$m \times 10^6$.	$S = p_r/p_\infty$.	$r \times 10^7$.
cm.	°	°	°	*Grams.*		*cm.*
10	20	+ 3.2	+14.8	10.0	2.42	1.44
20	20	−15.3	+10.2	18.3	6.21	.75
30	20	−36.1	+ 3.2	22.8	21.4	.48
These may be compared with the case of water vapor.						
8.5	20	+ 5.8	+14.7	2.6	2.17	1.65
17	20	− 9.6	+ 8.8	4.6	5.68	.77
22	20	−18.9	+ 4.6	5.5	11.1	.58
30	20	−36.1	− 3.5	6.4	69.7	.35

We may infer from the table that in a perfect apparatus and for true pressure differences† water fog particles would reach freezing (0° C.) at $\delta p = 24$ cm. and alcohol fog particles at $\delta p = 34.5$ cm. Moreover, for the same corona there must be on the average about 3.5 times more particles in the alcoholic fog than in the water fog, which accounts for the opaqueness of the former.

For the reasons adduced it is not worth while to express the results otherwise than in round numbers, for the data involved are inevitably crude. The assumption of the law of adiabatic cooling as far as − 36° C. is questionable, in view of the admixture of saturated vapor; but as the densities of vapor are for alcohol about 8 per cent that of air and for water vapor about 7 per cent, this approximation in a rarefied atmosphere like the use of Boyle's law for a wet gas is probably admissible. It is different, however, with the latent heat of the vapor, which is required at the low temperatures, but is known (as a rule) only at temperatures near the boiling-point. From this and similar points of

* C. T. R. Wilson: Phil. Trans., London, vol. 189, 1897, p. 300.

† δp computed as $p - p_2$ in the way shown in Chapter II, and not the apparent value observed at the fog chamber.

view, measurements of latent heat for the more common vapors at very low temperatures would be desirable.

Finally, the point at which the drop in pressure ceases to be efficient, on account of the increasingly rapid inward radiation of heat from the vessel, is the most serious of the outstanding errors. I have endeavored to diminish it compatibly with the desideratum of a large and easily adjusted fog chamber by successively increasing the bore of the exhaust pipes and stopcocks; and this plan has been in the large measure successful. The extent to which the error is present, as the drop in pressure increases more and more, is nevertheless left unanswered. If the upper inflection of the distribution curve (fig. 56) is a criterion, *i. e.*, the occurrence of identical terminal coronas for successively increasing exhaustions, the fog chamber with water-air is efficient to about $\delta p = 31$ or 32 cm., with water and carbon dioxide to about $\delta p = 37$ cm., with alcohol and air to about $\delta p = 20$ cm. In the former case the vapor would be cooled from 20° to about -10° C. even after condensation; in the latter case to about $+10^\circ$. On general principles and in view of the low temperature of the water, it would seem probable that the efficiency of the fog chamber must vanish gradually. But the appearance of the curves is such as if the action were unimpaired up to a given terminal drop in pressure.

In every case the fog particles with the surrounding medium of vapor soon reach the temperature of the air again, so that additional moisture must arrive from somewhere. It is remarkable that the marked constancy of the water coronas in perfectly tight apparatus during this period gives no evidence of the evaporation; while the alcohol coronas decrease one-half in aperture or the preponderating fog particles actually grow. Even if this is compatible with the evaporation of the smaller particles, there is again no evidence for it. Much of the moisture must therefore come from the wet cloth and the water within the vessel, which are not cooled by the expansion.

80. Size of the nuclei.—Here it may be worth while to inquire into the reason why the precipitation in alcohol is apparently so much easier; or, what is the same thing, into the estimated size of the nucleus on which precipitation takes place in these several cases. The Kelvin equation as modified by Helmholtz* may be used for this purpose, as was done by the latter and by Wilson† in the form $p_r/p_\infty = \epsilon^{2T/Rs\vartheta r}$ where p_r and p_∞ are the vapor pressures at the convex areas of radius r and radius infinity, respectively, T the surface tension of the liquid of density (s), R the gas constant of its vapor at the absolute temperature (ϑ).

*Helmholtz: Weid. Ann., XXVII, p. 524, 1886.
†Wilson: Phil. Trans., vol. 189, p. 305, 1897.

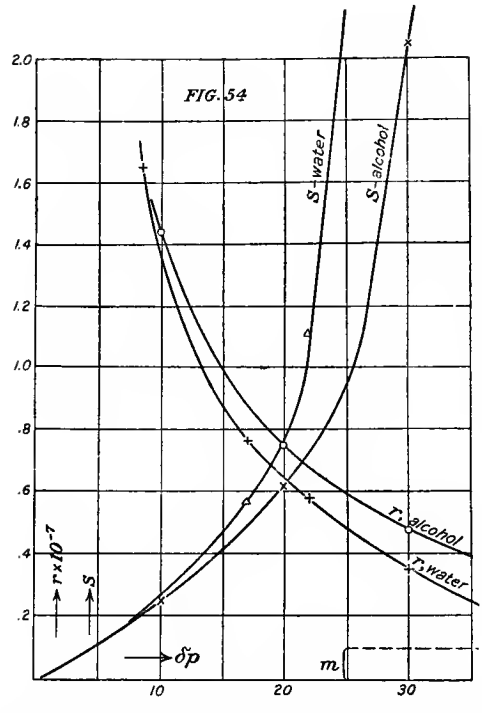

FIG. 54.—Supersaturations (S) of media air-water and alcohol-water, and estimated radius (r cm.) of smallest efficient nuclei, at different exhaustions (δp). m, molecular radius. Table 45.

Since p_r is the adiabatically reduced vapor pressure (without condensation) in the volume expansion due to the drop of pressure (δp) and p_∞ the normal vapor pressure at the same temperature ($\vartheta = 273^\circ + t_2$ in table 1), r follows from the equation. The values of p_r/p_∞ and r so found are both given in table 45, and have been constructed in the chart (fig. 54), where their relation to the usual order of molecular size is also indicated. Clearly these values of r, the radius of the nuclei differing so little from molecular radii (say 10^{-8}), can only indicate an order of values; for apart from the difficulties above enumerated in computing ϑ, r depends on surface tension (T), which has no meaning for molecular dimensions. Granting this, it is none the less remarkable that the values of r obtained should be so nearly alike for water and alcohol where different constants (T, R, s, etc.) occur throughout; in other words, that at a given temperature a given drop of pressure will condense both vapors on nuclei of about the same size.

In so far as these estimates are admissible it follows that the alcohol-air nucleus is larger than the water-air nucleus, since in the former case coronal condensation begins at about $\delta p = 15$ cm. where $r = 10^{-7}$ cm. and in water vapor it begins at $\delta p = 26$ cm. where $r = 4 \times 10^{-8}$ cm. about, less than half as large. These relations once established are retained through all successions of nuclei, as the following data for alcohol vapor in comparison with water vapor show. It is a little difficult to understand why the ionized nuclei in alcohol vapor should, like the colloidal nuclei, be larger than the corresponding cases for water vapor, unless the ions are aggregated vapor nuclei, a point of view tentatively advanced elsewhere; but this larger alcohol nucleus suggests that it is primarily

TABLE 46.—Colloidal nuclei and ions in alcohol vapor, energized or not; 4-inch cock.

	δp.	s.	Corona.	$n \times 10^{-3}$.
I. April 23. Not energized	30.8	10	[1]w r′	1,060
	28.4	10	[1]w r′	1,005
	26.0	10	[1]w r′	950
	23.0	11	[1]w y′	1,100
	21.1	10	[1]w c	615
	19.1	7.7	g B P	385
	17.3	4.8	cor	108
	16.0	2.4	cor	11
	4.7	1.5	cor	4
	13.4	1.1	cor	3
	12.3	(?)	[2]	0
	10.2	(?)	[3]	0
	19.9	(?)	[2]	0
	12.7	0	[3]	0
	16.7	5.0	cor	115
	18.5	7.7	g B P	380
	20.0	10.5	w r′	680
II. April 24	34.0	10	[1]w r′	940
	42.0	10	[1]w r′	1,040
	38.8	11	[2]w o′	1,170
	34.2	11	[1]w o′	1,110
	32.2	11	[1]w o′	1,080
	29.3	12	[1]w y′	1,270
	26.8	....	[1]w y′	1,210
	24.0	....	[1]w y′	1,120
	21.9	11	[1]w r′	720
	20.0	10	[1]w c	600
	18.3	8.2	w y	340
	16.7	3.5	cor	38
	15.0	1.0	cor	3
Later	14.8	1	cor	3
	16.3	5.0	[3]w r′	115
	18.3	7.6	w y b	320
	19.5	9.0	w r′	585
	21.7	10.5	w r′	720
	22.0	10.5	w r′	740
April 25	26.0	12	w y′	1,190
III. X-rays on. $D = 15$ cm	25.2	[4]12	w y′	1,160
	17.7	12	w y′	920
	15.1	11	w r′	650
	14.0	8.4	w y B	275
	12.9	2.6	cor	13
	11.5	.5	(?)	0
	11.5	.0	(?)	0
X-rays off	11.0	[5].0	....	0
IV. X-rays on. $D = 15$ cm	12.4	[5].0	....	0
	13.2	5.1	cor	101
	14.2	8.1	w B P	275
	15.1	10.	w r′	490
	16.1	10.5	w r′	580
April 26	36.6	11	w y′	1,420

[1] Accompanied by dense fogs, rapidly subsiding, with coronas dwindling.
[2] Small coronas probably due to shaking.
[3] All coronas accompanied by dense fogs.
[4] Coronas decreased in size during subsidence, more than one-half.
[5] Coronas often due to solutional nuclei; produced by shaking.

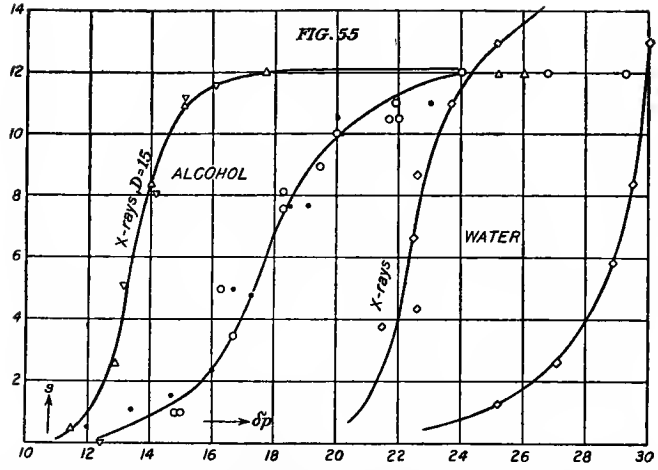

FIG. 55.—Aperture of coronas (s), observed at different exhaustions (δp), in media of alcohol-air, water-air, energized or non-energized. Table 46.

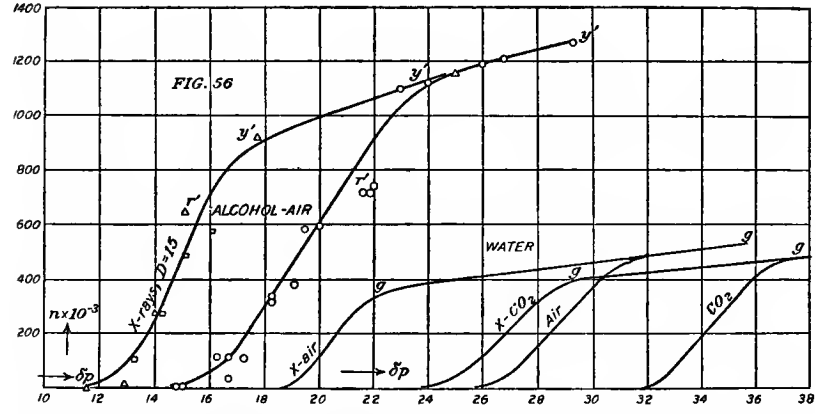

FIG. 56.—Efficient nucleation n in energized or non-energized media of alcohol-air and water-air, at different exhaustions (δp). Table 46.

the saturated vapor which furnishes the colloidal nuclei and that the gas is only secondarily involved.

81. Data for alcohol vapor.—The behavior of alcohol vapor is shown in the usual way in table 46, where δp is the sudden fall in pressure from atmospheric pressure producing the corona of the angular diameter $s/30$, when the eye and the source of light are at distances 40 and 250 cm. on the opposed sides of the fog chamber. The nucleation n is computed in the way given above, section 79, and indicates the number of

nuclei in the *exhausted* fog chamber. It is assumed, therefore, that the nuclei are reproduced more quickly than they can be withdrawn by the exhaustion. Measurement of s is not very satisfactory, as the coronas are blurred and accompanied by dense fogs and changes rapidly on subsidence. The effect of X-radiation is shown in parts III and IV of the table leading to the same terminal corona as for the non-energized vapor.

The results have been given graphically in figs. 55 and 56, the former referring to coronas (s), the latter to nuclei (n), in connection with earlier results for media of water-air and water-carbon dioxide, the same condensation apparatus and method underlying all experiments. One may notice at once that in the cases CO_2-water and air-water, both for the non-energized and for the energized state, the observed data would be obtained by shifting the air-water diagram as a whole to the right, as if the cooling in case of CO_2-water vapor were less efficient. The graphs are of the same kind, nearly parallel, and all of them (energized or not) terminate in the same asymptote or large green-blue-purple corona.

The alcohol curves are different from these chiefly in three respects: (1) Though the graphs both for the non-energized and energized states again terminate in the same asymptote, this is not the green-blue-purple corona, but the white-yellow corona which lies slightly below it; (2) the curves as a whole lie with a somewhat larger slope in a region of much lower exhaustions (δp); (3) the number of nuclei caught in alcohol vapor is relatively very large. The second and third observations have already been discussed. The first deserves especial consideration. The question occurs at once why both the energized and the non-energized curves should terminate in the same final corona, irrespective of the size of the nuclei, and why this should be lower for alcohol than for water. For the ionized state one might infer that the total number of ions has been precipitated, as is actually the case for low ionization; but if for strong ionization this were true for alcohol vapor it could not be true for water vapor where the number of ions caught is less than one-half the number in alcohol. In general, it is improbable that the terminal corona for ions should in such a case be the same as the terminal corona for colloidal nuclei.

The explanation which seems plausible to me is this: Each nucleus must drain the air of its supersaturated moisture within a certain radius, large as compared with the size of the nucleus and increasing in the lapse of time.

A limit of the phenomenon will be reached when for an indefinite number of graded nuclei the enveloping spheres free from supersatu-

ration form a system in contact. In case of water vapor the distance between centers would be 0.014 cm.; in case of alcohol 0.010 cm., distances which are both enormous as compared with the estimated size of nuclei (r, table 45, fig. 54). The greater distance which belongs to water vapor would be in keeping with its greater diffusivity, though this surmise does not work out for water-carbon dioxide as compared with water-air. At all events, when the limiting number of nuclei has been captured, the apparatus is powerless to produce condensation on a greater number of nuclei, be they relatively large as the ions or small as the colloidal nuclei, however many other inefficient nuclei may be present.

ABSENCE OF COLLOIDAL NUCLEI IN STRONG ODORS.

82. Introductory.—Throughout the course of my work I have been endeavoring to find whether bodies with strong odors and presumably large molecules could be regarded as a source of colloidal nuclei; or whether there is any relation between the colloidal nucleus and the odors. In case of carbon disulphide, from which nuclei apparently escape spontaneously, this would seem to be the case; but it is yet to be proved that vapor of carbon disulphide, if carefully filtered, nevertheless still produces colloidal nuclei in the fog chamber. In the present instance it is not improbable, if relatively few CS_2 molecules are oxidized SO_3, that sulphuric acid nuclei are the result. The experiment which has already been discussed is well worth while; but I did not make it, in the fear of contaminating the vacuum chamber. The following experiments show, however, that even in the extreme cases odors are due to molecules, and that in relation to the fog chamber, apparently large molecules are still quite negligibly small in comparison with the colloidal nuclei.

83. Data for camphor, turpentine, naphthalene.—The results obtained are given in table 47 in the usual way. The glass fog chamber was provided with a hole in the (thick) bottom, about 2 cm. in diameter and closed with a rubber cork. It was free from leakage from without. The bodies to be examined were introduced through the hole in question, and suspended in the middle of the fog chamber by aid of a wire-gauze tube 20 cm. long and 2 cm. in diameter. After putting this tube in place the air was carefully cleansed by precipitation of dust.

On May 5, 6, and 7, after putting the apparatus together, the medium within was first examined without introducing the odoriferous body. The internal sources of spurious nucleation gradually vanish. The

TABLE 47.—Miscellaneous experiments. Water nuclei effect of metal surfaces, of odors, etc. $\delta p = p - p_3$. Four-inch pipes and plug cock.

Date, etc.	δp.	s.	Corona.	$n \times 10^{-3}$.
May 5. Wet cloth lining in exhaust tube..	30.8	9.4	w r g′	240
	30.6	[1]6.5	cor	105
	30.8	10.0	w r g′	260
May 6	30.8	12.0	wy bg	380
May 6	30.8	[1]11.0	w r g	275
	30.8	11.0	w r g	275
	30.5	10.0	w p g	230
May 7	30.6	11.0	w y′ g	380
Examination of odors:[2]				
May 8. Air only	30.7	11	w r g	305
	30.6	11	w r g	275
May 9. Air, camphor in	30.8	11	w o g	305
	30.8	11	w y g	380
May 10. Camphor	30.8	13	g′ to gy	410
	30.8	13	g′	455
May 11. Camphor	30.8	13	g′ to gy	425
Air without camphor	30.6	13	g′ to gy	425
May 12. Air	30.6	12	y o	410
May 13. Turpentine	30.7	([3])	g y o	410
May 15. Naphthalene[4]	30.6	13	g to gy	425
	30.6	13	g B P	455
	30.8	13	g B P	455

[1] Foreign nuclei not absent in second exhaustion.
[2] Hole drilled in bottom of glass fog chamber, closed by rubber cork.
[3] Apparatus blurred.
[4] Enlargement of coronas due to second (smaller) exhaustions.

exhaust pipes were cloth-lined and the cloth kept wet to guard against minor saturation error. On May 8, with the introduction of camphor, the nucleation apparently rises to a maximum (g-b-p. corona); but the same result is maintained after the removal of the camphor and the gauze (tested in many observations not recorded in the tables). Hence the camphor nuclei can not be larger than the colloidal nuclei of air-water; for the presence or absence of camphor within a fog chamber is inappreciable. The same conclusion follows from the experiments with turpentine (where the walls of the fog chamber were speedily blurred from distillation of small quantities out of the lamp wick holding the liquid) and from naphthalene. It is fair to conclude that presumably large molecules are nevertheless bodies of an inferior order of size relative to the colloidal nuclei of dust-free air.

84. Summary.—Media of coal gas and water require higher exhaustion than media of air and water, media of carbon dioxide and water higher than coal gas and water, to precipitate condensation in like degree,

other things being equal. On the other hand, media of alcohol and water require smaller exhaustion to precipitate an alcohol fog in corresponding degree. The general character of the phenomena in all these several cases are, however, the same. Their relation to each other when the media are energized in like manner by the X-rays is also the same. (*Cf.* fig. 56.)

It does not follow, therefore, that wet coercible gases like carbon dioxide and coal gas contain larger colloidal nuclei than wet air. The apparent result would be quite the reverse of this. Neither can the difference be explained in terms of the respective value of the ratio of specific heats (γ); for in relation to condensation, the order is air, coal gas, carbon dioxide; in relation to γ, air, carbon dioxide, coal gas. The probable occurrence of large colloidal nuclei in media of alcohol and air and relatively small colloidal nuclei in water and air seems to show that the colloidal nuclei are primarily to be associated with the saturated vapor, and that the gas involved is of secondary importance. It can not be a question of mere solubility of gas in the vapor, for this is strongest in water and carbon dioxide, in which there is no evidence of large nuclei. The curves of distribution of number with size are again such as to suggest a common law of equilibrium.

The presence of strong odors (camphor, naphthalene, turpentine, etc.) in the fog chamber is without an appreciable effect. Hence the colloidal nuclei can not be large molecules merely, and colloidal nuclei can not be ascribed to chemical impurities in the gas.

Continued slow exhaustion seems to be favorable to the growth of fog particles and the formation of rain.

Both for the energized and for the non-energized state, the graphs for the same media, though referring to nuclei of widely differing sizes (ions, colloidal nuclei), again terminate in the same asymptote, or end in the same terminal corona. This is not identical for different media, however, the corona being of lower order though denser for alcohol and air, of higher order but thinner for water and air, for instance. The number of nuclei caught (*cæt. par*) in alcohol and air is much larger than in water and air. When the limiting number of nuclei has been reached by condensation, the system is powerless (in a given apparatus) to condense on a greater number of nuclei, be they relatively large like the ions or small like the colloidal nuclei.

CHAPTER V.

THE COTEMPORANEOUS VARIATIONS OF THE NUCLEATION AND THE IONIZATION OF THE ATMOSPHERE OF PROVIDENCE.

By Lulu B. Joslin.

85. Introduction.—The results obtained by Professor Barus,* showing a characteristic succession of the values of atmospheric nucleation throughout the year, suggested a parallel inquiry into the variations of the number of ions in the atmosphere in the lapse of time. The present work was therefore undertaken at his instigation, and observations systematically carried forward from August, 1905, to April, 1906.

In addition to the main purpose in view, it was hoped that a number of subsidiary questions might be answerable. Thus a large part of the nucleation of Providence is of local origin and enters the atmosphere with other products of combustion. Initially these nuclei were either highly ionized themselves, or at least the atmosphere originally received an accession of ions and nuclei in proportional quantities. It is therefore of interest to inquire whether any of the ionization survives, or whether there is any connection observable between corresponding changes of the nucleation and the ionization of a given place. The results, which are carefully tabulated in the present paper, seem to show that there is no such connection whatever; or that the persistent ionization arises from, and is maintained by, causes which are quite distinct from the nucleation. No evidence has been found to suggest that the ionization is either emitted or absorbed by the nucleation, whence it follows that the ionization arises from causes wholly non-local. Apart from these main purposes, the data are interesting as a continuous record of ionization (which will be supplemented in the future), though, as yet, sufficient time has not elapsed to ascertain whether the opposition in the monthly positive and negative ionizations found in the sequel is real or incidental. (*Cf.* fig. 62.)

Finally, I may add that work to investigate a possible relation between the nucleation and the ionization of the atmosphere was undertaken in Helgoland and on the coast of the Ostsee by Prof. G. Lüdeling† in 1902 and 1903, using Aitken's dust-counter. The time during which observations were recorded (August 21 to September 16, 1902, June 17 to July 4, 1903) were insufficient to warrant general conclusions, however, apart from the interesting special investigations which Professor Lüde-

* Smithsonian Contrib., xxxiv, No. 1625, chap. ix, 1906; Carnegie Institution publication No. 40, January, 1906, chaps. iv and v.

† Two papers in the Veröffentl. Königlich Preussischen Meteorologischen Instituts, Berlin, 1904.

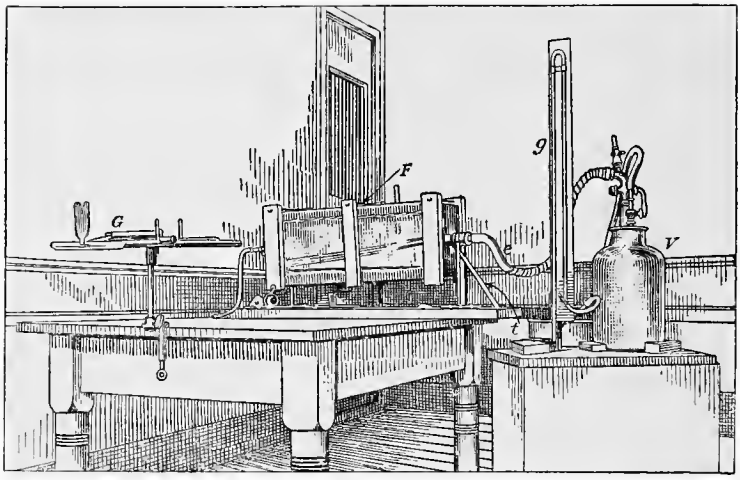

FIG. 57*a*.—Disposition of coronal apparatus for measuring atmospheric nucleation ("dust"). *V*, vacuum chamber; *F*, fog chamber; *G*, goniometer; *g*, gage; *e*, exhaustion pipe; *t*, support for trunnions. Influx pipe at left end of fog chamber.

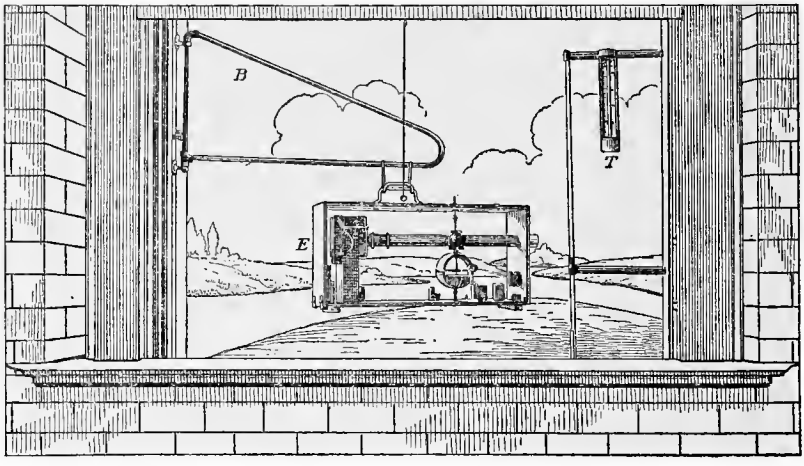

FIG. 57*b*.—Disposition of apparatus for measuring atmospheric ionization. *E*, Ebert's apparatus; *B*, swiveled brackets sustaining the same; *T*, thermometers.

ling's paper contains. Reference should also be made to P. Langevin's* important discovery of slow-moving ions in the atmosphere and to the work of M. Bloch,† but comparisons of this nature are quite beyond the scope of the present straightforward experimental research.

86. Measurements of nucleation.—Number of nuclei in the atmosphere were measured by aid of the corona of cloudy condensation, in the way

*P. Langevin: Bull. Soc. Franç. de Phys., p. 79, 1905.

†Bloch: "Recherches sur la conductibilité électrique, etc.," Paris, 1904. See C. T. R. Wilson, Trans. Intern. Congress, St. Louis, vol. 1, p. 365.

fully described by Professor Barus (*loc. cit.*, chap. 8), and the same apparatus (fig. 57*a*) which had proved efficient in the earlier investigations was used throughout the present experiments. *F* is the revoluble wood fog chamber with plate-glass windows, *V* the vacuum chamber, *i* the influx, *e* the exhaustion pipe, *g* the gage, *G* the goniometer. Source of light beyond *F* is not shown. Two or more observations were usually made daily, together with the meteorological elements of wind, weather, and similar data. The ionizations referred to below, section 91, were taken in the same place.

87. Data for nucleation.—In table 48 the first column shows the day and month, the second the time in hours and tenths of an hour. The third gives the current weather, F denoting fair, F′ partly fair, C′ partly cloudy, C cloudy, R rain, Sn snow, etc. The temperature of the fog chamber. (°C.) and the temperature of the atmosphere (°F.) follow. The remaining columns show the data referring to the coronas, the sixth giving the diameters (*s*) of the coronas at the end of a radius of 30 cm. Hence $s/30$ is nearly their angular diameter when the eye and the source of light are at distances 85 cm. and 250 cm. on opposite sides of the fog chamber. The seventh column indicates the colors of the successive annuli of the coronas, reckoned from within outward, w denoting white, r red, o orange, y yellow, g green, b blue, p purple, etc. A vertical line (|) shows an indeterminable color, a prime (′) an approach to a color, etc. The last column gives the number of nuclei in thousands per cubic centimeter, deduced from the amount of water precipitated per cubic centimeter, and the sizes of particles in successive coronas, as listed by Professor Barus (*loc. cit.*).

88. Remarks on the table of nucleation.—With regard to the individual observations very little can be adduced that has not already appeared in the earlier work. Conformably with the mild winter, the nucleation as a whole is relatively low, an unfortunate occurrence in its bearing on the purposes of the present work; but deductions of this character will be brought forward with advantage in connection with the daily and monthly mean nucleations below. It is rather curious that the forest fires on Cape Cod in the early May and the powder combustion on July 4 produce so little impression; on the other hand, the cold weather in August is at once marked by large coronas.

89. Mean daily nucleation.—The data of table 48 have been averaged for the successive days in table 49, with other data at once intelligible. The results, if given graphically with the current days as abscissas, the corresponding mean nucleations in thousands per cubic centimeter as ordinates, show no new points of view. One may note the rare occurrence of the large g-b-p coronas so frequently met in the high nucleations of the preceding winter.

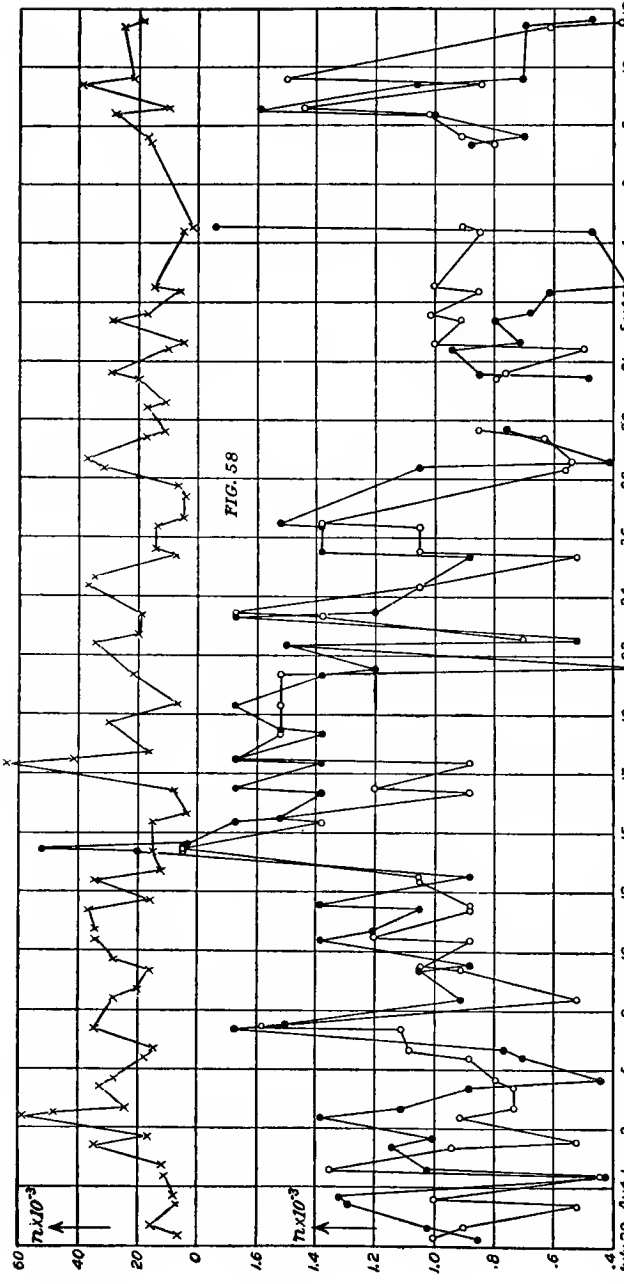

FIG. 58.—*Lower curves:* Daily ionization (*i*, thousands of ions per cubic centimeter) at the times given from August, 1905, to March, 1906. Positive values marked by open, negative by black circles. Observations connected by straight lines. *Upper curve:* Daily nucleations (*n*, in thousands of nuclei per cubic centimeter) observed at the same time. Table 49.

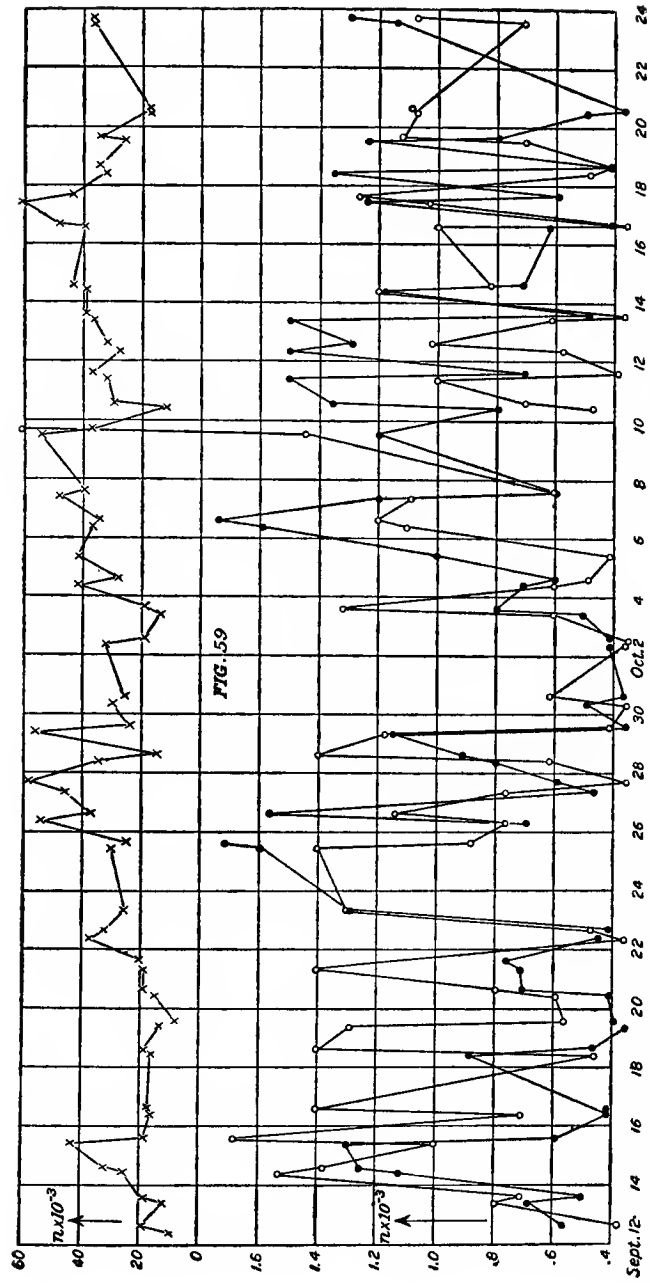

FIG. 59.—*Lower curves:* Daily ionization (*i*, thousands of ions per cubic centimeter) at the times given from August, 1905, to March, 1906. Positive values marked by open, negative by black circles. Observations connected by straight lines. *Upper curve:* Daily nucleations (*n*, in thousands of nuclei per cubic centimeter) observed at the same time. Table 49.

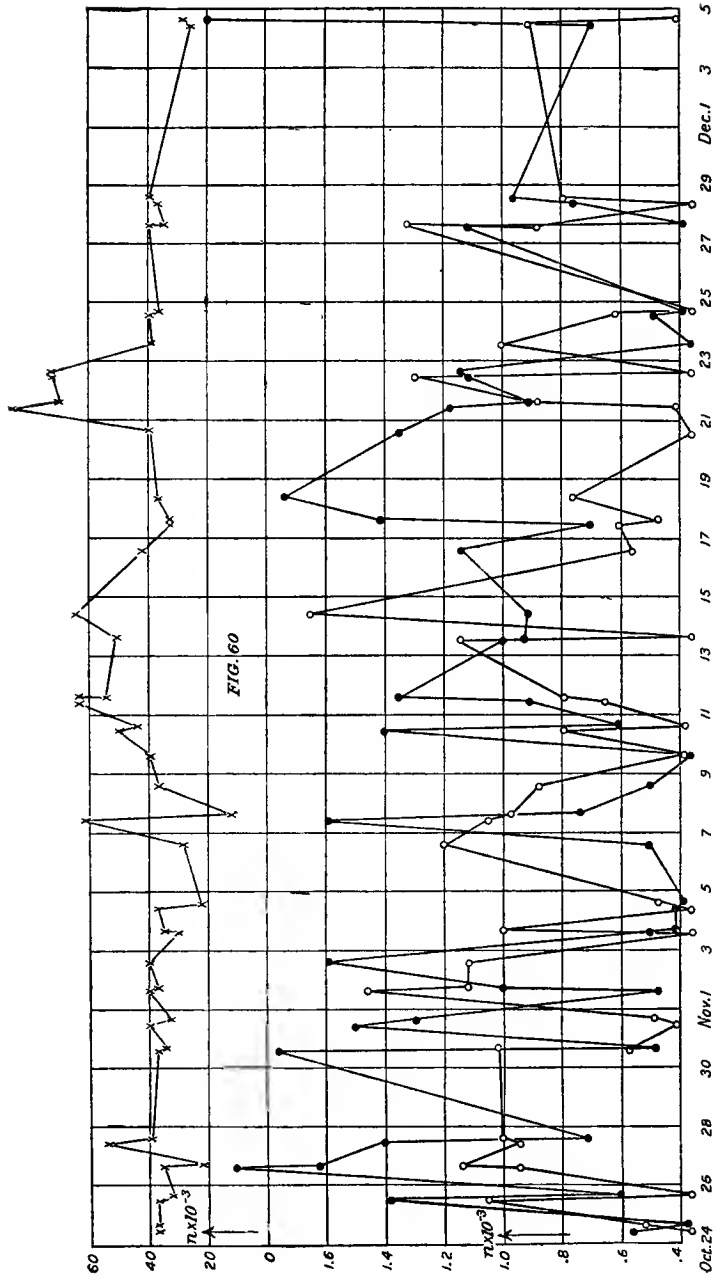

FIG. 60.—*Lower curves:* Daily ionization (*i*, thousands of ions per cubic centimeter) at the times given from August, 1905, to March, 1906. Positive values marked by open, negative by black circles. Observations connected by straight lines. *Upper curve:* Daily nucleations (*n*, in thousands of nuclei per cubic centimeter) observed at the same time. Table 49.

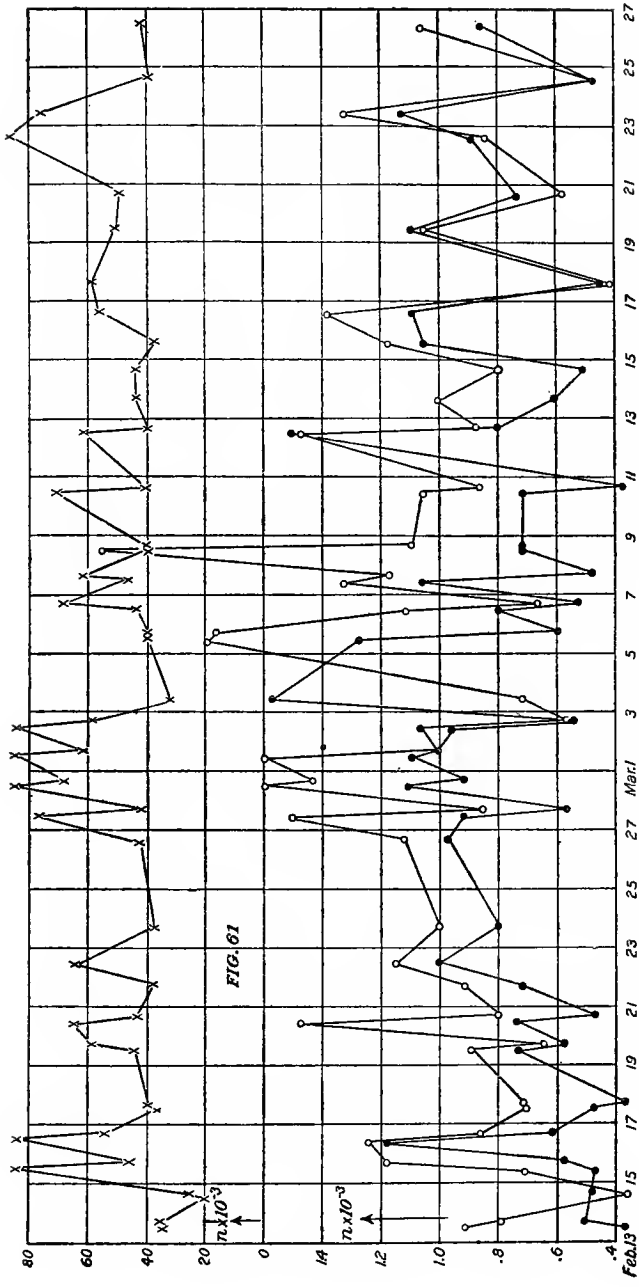

FIG. 61.—*Lower curves*: Daily ionization (*i*, thousands of ions per cubic centimeter) at the times given from August, 1905, to March, 1906. Positive values marked by open, negative by black circles. Observations connected by straight lines. *Upper curve*: Daily nucleations (*n*, in thousands of nuclei per cubic centimeter) observed at the same time. Table 49.

TABLE 48.—Showing the number of nuclei, n, per cub. cm., in the atmosphere at the times (in days and hours) stated. The temperature given in degrees F. refers to the atmosphere, the temperature in degrees C. to the fog chamber.

Date.	Time.	Weather.	°C.	°F.	s.	Corona.	$n \times 10^{-3}$.
1905.	*Hours.*						
May 4	9.8	C	21	50	3.2	cor	11.3
	12.7	C	21	53	3.2	cor	11.3
	6.2	F	21	53	3.2	cor	11.3
5	9.4	F	20	57	4.9	w B P	41.7
	6.0	F	20	54	4.6	cor	34.8
6	9.6	F	20	68	5.9	w C g	68
	12.7	C	21	75	6.6	w o g	90
	1.1	..	..	..	5.8	w P cor	64.5
	6.0	C	21	68	4.9	w o g	41.7
7	9.7	C′	21	75	4.8	w o g	39.5
	1.5	C′	21	84	4.8	w o g	39.5
	6.8	F	22	73	3.8	cor	19
8	9.0	F	21	60	6.7	w o g	92.5
	9.5	F	21	65	7.1	w y g	100
	3.0	F	21	65	4.8	w r g	39.5
9	9.8	R	20	61	4.8	w r g	39.5
	1.4	F	21	65	4.9	w B P	41.7
	6.3	F	20	59	4.6	w o g	34.8
10	9.6	F	19	60	5.6	w o g	58.7
	3.3	F	19	68	4.7	w o g	37.2
	6.2	F	..	66	4.7	...	37.2
11	9.3	F	19	66	5.6	w c g	58.7
	6.2	F	20	65	4.5	w r g	32.4
12	3.2	C′	20	68	3.8	cor	19
	6.0	C′	..	66	4.7	...	37.2
13	9.4	C′	..	60	4.6	...	34.8
	2.8	C	18	62	3.6	cor	16.2
	6.3	C	..	55	3.2	cor	11.3
14	9.8	C	19	59	3.3	cor	12.5
	1.4	R	19	49	3.8	cor	19
	6.2	R′	19	61	3.8	cor	19
15	9.1	C	19	60	4.5	w r g	32.4
	3.8	C′	19	67	3.6	w r g	16.2
	6.3	C	19	61	3.6	w r g	16.2
16	9.3	C	18	55	3.5	w r g	15
	3.4	R′	18	52	3.1	w r g	10.2
17	9.3	C	18	49	3.6	cor	16.2
	6.0	C	17	49	3.9	cor	20.5
18	9.4	C	16	55	3.7	cor	17.5
	2.8	F	18	65	4.6	g B P	34.8
	5.0	F	18	64	...	...	....
19	10.0	C′	18	65	4.5	w r g	32.4
	6.0	C′	18	66	4.6	w r g	34.8
20	10.3	F	17	57	6.0	w c g	70.5
	6.3	F	18	58	3.9	cor	20.5
21	9.4	F	18	59	4.6	g B P	34.8
	3.2	F	18	65	3.5	cor	15
22	9.1	F	17	64	4.7	cor	37.2
	3.7	F	18	69	4.6	cor	34.8
23	9.0	C′	18	60	5.2	w P cor	48.2
	6.5	F	18	59	4.6	w r g	34.8
24	9.3	F	17	59	6.1	w r g	73.3
	6.7	F	17	60	4.1	cor	24
25	9.3	F	17	65	6.2	w r g	76.5

TABLE 48.—Continued.

Date.	Time.	Weather.	°C.	°F.	s.	Corona.	$n \times 10^{-3}$.
1905.	*Hours.*						
May 25	3·3	F	18	69	4.8	w B P	39·5
26	9·2	F	18	72	4.8	w o g	39·5
	6.0	F	19	69	4·3	cor	28
27	8.8	C	19	69	3.8	cor	19
	6.7	R′	20	67	3.6	cor	16.2
28	9.8	F	20	77	4·3	w r g	28
	5.0	F	20	75	4·7	w r g	37.2
29	9.4	F	20	74	3·9	w r g	20.5
30	9.4	C	21	63	3.4	cor	13.8
	3·3	F	21	70	3.4	cor	13.8
31	9.0	F	20	64	3.2	cor	11·3
June 1	9.2	C	18	60	3.5	cor	15
	4.0	F	19	64	3.5	cor	15
2	9.9	F	19	65	4.7	cor	37.2
3	6.0	F	19	69	4·3	cor	28
4	9.5	F	19	70	4.8	w P cor	39·5
	5.0	F	19	71	3.7	cor	17·5
5	9·3	F	20	73	3·7	cor	17·5
6	9.9	R	21	63	2.9	cor	8·3
7	9.7	C	18	58	4.6	cor	34.8
8	9.2	R′	18	50	4.1	cor	24
	6.4	F	18	55	4.1	cor	24
9	9.4	F	17	66	5.4	w B cor	54.2
	5.8	F	19	69	4.0	cor	22
10	9.2	F	19	73	5.2	w	48.2
	6.1	F	20	75	4.0	cor	22
11	11.3	F	19	71	3·9	cor	20.5
	6.0	C	19	66	3.4	cor	13.8
12	9.5	R	19	65	4.7	cor	37.2
	5.5	R	19	62	3·9	cor	20.5
13	9·5	C	20	69	4.4	w r g	30
14	9.6	F	20	73	4.4	w r g	30
15	9.6	F	21	81	5.7	w r g	61.5
	6.0	F	22	76	3.8	cor	19
16	9.7	F	22	79	4.6	cor	34.8
	5.6	F	23	78	4·3	cor	28
17	9·5	F	22	73	4.2	cor	25.8
18	10.9	F	23	86	5.0	cor	43.8
	5.4	F	24	84	3.1	cor	10.2
19	10.8	F	20	62	2.8	cor	7·3
20	12.4	R	18	58	3·3	cor	12.5
22	10.4	C	20	69	4.1	cor	24
23	10.2	F	21	82	3.0	cor	9·3
24	10.0	C	21	74	4.8	w B P	39·5
	6.0	F	21	76	4.2	cor	25.8
25	11.4	F	21	82	3·7	cor	17·5
26	10.5	F	23	82	3·9	cor	20.5
27	10.0	F′	21	67	4.4	w r	30.0
28	11.0	F	20	70	4.8	g b P	39·5
	6.0	F	21	71	3·9	cor	20.5
29	10.3	F	21	76	4.8	w o cor	39·5
	6.6	F	21	77	3.6	cor	16.2
30	10.9	F	21	80	4.6	w y′	34.8
July 1	10.6	F	22	76	4.1	cor	24
	6.0	F	..	73	4.6	cor	34.8

TABLE 48.—Continued.

Date.	Time.	Weather.	°C.	°F.	*s.*	Corona.	$n \times 10^{-3}$.
1905.	*Hours.*						
July 2	12.0	R′	23	72	3.8	cor	19
3	11.3	C′	22	77	3.5	cor	15
4	11.2	F	23	86	4.7	w o	37.2
	6.5	F	23	81	3.1	cor	10.2
5	10.8	F	23	73	3.2	cor	11.3
6	9.8	C	23	72	2.9	cor	8.3
	5.5	F	23	72	3.9	cor	20.5
7	10.7	C′	23	79	5.9	w c g	68
8	12.0	C′	23	82	4.6	w r g	34.8
	4.0	F	..	80	4.2	w c g	25.8
9	11.0	F	24	85	4.6	g b p	34.8
	6.0	F	24	84	2.4	cor	4.6
11	10.3	F	26	85	4.7	w r g′	37.2
	4.5	C′	26	88	4.1	cor	24
12	10.6	F	26	89	5.4	w P cor	54.2
	6.0	F	27	85	3.7	cor	17.5
13	11.0	C′	26	88	4.9	w B cor	41.7
	5.7	F	..	84	3.7	cor	17.5
14	10.0	F	26	84	4.7	g B P	37.2
	5.5	F	27	83	4.4	w r	30
15	10.4	F	26	82	4.0	cor	22
	....	F	26	..	3.1	cor	10.2
16	10.7	F	25	78	3.8	w r	19
17	12.5	R′	26	85	3.5	cor	15
	5.3	R′	26	90	4.1	w r g	24
18	10.7	F	26	91	4.7	....	37.2
19	10.7	F	27	92	4.1	cor	24
	6.0	R	28	84	4.1	cor	24
20	10.5	F	27	86	4.2	cor	25.8
	6.0	F	27	82	3.3	cor	12.5
21	10.6	F	26	77	4.3	w o	28
	6.0	F	26	79	3.0	cor	9.3
22	10.5	F	25	80	5.5	w c g	56.2
	6.0	C	..	73	3.0	cor	9.3
23	10.3	R	25	65	2.2	cor	3.3
	6.5	C	..	67	1.8	cor	1.9
24	10.3	C	23	73	4.0	cor	22
25	10.2	C	23	77	4.5	w o cor	32.4
	6.0	F	23	77	3.7	cor	17.5
27	10.5	F	22	80	4.2	w r g	25.8
	4.7	F	23	81	4.6	w r g	34.8
29	9.8	C	23	76	2.6	cor	5.9
	4.6	R	24	73	3.5	w r g	15
30	10.6	R	..	75	2.2	cor	3.3
	6.0	R′	24	70	2.4	cor	4.6
31	10.3	C	23	66	2.7	cor	6.6
	4.3	C	23	67	2.8	cor	7.3
Aug. 1	10.4	R	22	63	3.2	cor	11.3
	6.0	R	21	65	3.2	cor	11.3
2	10.0	F	21	76	4.6	w r g	34.8
	6.0	C′	22	75	3.6	cor	16.2
3	9.6	F	21	75	5.6	w c g	58.7
	12.7	F	21	81	5.2	w P cor	48.2
	5.1	F	..	76	4.1	cor	24
4	9.7	F	21	78	4.5	g B P	32.4

TABLE 48.—Continued.

Date.	Time.	Weather.	°C.	°F.	*s*.	Corona.	$n \times 10^{-3}$.
1905.	*Hours.*						
Aug. 4	5.5	F	22	75	4.3	cor	28
5	9.7	C′	23	77	3.7	cor	17.5
	6.0	F	23	73	3.4	cor	13.8
6	10.7	F	23	80	4.0	cor	22
	6.0	F	23	76	3.2	cor	17.5
7	9.4	F	23	82	4.6	w r g	34.8
	....	R′	24	79	3.9	....	20.5
8	10.0	R′	24	77	4.3	w r g	28
	6.0	C′	25	80	3.9	....	20.5
9	9.6	C	24	76	3.6	....	16.2
	6.4	R	25	73	4.3	w r g	28
10	9.6	F	24	81	4.6	g B P	34.8
	6.0	C	..	79	4.6	w r g	34.8
11	9.8	C′	25	80	4.7	w o cor	37.2
	6.0	F	27	80	3.6	cor	16.2
12	10.5	C′	26	85	4.6	g B P	34.8
	6.0	C	26	79	3.3	cor	12.5
13	10.7	C	26	86	2.2	cor	3.3
	6.0	C′	26	78	3.2	cor	11.3
14	9.7	F	25	72	3.5	cor	15
15	10.7	R	23	66	3.5	cor	15
	6.3	R′	23	60	2.3	cor	4
16	11.6	R′	21	60	2.9	cor	8.3
17	10.5	F	20	70	6.5	w o g	86.5
	12.5	F	20	74	4.9	g′ B P	41.7
	6.5	F	20	66	3.6	cor	16.2
18	10.4	F	20	70	4.4	w r g	30
19	9.8	F	20	68	2.7	cor	6.6
20	11.0	F	19	69	4.0	cor	22
21	10.5	F	20	77	4.0	cor	22
22	10.3	F	22	83	4.6	g B P	34.8
	6.2	C′	23	80	3.9	....	20.5
23	10.4	F	22	82	3.8	....	19
24	10.7	F	23	85	4.7	w o g	37.2
	6.0	R	25	79	4.6	g B P	34.8
25	10.4	R′	23	66	2.8	cor	7.3
	6.0	C	..	67	3.5	w r g	15
26	10.7	F	22	70	3.4	w r g	13.8
	6.0	F	22	68	2.5	cor	5.2
27	10.1	R′	21	60	2.4	cor	4.6
	6.5	C′	21	59	2.7	cor	6.6
28	9.8	F	19	65	4.5	g B P	32.4
	6.0	F	20	65	4.7	w r g	37.2
29	10.0	F	20	72	3.7	cor	17.5
	3.0	F	20	75	3.2	cor	11.3
30	10.8	C	20	73	3.9	cor	20.5
	3.7	R	21	74	4.4	w r g	30
31	10.0	R	20	64	3.1	cor	10.2
	3.0	C	20	69	2.5	cor	5.2
Sept. 1	10.6	C	20	69	4.4	w r g	30
	3.0	R	20	67	3.7	cor	17.5
2	9.7	C′	20	70	2.6	cor	5.9
	1.5	C′	20	70	3.5	w g r p	15
4	10.5	R	21	69	2.5	cor	5.2
	1.7	R′	21	72	2.0	cor	2.5

TABLE 48.—Continued.

Date.	Time.	Weather.	°C.	°F.	*s.*	Corona.	$n \times 10^{-3}$.
1905.	*Hours.*						
Sept. 7	10.3	F	20	71	3.6	cor	16.2
	3.3	C	20	71	3.7	cor	17.5
8	10.2	F	20	70	4.3	w r g	28
	2.5	F	20	74	3.1	cor	10.2
9	9.7	F	20	74	4.8	w r g	39.5
	2.5	F	20	78	4.0	w r g	22
11	9.9	F	21	72	4.2	cor	25.8
	2.5	C	21	71	3.8	cor	19
12	10.2	R	20	63	3.1	cor	10.2
	2.7	R	21	66	3.8	cor	19
13	10.3	C	20	70	3.3	cor	12.5
	2.4	C	20	74	3.8	cor	19
14	10.4	F	18	57	4.2	cor	25.8
	2.5	F	18	62	4.5	y g p	32.4
15	10.4	F	15	62	5.0	w r g	43.8
	2.5	F	17	64	3.8	cor	19.0
16	10.5	C	17	62	3.6	cor	16.2
	2.0	C	18	64	3.7	cor	17.5
18	10.0	C	18	68	3.6	cor	16.2
	3.6	C	19	71	3.8	cor	19
19	9.8	R	19	68	3.4	cor	13.8
	3.3	C	19	69	2.9	cor	8.3
20	10.3	C	19	67	3.5	cor	15
	3.7	C	20	69	3.8	cor	19
21	8.7	F	19	67	3.8	cor	19
	3.4	F	19	74	3.9	cor	20.5
22	9.8	F	19	70	4.7	y g p	37.2
	5.0	F	21	75	4.5	y g p	32.4
23	9.0	F	19	67	4.2	cor	25.8
25	11.0	F	18	61	4.4	cor	30
	2.7	F	18	62	3.9	cor	20.5
26	9.0	F	17	50	5.4	w r g	54.2
	3.7	F	17	58	4.7	cor	37.2
27	9.0	F	16	52	5.1	w r g	46
	5.5	F	16	60	5.6	w r g	58.7
28	9.5	F	16	65	4.6	y g p	34.8
	3.5	F	18	74	3.5	cor	15
29	9.2	F	17	63	5.5	w r g	56.2
	2.5	F	18	69	4.1	cor	24.0
30	9.0	F	18	63	4.4	y g p	30
	3.3	F	20	71	4.2	cor	25.8
Oct. 2	9.2	C	18	62	4.5	cor	32.4
	2.7	C	18	65	3.8	cor	19
3	10.0	F	19	72	3.4	cor	13.8
	2.8	F	19	75	3.8	cor	19
4	9.8	F	18	71	4.9	cor	41.7
	2.9	F	19	76	4.3	cor	28
5	10.5	F	19	76	4.9	y g p	41.7
6	9.3	F	18	58	4.7	y g p	37.2
	3.1	F	18	63	4.6	cor	34.8
7	9.1	F	17	56	5.2	cor	48.2
	2.6	F	17	63	4.8	cor	39.5
9	12.1	F	18	74	5.4	w r g	54.2
	4.5	F	18	71	4.7	cor	37.2
10	9.9	F	16	58	3.7	cor	17.5

TABLE 48.—Continued.

Date.	Time.	Weather.	°C.	°F.	*s.*	Corona.	$n \times 10^{-3}$.
1905.	*Hours.*						
Oct. 10	2.5	F	17	64	4.4	w r g	30
11	9.8	C	16	56	4.5	w r g	32.4
	2.2	C	16	58	4.7	w r g	37.2
12	9.0	F	16	54	4.3	w r g	28
	2.7	F	17	59	4.5	w r g	32.4
13	11.0	F	16	56	4.7	y g p	37.2
	2.6	C	16	58	4.8	y g p	39.5
14	10.0	F	17	61	4.8	y g p	39.5
	2.6	F	18	68	5.0	y g p	43.8
16	2.5	F	20	75	4.8	y g p	39.5
	4.7	F	20	73	5.2	w B cor	48.2
17	10.3	F	18	60	5.7	w r g	61.5
	2.7	F	18	63	5.0	w r g	43.8
18	9.2	F	18	61	4.5	cor	32.4
	2.7	F	18	66	4.6	cor	34.8
19	12.0	C	19	75	4.2	cor	25.8
	3.5	C	20	72	4.6	g P cor	34.8
20	11.6	R	19	60	3.7	cor	17.5
	2.6	R	18	60	3.7	cor	17.5
23	12.2	F	17	52	4.7	g B	37.2
	4.3	F	17	52	4.7	g B	37.2
24	10.2	F	16	54	4.7	cor	37.2
	2.7	F	17	61	4.7	y g p	37.2
25	12.1	F	17	55	4.7	w r g	37.2
	4.1	C	18	54	4.5	w B	32.4
26	2.7	C	18	46	4.6	w r g	34.8
	4.6	F	18	43	4.0	B g	22
27	11.0	F	17	50	5.4	g B P	54.2
	2.8	F	18	53	4.8	y g B	39.5
30	2.7	F	18	52	4.7	y g B	37.2
	4.3	F	18	47	4.6	w r g	34.8
31	11.5	C	18	54	4.8	w Br g	39.5
	3.7	C	19	54	4.5	w r g	32.4
Nov. 1	3.0	F	18	64	4.8	g B P	39.5
	5.6	F	19	54	4.7	w Br B	37.2
3	3.7	C	18	50	4.4	w r g	30
	5.0	C	18	48	4.6	w r g	34.8
4	10.2	F	18	53	4.7	w r g	37.2
	2.4	F	17	52	4.0	w Br B	22
6	2.7	R	17	51	4.3	w r g	28
7	10.5	F	18	48	5.7	w r g	61.5
	3.0	C	18	48	3.7	w Br B	17.5
8	3.0	C	19	48	4.7	w Br B	37.2
9	2.6	C	19	45	4.8	w Br B	39.5
10	11.1	F	21	46	5.3	g B P	50.5
	3.2	C	20	45	5.0	w Bz B	43.8
11	9.5	F	20	40	6.2	w r g	76.5
	10.5	F	20	42	6.8	y g	95
12	2.5	F	21	49	5.4	g B P	54.2
13	3.2	F	23	56	5.3	g B P	50.5
14	10.7	F	20	28	6.6	y g	90
16	2.5	C	20	51	4.9	w Br B	41.7
17	11.2	F	19	44	4.5	cor	32.4
	2.7	F	19	45	4.5	w e g	32.4
18	9.8	F	21	44	4.7	y g	37.2

TABLE 48.—Continued.

Date.	Time.	Weather.	°C.	°F.	*s*.	Corona.	$n \times 10^{-3}$.
1905.	*Hours.*						
Nov. 20	2.7	F	20	38	4.8	w Br B	39.5
21	10.6	F	20	46	6.5	y g	86.5
	3.3	F	21	52	6.0	w r g	70.5
22	12.1	F	20	52	6.1	w r g	73.3
	4.0	C	20	52	6.1	w r g	73.3
23	2.7	F	22	59	4.8	w Br B	39.5
24	2.5	F	22	63	4.8	w Br B	39.5
	5.3	F	22	55	4.7	w Br B	37.2
27	3.5	F	18	45	4.8	w Br B	39.5
	5.0	F	18	42	4.6	w Br B	34.8
28	10.4	C	19	38	4.7	w B g	37.2
	3.0	C	19	37	4.8	w B g	39.5
Dec. 4	12.1	F	21	39	4.2	cor	25.8
	2.7	F	20	37	4.3	w Br B	28
5	11.0	F	20	30	5.7	w r g	61.5
	2.7	F	19	36	5.4	w Br B	54.2
6	12 2	C	20	40	5.6	w r g	58.7
	3.0	C	20	40	4.6	w B g	34.8
7	2.7	F	19	46	4.8	w B g	39.5
8	11.2	F	22	50	4.9	w Br B	41.7
	3.2	F	22	53	5.4	w Br B	54.2
9	10.7	C	22	42	3.9	cor	20.5
11	3.0	C	20	34	5.6	w r g	58.7
12	10.7	C	21	28	4.7	w Br B	37.2
	2.7	F	20	35	5.0	w g B	43.8
13	12.2	F	22	44	6.1	w r g	73.3
	3.5	F	22	45	5.7	w g B	61.5
14	3.7	F	22	34	5.8	w g P	64.5
15	11.1	C	22	22	6.5	y g	86.5
16	3.5	C	21	32	5.0	w g P	43.8
18	4.0	F	23	46	6.7	g b P	92.5
19	10.5	F	23	42	4.7	w Br g	37.2
	2.5	C	23	46	4.7	w Br g	37.2
20	10.6	F	23	45	5.2	g b P	48.2
	3.9	F	23	47	4.8	w Br g	39.5
21	10.7	R	23	46	3.8	cor	19
	3.1	R′	23	52	4.9	w g P	41.7
1906.							
Jan. 1	3.7	F	23	36	4.6	w r g	32.4
2	10.7	F	22	31	5.7	w r g	61.5
	3.5	C	21	36	5.6	w B P	58.7
3	11.7	F	20	32	4.7	g B P	37.2
	3.4	C	20	34	4.8	w Br g	39.5
4	1.0	R′	22	58	5.0	g B P	43.8
	3.2	C	22	57	6.2	w r g	76.5
5	10.0	F	23	43	6.0	w r g	70.5
	2.7	F	22	44	5.3	w Br P	50.5
6	10.6	C	21	38	5.9	w r g	68
	4.3	F	20	37	5.9	w r g	68
8	12.5	C	19	27	4.7	w Br g	37.2
	4.5	Sn	20	26	4.7	w Br g	37.2
9	11.0	F	20	20	6.7	y g	92.5
	3.0	F	19	26	6.5	y g	86.5
10	4.0	F	18	25	6.4	w r g	83.5
11	12.2	F	19	32	5.9	w r g	68
	5.0	F	19	31	6.4	w r g	83.5
12	11.2	F	22	51	5.9	w r g	68

TABLE 48.—Continued.

Date.	Time.	Weather.	°C.	°F.	*s*.	Corona.	$n \times 10^{-3}$.
1906.	*Hours.*						
Jan. 12	4.8	F	22	47	5.6	w r g	58.7
13	10.5	F	21	38	4.5	cor	32.4
	3.3	C	21	36	3.8	w Br P	19
15	10.0	F	21	31	4.9	w Br P	41.7
16	11.5	R′	20	49	4.8	w r g	39.5
	3.5	R′	22	49	5.5	g B P	56.2
17	10.1	F	20	39	6.0	w r g	70.5
	3.5	F	18	40	4.7	w Br B	37.2
18	12.3	R′	18	44	4.9	g P r	41.7
	4.8	C	19	43	5.1	w Br P	46
19	10.0	F	19	39	4.6	w Br g	34.8
	2.7	F	20	41	5.8	w Br P	64.5
20	10.4	C	20	35	4.8	g Br	39.5
	3.2	R′	20	40	4.9	g Br	41.7
22	12.5	C	23	53	4.5	w Br g	32.4
	4.0	F	22	51	4.7	w Br g	37.2
23	10.3	F	22	63	5.0	w Br P	43.8
	5.0	F	23	63	5.1	w Br P	46
24	10.1	F	20	43	6.5	y g	86.5
25	9.8	F	20	26	5.3	w Br P	50.5
	3.2	F	19	26	4.5	w Br P	32.4
26	10.0	F	19	29	4.8	w Br g	39.5
	3.3	F	19	39	4.5	w Br g	32.4
27	10.2	F	20	37	6.3	y G	80.5
	4.4	F	20	46	4.9	w Br P	41.7
29	12.0	F	20	29	6.8	y G	95
	3.7	F	20	33	4.9	g Pr	41.7
30	10.5	F	20	41	6.1	w r g	73.3
	3.0	F	20	49	5.1	w Br B	46
31	12.3	F	21	52	4.7	w Br g	37.2
	3.3	F	21	49	4.5	w Br g	32.4
Feb. 1	12.2	F	21	43	6.0	G r g	70.5
	5.0	F	21	43	5.1	w Br P	46
2	11.0	F	19	20	6.5	y G	86.5
	5.0	F	17	14	5.5	w r b o g	56.2
3	10.2	F	18	9	6.2	w r g	76.5
	6.2	F	18	19	6.1	w r g	73.3
4	10.1	F	20	35	5.0	w P cor	43.8
	12.5	F	20	39	5.2	w P cor	48.2
	6.3	F	21	37	4.6	cor	34.8
5	5.0	..	22	39	4.7	cor	37.2
6	9.5	F	21	20	6.8	g B P	95
	11.3	F	21	21	6.4	w r g	83.5
	3.5	F	21	23	5.2	cor	48.2
7	10.5	Sn′	19	15	6.0	w r g	70.5
	12.1	Sn′	18	18	6.7	w o b g	92.5
	3.6	F	19	24	6.0	w r g	70.5
	6.1	..	19	22	5.9	w r g	68
8	9.5	F	20	19	5.9	w r g	68
	11.7	F	20	29	4.8	g B′	39.5
	3.0	F	19	34	4.8	w r g	39.5
	5.6	F	19	31	5.8	w r g	64.5
9	11.2	R	21	38	4.6	w r g	34.8
	4.8	C	21	35	4.8	w P cor	39.5
10	9.7	F	22	32	4.8	g B P	39.5
	12.8	F	21	36	4.8	g B P	39.5
	5.2	F	22	35	4.8	g B P	39.5

TABLE 48.—Continued.

Date.	Time.	Weather.	°C.	°F.	*s*.	Corona.	$n \times 10^{-3}$.
1906.	*Hours.*						
Feb. 11	9.8	F	22	22	6.5	yo bg	86.5
	12.0	F	..	27	6.0	w r g	70.5
	5.0	F	22	28	4.8	w r o g	39.5
12	9.6	F	22	34	5.3	w r g	50.5
	1.5	F	21	41	4.8	cor	39.5
	3.5	C	20	40	4.4	cor	30
13	12.2	R	22	42	4.6	g B P	34.8
	6.0	C	23	40	4.6	cor	34.8
14	12.3	C′	23	47	3.9	cor	20.5
	4.1	C	23	48	4.2	cor	25.8
15	1.0	C	20	24	6.8	g B P	95
	5.1	F	21	25	5.1	g Br	46
16	12.3	F	20	26	6.5	y g	86.5
	5.0	F	21	34	5.4	w r o b g	54.2
17	12.3	F	21	30	4.7	w Br g	37.2
	4.0	F	21	40	4.8	g Br	39.5
19	12.3	F	22	44	5.0	y g	43.8
	5.0	C	22	43	5.6	w Br P	58.7
20	11.3	F	22	42	5.8	w Br P	64.5
	4.7	F	22	47	5.0	w Br P	43.8
21	5.1	R	23	54	4.7	g B P	37.2
22	11.0	F	24	51	5.8	w r g	64.5
23	5.0	F	22	45	4.7	w Br g	37.2
26	4.3	F	21	45	4.9	w Br g	41.7
27	11.5	F	20	35	6.2	y g	76.5
	5.0	F	19	33	4.9	g Br	41.7
28	12.2	F	18	21	6.7	y g	92.5
	5.0	F	18	22	5.9	w r g	68
March 1	12.5	F	17	27	6.7	y g	92.5
	5.0	F	18	32	5.7	w r g	61.5
2	11.5	F	19	36	6.4	y g	83.5
	5.7	F	20	40	5.6	w r g	58.7
3	10.7	R′	21	36	4.5	cor	32.4
5	12.5	F	22	44	4.8	w b P	39.5
	4.7	F	22	45	4.8	w g p r	39.5
6	11.7	F	21	36	5.0	w b p	43.8
	5.0	F	21	38	5.9	w r g	68
7	12.5	C	20	43	5.1	w h p	46
	4.0	C	20	43	5.7	w r g	61.5
8	12.2	C	21	47	4.8	g br	39.5
	5.0	F	22	45	4.8	g br	39.5
10	11.5	F	19	44	6.0	y g	70.5
	3.5	F	20	47	4.8	w br P	39.5
12	1.2	F	18	40	5.7	w br g	61.5
	4.2	F	20	39	4.8	g br	39.5
13	5.0	C	19	32	5.0	w br g	43.8
14	4.0	F	20	33	5.0	g br	43.8
15	1.5	Sn	00	26	4.7	w br g	37.2
16	3.2	F	00	40	5.5	w br g	56.2
17	3.7	F	22	33	5.6	w br g	58.7
19	10.7	C	22	35	5.3	w br g	50.5
20	3.7	C	21	36	5.2	w br p	48.2
22	3.4	F	22	38	6.5	y g	86.5
23	10.8	F	22	24	6.2	y g	76.5
24	3.5	F	21	33	4.8	g br	39.5
26	10.8	C	22	36	4.9	w br p	41.7

TABLE 49.—Mean daily nucleations, corresponding to table 48.

Date.	$n \times 10^{-3}$	Date.	$n \times 10^{-3}$	Date.	$n \times 10^{-3}$
1905.		1905.		1905.	
May 4	11	June 28	30	Aug. 25	11
5	38	29	28	26	9
6	66	30	35	27	6
7	33	July 1	31	28	35
8	96	2	19	29	14
9	38	3	15	30	25
10	44	4	24	31	8
11	46	5	11	Sept. 1	24
12	32	6	14	2	10
13	21	7	68	4	4
14	14	8	30	7	17
15	22	9	20	8	19
16	13	11	31	9	31
17	18	12	36	11	22
18	26	13	30	12	15
19	34	14	34	13	16
20	46	15	16	14	29
21	25	16	19	15	31
22	36	17	19	16	17
23	42	18	37	18	18
24	49	19	24	19	11
25	58	20	19	20	17
26	34	21	19	21	20
27	18	22	33	22	35
28	33	23	3	23	26
29	21	24	22	25	25
30	14	25	25	26	46
31	11	27	30	27	52
June 1	15	29	10	28	25
2	37	30	4	29	40
3	28	31	7	30	28
4	29	Aug. 1	11	Oct. 2	26
5	18	2	25	3	16
6	8	3	65	4	35
7	35	4	30	5	42
8	24	5	16	6	36
9	38	6	20	7	44
10	35	7	28	9	46
11	17	8	24	10	24
12	29	9	22	11	35
13	30	10	35	12	36
14	30	11	26	13	38
15	40	12	24	14	42
16	31	13	7	16	44
17	26	14	15	17	53
18	27	15	9	18	34
19	7	16	8	19	30
20	12	17	72	20	17
21	..	18	30	23	37
22	24	19	7	24	37
23	9	20	22	25	35
24	33	21	22	26	28
25	17	22	28	27	47
26	20	23	19	30	36
27	30	24	36	31	36

TABLE 49.—Continued.

Date.	$n \times 10^{-3}$	Date.	$n \times 10^{-3}$	Date.	$n \times 10^{-3}$
1905.		1905.		1906.	
Nov. 1	38	Dec. 21	30	Feb. 9	38
2	39	1906.		10	39
3	32	Jan. 1	32	11	65
4	30	2	60	12	40
6	28	3	38	13	35
7	39	4	60	14	23
8	37	5	60	15	70
9	39	6	68	16	70
10	47	8	37	17	38
11	70	9	89	19	51
13	50	10	83	20	54
14	90	11	76	21	37
16	42	12	63	22	64
17	32	13	26	23	37
18	37	15	42	26	42
20	39	16	48	27	59
21	78	17	54	28	75
22	73	18	44	Mar. 1	72
23	39	19	50	2	71
24	38	20	41	3	32
27	37	22	35	5	39
28	38	23	45	6	56
Dec. 4	27	24	86	7	54
5	58	25	41	8	39
6	47	26	36	10	55
7	39	27	61	12	50
8	48	29	68	13	44
9	20	30	60	14	44
11	59	31	35	15	37
12	40	Feb. 1	58	16	56
13	67	2	71	17	59
14	64	3	75	19	50
15	86	4	42	20	48
16	44	5	37	22	86
18	92	6	76	23	76
19	37	7	75	24	39
20	44	8	53	26	42

TABLE 50.—Mean monthly nucleations corresponding to table 48.

Date.	$n \times 10^{-3}$.	Date.	$n \times 10^{-3}$.
1905.		1905.	
November...	53	August.....	23
December...	69	September...	24
January.....	66	October.....	35
February....	71	November...	45
March	47	December...	50
April	40	1906.	
May.....	35	January.....	53
June.....	26	February....	53
July.....	27	March	52

90. Mean monthly nucleations.—The data of table 48 suffice for the determination of the average nucleations per month, care being taken to omit the days on which no observations were taken. Table 50 contains the results.

These data are shown in the lower graphs of fig. 62. What is remarkable is the gradual rise of the curve to a persistent maximum reaching nearly into April. True, the winter was relatively mild and the spring relatively cold; but one would not be prepared to predict nucleations so uniformly maintained between November and April. The distribution is in fact peculiar, as may be seen by comparing it with the nucleation of the preceding years since 1902, in fig. 63. The uniformity of the new curve, the absence of maxima in December, are striking. One may note the upward march of the successive curves 1902–03, 1903–04, 1904–05.

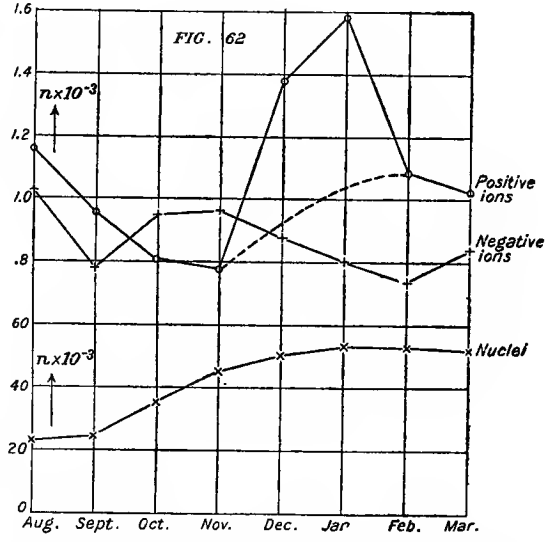

FIG. 62.—Average monthly ionization (thousands per cubic centimeter), positive and negative as stated, and nucleations (thousands per cubic centimeter), observed between August, 1905, and March, 1906.

91. Measurement of ionization.—To determine the number of ions in the atmosphere, Ebert's* well-known apparatus was used. This consists of a tubular condenser, the inner coat of which is charged and in contact with a graduated electroscope. The air to be examined is passed through the condenser by an aspirator-fan propelled by clockwork. The air delivery of the machine is also carefully standardized.

In order to test the same air which yielded the nuclei for the preceding measurement, the electrical apparatus (*E*, fig. 57*b*) was swung from the outside of a window on a long swivel bracket (*B*). In this way it could be drawn near the window for charging and examination with appropriate

* H. Ebert: Illus. Aëronaut. Mittheilungen, October, 1902, pp. 1–10.

lenses or moved to a reasonable distance away from the window during the passage of the air to be tested. In winter all measurements must be made with a galvanoscope on the outside of the house. Thermometers are shown at T.

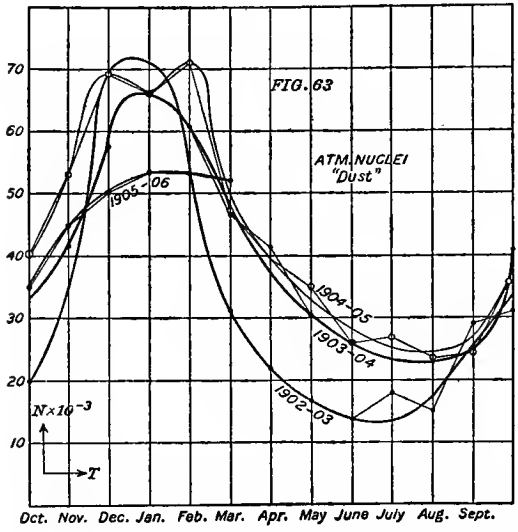

FIG. 63.—Atmospheric nucleation (thousands per cubic centimeter) from October, 1902, to March, 1906.

The difficulties encountered in using this apparatus in cold weather will be investigated later (section 94). Here some reference to its constants is in place. The quantity of air passed through the condenser in the fiducial time (about 10 minutes) was 1.0357×10^6 cubic centimeters; the capacity of the condenser 17.74 cm. Hence if V is the drop of potential in volts during the fiducial time specified,

$$Q = 17.7 \frac{V/300}{1.0357 \times 10^6} = \frac{V}{17.52 \times 10^6}$$

denotes the charge in 1 cubic centimeter of air. As 3.4×10^{-10} is the electrostatic charge per electron,

$$n \times 10^{-3} = \frac{Q}{3.4 \times 10^{-7}} = \frac{V}{6}, \text{ nearly,}$$

shows the number of ions per cubic centimeter. Measurements to find their velocity were not made, as this would have carried me too far from the purposes of this paper.

I may add that a similar apparatus was installed, in which the winter indraft of cold air (through a condenser), measured by an anemometer, was utilized. The object here was to determine the hourly variations of ionization. Though many observations were taken, their meaning is vitiated by the temperature discrepancy mentioned in section 94. For this reason, perhaps, a periodicity similar to the one discovered by Wood and Campbell (Nature, April, 1906, p. 583) with stagnant air was not detected.

92. Data for ionization.—In table 51 the date and hour are given in the first and second columns. The fall of potential, $V-v$ (v being the fall in the absence of the aspirator air current), in volts, during the ten minutes of observation, is shown in the fourth column, marked "volts." From this the charge (Q) in electrostatic units per cubic meter, and the number of ions (n) in thousands per cubic centimeter, are computed. The sign of the charges is indicated in each case, and q denotes their ratio (Q_+/Q_-). The correction (v) is regarded as negligible.

TABLE 51.

Date.	Time.	Volts.	Q.	$n \times 10^{-3}$.	Date.	Time.	Volts.	Q.	$n \times 10^{-3}$.
1905.					1905.				
July 26	4.0	3.7	+0.21	0.62	Aug. 9	9.2	10.9	+0.62	1.82
		4.6	+ .26	.76			1.7	− .10	.29
		5.1	+ .29	.85			8.2	+ .47	1.38
		7.8	+ .45	1.32			5.2	− .30	.88
		6.1	+ .35	1.03			6.3	+ .36	1.05
	5	5.9	+ .34	1.00			4.2	− .24	.70
29	9.2	5.0	+ .29	.85			6.3	+ .36	1.05
		5.9	− .34	1.00			4.2	− .24	.70
	4.0	6.3	+ .36	1.02		12.3	5.2	+ .30	.88
		4.2	− .24	.70			6.3	− .36	1.05
31	10.0	7.7	+ .44	1.29	10	9.5	8.2	+ .47	1.38
		3.0	− .18	.52			5.2	− .30	.88
	3.0	7.8	+ .45	1.32		12	7.2	+ .41	1.20
		5.9	− .34	1.00			7.2	− .41	1.20
Aug. 1	10.0	2.6	+ .15	.44	11	10	6.3	+ .36	1.05
		2.6	− .15	.44			5.2	− .30	.88
	3.0	6.3	+ .36	1.02		12.3	8.2	+ .47	1.38
		8.1	− .46	1.35			5.2	− .30	.88
2	9.2	6.9	+ .39	1.14	12	9.0	6.3	+ .36	1.05
		5.6	− .32	.94			6.3	− .36	1.05
	4.0	5.9	+ .34	1.00		12.0	5.2	+ .30	.88
		3.1	− .18	.52			6.3	− .36	1.05
3	10.0	8.2	+ .47	1.38	14	9.4	11.9	+ .68	2.00
		5.5	− .31	.91			11.0	− .63	1.85
	4.3	6.7	+ .38	1.11		11.3	13.8	+ .79	2.32
		4.4	− .25	.73			11.0	− .63	1.85
4	10.0	5.3	+ .30	.88		12.3	11.0	+ .63	1.85
		4.4	− .25	.73			11.0	− .63	1.85
	4.3	2.6	+ .15	.44	15	10	10	+ .57	1.67
		4.8	− .27	.79			8.2	− .47	1.38
5	10.0	4.2	+ .24	.70			10.0	+ .57	1.67
		5.3	− .30	.88			8.2	− .47	1.38
	4.0	4.6	+ .26	.76			9.1	+ .52	1.52
		6.5	− .37	1.08			27.8	....	....
7	9.4	10.0	+ .57	1.67		12.3	9.1	+ .52	1.52
		6.7	− .38	1.11			9.1	− .52	1.52
	12.3	9.0	+ .51	1.50	16	10	8.2	+ .47	1.38
		9.5	− .54	1.58			5.2	− .30	.88
8	10.0	5.5	+ .31	.91		1.0	10.0	+ .57	1.67
		3.2	− .18	.52			7.2	− .41	1.20
9	9.2	6.3	+ .36	1.05	17	10.0	8.2	+ .47	1.38
		5.5	− .31	.91			5.2	− .30	.88

TABLE 51.—Continued.

Date.	Time.	Volts.	Q.	$n \times 10^{-3}$.	Date.	Time.	Volts.	Q.	$n \times 10^{-3}$.
1905.					1905.				
Aug. 17	12.3	10.0	+0.57	1.67	Sept. 2	9.7	3.7	−0.21	0.61
		10.0	− .57	1.67		1.4	6.0	+ .34	1.00
18	10.0	8.2	+ .47	1.38			2.2	− .12	.37
		9.1	− .52	1.52	4	10.5	5.1	+ .29	.85
	12.0	9.1	+ .52	1.52			2.8	− .16	.47
		9.1	− .52	1.52		1.7	5.4	+ .31	.91
19	9.0	10.0	+ .57	1.67			10.4	− .59	1.74
		9.1	− .52	1.52	7	10.3	4.8	+ .27	.80
	12.0	....	....	....			5.3	− .30	.88
		....	....	....		3.3	5.4	+ .31	.91
21	10.0	8.2	+ .47	1.38			4.2	− .24	.70
		9.1	− .52	1.52	8	10.2	7.1	+ .40	1.18
	1.0	7.2	+ .41	1.20			6.5	− .37	1.09
		2.1	− .12	.35		2.5	8.6	+ .49	1.44
22	10	6.3	+ .36	1.05			9.5	− .54	1.59
		6.3	− .36	1.05	9	9.7	5.0	+ .28	.84
	1.0	3.1	+ .18	.52			6.4	− .36	1.06
		4.2	− .24	.70		2.2	8.9	+ .51	1.50
23	9.3	10.0	+ .57	1.67			4.2	− .24	.70
		8.2	− .47	1.38	11	9.9	3.7	+ .21	.61
	12.0	7.2	+ .41	1.20			4.1	− .23	.69
		10.0	− .57	1.67		2.4	2.3	+ .13	.38
24	10.0	6.3	+ .36	1.05			2.8	− .16	.47
		6.3	− .36	1.05	12	10.1	10.8	+ .61	1.79
	12.0	4.2	+ .24	.70			1.9	− .11	.32
		5.2	− .30	.88		2.7	2.2	+ .12	.36
25	10.0	5.2	+ .30	.88			3.3	− .19	.56
		3.1	− .18	.52	13	10.3	4.8	+ .27	.79
	1.0	8.2	+ .47	1.38			4.0	− .23	.68
		6.3	− .36	1.05		2.3	4.2	+ .24	.70
26	9.0	8.2	+ .47	1.38			3.0	− .17	.50
		6.3	− .36	1.05	14	10.4	9.2	+ .52	1.53
	12.0	9.1	+ .52	1.52			6.7	− .38	1.12
		8.2	− .47	1.38		2.5	8.2	+ .47	1.38
28	10.4	6.2	− .35	1.05			7.6	− .43	1.25
		3.4	+ .19	.56	15	10.4	6.0	+ .34	1.00
	2.7	2.4	− .14	.41			7.7	− .44	1.29
		3.2	+ .18	.54		2.5	10.1	+ .57	1.68
29	9.9	3.7	+ .21	.63			3.5	− .20	.59
		3.7	− .21	.63	16	10.5	4.2	+ .24	.70
	2.6	5.0	+ .29	.86			2.4	− .14	.41
		4.5	− .25	.76		2.0	8.3	+ .47	1.40
30	10.5	4.8	+ .27	.79			2.4	− .14	.41
		3.0	− .17	.48	18	10.0	2.8	+ .16	.47
	2.6	4.5	+ .25	.76			5.3	− .30	.88
		5.1	− .29	.85		3.5	8.3	+ .47	1.40
31	10.0	3.0	+ .17	.50			2.8	− .16	.47
		5.6	− .32	.94	19	9.8	7.7	+ .44	1.29
	2.7	5.9	+ .34	1.00			1.8	− .10	.31
		4.2	− .24	.71		3.3	3.3	+ .19	.56
Sept. 1	10.5	5.4	+ .31	.91			2.3	− .13	.38
		4.7	− .27	.79	20	10.2	3.5	+ .20	.59
	3	6.8	+ .39	1.14			1.2	− .07	.20
		.4	− .23	.67		3.7	4.7	+ .27	.79
2	9.7	5.1	+ .29	.85			4.2	− .24	.70

TABLE 51.—Continued.

Date.	Time.	Volts.	Q.	$n \times 10^{-3}$.	Date.	Time.	Volts.	Q.	$n \times 10^{-3}$.
1905.					1905.				
Sept. 21	8.7	8.3	+0.47	1.40	Oct. 7	2.6	3.5	−0.20	0.59
		4.2	− .24	.70	9	12 1	8.7	+ .50	1.46
	3.5	4.5	+ .26	.76			7.2	− .41	1.20
		4.6	− .26	.76		4.5	16.6	+ .95	2.79
22	9.8	1.9	+ .11	.32			2.4	− .14	.41
		2.6	− .15	.44	10	9.9	2.8	+ .16	.47
	5.0	2.8	+ .16	.47			4.8	− .27	.79
		2.4	− .14	.41		2.5	4.2	+ .24	.70
23	9.0	7.8	+ .44	1.30			8.1	− .46	1.35
		7.7	− .44	1.29	11	9.8	6.0	+ .34	1.00
25	11.0	8.3	+ .47	1.40			8.9	− .51	1.50
		9.5	− .54	1.59		2.2	2.3	+ .13	.38
	2.7	5.3	+ .30	.88			4.2	− .24	.70
		10.1	− .58	1.71	12	9.0	3.4	+ .19	.57
26	9.0	4.5	+ .26	.76			8.9	− .51	1.50
		4.1	− .23	.69		2.7	6.3	+ .36	1.02
	3.7	6.8	+ .39	1.14			7.7	− .44	1.29
		9.3	− .53	1.56	13	11.0	3.7	+ .21	.61
27	9.0	4.5	+ .26	.76			8.9	− .51	1.50
		2.7	− .15	.46		2.6	1.4	+ .08	.23
	5.5	1.1	+ .06	.19			3.0	− .17	.48
		3.5	− .20	.59	14	10.0	7.2	+ .41	1.20
28	9.5	3.7	+ .21	.61			7.1	− .40	1.18
		4.8	− .27	.79		2.6	4.9	+ .28	.82
	3.4	8.3	+ .47	1.40			4.2	− .24	.70
		5.4	− .31	.91	16	2.5	5.9	+ .34	1.00
29	9.2	7.0	+ .40	1.17			3.7	− .21	.61
		6.8	− .39	1.14		4.7	1.4	+ .08	.23
	2.5	2.4	+ .14	.41			2.4	− .14	.41
		1.8	− .10	.31	17	10.3	6.1	+ .35	1.03
30	9.0	1.9	+ .11	.32			7.4	− .42	1.23
		3.0	− .17	.48		2.7	7.5	+ .43	1.26
	3.2	3.7	+ .21	.61			3.5	− .20	.59
		1.4	− .08	.23	18	9.2	3.0	+ .17	.48
Oct. 2	9.1	2.3	+ .13	.38			8.0	− .46	1.35
		2.4	− .14	.41		2.7	2.4	+ .14	.41
	2.7	1.8	+ .10	.31			2.4	− .14	.41
		2.4	− .14	.41	19	12	4.2	+ .24	.70
3	10.0	3.6	+ .20	.60			7.4	− .42	1.23
		3.0	− .17	.50		3.5	6.7	+ .38	1.12
	2.8	7.9	+ .45	1.31			4.8	− .27	.79
		4.8	− .27	.79	20	11.6	6.4	+ .36	1.07
4	9.8	3.6	+ .20	.60			2.8	− .16	.47
		4.2	− .24	.70		2.6	6.5	+ .37	1.09
	2.9	3.0	+ .17	.48			1.9	− .11	.32
		3.6	− .20	.60	23	12.2	4.2	+ .24	.70
5	10.5	2.4	+ .14	.41			6.9	− .39	1.14
		6.0	− .34	1.00		4.3	6.4	+ .36	1.07
6	9.2	6.6	+ .38	1.11			7.7	− .44	1.29
		9.5	− .54	1.59	24	10.2	1.7	+ .10	.29
	3.1	7.2	+ .41	1.20			3.3	− .19	.56
		10.4	− .59	1.74		2.7	3.1	+ .18	.52
7	9.2	6.5	+ .37	1.09			1.8	− .10	.31
		6.6	− .38	1.11	25	12.1	6.2	+ .35	1.05
	2.6	3.6	+ .20	.60			8.2	− .47	1.38

TABLE 51.—Continued.

Date.	Time.	Volts.	Q.	$n \times 10^{-3}$.	Date.	Time.	Volts.	Q.	$n \times 10^{-3}$.
1905.					1905.				
Oct. 25	4.0	1.4	+0.08	0.23	Nov. 14	10.7	5.4	−0.31	.91
		3.6	− .20	.60	16	2.5	3.3	+ .19	.56
26	2.7	5.6	+ .32	.94			6.8	− .39	1.14
		11.3	− .65	1.91	17	11.2	3.6	+ .20	.60
	4.6	6.9	+ .39	1.14			4.2	− .24	.70
		9.6	− .55	1.62		2.7	2.8	+ .16	.47
27	11.0	5.6	+ .32	.94			8.4	− .48	1.41
		8.3	− .47	1.40	18	9.8	4.6	+ .26	.76
	2.8	6.0	+ .34	1.00			10.4	− .59	1.74
		4.2	− .24	.71	20	2.7	1.7	+ .10	.29
30	2.5	3.4	+ .19	.57			8.1	− .46	1.35
		10.5	− .60	1.76	21	10.6	2.4	+ .14	.41
	4.7	6.3	+ .36	1.02			7.1	− .40	1.18
		3.0	− .17	.48		3.2	5.3	+ .30	.88
31	11.4	2.4	+ .14	.41			5.4	− .31	.91
		8.9	− .51	1.50	22	12.1	7.7	+ .44	1.29
	3.7	3.0	+ .17	.48			6.6	− .38	1.11
		7.7	− .44	1.29		4.0	1.8	+ .10	.31
Nov. 1	3.0	8.7	+ .50	1.46			6.8	− .39	1.14
		2.8	− .16	.47	23	2.7	5.9	+ .34	1.00
	5.6	6.7	+ .38	1.12			1.8	− .10	.31
		6.0	− .34	1.00	24	2.5	3.7	+ .21	.61
2	2.4	6.7	+ .38	1.12			3.0	− .17	.48
		9.5	− .54	1.59		5.3	1.8	+ .10	.31
3	2.7	1.8	+ .10	.31			2.3	− .13	.38
		3.0	− .17	.50	27	3.4	5.3	+ .30	.88
	5.0	6.0	+ .34	1.00			6.6	− .38	1.11
		2.4	− .14	.41		5.3	7.8	+ .45	1.32
4	10.2	1.4	+ .08	.23			2.3	− .13	.38
		2.4	− .14	.41	28	10.5	1.8	+ .10	.31
	2.4	2.8	+ .16	.47			4.5	− .26	.76
		2.2	− .12	.36		3.0	4.8	+ .27	.79
6	3.0	7.2	+ .41	1.20			5.7	− .32	.96
		3.0	− .17	.50	Dec. 4	12.0	5.4	+ .31	.91
7	10.6	6.2	+ .35	1.05			4.2	− .24	.70
		9.5	− .54	1.59		2.7	2.4	+ .14	.41
	2.8	5.8	+ .33	.97			11.9	− .68	2.0
		4.4	− .25	.73	5	11.0	12.7	+ .73	2.15
8	3.0	5.3	+ .30	.88			11.9	− .68	2.00
		3.0	− .17	.50		2.7	12.0	+ .68	2.01
9	2.5	2.3	+ .13	.38			6.9	− .39	1.14
		11.1	− .63	1.85	6	12.2	9.5	+ .54	1.59
10	11.1	4.7	+ .27	.79			3.0	− .17	.50
		8.3	− .47	1.40		2.7	2.8	+ .16	.47
	3.0	1.8	+ .10	.31			3.6	− .20	.60
		3.6	− .20	.60	7	2.7	10.5	+ .60	1.76
11	10.5	3.9	+ .22	.65			4.5	− .26	.76
		5.4	− .31	.91	8	11.2	9.5	+ .54	1.59
	2.5	4.8	+ .27	.79			2.4	− .14	.41
		8.1	− .46	1.35		3.2	7.3	+ .42	1.24
13	12.4	6.8	+ .39	1.14			2.3	− .13	.38
		6.0	− .34	1.00	9	10.7	6.7	+ .38	1.12
	3.2	.9	+ .05	.16			5.9	− .34	1.00
		5.6	− .32	.94	11	3.0	7.6	+ .43	1.25
14	10.7	9.8	+ .56	1.65			4.9	− .28	.82

TABLE 51.—Continued.

Date.	Time.	Volts.	Q.	$n \times 10^{-3}$.	Date.	Time.	Volts.	Q.	$n \times 10^{-3}$.
1905.					1906.				
Dec. 12	10.7	11.0	+0.63	1.85	Jan. 9	11.0	9.3	+0.53	1.56
		1.4	− .08	.23			3.8	− .22	.65
	2.7	4.7	+ .27	.79		3.0	10.5	+ .60	1.76
		5.9	− .34	1.00			5.1	− .29	.85
13	12.2	11.3	+ .65	1.91	10	3.5	10.6	+ .60	1.78
		9.5	− .54	1.59			1.4	− .08	.23
	3.5	7.7	+ .44	1.29	11	12.5	9.7	+ .55	1.62
		4.4	− .25	.73			4.2	− .24	.70
14	3.7	1.9	+ .11	.32		4.7	13.4	+ .76	2.02
		4.7	− .27	.79			2.4	− .14	.41
15	11.0	12.7	+ .73	2.15	12	11.2	4.1	+ .23	.69
		4.7	− .27	.79			3.2	− .18	.54
16	3.5	14.3	+ .82	2.41		4.8	6.5	+ .37	1.09
		3.4	− .19	.57			3.4	− .19	.57
18	4.0	8.4	+ .48	1.41	13	10.5	16.0	+ .91	2.68
		2.9	− .16	.49			6.7	− .38	1.12
19	10.5	6.7	+ .38	1.12		3.2	?21.5	+1.23	3.62
		4.1	− .23	.69			2.3	− .13	.38
	2.4	7.6	+ .43	1.25	15	10.0	6.7	+ .38	1.12
		14.8	− .84	2.47			5.9	− .34	1.00
20	10.5	6.8	+ .39	1.14	16	11.5	6.6	+ .38	1.11
		4.9	− .28	.82			1.9	− .11	.32
	3.9	6.0	+ .34	1.00		3.4	5.7	+ .32	.96
		4.7	− .27	.79			3.7	− .21	.63
21	10.5	11.3	+ .65	1.91	17	10.0	7.0	+ .40	1.17
		6.5	− .37	1.09			1.9	− .11	.32
	3.0	3.7	+ .21	.61		3.5	7.0	+ .40	1.17
		3.0	− .17	.48			5.3	− .30	.88
1906.					18	12.2	7.1	+ .40	1.18
Jan. 1	3.7	11.3	+ .65	1.91			1.7	− .10	.29
		4.6	− .26	.76		4.8	3.4	+ .19	.57
2	10.7	19.0	+2.09	6.01			1.1	− .06	.18
		10.2	− .58	1.70	19	9.9	6.6	+ .38	1.11
	3.5	18.0	+1.03	3.01			4.2	− .24	.70
		4.4	− .25	.73		2.7	9.7	+ .55	1.62
3	11.7	9.5	+ .54	1.59			7.7	− .44	1.29
		7.0	− .40	1.17	20	10.3	7.1	+ .40	1.18
	3.3	9.7	+ .55	1.62			3.1	− .18	.52
		1.4	− .08	.23		3.2	2.8	+ .16	.47
4	12.8	8.1	+ .46	1.35			3.7	− .21	.61
		2.4	− .14	.41	22	12.5	7.8	+ .45	1.32
	3.2	2.3	+ .13	.38			5.4	− .31	.91
		4.2	− .24	.70		4.0	4.7	+ .27	.79
5	10.0	11.9	+ .68	2.00			6.3	− .36	1.02
		7.5	− .43	1.26	23	10.3	5.3	+ .30	.88
	2.7	10.1	+ .57	1.68			3.4	− .19	.57
		13.7	− .78	2.29		5.0	8.1	+ .46	1.35
6	10.6	9.2	+ .52	1.53			2.3	− .13	.38
		5.4	− .31	.91	24	10.0	8.4	+ .48	1.41
	4.3	11.3	+ .65	1.91			9.6	− .55	1.62
		5.8	− .33	.97	25	9.8	11.2	+ .64	1.88
8	12.5	12.5	+ .71	2.01			4.3	− .24	.73
		6.5	− .37	1.09		3.1	7.2	+ .41	1.20
	4.5	13.0	+ .74	2.02			4.2	− .24	.70
		7.2	− .41	1.20	26	10.0	8.9	+ .51	1.50

TABLE 51.—Continued.

Date.	Time.	Volts.	Q.	$n \times 10^{-3}$.	Date.	Time.	Volts.	Q.	$n \times 10^{-3}$.
1906.					1906.				
Jan. 26	10.0	1.9	−0.11	0.32	Feb. 8	9.8	4.8	+0.27	0.79
	3.3	11.3	+ .65	1.91		12.6	5.2	+ .30	.88
		3.0	− .17	.48			11.2	− .64	1.88
27	10.2	7.5	+ .43	1.26		3.4	8.6	+ .49	1.45
		4.9	− .28	.82			3.3	− .19	.56
	4.4	8.0	+ .46	1.35		4.8	3.8	+ .22	.64
		1.8	− .10	.31			3.9	− .22	.66
29	12	16.1	+ .92	2.70	9	11.5	7.7	+ .44	1.30
		5.0	− .28	.84			6.2	− .35	1.04
	3.7	10.0	+ .57	1.67			1.9	+ .11	.33
		6.2	− .35	1.05		4.9	5.9	+ .34	1.00
30	10.5	5.3	+ .30	.88			1.4	− .08	.23
		7.2	− .41	1.20	10	9.9	5.4	+ .31	.91
	3.0	4.8	+ .27	.79			3.3	+ .19	.56
		4.2	− .24	.70		10.6	2.8	− .16	.47
31	12.3	8.3	+ .47	1.40		10.6	4.2	+ .24	.71
		7.5	− .43	1.26		12.5	8.1	+ .46	1.37
	3.2	8.9	+ .51	1.50			4.6	− .26	.76
		6.5	− .37	1.09		5.0	3.7	+ .21	.62
Feb. 1	12.0	11.1	+ .63	1.87			3.3	− .19	.56
		6.9	− .39	1.14	11	10.2	12.3	+ .70	2.06
	5.0	6.8	+ .39	1.14			6.0	− .34	1.00
		1.8	− .10	.31			6.5	+ .37	1.10
2	11.0	12.3	+ .70	2.07		11	6.4	− .37	1.08
		7.0	− .40	1.17			6.7	+ .38	1.12
	5.0	11.9	+ .68	2.00		4.5	7.0	+ .40	1.18
		2.4	− .14	.41			4.3	− .24	.73
3	10.2	9.5	+ .54	1.59			6.1	+ .34	1.03
		4.7	− .27	.79	12	9.7	8.7	+ .50	1.47
	6.0	1.8	+ .17	.52			7.8	− .45	1.30
		3.5	− .20	.59		12	7.7	+ .44	1.30
4	10.0	8.6	+ .49	1.44			8.7	− .50	1.47
		6.8	− .39	1.15		3	7.8	+ .45	1.32
	12.4	3.7	+ .21	.62			3.4	− .19	.57
		8.4	− .48	1.40	13	12.5	5.4	+ .31	.91
	6.2	5.6	+ .32	.94			.0	.0	.0
		6.0	− .34	1.00		5.7	4.7	+ .27	.79
5	5.0	9.0	+ .51	1.50			3.0	− .17	.50
		1.4	− .08	.23	14	12.5	5.4	+ .31	.91
6	9.5	7.7	+ .44	1.30			.5	− .03	.09
		2.9	− .17	.50		4.7	1.6	+ .09	.28
	11.6	7.6	+ .43	1.28			2.9	− .16	.48
		1.4	− .08	.23	15	12.5	4.2	+ .24	.70
	12.1	4.4	+ .25	.73			2.8	− .16	.47
		4.1	+ .23	.69		5.2	7.1	+ .40	1.18
	3.0	2.2	− .13	.38			3.4	− .19	.57
		.9	+ .05	.15	16	12.5	7.3	+ .42	1.24
7	9.9	2.5	+ .14	.43			7.1	− .40	1.18
		5.3	− .30	.89		5.0	5.0	+ .29	.86
	12.	10.3	+ .59	1.74			3.7	− .21	.61
		10.1	− .58	1.70	17	12.2	4.2	+ .24	.70
	3.6	9.0	+ .51	1.51			2.8	− .16	.47
		4.1	− .23	.69		3.4	4.2	+ .24	.71
	6.2	2.8	+ .16	.47			1.7	− .10	.29
		5.4	− .31	.89	19	12.2	5.3	+ .30	.89

TABLE 51.—Continued.

Date.	Time.	Volts.	Q.	$n \times 10^{-3}$.	Date.	Time.	Volts.	Q.	$n \times 10^{-3}$.
1906.					1906.				
Feb. 19	12.2	4.4	−0.25	0.73	Mar. 6	5.0	4.0	+0.22	0.66
	5.0	3.8	+ .22	.64			3.1	− .18	.52
		3.4	− .19	.57	7	12.5	7.9	+ .45	1.32
20	11.2	8.7	+ .50	1.47			6.2	− .35	1.05
		4.3	− .24	.73		3.7	4.0	+ .22	1.17
	5.0	4.7	+ .27	.79			2.8	− .16	.47
		2.8	− .16	.47	8	12.2	7.3	+ .42	2.15
21	5.3	5.4	+ .31	.91			4.2	− .24	.71
		4.2	− .24	.71		5.0	3.7	+ .21	1.09
22	12.0	6.8	+ .39	1.15			4.2	− .24	.71
		6.0	− .34	1.00	10	11.5	6.2	+ .35	1.05
23	4.7	6.0	+ .34	1.00			4.2	− .24	.71
		4.7	− .27	.79		3.5	5.1	+ .29	.85
26	4.3	8.1	+ .46	1.37			1.4	− .08	.23
		5.8	− .33	.97	12	1.2	8.7	+ .50	1.47
		6.7	+ .38	1.12			9.0	− .51	1.50
27	11.5	9.0	+ .51	1.50		4.2	5.2	+ .29	? .87
		5.5	− .31	.91			4.7	− .27	.79
	5.0	5.1	+ .29	.85	13	5	5.9	+ .34	1.00
		3.3	− .19	.56			3.6	− .20	.60
28	12.2	9.4	+ .54	1.59	14	4	4.8	+ .27	.79
		6.6	− .38	1.11			3.1	− .17	.50
	5.0	8.5	+ .48	1.43	15	1.5	7.0	+ .40	1.17
		5.6	− .31	.91			6.2	− .35	1.05
Mar. 1	12.5	9.4	+ .54	1.59	16	3.2	8.3	+ .47	1.38
		6.5	− .37	1.09			3.7	− .21	1.09
	5.0	5.9	+ .34	1.00	17	3.7	2.4	+ .14	.41
		6.0	− .34	1.00			2.6	− .15	.44
2	11.5	6.3	+ .36	1.06	19	10.7	6.2	+ .35	1.05
		5.7	− .32	.96			3.7	− .21	1.09
	5.7	3.3	+ .19	.56	20	3.7	3.4	+ .19	.57
		3.2	− .18	.54			4.4	− .25	.73
3	10.7	4.2	+ .24	.71	22	3.4	5.0	+ .28	.84
		9.3	− .53	1.57			5.2	− .30	.88
5	12.5	10.6	+ .61	1.79	23	10.7	7.9	+ .45	1.32
		7.5	− .43	1.26			6.7	− .38	1.12
	4.5	10.5	+ .60	1.76	24	3.5	2.8	+ .16	.47
		3.5	− .20	.59			2.8	− .16	.47
6	11.5	6.6	+ .38	1.11	26	10.8	6.4	+ .36	1.06
		4.8	− .27	.79			5.1	− .29	.85

93. Remarks on the tables.—Perhaps the most expeditious way of digesting this large body of observations is to plot them graphically (as above, figs. 58–61) in relation to time. This was carefully done throughout, and the statements now to be made refer to this summary. It is not probable that positive and negative ions will show the same fluctuations in number, but a general similarity in the trend of the curves may be anticipated.

Beginning with August, 1905, the positive and negative ionizations usually vary in the same sense, though rarely in the same absolute magni-

tude. There being but two observations, as a rule, for the day, the nature of the fluctuations is not referable to periods; and indeed there is as liable to be a rise as a fall of values during the middle hours of the day. Towards the end of the month and in the beginning of September there is an absence of agreement in the march of positive and negative ionizations. Frequently the variation of one ionization is apt to lag behind the other.

After the 7th of September the positive and negative variations tend to take the same sign again, but the agreement in the course of a month is less marked than before.

In October the earlier observations are as a rule in the same phase until October 10, where the first of a series of anomalies occurs, to be specially considered later (section 94). While the data throughout the remaining part of October are regular, there are similarly displaced variations towards the end, which run quite into the next month.

During November similarity of variation of the positive and negative ionization may still be recognized, but in December the divergence of data is so marked that it is not possible to coordinate them; and the same discrepancy shows itself in January, both as regards the signs of variations and their absolute values. One may note, moreover, that the positive curve (the observations for which were first taken) is more irregular in its march and fluctuates between relatively enormous values. Though there is some agreement in phase between January 18 and 25, the anomalies increase again at the close of the month.

The attempt was therefore made in February (section 94) to account for and remove these discrepancies, and though this was but partially successful, the positive and negative results during the remainder of the season again return to an unmistakable agreement in character. There is, moreover, a curious parallelism between the general march of the nucleation curves and the ionization after February 15 as far as March. In the latter month the positive and negative ionizations, though at first fluctuating and uncertain, are finally in very close agreement.

From what has been stated it appears that the positive results during December and January are liable to be untrustworthy. The negative results, which were taken after the positive, show less irregular fluctuation and are in a measure acceptable throughout the eight months of observation.

94. Errors of measurement.—The abnormal data during the occurrence of cold weather, and as a rule in December and January, show that some grave error must here have crept into the results. As every part of the condenser and appurtenances functioned faultlessly, this error is liable

to be found in the galvanoscope. Changes of temperature produce vortical currents in the capsule which modify the deflections of the aluminum foils. In the mean ranges, one scale part of double deflection is equivalent to about 6 volts, or to 1,000 ions per cubic centimeter. Therefore, the presence of any secondary disturbance like the one in question is of very serious consequence. Prior to measurement, the apparatus was naturally left in the cold air out of doors until temperature uniformity was presumable; but this is not sufficient, as the special observations in the early part of February show, even for a galvanoscope dried with sodium.

Turning first to the leakages due to conduction, etc. (v in the above equation), direct experiments made at different times showed values of 0.073, 0.067, 0.120 volt per minute, or less than 0.9 volt for the ten minutes of observation. This is equivalent to an excess of 150 ions per cubic centimeter. As it is applied equally to the positive and to the negative ions, is independent of the size of the deflections, and the same no matter whether the deflections on both sides are equal or not, it has no bearing on the outstanding errors in question. It was not deducted from the ionizations (n) of table 53, which are therefore slightly too large.

Trials made between February 4 and 11 showed that in almost every case the first measurements (whether for positive or negative ions), even after the galvanoscope had been exposed to the cold air for some time, are too large. This discrepancy may at times extend to the second and third observations (February 6, 9, 11). Thus on February 9 the estimated positive ionization would be a thousand and zero, for instance. Usually, however, the second and third observations are liable to be trustworthy (February 6, 10, 11, etc.). Hence electroscopic apparatus which can not be left permanently out of doors, but is taken from a warm room into the cold atmosphere, even if it is sodium dried, is not liable to show warrantable results after mere waiting for uniform temperature. It seems additionally necessary to pass a large volume of cold air through the condenser, or to make successive measurements in series. The observer is usually in doubt, whenever the positive and negative ionizations differ widely, so that at least three tests must be made. The tendency of the apparatus to show spurious results is usually indicated by an inequality of deflections of the foils on either side of the vertical. They may increase to a maximum after charging and then decrease regularly. The latter probably finds an explanation in the gradual cessation of a down-pouring cold air current near the sides of the capsule of the galvanoscope, but the persistence of unequal deflections must follow from other causes. Remembering that the air is desiccated internally with metallic sodium, it seems hardly creditable that there can be a precipitation of moisture from this dried air on the aluminum foils; and yet the behavior is such

as if a moisture gradient from the foil nearest the sodium to that more remote were permanently maintained. In such a case there would be slight but unequal precipitation of vapor on the two foils, in an apparatus passing from warm to cold, and persistence would be due to freezing. The only other explanation is the possibility of charges on the very cold glass and on other insulators which can not be earthed.

95. Mean daily ionization.—As in the preceding case, the observations were now averaged for single days. The results are given in detail in table 52. If given in the charts with the number of ions in thousands per cubic centimeter laid off vertically, very little that is new may be taken from these figures, and they are therefore omitted. They serve, however, as a basis for the monthly ionizations which follow, and in comparing the ionizations with the nucleation of the atmosphere these charts are useful. Thus, it would be difficult to detect synchronism in August, September, October, November, December; but from the middle of January to the end of February suspicions of this kind would be justified.

TABLE 52.—Mean daily ionizations corresponding to table 51.

Date.	Positive ions. $n \times 10^{-3}$	Negative ions. $n \times 10^{-3}$	Date.	Positive ions. $n \times 10^{-3}$	Negative ions. $n \times 10^{-3}$	Date.	Positive ions. $n \times 10^{-3}$	Negative ions. $n \times 10^{-3}$
1905.			1905.			1905.		
July 26	0.90	....	Aug. 28	0.55	0.73	Sept. 29	0.79	0.72
29	.93	0.85	29	.74	.69	30	.46	.36
31	1.30	.76	30	.78	.66	Oct. 2	.34	.41
Aug. 1	.73	.89	31	.75	.82	3	.95	.64
2	1.07	.73	Sept. 1	1.02	.73	4	.54	.65
3	1.24	.82	2	.62	.49	5	.41	1.00
4	.66	.76	4	.88	1.10	6	1.15	1.66
5	.73	.98	7	.85	.79	7	.84	.85
7	1.58	1.34	8	1.31	1.34	9	2.12	.80
8	.91	.52	9	1.17	.88	10	.58	1.07
9	1.20	.75	11	.49	.58	11	.69	1.10
10	1.29	1.04	12	1.07	.44	12	.79	1.39
11	1.21	.88	13	.75	.59	13	.42	.99
12	.96	1.05	14	1.45	1.18	14	1.01	.94
14	2.05	1.85	15	1.34	.94	16	.61	.51
15	1.59	1.42	16	1.05	.41	17	1.14	.86
16	1.52	1.04	18	1.43	.67	18	.44	.38
17	1.52	1.27	19	.92	.34	19	.91	1.01
18	1.45	1.52	20	.69	.45	20	1.08	.39
19	1.67	1.52	21	1.08	.73	23	.89	1.21
21	1.29	.93	22	.39	.42	24	.40	.43
22	.78	.87	23	1.30	1.29	25	.64	.99
23	1.43	1.52	25	1.14	1.65	26	1.04	1.76
24	.87	.96	26	.95	1.12	27	.97	1.08
25	1.13	.78	27	.47	.52	30	.79	1.12
26	1.45	1.21	28	1.00	.85	31	.44	1.39

TABLE 52.— Mean daily ionizations corresponding to table 51.— Continued.

Date.	Positive ions. $n \times 10^{-3}$	Negative ions. $n \times 10^{-3}$	Date.	Positive ions. $n \times 10^{-3}$	Negative ions. $n \times 10^{-3}$	Date.	Positive ions. $n \times 10^{-3}$	Negative ions. $n \times 10^{-3}$
1905.			1905.			1906.		
Nov. 1	1.29	0.73	Dec. 21	1.26	0.78	Feb. 9	0.87	0.63
2	1.12	1.59	1906.			10	.83	.59
3	.65	.45	Jan. 1	1.91	.76	11	1.29	.93
4	.35	.38	2	4.51	1.21	12	1.36	1.11
6	1.20	.50	3	1.60	.70	13	.85	.50
7	1.01	1.16	4	.86	.55	14	.59	.28
8	.88	.50	5	1.84	1.77	15	.94	.52
9	.38	1.85	6	1.72	.94	16	1.05	.89
10	.55	.50	8	2.01	1.14	17	.70	.38
11	.72	1.13	9	1.66	.75	19	.76	.65
13	.60	.97	10	1.78	.23	20	1.13	.60
14	1.65	.91	11	1.83	.55	21	.91	.71
16	.56	1.14	12	.89	.55	22	1.15	1.00
17	.53	1.05	13	3.15	.75	23	1.00	.79
18	.76	1.74	15	1.12	1.00	26	1.24	.97
20	.29	1.35	16	1.03	.47	27	1.17	.73
21	.64	1.04	17	1.17	.60	28	1.51	1.01
22	.80	1.13	18	.87	.23	Mar. 1	1.29	1.04
23	1.00	.31	19	1.36	.99	2	.81	.75
24	.46	.43	20	.82	.56	3	.71	1.57
27	1.10	.74	22	1.05	.96	5	1.78	.92
28	.55	.86	23	1.11	.47	6	.88	.65
Dec. 4	.66	1.35	24	1.41	1.62	7	1.24	.76
5	2.08	1.57	25	1.54	.71	8	1.62	.71
6	1.03	.55	26	1.70	.40	10	.95	.47
7	1.76	.76	27	1.30	.56	12	1.17	1.14
8	1.41	.39	29	2.18	.94	13	1.00	.60
9	1.12	1.00	30	.83	.95	14	.79	.50
11	1.25	.82	31	1.45	1.17	15	1.17	1.05
12	1.32	.61	Feb. 1	1.50	.72	16	1.38	1.09
13	1.60	1.16	2	2.03	.79	17	.41	.44
14	.32	.79	3	1.05	.69	19	1.05	1.09
15	2.15	.79	4	.93	1.18	20	.57	.73
16	2.41	.57	5	1.50	.23	22	.84	.88
18	1.41	.49	6	.83	.37	23	1.32	1.12
19	1.18	1.58	7	1.03	1.04	24	.47	.47
20	1.07	.81	8	.94	1.03	26	1.06	.85

96. Mean monthly ionizations and conclusion.—The straightforward way of arriving at a conclusion as to the presence or absence of a relation between the nucleation and the ionization of the atmosphere consists in comparing the average monthly values for both cases. This is done in table 53, and graphically in fig. 62.

The curve showing the distribution of negative ions is probably the more trustworthy, as these observations were made last. The positive distribution curve is too high in December and January for the reasons already stated, and its more probable course during these two months is indicated by the dotted line. It seems exceedingly curious that whereas

the fluctuations of positive and negative ionization in successive observations, on the same or on succeeding days, usually show the same sign, although not the same absolute value, this is not in general the case with the monthly ionizations. The two curves of fig. 62 throughout the greater part of their course vary in opposite directions.

TABLE 53.—Mean monthly ionizations, corresponding to table 51.

Date.	Positive ions. $n \times 10^{-3}$	Negative ions. $n \times 10^{-3}$
1905.		
Aug.	1.16	1.02
Sept.	.95	.78
Oct.	.80	.94
Nov.	.77	.96
Dec.	1.38	.88
1906.		
Jan.	1.58	.80
Feb.	1.09	.73
Mar.	1.03	.84

Compared with the uniform curve for nucleation the appearance of the ionization curve is sufficiently distinctive. One might perhaps be inclined to refer the dip in the negative curve between November and February to the more marked "absorption" of the negative ions by the increasing nucleation. But the two curves are not sufficiently similar and there is no reason why the absorbed ion should fail to have a record in the condenser. The only conclusion to be drawn from the results for the distribution of either the positive or the negative ions is this, that there is no discernible relation between the number of ions and the number of Aitken nuclei present in the atmosphere at any time, or that the two distributions result from entirely distinct causes. The ionization of a given region is independent of artificial local contributions, however abundant these may be.

CHAPTER VI.

THE VARIATIONS OF THE COLLOIDAL NUCLEATION OF DUST-FREE AIR IN THE LAPSE OF TIME.

97. Introductory.—Above (Chapter I, section 26, *et seq.*) and in my address* before the Physical Society, I gave an account of observations made several times daily since May 9, 1905, in a search for the possible occurrence of an ultra-mundane radiation. The work was there summarized as follows:

> Using the most sensitive condensation method, *i. e.*, that depending on the depression of the limiting asymptote of non-energized, dust-free air, no change of the quality of scrupulously filtered atmospheric air has thus far been detected. . . . Naturally [ions] would vanish during the slow passage of air through the filter, but fresh ions should be reproduced within the fog chamber by the same agency which generates them without. . . . Probably, therefore, the coronal method is as yet inadequately sensitive to cope with variations of the small nucleations specified.

The ions, which are relatively large nuclei, withdraw much of the available moisture which would otherwise be precipitated on the colloidal nuclei of dust-free air. Hence the size of the terminal corona is diminished. The advantage of the method is its independence of the drop in pressure if this exceeds a certain value.

Since the discovery announced by A. Wood and A. R. Campbell† on the probability of cosmical radiation as evidenced by the existence of a daily period of the same, showing maximum ionization between 8 and 10 A. M. and 10 P. M. and 1 A. M., minimum ionization at about 2 P. M. and 4 A. M., I have taken the subject up again. It seems possible that I overestimated the sensitiveness of the earlier method. I have therefore changed it in the present experiment, replacing the large terminal coronas by the small coronas very near the fog limit.

98. Method and data.—The observations, in other words, are now made with a drop in pressure, but just sufficient to produce coronal condensation on the larger colloidal nuclei of dust-free air ($\delta p = 21$ cm.). The sizes of coronas vary rapidly with the pressure difference and hence with the barometer, p, etc., and great care must be taken with these details. This, however, has been done and the results obtained are given in table 54 and in the chart (fig. 64).

---

* Physical Review, XXII, p. 105, 1905; also p. 109, on Radiant fields.

† Nature, vol. 73, p. 583, 1906.

The table gives the angular diameter (s) of the successive coronas, and other data to be presently explained, from which the number of nuclei (n) per cubic centimeter may be obtained. Observations were

TABLE 54.—Colloidal nucleation (s) of dust-free air near the fog limit in their time variations, observed two or more times daily. $\delta p = 27$ cm. (observed at fog chamber, isothermally) $= p - p_3$. Computed $\delta p = p - p_2 = 21$ cm.

Date.	Time.	$p - p_3$.	s.	p.	s^1.	$n \times 10^{-3}$.
1906.	*h.* *m.*					
May 21	9 30	27.4	3.6	76.4	3.2	9.7
	12 0	26.7	2.1	....	2.8	6.1
	5 30	27.3	3.0	.3	2.7	5.9
22	9 15	.1	2.9	.7	3.1	8.5
	3 00	.3	3.1	.6	3.0	7.7
23	9 15	.3	2.9	.4	2.7	6.1
	3 15	.5	4.4	.1	3.7	16
24	9 30	.0	2.8	.0	2.8	6.3
	4 00	.1	3.5	75.8	3.2	9.7
25	9 00	.2	4.3	.6	3.8	18
26	8 50	.4	4.9	.4	4.0	19
	3 10	.2	4.9	.3	4.2	22
27	10 25	.1	4.2	.2	3.6	15
	4 25	.1	4.9	.0	4.2	22
28	9 5	27.3	5.2	75.0	4.2	22
	3 45	.1	5.4	74.9	4.6	30
29	11 00	.1	4.9	75.1	4.2	22
	3 50	.1	4.9	.2	4.3	25
30	8 50	.1	2.9	.9	2.7	6
	3 10	.3	3.9	.8	3.3	11
31	9 30	.0	3.0	.9	2.9	7
	2 45	.0	4.5	.6	4.3	25
June 1	9 30	.2	3.9	.7	3.4	12
	2 45	26.9	3.9	....	3.9	17
2	9 5	27.0	3.7	.6	3.5	13
	2 45	.1	3.7	.6	3.3	11
3	10 00	.3	4.9	.9	4.4	26
	4 30	.2	4.2	.9	3.8	18
4	8 30	27.1	3.1	76.4	3.0	8
	3 35	.3	4.3	.2	4.0	19
5	9 20	.1	3.9	75.9	3.7	16
	3 20	.1	4.2	.6	3.8	18
6	10 6	.1	5.0	.1	4.3	24
	3 20	.2	5.9	74.8	4.9	37
7	9 10	.3	4.9	75.6	4.2	22
	3 45	.3	4.8	.9	4.3	25
8	9 25	.1	3.6	76.2	3.6	15
	2 45	.4	4.6	.0	4.0	19
9	9 10	.3	5.0	75.5	4.3	25
	2 45	26.9	3.5	.0	3.1	8
	8 15	27.3	5.1	.1	4.1	20
	9 20	.3	5.1	.3	4.2	22
10	9 55	.2	5.1	.2	4.3	25
	3 15	.3	5.6	.0	4.6	30
	6 15	.2	5.1	.1	4.3	25
11	8 40	.2	4.9	.5	4.3	25
	2 55	.1	4.2	.6	3.8	18

TABLE 54, continued.—Colloidal nucleation (s) of dust-free air near the fog limit in their time variations, observed two or more times daily. $\delta p = 27$ cm. (observed at fog chamber, isothermally) $= p - p_3$. Computed $\delta p = p - p_2 = 21$ cm.

Date.	Time.	$p - p_3$.	s.	p.	s^1.	$n \times 10^{-3}$.
1906.	*h.* *m.*					
June 11	6 5	0.1	3.6	0.8	3.3	11
12	8 45	27.1	3.0	76.3	3.0	8
	12 00	.2	3.4	.3	3.3	11
	3 00	.0	2.8	.2	2.9	7
13	9 00	.1	2.5	.7	2.7	6
	11 40	.1	2.5	.7	2.7	6
	2 35	.2	3.0	.6	3.0	8
	6 5	.2	3.5	.5	3.5	13
14	9 35	.2	3.9	.2	3.7	16
	12 20	.0	2.9	.0	2.9	7
	3 30	.2	4.0	75.8	3.6	15
	6 10	.1	3.7	.7	3.4	12
15	9 20	.1	4.2	.7	3.9	18
	12 00	.2	4.2	.7	3.7	16
	2 40	.1	4.5	.7	4.2	22
	6 00	.1	3.6	.8	3.3	11
16	9 50	.4	4.7	.9	4.1	21
	3 45	.2	4.1	....	3.7	16
17	10 00	.1	4.0	.6	3.6	15
	12 00	.3	5.3	.6	4.6	30
	3 25	.3	5.1	.6	4.5	28
	6 10	26.8	2.8	.7	3.0	8
18	9 15	27.1	3.0	76.0	2.9	7
	12 35	.0	3.0	75.9	2.9	7
	3 00	.2	3.9	.9	3.5	13
	6 00	.2	3.8	.8	3.4	12
19	11 00	.1	3.5	.6	3.1	8
	12 55	.2	4.4	.6	3.8	18
	3 40	.2	4.6	.6	4.0	19
20	5 35	.1	4.1	.7	3.8	18
21	10 15	.3	4.0	.8	3.6	14
	1 00	.1	3.8	.7	3.5	13
	3 10	.1	3.7	.6	3.3	11
	6 20	.1	3.8	....	3.4	12
22	9 15	.1	4.4	.3	3.8	18
	12 10	.1	4.2	.3	3.6	15
	2 50	.2	5.5	.2	4.7	33
	6 10	.2	5.3	....	4.5	28

made at about 9 A. M. and 3 P. M., as near the time of the Wood and Campbell maxima and minima as my duties permitted, on the successive days and hours given by the abscissas.

99. Deductions.—Figure 64 shows in the first place that, in general, minima and maxima of nucleation would have to appear at about the time at which Wood and Campbell observed maxima and minima,

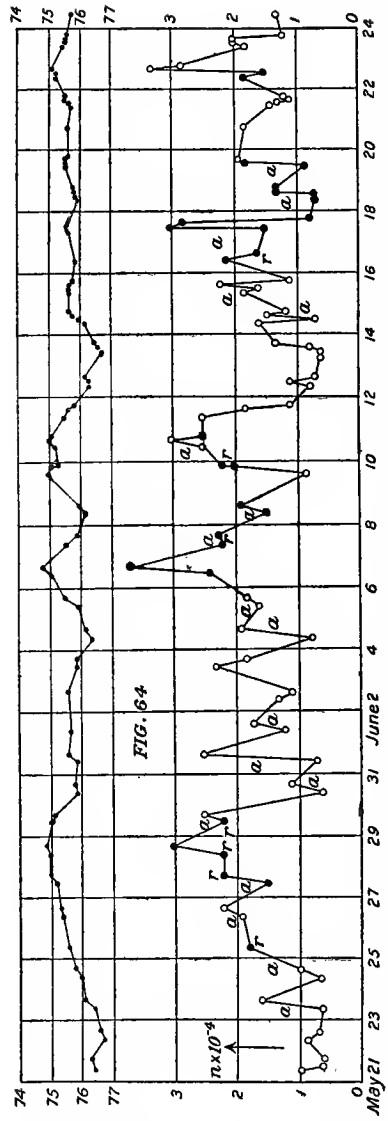

FIG. 64.—Nucleations in ten thousands of colloidal nuclei per cubic centimeter of dust-free air observed on the days and hours given by the abscissas. The branches *a* are in agreement with the Wood-Campbell discovery; the branches *e* show a tendency to inversion; *r* denotes rain. Table 54. Apparatus I. The upper curve (positive downward) shows the initial pressure within the fog chamber and is equivalent to the fluctuations of the barometer.

respectively; or that an inversion of Wood and Campbell's results is a question, since there is usually incremented nucleation in the afternoon as compared with the morning. This, however, may be explained, if the ions are large, even in comparison with the larger gradations of colloidal nuclei. Fewer of these will therefore be captured in proportion as the ionization is larger. Hence the figure shows at *a* an *apparent* corroboration of Wood and Campbell's results; at *e* an omission or inversion of the periods. But the *e*'s are much fewer in number, and in comparison with the amplitude of the *a*'s, the *e*'s are frequently neutral.

In the second place, the high nucleation during the period of rain is noteworthy. Here, then, few ions were present. As there is a modification of the atmospheric potential gradient during this time, one might favor an explanation on similar lines to the ideas suggested by Richardson.*

100. Effect of the barometer.—In the further development of the investigation on the time variations of the efficient colloidal nucleation in filtered air, the results are of the same character as those already dis-

* Nature, LXXIII, p. 607, 1906.

cussed; but the dependence of the nucleation on the *fluctuations of the barometer* now shows itself even more obtrusively than before. The minima of atmospheric pressure coincide with maxima of colloidal nucleation, and therefore (by inference but not necessarily) with minima of ionization of the dust-free air, both in the daily and in the weekly periods of observation. Maximum pressure, therefore, would correspond to maximum ionization as if the radiant energy originated in the compression of the atmosphere, or were dependent on the mass of the atmosphere bearing on a given place. This would, if finally substantiated, be an important inference, but no more so than the more direct correlative result that minimum pressure and maximum colloidal nucleation of dust-free air go together.

At the same time, since the change of absolute temperature (τ) due to a sudden expansion equivalent to a drop (δp) at a barometric pressure (p) and vapor pressure (π) may be written

$$\frac{\tau_2}{\tau_1} = \left(1 - \delta p/(p-\pi)\right)^{(k-c)/k}$$

the correction for the changes of the barometer are in the same sense as the observed changes in nucleation. These corrections are found by varying the numerator of $\delta p/(p-\pi)$ and observing the effect on the angular diameter of the corona. While I can see no room for error, it must nevertheless be acknowledged that the present method of small exhaustion, though possibly more sensitive, is not as straightforward as the method mentioned in my address, where no variation could be detected, the terminal corona remaining unchanged.

At the present stage of investigation, therefore, the need of any external radiation has ceased to be obvious; and the results, if they exceed the barometer correction, are most directly referable to changes of pressure within the gas, the number of colloidal nuclei being greatest when the pressure is least.

101. Corrections.—In table 54 and the following table 55, p is the barometric pressure; p_3 the final pressure when fog chamber and vacuum chamber are in communication; p_2 the (computed) pressure which would be observed in the fog chamber if it could be instantly separated from the vacuum chamber after exhaustion. Hence the true drop in pressure is $\delta p = p - p_2$ while $\delta p = p - p_3$ is observed. The initial pressure (p) differs from the atmospheric pressure by a few millimeters, due to the leakage of the 4-inch stopcock from fog chamber to vacuum chamber. As it is impossible to retain the same value of p and δp throughout, a correction must be applied, seeing that the adiabatic cooling is given by $\tau_2/\tau_1 = (1 - \delta p/(p-\pi))^{(k-c)/k}$, where π is the vapor pressure of water. By varying

δp from 26 to 28 cm. and observing the changes of s (angular coronal diameter) when p is constant, a table was investigated from which reductions could at once be made to $\delta p = 27$ cm. and $p = 76$ cm.; for instance,

δp = 26.8 cm.	δs = +0.34	p = 75.8	δs = −0.11
26.9	+ .17	75.9	− .06
27.0	+ .00	76.0	+ .00
27.1	− .15	76.1	+ .06
27.2	− .30	76.2	+ .11

The value of s corrected for both pressures is given in this table.

In the same way the case of apparatus II (to be described presently) was treated, the reductions being much larger here. Thus the data (barometer, 75.5; temperature, 21.4° C.)

δp = 24.9	s = 1.7	δp = 25.6	s = 3.1
25.6	3.6	26.2	5.2
26.4	5.6	25.6	2.9
24.8	1.0		

were consecutively observed, showing that the coronas after long waiting are much larger than when obtained in succession. The efficient nucleation of the fog chamber increases in the lapse of time, probably from the evanescence of water nuclei associated even with small coronas. From these results corrections of the form

δp = 25.5	δs = +0.27	B = 75.9	δs = −0.08
25.6	+ .00	76.0	+ .00
25.7	+ .27	76.1	+ .08

were made out. These examples show how critically important these corrections are, and how difficult it will be to decide whether anything more than the barometer fluctuation is being observed.

102. Further data.—It follows from section 101 that there would be a chance for error in the unavoidable leakage of the stopcock, and the best method of coming to a decision would consist in the installation of a second fog chamber, side by side with the other, but containing a smaller exhaust pipe (2 inches in diameter, 18 inches long) and therefore a more perfect stopcock.

Fig. 65 shows two fog chambers (F and F') and appurtenances in place, each with an independent vacuum chamber (V and V') and goniometer. Other parts will be easily recognized.

Table 55 and chart 66 contain the new data, the old fog chamber (4-inch cock) being marked I, the new fog chamber (2-inch cock), marked II. The latter was first tested at different values of δp, and $\delta p = 25.6$

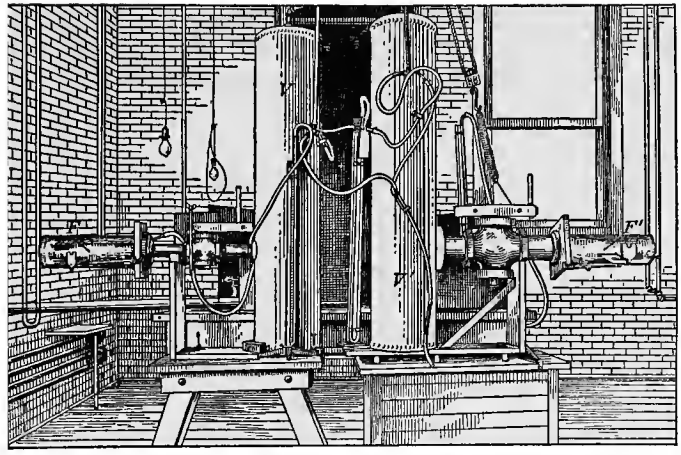

FIG. 65.—Independent fog chambers with 2-inch and 4-inch efflux side by side. Vacuum chambers, V and V'; fog chambers, F and F'.

finally selected. At the outset the values of s may be uncertain, because of internal sources of nucleation and similar difficulties.

Four observations were usually made daily. Data corresponding to I and II are distinguished by subscripts, and those of II were usually observed about five minutes after the time given for I. One may note the much greater efficiency of the apparatus with 2-inch pipes as compared with the other with 4-inch pipes, the reason for which is not easily seen. As a whole the observations for apparatus I during the end of June and the beginning of July run parallel to the barometric decrement, and the astonishingly high values on June 29 and 30 occur during a period

TABLE 55.—Colloidal nucleations near the fog limit in their time variations. Fog chamber I with 4-inch exhaust pipes; $\delta p = p - p_3 = 27$ cm.; II with 2-inch exhaust pipes; $\delta p = p - p_3 = 25.6$ cm.; $p - p_2 = 21$ cm. and 20 cm., respectively.

Date.	Time.		$\delta p_1 = p - p_3$	s_1.	p.	s'_1.	$n \times 10^{-3}$	$\delta p_2 = p - p_3$	s_2.	s'_2.	$\frac{n_2}{10^3} \times$
	h.	*m.*									
June 23	9	15	27.1	4.3	75.5	3.8	18	[1]27.6	7.3	6.4	75
	12	35	.1	4.5	.6	4.1	20	.4	7.7	7.4	86
	3	15	.2	4.6	.6	4.1	20	.4	7.3	7.0	82
	5	50	.0	3.6	.6	3.4	12	.3	7.1	7.0	82
24	10	20	.1	3.8	.8	3.5	13	.2	7.5	7.9	93
	12	50	.0	4.1	.7	3.9	18	[2]26.5	5.2	5.0	38
	4	15	.1	3.9	.7	3.6	15	.6	5.1	4.6	30
	6	20	.1	4.3	.7	4.0	19	.5	5.5	5.3	45
25	9	10	.2	5.1	.7	4.6	30	.5	6.0	5.8	57
	12	10	.1	4.0	.8	3.7	16	.5	4.9	4.7	32

[1] Early results. [2] Results in succession.

TABLE 55.—Continued.

Date.	Time.		$\delta p_1 = p - p_3$	s.	p.	s'_1.	$n \times 10^{-3}$	$\delta p_2 = p - p_3$	s_2.	s'_2.	$n_2 \times 10^{-3}$.
	h.	*m.*									
June 25	3	35	27.1	4.2	75.8	3.9	18	26.5	5.0	4.8	34
	6	10	.1	3.0	.7	2.7	6	.5	5.3	5.1	40
26	9	30	27.1	4.0	76.0	3.9	17	....	...	...	..
	12	20	.1	4.1	75.9	3.9	17	26.5	4.9	4.8	34
	12	35	....	...	.9	...	..	25.6	2.1	2.0	2
	2	40	27.2	5.1	.9	3.7	16	.6	2.6	2.5	4
	5	30	.2	4.7	.9	4.3	25	.6	2.6	2.5	4
27	9	10	.2	4.9	.8	4.5	28	.6	2.7	2.5	4
	12	25	.1	4.9	.7	4.6	32	.6	2.7	2.5	4
	3	00	.1	4.1	.6	3.7	16	.6	3.5	3.2	9
	6	5	.2	4.8	.6	4.2	22	.5	3.5	3.4	11
28	9	5	.3	5.7	.9	5.2	43	.6	3.0	3.0	7
	12	5	.1	4.9	.9	4.7	33	.5	3.0	3.2	9
	3	30	.2	5.1	.8	4.7	33	.5	2.8	2.6	5
29	9	00	.1	5.0	.3	4.5	28	.7	3.7	2.9	7
	12	30	.5	7.0	.2	5.8	59	.6	3.8	3.3	10
	12	40	.2	5.1	.2	4.3	25	....	...	...	..
	2	55	.2	5.4	.2	4.6	30	25.6	3.7	3.2	9
	6	00	.2	5.0	.2	4.2	22	.6	3.8	3.2	9
30	9	25	.5	7.0	.2	5.8	59	.7	4.4	3.6	14
	12	30	.1	5.3	.1	4.6	30	.6	3.2	2.6	5
	3	5	.1	5.3	.2	4.7	33	.6	4.0	3.3	10
	5	50	.1	5.3	.3	4.7	33	.6	4.3	3.7	16
July 1	10	00	27.2	5.1	75.6	4.6	30	25.6	3.3	3.0	7
	12	10	.1	4.5	.6	4.1	20	.6	3.2	2.9	7
	1	45	.1	4.1	.6	3.7	43	.7	3.6	2.9	7
	6	25	.2	5.2	.6	4.7	33	.5	2.9	2.9	7
2	9	15	.4	5.7	.6	4.9	37	.6	3.6	3.3	10
	12	30	.1	4.6	.6	4.2	22	.6	3.6	3.3	10
	2	20	.3	5.5	.5	4.8	36	.6	4.2	3.8	17
	6	00	.2	5.5	.5	4.9	37	.6	3.7	3.3	10
3	9	40	.3	5.6	.5	4.9	37	.6	3.8	3.4	11
	12	30	.2	5.3	.5	4.7	33	.6	3.5	3.1	9
	2	00	.3	5.3	....	4.6	30	.6	3.6	3.2	9
	6	50	.2	5.3	.5	4.6	30	.6	3.9	3.5	13
4	9	15	.2	5.3	.2	4.5	28	.6	4.1	3.5	13
	12	00	.1	5.0	....	4.4	26	.7	4.4	3.5	13
	4	50	.2	5.2	.3	4.5	28	.6	4.3	3.7	16
	6	5	.3	5.2	.5	4.5	28	.6	3.5	3.1	8
5	8	55	.2	4.0	76.5	3.9	18	.6	2.8	3.2	9
	12	10	.4	4.7	.5	4.4	27	....	...	...	..
	2	45	.2	3.7	.5	3.7	16	.6	2.1	3.6	14
	6	20	.2	3.3	.7	3.4	12	.6	1.9	2.4	4
6	9	50	27.2	3.7	77.1	4.0	19	25.6	1.9	2.8	6
	12	35	.1	2.7	.0	3.1	9	.6	1.8	2.6	5
	12	45	.2	2.9	.0	3.1	8	....	...	...	..
	3	15	.2	3.3	76.9	3.5	13	25.6	1.9	2.6	5
	6	10	.3	3.8	.9	3.9	19	.6	1.5	2.2	3
7	9	20	.2	3.6	.7	3.6	15	.6	2.5	3.1	8
	2	25	.2	4.2	....	4.2	22	.0	1.5	3.6	14
	7	45	.2	3.7	76.4	3.5	14	.6	3.5	3.8	17
8	8	50	.2	4.2	.2	3.9	18	.4	2.8	3.5	13
	9	00	.2	3.8	.2	3.6	15	....	...	...	..
	2	55	.2	4.3	.1	4.0	20	.6	2.7	2.8	6
	5	40	.3	4.9	.0	4.4	27	.6	3.0	3.0	7

TABLE 55.—Continued.

Date.	Time.	$\delta p_1 = p - p_3$	s_1.	p.	s'_1.	$n \times 10^{-3}$	$\delta p_2 = p - p_3$	s_2.	s'_2.	$n_2 \times 10^{-3}$.
	h. *m.*									
July 9	9 00	27.2	5.2	75.8	4.8	35	25.4	3 3	3.5	13
	2 30	.2	5.1	.7	4.6	30	.6	4.1	3.7	16
	5 50	.2	4.8	.6	4.3	25	.6	4.1	3.8	17
10	9 05	.2	5.2	.6	4.7	33	.7	4.0	3.4	11
	2 45	.4	5.7	.5	4.8	35	.6	4.0	3.6	14
	5 45	.2	5.0	....	4.5	29	.4	2.8	3.0	7
11	9 05	.2	4.6	76.2	4.4	27	.5	2.6	3.0	7
	2 15	.2	3.9	.2	3.7	16	....	...	...	...
	5 20	.2	3.9	.2	3.7	16	....	...	...	...

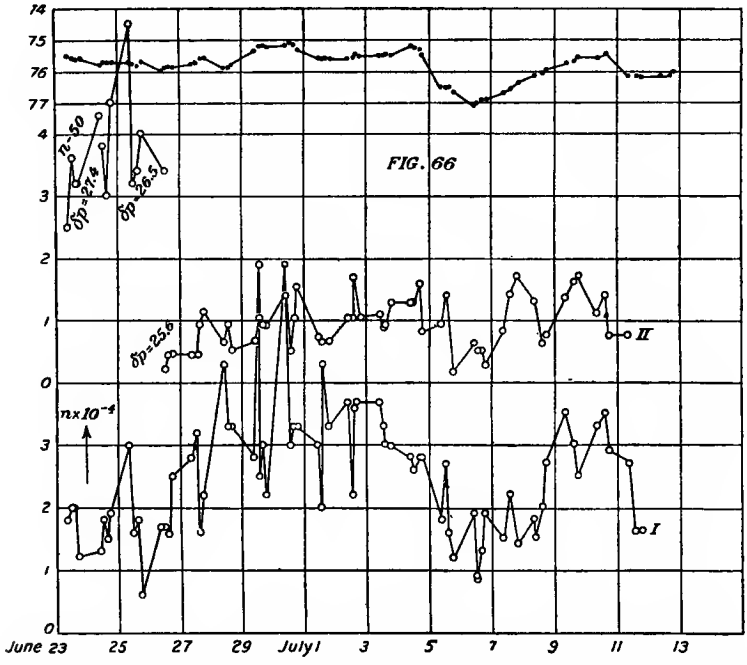

FIG. 66.—Data of fig. 64 continued for apparatus I (fog chamber with 4-inch pipes) and apparatus II (fog chamber with 2-inch pipes), adjusted for different exhaustions ($\delta p = 27.3$ and 25.6 cm., respectively). Table 55.

of exceptionally low barometer. The daily details of the barometer are not as a rule reproduced.

In case of apparatus II, if the initial observations $\delta p = 27.4$ be overlooked, the data for $\delta p = 26.5$ are not unlike magnified parts of the corresponding curve for apparatus I. The chief observations for apparatus II in June ($\delta p = 25.6$ or computed $\delta p = 20$ just above the fog

limit) do not in their details, it is true, agree with the curves for apparatus I, except to some degree on June 29 and 30. As a whole, however, they also strikingly follow the march of the decrement of the barometer. One may note, moreover, that it is not necessary that the curves for apparatus I and II should quite agree. If, for instance, the preponderating nuclei in the former case are colloidal, and in the latter case ions, one should expect an inverse curve; for the ions in I would decrease the number of efficient nuclei, whereas in II they would increase their number. Decision must be deferred for further observation.

In July the two fog chambers again fail to agree in their daily fluctuations, but both nevertheless follow the barometer closely, in their broader variations. The different sizes of coronas imply different ratios of ions and colloidal nuclei, and hence detailed agreement should not be anticipated. On July 12 the fog chambers were subjected to modifications and it was therefore concluded to terminate the preliminary series of observations at that point, reserving further record and comment for a subsequent report.

103. Conclusion.—It appears, therefore, at the present stage of progress of the investigation on the time variation of the number of larger colloidal nuclei in dust-free wet air, that the meaning of the above results is not quite clear. The probable occurrence of an effect due to anything like cosmical radiation may, however, be regarded as excluded. The nucleation curves vary in their broad contours with the barometer, being a maximum when the atmospheric pressure is least. Nevertheless the two fog chambers do not, in their detailed variation, show appreciable accordance; rather the reverse of this, and yet such a result may be due to differences in the ratios of nuclei and ions entrapped in the differently adjusted chambers. No. II in the above work (Chapter II, section 53) shows apparent excess in the region of ions as compared with No. I. As a whole the data for the time variation can not be regarded as quite trustworthy, since the correction to be added for variation of barometric pressure and the drop of pressure are in the same sense as the residual effect observed. If some obscure factor in the make-up of these corrections has been overlooked, the results may possibly be attributed to it.

From another point of view adequate explanation is now at hand, why in the above investigations it was found impossible to secure reasonably coincident results in the case of those groups of nuclei which lie in the region of the larger colloidal nuclei and of the ions; and it is chiefly for this reason that the results of this chapter are included in the present report.